



**THE UNITED STATES PATENT AND TRADEMARK OFFICE**

Applicant:	Sharon Erickson	Attorney Docket #:	GNE-0073
Serial No.	11/949,351	Group Art Unit	1643
Filing Date	12/03/2007	Examiner:	Natarajan, Meera
Customer No.:	35489	Confirmation No.:	4598
Title:	<b>METHODS OF TREATMENT USING ANTI-ErbB ANTIBODY MAYTANSINOID CONJUGATES</b>		

**FILED VIA EFS**

Commissioner for Patents  
P.O. Box 1450  
Alexandria, VA 22313-1450

**DECLARATION OF MARK X. SLIWKOWSKI, Ph.D.**

I, MARK X. SLIWKOWSKI, Ph.D. declare and say as follows: -

1. I obtained a B.S. in Animal Science and Agricultural Biochemistry from the University of Delaware, a Ph.D. in Biochemistry with minor in Physical Chemistry from North Carolina State University, and completed postdoctoral training at the National Institutes of Health, National Heart, Lung and Blood Institute, Laboratory of Biochemistry.

2. After six years of research experience at Triton Biosciences, Inc. (Berlex Biosciences, Inc.), I joined Genentech, Inc. in 1991 as a senior scientist, where my current title is Senior Staff Scientist, Research Oncology.

3. During my employment at Genentech, I have worked on a number of programs involving drugs directed against the human epidermal growth factor receptor family (also known as the HER or ErbB family). Members of the ErbB family are frequently activated in a number of proliferative diseases including cancer. Along with colleagues at Genentech, I have studied various aspects of the ErbB receptor activation process including the biochemical nature of the receptor complexes, the activation of signal transduction pathways, and the resultant biological outcomes. Our studies have also focused on research toward the development of ErbB inhibitors for treating proliferative disorders such as cancer, as well as the elucidation of the molecular mechanisms by which such inhibitors act. Our investigations and those of my predecessors at Genentech have contributed to the development of a number of therapeutic approaches that

target the ErbB receptor family, including the anti-ErbB2 antibody trastuzumab, which is marketed under the tradename Herceptin<sup>®</sup>. Working closely with other groups at Genentech and in collaboration with ImmunoGen, Inc., we have also developed T-DM1, a therapeutic immunoconjugate in which trastuzumab is conjugated to the cytotoxic maytansinoid “DM1” for the treatment of tumors that express ErbB2.

4. My Scientific Curriculum Vitae, including my list of publications, patents, pending patent applications, and awards, is enclosed as **Exhibit A** and forms part of this Declaration.

5. I am familiar with and understand the disclosure of the above-identified patent application and the pending claims, including the new claims added concurrently with filing the present Declaration. Independent Claim 40 is directed to an immunoconjugate comprising the humanized anti-ErbB2 antibody huMAb4D5-8 conjugated to a maytansinoid. The antibody huMAb4D5-8 is the same antibody as trastuzumab and is a humanized form of the mouse monoclonal antibody “4D5.” (See the above-identified patent application at page 61, para. [0216].) All other claims depend, directly or indirectly, from claim 40. I am also familiar with and understand the Office Action mailed on June 8<sup>th</sup>, 2010, in connection with the above-identified patent application, and the references cited in that Office Action.

6. According to the Office Action, the claimed invention would have been obvious to one of ordinary skill in the art at the time the invention was made over the combination of U.S. Patent No. 5,208,020 (referred to hereinafter as “Chari et al.”) and U.S. Patent No. 6,054,297 (referred to hereinafter as “Carter et al.”). Chari et al. allegedly teach a composition comprising one or more maytansinoids (col. 6-8) linked to a monoclonal antibody or antibody fragment, where the monoclonal antibody is selective for tumor cell antigens. Carter is cited for disclosing humanized 4D5 antibodies, including huMAb4D5-8, and for allegedly teaching that the humanized 4D5 antibodies may be used as immunotoxins, conjugated with a cytotoxic moiety (col. 44). The Examiner recognizes that Chari et al. do not teach an anti-ErbB2 antibody conjugated to a maytansinoid, let alone conjugates comprising the specific humanized anti-ErbB2 antibody, huMAb4D5-8, conjugated to a maytansinoid. The finding of obviousness is based on the assertion that one of ordinary skill would have been motivated to make the claimed

antibody-maytansinoid conjugates because such conjugates fall within the scope of the immunotoxins of Carter et al. and because Carter et al. teach that ErbB2 is amplified or overexpressed in human malignancies.

7. The conclusion drawn by the Examiner from the combined disclosures of Chari et al. and Carter et al. disregards a large body of additional relevant knowledge in the pertinent art at the time the present invention was made, and is therefore incorrect.

8. As it is recognized in the Office Action, at the time the present invention was made it was known that ErbB2 (also known as HER2) is amplified and overexpressed in breast and ovarian cancers, and such overexpression is correlated with poor prognosis. (See Carter et al. and application at page 2, para. [0006].) HER2 was also known to be overexpressed in a number of other carcinomas. (*Id.*) It was also known that HER2 is expressed in normal tissues at levels similar to those found in non-HER2-amplified, non-HER2-overexpressing breast cancers and breast cancer cell lines. For example, HER-2 protein was identified on cell membranes of normal epithelial cells in the gastro-intestinal, respiratory, reproductive, and urinary tract as well as in the skin, breast and placenta, demonstrating that HER2 is normally a membrane constituent of a variety of epithelial cell types. (See abstract, Press et al., *Oncogene* 5(7):953-62, 1990 - **Exhibit B.**)

9. The Office Action also recognizes that at the time the present invention was made huMAB4D5-8 (marketed under the tradename Herceptin<sup>®</sup>) was known (see, Carter et al. cited in the Office Action). Indeed, Herceptin<sup>®</sup> was approved by the FDA in 1998 (well prior to the March 16, 2000 priority date of this application) for the treatment of metastatic HER2-overexpressing breast cancer, either as an initial treatment in combination with chemotherapy (paclitaxel), or as a monotherapy after prior treatment with chemotherapy. Herceptin<sup>®</sup> was later approved in 2006 as part of a multi-agent regimen for the adjuvant (post-surgical) treatment of HER2-overexpressing breast cancer. In 2008, Herceptin<sup>®</sup> received further approvals from the FDA for treatment in the adjuvant setting. Although Herceptin<sup>®</sup> is a breakthrough in the treatment of HER2-overexpressing breast cancer, most patients treated with Herceptin<sup>®</sup> in the metastatic setting relapsed after experiencing a period of clinical benefit. (See application, page 5, para. [0014].)

10. At the time the present invention was made, maytansinoids were also known as a family of cytotoxic molecules that include maytansine and its derivative DM1. Before the priority date of the present application, it was reported that maytansine acts as a very potent mitotic inhibitor by inhibiting microtubule polymerization. (See, Rao et al., *Cancer Research* 39:3152-3155, 1979 – **Exhibit C**; and Remillard et al., *Science* 189:1002-1005, 1975 – **Exhibit D**.) Microtubules are necessary for segregation of chromosomes during mitosis, and disruption of microtubules blocks mitosis, thereby inhibiting cell proliferation. Treatment of human cells in vitro with maytansine was reported to result in up to approximately 75% of cells accumulating in mitosis, depending on the concentration of maytansine and duration of exposure. (See **Exhibit C**, e.g., Chart 1.) Indeed, it was reported that sensitivity of cells to the cytotoxic effect of maytansine was cell cycle-dependent, *with cells synchronized in G1 being the most resistant to maytansine*. (See **Exhibit C**, e.g., abstract and page 3155, col. 1, last para.) Thus, it was known before the priority date that maytansine and related maytansinoids, such as DM1, were cytotoxic agents that exerted their cytotoxic effects during M-phase mitosis.

11. However, in addition to the state of the art knowledge detailed in paragraphs 8-10, at the time the present invention was made one of ordinary skill in the art would have been also aware of studies into the mechanism of action of the antibody 4D5. Those studies demonstrated that 4D5 is cytostatic (not cytotoxic), meaning that 4D5 acts on tumors expressing ErbB2 by arresting the cell cycle. The enclosed article by Lewis et al. (*Cancer Research* 56:1457-1465, 1996 – **Exhibit E**) shows that 4D5 has a cytostatic effect, and in particular, it reduces the number of S-phase cells, thus suggesting that 4D5 causes a G0/G1 block. (See Lewis, e.g., at page 1460, column 2, lines 11-13; page 1461, column 1, to 1462, column 2, 1st paragraph; Figure 5; and page 1464, lines 32-33.) Those findings were consistent with earlier studies reporting that 4D5 had a cytostatic, anti-proliferative effect in vitro on SK-BR-3 cells grown in monolayer, and 4D5 completely suppressed colony formation by SK-BR-3 cells in soft agar. (See Hudziak et al., *Molecular and Cellular Biology* 9(3):1165-1172, 1989 – **Exhibit F**, e.g., at page 1168, col. 2, through page 1169, col. 1; and page 1171, col. 1, para. 3) Taken together, those findings indicated that 4D5, and therefore huMAb4D5-8, act at least in part by arresting breast cancer cells in the G0/G1 phase of the cell cycle, which precedes the subsequent S, G2 and M (mitosis) phases of the cell cycle. Those findings, which were made before the priority date of the present application, were subsequently confirmed after the priority date by Lane et al., who reported that

4D5 arrested 96% of BT474 cells, a breast carcinoma cell line that overexpresses HER2, in the G1 phase of the cell cycle. (See Lane et al., *Molecular and Cellular Biology*, 20(9):3210-3223, 2000 – **Exhibit G**, e.g., at page 3214, col. 2.)

12. Thus, it was known well before the present invention was made that the cytostatic mechanism of the 4D5 antibody and, consequently, humanized huMab4D5-8, works in opposition to the cytotoxic mechanism of maytansinoids, which inhibit mitosis by inhibiting microtubule polymerization, and therefore require cells to be proliferating in order to act. Accordingly, contrary to the Office Action, at the time the present invention was made, one of skill in the art would not have been motivated to select huMab4D5-8 as a humanized anti-HER2 antibody for conjugation to a maytansinoid, such as DM1, since it would have expected that huMab4D5-8 would arrest cancer cells in the pre-mitotic G0/G1 phase of the cell cycle before DM1 would even have the opportunity to act. Therefore, based on the seemingly incompatible mechanisms of huMab4D5-8 and DM1, one skilled in the art at the time the present invention was made would have expected huMab4D5-8 to oppose and possibly prevent the effects of DM1, if those two agents were linked together in an immunoconjugate. Indeed, recent data from my laboratory here at Genentech demonstrate that huMab4D5-8 retains all of its biological mechanisms of action, including its cytostatic activity, when conjugated to DM1.

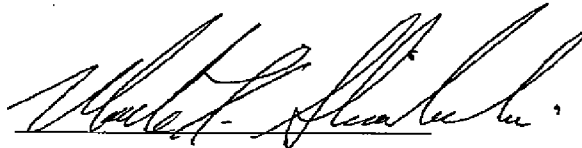
13. Moreover, before the priority date, the utility of immunoconjugates was often limited due to the expression of the targeted antigen on normal as well as cancerous cells, even where the antigen was expressed at higher levels on cancerous cells relative to normal cells. For example, Trail and Bianchi cautioned that “[i]t is therefore necessary to balance the relative selectivity of the MAb [i.e., the selectivity of the targeting monoclonal antibody for cancerous cells over normal cells] with the potency of the agent delivered.” (See Trail and Bianchi, *Current Opinion in Immunology* 11:584-588, 1999 – **Exhibit H**, page 584, col. 1, para. 2.) If that balance is not achieved, e.g., if a potent cytotoxic agent exerts its effect on too many normal cells, then toxicity may result. Trail and Bianchi further cautioned that “[t]he use of extremely toxic drugs requires careful MAb [monoclonal antibody] selection as *even low levels of expression of the targeted antigen by normal cells may lead to significant toxicity.*” (**Exhibit H**, page 585, col. 1, para. 1, emphasis added.)

14. Accordingly, even if huMAb4D5-8 had not negated the cytotoxicity of DM1 (an outcome which would not have been expected), it would nonetheless have been unpredictable as to whether a huMAb4D5-8-DM1 immunconjugate would have achieved an appropriate balance between antibody selectivity (i.e., for cancerous cells versus normal cells) and potency of the cytotoxic agent. HER2 is expressed on normal cells as well as being overexpressed on certain breast cancer cells and other cancer cells. Therefore, even if DM1 exerted its cytotoxicity notwithstanding its being conjugated to huMAb4D5-8, it would have been unpredictable whether such an immunconjugate would have been unacceptably toxic due to delivery of DM1 to normal cells expressing HER2. The present application addresses this unpredictability, reporting that “*HERCEPTIN®-DM1 does not kill normal human cells, indicating a selective activity,*” based on studies in which “[t]he effect of various concentrations of HERCEPTIN®-DM1 on hummman [sic, human] mammary epithelial cells, human hepatocytes and human small airway epithelial cells was investigated.” (Application at pages 65-66, para. [0229], emphasis added.) I have personal knowledge of those studies, and I confirm that the human cells used in those studies expressed HER2 at levels similar to those found in non-HER2-amplified, non-HER2-overexpressing breast cancers and breast cancer cell lines, consistent with the observations of Press et al. (**Exhibit B**). At the time the invention was made, it would have been expected that the level of HER2 expression on normal cells would lead to unacceptable cytotoxic side-effects for such an immunconjugate. However, surprisingly, we found that this was not the case. Moreover, the present application reports extensive dose-response studies in a novel mouse model for HER2 non-responsive breast cancer, concluding that “[t]he fact that the effect of HERCEPTIN®-DM1 is dose-dependent suggests that in an actual clinical setting, the strategy is likely to provide a considerable maneuver of doses to achieve the best anti-tumor activity.” (See application at page 69, para. [0237].) Those findings enhanced the likelihood that a therapeutic window could be achieved and that toxicity in a clinical setting could be managed. Thus, even if huMAb4D5-8 did not negate the cytotoxicity of DM1 (an outcome which would not have been predicted), the present application addresses the unpredictability in the art as to whether a huMAb4D5-8-DM1 immunconjugate would have struck an appropriate balance between antibody selectivity and potency of the cytotoxic agent.

15. On the basis of the explanations set forth in this Declaration and the enclosed evidence, it is my considered scientific opinion that at the time the present invention was made one of ordinary skill in the art would have expected huMAb4D5-8 to oppose the action of a maytansinoid such as DM1 and therefore would not have been motivated to select huMAb4D5-8 as a humanized anti-HER2 antibody for conjugation to a maytansinoid, nor would it have been at all predictable that a huMAb4D5-8--maytansinoid conjugate would effectively and safely treat HER2 overexpressing cancer with a reasonable expectation of success.

16. I declare further that all statements made in this Declaration of my own knowledge are true and that all statements made on information and belief are believed to be true and further, that these statements are made with the knowledge that willful statements and the like so made are punishable by fine or imprisonment, or both, under Section 1001 of Title 18 of the United States Code and that such willful false statements may jeopardize the validity of the application or any patent granted thereon.

Dated: 30 June 2010



MARK X. SLIWKOWSKI, Ph.D.



# **EXHIBIT A**

MARK X. SLIWKOWSKI

Genentech, Inc.  
Research Oncology  
1 DNA Way, MS 72 Room 10.489  
South San Francisco, CA 94080  
650/225-1247 Ph.  
650/438-4759 Cell  
650/225-5770 Fax  
marks@gene.com

Home  
42 Oak Creek Lane  
San Carlos, CA 94070  
650/364-8217

EDUCATION

National Institutes of Health (1982-1985)  
National Heart, Lung and Blood Institute, Laboratory of Biochemistry  
Staff Fellow with Dr. Thressa C. Stadtman

North Carolina State University (1978-1981)  
Ph.D. in Biochemistry with minor in Physical Chemistry  
Advisor: Dr. Harold E. Swaisgood

University of Delaware (1972-1976)  
B.S. in Animal Science and Agricultural Biochemistry (Pre-Vet)

EXPERIENCE

GENENTECH, INC.

Staff Scientist

2002-present

**HER3-EGFR Dual Antibody Project (DAF) (2006-present)** Late Stage Research Team Leader responsible for moving project into Early Clinical Development (ECD). Current member of ECD core team.

**Armed Antibody Program (2003-present)** Lead multi-disciplinary research and development team efforts to assess arming monoclonal with cytotoxic agents. Served as the major liaison in coordinating collaboration with outside companies.

**Trastuzumab-DM1 Program (2004)** Research team leader and early development team leader. Considered prototype for armed antibody platform. Current member of T-DM1 core team. Participate in development program.

Director

2003-2008

Formed Translational Oncology Department. Managed expansive growth from 2004-2007, including small molecule expertise. Managed Director of Assay & Automation Technology from 2005-2007.

Senior Scientist

1991-2001

**Heregulin (1991-1996)** Participated in the initial characterization of heregulin. Helped define a role for HER2/ErbB2 as a co-receptor with HER3, HER4 and EGFR.

**HERCEPTIN® (1993-present)** Member of the core project team throughout Phase II and Phase III clinical development. Responsibilities included studies on the development of an *in vitro* diagnostic assay, mechanism of action, mechanism of cardiotoxicity, coordinating biological and biochemical assays, obtaining data to support new clinical indications and designing studies to test novel chemotherapeutic combinations. Also responsible for managing all extramural research activities.

**Pertuzumab (1997-present)** As part of our heregulin studies, recognized the potential of blocking ligand-activated HER2 as an anti-cancer therapy. Led research and developmental research teams. Participated on developmental assessment team that resulted in rhuMAb 2C4/pertuzumab being moved into development in August 2000. Helped facilitate Roche decision to co-develop rhuMAb 2C4. Currently lead research effort and serve on pertuzumab core team.

**Tarceva®(2000-2007)** One of several Genentech employees that encouraged Business Development to pursue in-licensing OSI-774. Participated in due diligence team. Led research effort on Tarceva and serve on Tarceva core team.

**Triton Biosciences, Inc. (Berlex Biosciences, Inc.)**

**Staff Scientist** 1990 - 1991  
Initiated a program for the identification and isolation of ligands for receptor tyrosine kinases. Participated in project to establish structure-activity relationship for TGF $\alpha$ . Supervised protein and peptide chemistry laboratories consisting of 2 scientists and 5 research associates.

**Senior Research Scientist** 1987 - 1990  
Project Leader for development stage of HTLV-1 program. (Interdisciplinary team consisting of 3 scientists and 8 research associates.) Developed folding procedure for TGF $\alpha$ . Collaborated extensively with Immunology group on projects involving differentiation and cytotoxicity.

**Research Scientist** 1985 - 1987  
One of the first bench scientists hired. Established protein chemistry laboratory purified recombinant retroviral proteins for development of diagnostic viral immunoassay.

**NIH Postdoctoral Position** 1982 - 1985  
Studied mechanisms by which selenium is incorporated into bacterial proteins. Purified several selenium-containing proteins and gained extensive experience in peptide mapping.

**AWARDS**

Genentech Inc. Outstanding Commercial Collaborator Award, 2008  
North Carolina State University Outstanding Alumni Award, 2008  
Genentech Inc. Most Commercially Significant Patent Award, 2007 (Patent No. 7,097,840)  
Genentech Inc. Most Commercially Significant Patent Award, 2006 (Patent No. 6,949,245)  
Industry Scientist of the Year, Pharmaceutical Achievement Award, 2005  
Triton R&D Award, 1989  
Industrial Initiative for Science and Math Education Award, 1989  
American Society of Biological Chemistry Travel Grant, 1985  
Phi Lambda Upsilon Chemistry Honor Society, 1981  
Gamma Delta Sigma Agricultural Honor Society, 1981

Outstanding Graduate Student Teaching Award , 1979

**PROFESSIONAL AFFILIATIONS**

American Society of Clinical Oncology  
American Association for Cancer Research  
American Society for Biochemistry and Molecular Biology

**INVITED PRESENTATIONS (SINCE 2006)**

Van Andel Research Institute, Grand Rapids, June 2009  
Keystone Symposium, Whistler, BC, March 2009  
European Antibody Congress, Geneva, December 2008  
Istituto Nazionale Tumori of Milan, April 2008  
Oncology Leaders' Forum Boston, November 2007  
ASTRO Los Angeles, October 2007  
FASEB Symposium, Tucson, August 2007  
ESMO Congress, Istanbul, Turkey October 2006  
Congress of the International Assoc. for Breast Cancer Research, Montreal September 2006  
SPORE Breast Cancer Workshop, Baltimore, July 2006  
Stanford University May 2006  
Chair of New Biological Agents on the Horizon AACR Annual Meeting, Washington DC, April 2006  
Conference on Obstacles to Translational Medicine, San Francisco, March 2006  
Vanderbilt University, January 2006

**PEER REVIEW ACTIVITIES**

Department of Defense Breast Cancer Program  
*Nature* ad hoc  
*Oncogene* ad hoc  
*Cancer Research* ad hoc  
*Clinical Cancer Research* ad hoc  
*Cancer Cell* ad hoc

## PUBLICATIONS

1. Yao E, Zhou W, Lee-Hoeflich ST, Truong T, Haverty PM, Eastham-Anderson J, Lewin-Koh N, Gunter B, Belvin M, Murray LJ, Friedman LS, Sliwkowski MX, Hoeflich KP. Suppression of HER2/HER3-mediated growth of breast cancer cells with combinations of GDC-0941 PI3K inhibitor, trastuzumab, and pertuzumab. *Clin Cancer Res* 2009;15:4147-56.
2. Polson AG, Sliwkowski MX. Toward an effective targeted chemotherapy for multiple myeloma. *Clin Cancer Res* 2009;15:3906-7.
3. Makhija S, Amler LC, Glenn D, Ueland FR, Gold M, Dizon DS, Paton V, Lin C-Y, Januario T, Ng K, Strauss A, Kelsey SM, Sliwkowski MX, Matulonis U. Clinical activity of gemcitabine plus pertuzumab in platinum-resistant ovarian cancer, fallopian tube, or primary peritoneal cancer: low mRNA expression of the HER2-coreceptor HER3 may be predictive of pertuzumab activity. *J Clin Oncol* 2009;in press.
4. Krop IE, Beeram M, Modi S, Holden SN, Yu W, Girish S, Tibbitts J, Yi J-H, Sliwkowski MX, Jacobson FS, Lutzker SG, Burris HA. A Phase I Study of Trastuzumab-DM1, HER2 Antibody-Drug Conjugate, Given Every 3 Weeks to Patients with HER2+ Metastatic Breast Cancer *J Clin Oncol* 2009; to be submitted.
5. Junttila TT, Parsons K, Olsson C, Lu Y, Xin Y, Theriault J, Meng G, Totpal K, Kelley RF, Sliwkowski MX. Superior in vivo efficacy of afucosylated trastuzumab in the treatment of HER2 amplified breast cancer. to be submitted 2009.
6. Junttila TT, Akita RW, Parsons K, Fields C, Lewis Phillips GD, Friedman LS, Sampath D, Sliwkowski MX. Ligand-independent HER2/HER3/PI3K complex is disrupted by trastuzumab and is effectively inhibited by the PI3K inhibitor GDC-0941. *Cancer Cell* 2009;15:429-40.
7. Hollmen M, Maatta JA, Bald L, Sliwkowski MX, Elenius K. Suppression of breast cancer cell growth by a monoclonal antibody targeting cleavable ErbB4 isoforms. *Oncogene* 2009;28:1309-19.
8. Lewis Phillips GD, Li G, Dugger DL, Crocker LM, Parsons KL, Mai E, Blattler WA, Lambert JM, Chari RV, Lutz RJ, Wong WL, Jacobson FS, Koeppen H, Schwall RH, Kenkare-Mitra SR, Spencer SD, Sliwkowski MX. Targeting HER2-positive breast cancer with trastuzumab-DM1, an antibody-cytotoxic drug conjugate. *Cancer Res* 2008;68:9280-90.
9. Lee-Hoeflich ST, Crocker L, Yao E, Pham T, Munroe X, Hoeflich KP, Sliwkowski MX, Stern HM. A central role for HER3 in HER2-amplified breast cancer: implications for targeted therapy. *Cancer Res* 2008;68:5878-87.
10. Junutula JR, Raab H, Clark S, Bhakta S, Leipold DD, Weir S, Chen Y, Simpson M, Tsai SP, Dennis MS, Lu Y, Meng YG, Ng C, Yang J, Lee CC, Duenas E, Gorrell J, Katta V, Kim A, McDorman K, Flagella K, Venook R, Ross S, Spencer SD, Lee Wong W, Lowman HB, Vandlen R, Sliwkowski MX, Scheller RH, Polakis P, Mallet W. Site-specific conjugation of a cytotoxic drug to an antibody improves the therapeutic index. *Nat Biotechnol* 2008;26:925-32.
11. Carey KD, Garton AJ, Romero MS, Kahler J, Thomson S, Ross S, Park F, Haley JD, Gibson N, Sliwkowski MX. Kinetic analysis of epidermal growth factor receptor somatic mutant proteins shows increased sensitivity to the epidermal growth factor receptor tyrosine kinase inhibitor, erlotinib. *Cancer Res* 2006;66:8163-71.

12. Adams CW, Allison DE, Flagella K, Presta L, Clarke J, Dybdal N, McKeever K, Sliwkowski MX. Humanization of a recombinant monoclonal antibody to produce a therapeutic HER dimerization inhibitor, pertuzumab. *Cancer Immunol Immunother* 2006;55:717-27.
13. Agus DB, Gordon MS, Taylor C, Natale RB, Karlan B, Mendelson DS, Press MF, Allison DE, Sliwkowski MX, Lieberman G, Kelsey SM, Fyfe G. Phase I clinical study of pertuzumab, a novel HER dimerization inhibitor, in patients with advanced cancer. *J Clin Oncol* 2005;23:2534-43.
14. Jackson JG, St Clair P, Sliwkowski MX, Brattain MG. Blockade of epidermal growth factor- or heregulin-dependent ErbB2 activation with the anti-ErbB2 monoclonal antibody 2C4 has divergent downstream signaling and growth effects. *Cancer Res* 2004;64:2601-9.
15. Franklin MC, Carey KD, Vajdos FF, Leahy DJ, de Vos AM, Sliwkowski MX. Insights into ErbB signaling from the structure of the ErbB2-pertuzumab complex. *Cancer Cell* 2004;5:317-28.
16. Austin CD, De Maziere AM, Pisacane PI, van Dijk SM, Eigenbrot C, Sliwkowski MX, Klumperman J, Scheller RH. Endocytosis and sorting of ErbB2 and the site of action of cancer therapeutics trastuzumab and geldanamycin. *Mol Biol Cell* 2004;15:5268-82.
17. Sliwkowski MX. Ready to partner. *Nat Struct Biol* 2003;10:158-9.
18. Miller K, Meng G, Liu J, Hurst A, Hsei V, Wong WL, Ekert R, Lawrence D, Sherwood S, DeForge L, Gaudreault J, Keller G, Sliwkowski M, Ashkenazi A, Presta L. Design, construction, and in vitro analyses of multivalent antibodies. *J Immunol* 2003;170:4854-61.
19. Burgess AW, Cho HS, Eigenbrot C, Ferguson KM, Garrett TP, Leahy DJ, Lemmon MA, Sliwkowski MX, Ward CW, Yokoyama S. An open-and-shut case? Recent insights into the activation of EGF/ErbB receptors. *Mol Cell* 2003;12:541-52.
20. Akita RW, Sliwkowski MX. Preclinical studies with Erlotinib (Tarceva). *Semin Oncol* 2003;30:15-24.
21. Stamos J, Sliwkowski MX, Eigenbrot C. Structure of the epidermal growth factor receptor kinase domain alone and in complex with a 4-anilinoquinazoline inhibitor. *J Biol Chem* 2002;277:46265-72.
22. Ranson M, Sliwkowski MX. Perspectives on anti-HER monoclonal antibodies. *Oncology* 2002;63 Suppl 1:17-24.
23. Penuel E, Akita RW, Sliwkowski MX. Identification of a region within the ErbB2/HER2 intracellular domain that is necessary for ligand-independent association. *J Biol Chem* 2002;277:28468-73.
24. Agus DB, Akita RW, Fox WD, Lewis GD, Higgins B, Pisacane PI, Lofgren JA, Tindell C, Evans DP, Maiese K, Scher HI, Sliwkowski MX. Targeting ligand-activated ErbB2 signaling inhibits breast and prostate tumor growth. *Cancer Cell* 2002;2:127-37.
25. Yarden Y, Sliwkowski MX. Untangling the ErbB signalling network. *Nat Rev Mol Cell Biol* 2001;2:127-37.
26. Penuel E, Schaefer G, Akita RW, Sliwkowski MX. Structural requirements for ErbB2 transactivation. *Semin Oncol* 2001;28:36-42.
27. O'Shea S, Johnson K, Clark R, Sliwkowski MX, Erickson SL. Effects of in vivo heregulin beta1 treatment in wild-type and ErbB gene-targeted mice depend on receptor levels and pregnancy. *Am J Pathol* 2001;158:1871-80.

28. Mann M, Sheng H, Shao J, Williams CS, Pisacane PI, Sliwkowski MX, DuBois RN. Targeting cyclooxygenase 2 and HER-2/neu pathways inhibits colorectal carcinoma growth. *Gastroenterology* 2001;120:1713-9.
29. Lee H, Akita RW, Sliwkowski MX, Maihle NJ. A naturally occurring secreted human ErbB3 receptor isoform inhibits heregulin-stimulated activation of ErbB2, ErbB3, and ErbB4. *Cancer Res* 2001;61:4467-73.
30. Koeppen HK, Wright BD, Burt AD, Quirke P, McNicol AM, Dybdal NO, Sliwkowski MX, Hillan KJ. Overexpression of HER2/neu in solid tumours: an immunohistochemical survey. *Histopathology* 2001;38:96-104.
31. Riley JK, Sliwkowski MX. CD20: a gene in search of a function. *Semin Oncol* 2000;27:17-24.
32. Patel NV, Acarregui MJ, Snyder JM, Klein JM, Sliwkowski MX, Kern JA. Neuregulin-1 and human epidermal growth factor receptors 2 and 3 play a role in human lung development in vitro. *Am J Respir Cell Mol Biol* 2000;22:432-40.
33. Kurokawa H, Lenferink AE, Simpson JF, Pisacane PI, Sliwkowski MX, Forbes JT, Arteaga CL. Inhibition of HER2/neu (erbB-2) and mitogen-activated protein kinases enhances tamoxifen action against HER2-overexpressing, tamoxifen-resistant breast cancer cells. *Cancer Res* 2000;60:5887-94.
34. Carter P, Fendly BM, Lewis GD, Sliwkowski MX. Development of herceptin. *Breast Dis* 2000;11:103-11.
35. Agus DB, Akita RW, Fox WD, Lofgren JA, Higgins B, Maiese K, Scher HI, Sliwkowski MX. A potential role for activated HER-2 in prostate cancer. *Semin Oncol* 2000;27:76-83; discussion 92-100.
36. Zheng JL, Frantz G, Lewis AK, Sliwkowski M, Gao WQ. Heregulin enhances regenerative proliferation in postnatal rat utricular sensory epithelium after ototoxic damage. *J Neurocytol* 1999;28:901-12.
37. Sundaresan S, Penuel E, Sliwkowski MX. The biology of human epidermal growth factor receptor 2. *Curr Oncol Rep* 1999;1:16-22.
38. Sliwkowski MX, Lofgren JA, Lewis GD, Hotaling TE, Fendly BM, Fox JA. Nonclinical studies addressing the mechanism of action of trastuzumab (Herceptin). *Semin Oncol* 1999;26:60-70.
39. Schaefer G, Akita RW, Sliwkowski MX. A discrete three-amino acid segment (LVI) at the C-terminal end of kinase-impaired ErbB3 is required for transactivation of ErbB2. *J Biol Chem* 1999;274:859-66.
40. Pegram M, Hsu S, Lewis G, Pietras R, Beryt M, Sliwkowski M, Coombs D, Baly D, Kabbinnar F, Slamon D. Inhibitory effects of combinations of HER-2/neu antibody and chemotherapeutic agents used for treatment of human breast cancers. *Oncogene* 1999;18:2241-51.
41. Kern JA, Wakita R, Sliwkowski MX. Neuregulin receptor-mediated gene transfer by human epidermal growth factor receptor 2-targeted antibodies and neuregulin-1. *Cancer Gene Ther* 1999;6:537-45.
42. Jones JT, Akita RW, Sliwkowski MX. Binding specificities and affinities of egf domains for ErbB receptors. *FEBS Lett* 1999;447:227-31.
43. Aguilar Z, Akita RW, Finn RS, Ramos BL, Pegram MD, Kabbinnar FF, Pietras RJ, Pisacane P, Sliwkowski MX, Slamon DJ. Biologic effects of heregulin/neu differentiation factor on normal and malignant human breast and ovarian epithelial cells. *Oncogene* 1999;18:6050-62.

44. Sundaresan S, Roberts PE, King KL, Sliwkowski MX, Mather JP. Biological response to ErbB ligands in nontransformed cell lines correlates with a specific pattern of receptor expression. *Endocrinology* 1998;139:4756-64.
45. Jones JT, Ballinger MD, Pisacane PI, Lofgren JA, Fitzpatrick VD, Fairbrother WJ, Wells JA, Sliwkowski MX. Binding interaction of the heregulinbeta egf domain with ErbB3 and ErbB4 receptors assessed by alanine scanning mutagenesis. *J Biol Chem* 1998;273:11667-74.
46. Fitzpatrick VD, Pisacane PI, Vandlen RL, Sliwkowski MX. Formation of a high affinity heregulin binding site using the soluble extracellular domains of ErbB2 with ErbB3 or ErbB4. *FEBS Lett* 1998;431:102-6.
47. Fairbrother WJ, Liu J, Pisacane PI, Sliwkowski MX, Palmer AG, 3rd. Backbone dynamics of the EGF-like domain of heregulin-alpha. *J Mol Biol* 1998;279:1149-61.
48. Ballinger MD, Jones JT, Lofgren JA, Fairbrother WJ, Akita RW, Sliwkowski MX, Wells JA. Selection of heregulin variants having higher affinity for the ErbB3 receptor by monovalent phage display. *J Biol Chem* 1998;273:11675-84.
49. Zrihan-Licht S, Lim J, Keydar I, Sliwkowski MX, Groopman JE, Avraham H. Association of csk-homologous kinase (CHK) (formerly MATK) with HER-2/ErbB-2 in breast cancer cells. *J Biol Chem* 1997;272:1856-63.
50. Zhang D, Sliwkowski MX, Mark M, Frantz G, Akita R, Sun Y, Hillan K, Crowley C, Brush J, Godowski PJ. Neuregulin-3 (NRG3): a novel neural tissue-enriched protein that binds and activates ErbB4. *Proc Natl Acad Sci U S A* 1997;94:9562-7.
51. Westphal M, Meima L, Szonyi E, Lofgren J, Meissner H, Hamel W, Nikolics K, Sliwkowski MX. Heregulins and the ErbB-2/3/4 receptors in gliomas. *J Neurooncol* 1997;35:335-46.
52. Schaefer G, Fitzpatrick VD, Sliwkowski MX. Gamma-heregulin: a novel heregulin isoform that is an autocrine growth factor for the human breast cancer cell line, MDA-MB-175. *Oncogene* 1997;15:1385-94.
53. Sadick MD, Sliwkowski MX, Nuijens A, Bald L, Chiang N, Lofgren JA, Wong WL. Analysis of heregulin-induced ErbB2 phosphorylation with a high-throughput Kinase receptor activation enzyme-linked immunosorbant assay. *Anal Biochem* 1996;235:207-14.
54. Mincione G, Bianco C, Kannan S, Colletta G, Ciardiello F, Sliwkowski M, Yarden Y, Normanno N, Pramaggiore A, Kim N, Salomon DS. Enhanced expression of heregulin in c-erb B-2 and c-Ha-ras transformed mouse and human mammary epithelial cells. *J Cell Biochem* 1996;60:437-46.
55. Li W, Park JW, Nuijens A, Sliwkowski MX, Keller GA. Heregulin is rapidly translocated to the nucleus and its transport is correlated with c-myc induction in breast cancer cells. *Oncogene* 1996;12:2473-7.
56. Li RH, Sliwkowski MX, Lo J, Mather JP. Establishment of Schwann cell lines from normal adult and embryonic rat dorsal root ganglia. *J Neurosci Methods* 1996;67:57-69.
57. Li R, Chen J, Hammonds G, Phillips H, Armanini M, Wood P, Bunge R, Godowski PJ, Sliwkowski MX, Mather JP. Identification of Gas6 as a growth factor for human Schwann cells. *J Neurosci* 1996;16:2012-9.



58. Lewis GD, Lofgren JA, McMurtrey AE, Nuijens A, Fendly BM, Bauer KD, Sliwkowski MX. Growth regulation of human breast and ovarian tumor cells by heregulin: Evidence for the requirement of ErbB2 as a critical component in mediating heregulin responsiveness. *Cancer Res* 1996;56:1457-65.
59. Jacobsen NE, Abadi N, Sliwkowski MX, Reilly D, Skelton NJ, Fairbrother WJ. High-resolution solution structure of the EGF-like domain of heregulin-alpha. *Biochemistry* 1996;35:3402-17.
60. Carver RS, Sliwkowski MX, Sitaric S, Russell WE. Insulin regulates heregulin binding and ErbB3 expression in rat hepatocytes. *J Biol Chem* 1996;271:13491-6.
61. Pietras RJ, Arboleda J, Reese DM, Wongvipat N, Pegram MD, Ramos L, Gorman CM, Parker MG, Sliwkowski MX, Slamon DJ. HER-2 tyrosine kinase pathway targets estrogen receptor and promotes hormone-independent growth in human breast cancer cells. *Oncogene* 1995;10:2435-46.
62. Morrissey TK, Levi AD, Nuijens A, Sliwkowski MX, Bunge RP. Axon-induced mitogenesis of human Schwann cells involves heregulin and p185erbB2. *Proc Natl Acad Sci U S A* 1995;92:1431-5.
63. Levi AD, Bunge RP, Lofgren JA, Meima L, Hefti F, Nikolics K, Sliwkowski MX. The influence of heregulins on human Schwann cell proliferation. *J Neurosci* 1995;15:1329-40.
64. Chu GC, Moscoso LM, Sliwkowski MX, Merlie JP. Regulation of the acetylcholine receptor epsilon subunit gene by recombinant ARIA: an in vitro model for transsynaptic gene regulation. *Neuron* 1995;14:329-39.
65. Sliwkowski MX, Schaefer G, Akita RW, Lofgren JA, Fitzpatrick VD, Nuijens A, Fendly BM, Cerione RA, Vandlen RL, Carraway KL, 3rd. Coexpression of erbB2 and erbB3 proteins reconstitutes a high affinity receptor for heregulin. *J Biol Chem* 1994;269:14661-5.
66. Groskreutz DJ, Sliwkowski MX, Gorman CM. Genetically engineered proinsulin constitutively processed and secreted as mature, active insulin. *J Biol Chem* 1994;269:6241-5.
67. Carraway KL, 3rd, Sliwkowski MX, Akita R, Platko JV, Guy PM, Nuijens A, Diamonti AJ, Vandlen RL, Cantley LC, Cerione RA. The erbB3 gene product is a receptor for heregulin. *J Biol Chem* 1994;269:14303-6.
68. Press MF, Pike MC, Chazin VR, Hung G, Udove JA, Markowicz M, Danyluk J, Godolphin W, Sliwkowski M, Akita R, et al. Her-2/neu expression in node-negative breast cancer: direct tissue quantitation by computerized image analysis and association of overexpression with increased risk of recurrent disease. *Cancer Res* 1993;53:4960-70.
69. Holmes WE, Sliwkowski MX, Akita RW, Henzel WJ, Lee J, Park JW, Yansura D, Abadi N, Raab H, Lewis GD, et al. Identification of heregulin, a specific activator of p185erbB2. *Science* 1992;256:1205-10.
70. Coates SR, Harris AJ, Parkes DL, Smith CM, Liu HL, Akita RW, Ferrer MM, Sampson EK, Brandis JW, Sliwkowski MX. Serological evaluation of Escherichia coli-expressed human T-cell leukemia virus type I env, gag p24, and tax proteins. *J Clin Microbiol* 1990;28:1139-42.
71. Ehrlich GD, Glaser JB, Abbott MA, Slamon DJ, Keith D, Sliwkowski M, Brandis J, Keitelman E, Teramoto Y, Papsidero L, et al. Detection of anti-HTLV-I Tax antibodies in HTLV-I enzyme-linked immunosorbent assay-negative individuals. *Blood* 1989;74:1066-72.

72. Sliwkowski MX, Stadtman TC. Selenoprotein A of the clostridial glycine reductase complex: purification and amino acid sequence of the selenocysteine-containing peptide. *Proc Natl Acad Sci U S A* 1988;85:368-71.
73. Sliwkowski MX, Stadtman TC. Selenium-dependent glycine reductase: differences in physicochemical properties and biological activities of selenoprotein A components isolated from *Clostridium sticklandii* and *Clostridium purinolyticum*. *Biofactors* 1988;1:293-6.
74. Sliwkowski MX, Swaisgood HE. Assay of enzyme-catalyzed oxygen-dependent disulfide bond formation. *Methods Enzymol* 1987;143:119-23.
75. Sliwkowski MX, Stadtman TC. Purification and immunological studies of selenoprotein A of the clostridial glycine reductase complex. *J Biol Chem* 1987;262:4899-904.
76. Sliwkowski MX, Stadtman TC. Incorporation and distribution of selenium into thiolase from *Clostridium kluyveri*. *J Biol Chem* 1985;260:3140-4.
77. Sliwkowski MX, Levine RL. Labeling of cysteine-containing peptides with 2-nitro-5-thiobenzoic acid. *Anal Biochem* 1985;147:369-73.
78. Hartmanis MG, Sliwkowski MX. Selenomethionine-containing thiolase and 3-hydroxybutyryl-CoA dehydrogenase from *Clostridium kluyveri*. *Curr Top Cell Regul* 1985;27:479-86.
79. Sliwkowski MX, Swaisgood HE, Clare DA, Horton HR. Kinetic mechanism and specificity of bovine milk sulphhydryl oxidase. *Biochem J* 1984;220:51-5.
80. Sliwkowski MX, Hartmanis MG. Simultaneous single-step purification of thiolase and NADP-dependent 3-hydroxybutyryl-CoA dehydrogenase from *Clostridium kluyveri*. *Anal Biochem* 1984;141:344-7.
81. Sliwkowski MX. Characterization of selenomethionine in proteins. *Methods Enzymol* 1984;107:620-3.
82. Sliwkowski MX, Sliwkowski MB, Horton HR, Swaisgood HE. Resolution of sulphhydryl oxidase from gamma-glutamyltransferase in bovine milk by covalent chromatography on cysteinylsuccinamidopropyl-glass. *Biochem J* 1983;209:731-9.
83. Sliwkowski MB, Sliwkowski MX, Swisgood HE, Horton HR. Nonidentity of sulphhydryl oxidase and gama-glutamyltransferase in bovine milk. *Arch Biochem Biophys* 1981;211:731-7.
84. Janolino VG, Sliwkowski MX, Swaisgood HE, Horton HR. Catalytic effect of sulphhydryl oxidase on the formation of three-dimensional structure in chymotrypsinogen A. *Arch Biochem Biophys* 1978;191:269-77.

#### ISSUED PATENTS

1. Akita, R. and Sliwkowski, M.X. US Patent #5968511, "ErbB3 antibodies," March 25<sup>th</sup>, 1997.
2. Akita, R. and Sliwkowski, M.X. US Patent #7285649, "ErbB3 antibodies," April 4<sup>th</sup>, 2001.

3. Schaefer, G. M. and Sliwowski, M.X. US Patent #6096873, "Gamma-Heregulin," July 10<sup>th</sup>, 1997.
4. Schaefer, G.M. and Sliwowski, M.X. US Patent #6500941, "Gamma-Heregulin," February 28<sup>th</sup>, 2000.
5. Schaefer, G.M. and Sliwowski, M.X. US Patent #6916624, "Gamma-Heregulin," July 12<sup>th</sup>, 2005.
6. Ballinger, M.D., Fairbrother, W.J., Jones, J.T., Sliwowski, M.X. and Wells, J.A. US Patent #6387638, "Heregulin Variants," July 17<sup>th</sup>, 1998.
7. Ballinger, M.D., Fairbrother, W.J., Jones, J.T., Sliwowski, M.X. and Wells, J.A., US Patent #7063961, "Heregulin Variants," February 22<sup>nd</sup>, 2002.
8. Ballinger, M.D., Fairbrother, W.J., Jones, J.T., Sliwowski, M.X. and Wells, J.A., US Patent #61365558, "Heregulin Variants," February 9<sup>th</sup>, 1998.
9. Fitzpatrick, V.D., Sliwowski, M.X. and Vandlen, R.L., US Patent #6696290, "ErbB2 and ErbB4 Chimeric Heteromultimeric Adhesins," March 12<sup>th</sup>, 1999.
10. Kern, J.A. and Sliwowski, M.X., US Patent #7153828, "Use of Heregulin as a Growth Factor," December 26<sup>th</sup>, 2006.
11. Cohen, R.L., Gardiner, M.B., Sliwowski, M.X. and Stelzer, G.T., US Patent #6573043, "Tissue Analysis and Kits Therefore," October 1998.
12. Cohen, R.L., Gardiner, M.B., Sliwowski, M.X. and Stelzer, G.T., US Patent #6905830, "Tissue Analysis and Kits Therefore," January 23<sup>rd</sup>, 2003.
13. Cohen, R.L., Gardiner, M.B., Sliwowski, M.X. and Stelzer, G.T., US Patent #7129051, "Tissue Analysis and Kits Therefore," October 29<sup>th</sup>, 2004.
14. Sliwowski, M.X., US Patent #6949245, "Humanized Anti-ErbB2 Antibodies and Treatment with Anti-ErbB2 Antibodies," June 23<sup>rd</sup>, 2000.
15. Agus, D.B., Scher, H.I. and Sliwowski, M.X., US Patent #7041292, "Treating Prostrate Cancer with Anti-ErbB2 Antibodies," June 23<sup>rd</sup>, 2000.
16. Blattler, W., Erickson, S., Schwall, R. and Sliwowski, M.X., US Patent #7097840, "Methods of Treatment Using Anti-ErbB Antibody Maytansinoid Conjugates," March 16<sup>th</sup>, 2001.
17. Cohen, R.L., Gardiner, M.B., Sliwowski, M.X. and Stelzer, G.T., US Patent #7344840, "Tissue Analysis and Kits Therefore," March 18<sup>th</sup>, 2008.
18. Cohen, R.L., Gardiner, M.B., Sliwowski, M.X. and Stelzer, G.T., US Patent #7468252, "Tissue Analysis and Kits Therefore," December 23<sup>rd</sup>, 2008.
19. Adams, C.W., Presta, L.G. and Sliwowski, M.X., US Patent #7537931, "Humanized Anti-ErbB2 Antibodies and Treatment with Anti-ErbB2 Antibodies," May 5<sup>th</sup>, 2006.

20. Adams, C.W., Presta, L.G. and Sliwkowski, M.X., US Patent #7498030, "Humanized Anti-ErbB2 Antibodies and Treatment with Anti-ErbB2 Antibodies," March 3<sup>rd</sup>, 2009.
21. Adams, C.W., Presta, L.G. and Sliwkowski, M.X., US Patent #7501122, "Treatment with Anti-ErbB2 Antibody Combinations," March 10<sup>th</sup>, 2009.
22. Adams, C.W., Presta, L.G. and Sliwkowski, M.X., US Patent #7485302, "Treatment with Anti-ErbB2 Antibodies and Chemotherapeutic Agents," February 3<sup>rd</sup>, 2009.
23. Gerritsen, M.E. and Sliwkowski, M.X., US Patent #7332579, "Antibodies to Human ErbB4," February 19<sup>th</sup>, 2008.

#### PENDING PATENTS

1. Akita, R. and Sliwkowski, M.X., Appl. No. 11/943490, "Isolated Nucleic Acids, Vectors, and Host Cells Encoding ErbB3 Antibodies," November 20<sup>th</sup>, 2007.
2. Akita, R. and Sliwkowski, M.X., Appl. No. 11/534830, "Isolated Nucleic Acids, Vectors, and Host Cells Encoding ErbB3 Antibodies," September 25<sup>th</sup>, 2006.
3. Schaefer, G.M. and Sliwkowski, M.X., Appl. No. 12/168032, "Gamma-Heregulin," July 3<sup>rd</sup>, 2008.
4. Fitzpatrick, V.D., Sliwkowski, M.X. and Vandlen, R.L., Appl. No. 11/536354, "Chimeric Heteromultimeric Adhesins," September 28<sup>th</sup>, 2006.
5. Sliwkowski, M.X., Appl. No. 11/154465, "Treatment with Anti-ErbB2 Antibodies and EGFR-Targeted Drugs," June 16<sup>th</sup>, 2005.
6. Sliwkowski, M.X., Appl. No. 11/690691, "Treatment with Anti-ErbB2 Antibodies," March 23<sup>rd</sup>, 2007.
7. Kelsey, S.M. and Sliwkowski, M.X., Appl. No. 11/770441, "Treatment with Anti-ErbB2 Antibodies," June 28<sup>th</sup>, 2007.
8. Bossenmaier, B., Kelsey, S.M., Koll, H., Muller, H.J. and Sliwkowski, M.X., Appl. No. 10/619754, "Methods for Identifying Tumors That Are Responsive to Treatment with Anti-ErbB2 Antibodies," July 14<sup>th</sup>, 2003.
9. Brunetta, P.G. and Sliwkowski, M.X., Appl. No. 12/193582, "Therapy of Non-Malignant Diseases or Disorders with Anti-ErbB2 Antibodies," August 18<sup>th</sup>, 2008.
10. Ebens, A.J., Jacobson, F.S., Polakis, P., Schwall, R.H. and Sliwkowski, M.X., Appl. No. 11/141344, "Antibody Drug Conjugates and Methods," May 31<sup>st</sup>, 2005.
11. Kelsey, S.M. and Sliwkowski, M.X., Appl. No. 11/490438, "Combination Therapy of HER Expressing Tumors," July 19<sup>th</sup>, 2006.

12. Ballinger, M.D., Fairbrother, W.J., Jones, J.T., Sliwowski, M.X. and Wells, J.A., Appl. No. 11/347808, "Heregulin Variants," February 2<sup>nd</sup>, 2006.
13. Fitzpatrick, V.D., Sliwowski, M.X., and Vandlen, R. L., Appl. No. 10/746176, "ErbB2 and ErbB3 Chimeric Heteromultimeric Adhesins," December 22<sup>nd</sup>, 2003.
14. Cohen, R.L., Gardiner, M.B., Sliwowski, M.X. and Stelzer, G.T., Appl. No. 12/331178, "Tissue Analysis and Kits Therefore," December 9<sup>th</sup>, 2008.
15. Sliwowski, M.X., Appl. No. 12/247850, "Treating Prostate Cancer with Anti-ErbB2 Antibodies," October 8<sup>th</sup>, 2008.
16. Erickson, S., Schwall, R., Sliwowski, M.X., and Blattler W., Appl. No. 11/488545, "Methods of Treatment Using Anti-erbB Antibody-Maytansinoid Conjugates," July 27<sup>th</sup>, 2006.
17. Erickson, S., Schwall, R., Sliwowski, M.X., and Blattler W., Appl. No. 11/949351, "Methods of Treatment Using Anti-erbB Antibody-Maytansinoid Conjugates," December 3<sup>rd</sup>, 2007.
18. Gerritsen, M.E. and Sliwowski, M.X., Appl. No. 12/215200, "ErbB4-Antagonists," June 24<sup>th</sup>, 2008.
19. Ebens, A.J. Jr., Jacobson, F.S., Polakis, P., Schwall, R.H., Sliwowski, M.X., and Spencer, S.D., Appl. No. 12/326721, "Antibody Drug Conjugates and Methods," December 2<sup>nd</sup>, 2008.
20. Ebens, A.J. Jr., Jacobson, F.S., Polakis, P., Schwall, R.H., Sliwowski, M.X., and Spencer, S.D., Appl. No. 12/0528938, "Antibody Drug Conjugates and Methods," March 21, 2008.
21. Doronina, S.O., Senter, P.D., Ebens, A.J. Jr., Kline, T.B., Polakis, P., Sliwowski, M.X., and Spencer, S.D., Appl. No. 11/833954, "Monomethylvaline Compounds Capable of Conjugation to Ligands," August 3<sup>rd</sup>, 2007.
22. Doronina, S.O., Senter, P.D., Ebens, A.J. Jr., Kline, T.B., Polakis, P., Sliwowski, M.X., and Spencer, S.D., Appl. No. 11/833959, "Monomethylvaline Compounds Capable of Conjugation to Ligands," August 3<sup>rd</sup>, 2007.
23. Doronina, S.O., Senter, P.D., Ebens, A.J. Jr., Kline, T.B., Polakis, P., Sliwowski, M.X., and Spencer, S.D., Appl. No. 11/833961 "Monomethylvaline Compounds Capable of Conjugation to Ligands," August 3<sup>rd</sup>, 2007.
24. Doronina, S.O., Senter, P.D., Ebens, A.J. Jr., Kline, T.B., Polakis, P., Sliwowski, M.X., and Spencer, S.D., Appl. No. 11/833964, "Monomethylvaline Compounds Capable of Conjugation to Ligands," August 3<sup>rd</sup>, 2007.
25. Berry, L., Phillips, G., and Sliwowski, M.X., Appl. No. 12/400988, "Combinations of an Anti-HER2 Antibody-Drug Conjugate and Chemotherapeutic Agents, and Methods of Use," March 10<sup>th</sup>, 2009.

26. Cairns, B., Chen, R., Frantz, G., Hillan, K.J., Koeppen, H., Phillips, H.S., Polakis, P., Smith, V., Spencer, S.D., Williams, P.M., Wu, T.D., Zhang, Z., and Sliwkowski, M.X., Appl. No. 11/733861, "Compositions and Methods for Diagnosis and Treatment of Tumor," April 11<sup>th</sup>, 2007.
27. Sliwkowski, M.X. and Elenius, K., Appl. No. 61/117903, "Anti-HER4 Antibodies," November 25, 2008.
28. Schaefer, G.M. and Sliwkowski, M.X. Appl. No. 11/173893, "Gamma-Heregulin," July 1<sup>st</sup>, 2005.
29. Adams, C.W., Presta, L.G. and Sliwkowski, M.X., Appl. No. 11/044749, "Humanized Anti-ErbB2 Antibodies and Treatment with Anti-ErbB2 Antibodies," January 27<sup>th</sup>, 2005.

# **EXHIBIT B**

# Expression of the HER-2/*neu* proto-oncogene in normal human adult and fetal tissues

Michael F. Press<sup>1</sup>, Carlos Cordon-Cardo<sup>2</sup> and Dennis J. Slamon<sup>3</sup>

<sup>1</sup>Department of Pathology, University of Southern California, 2011 Zonal Avenue, Los Angeles, California 90033; <sup>2</sup>Department of Pathology, Memorial Sloan-Kettering Cancer Center, 1275 York Avenue, New York, New York 10021; <sup>3</sup>Division of Hematology and Oncology, Department of Medicine, UCLA Medical School, Los Angeles, California 90024, USA

The HER-2/*neu* proto-oncogene is homologous with, but distinct from, the epidermal growth factor receptor. Current evidence indicates that this gene is frequently amplified and/or overexpressed in some human breast and ovarian cancers and that these alterations may be clinically important; however, little is known about the expression pattern of the gene in normal tissues. Using immunohistochemistry and northern blot analyses to identify the HER-2/*neu* protein and transcript respectively, we have evaluated a variety of normal adult and fetal tissues for HER-2/*neu* expression. HER-2/*neu* protein was identified on cell membranes of epithelial cells in the gastro-intestinal, respiratory, reproductive, and urinary tract as well as in the skin, breast and placenta. Northern hybridization confirmed the presence of the 4.5 kb transcript encoding the protein in these tissues. The amount of HER-2/*neu* message and protein was generally higher in fetal tissues than in the corresponding normal adult tissues. HER-2/*neu* expression levels in these normal tissues were similar to the levels found in non-amplified, non-overexpressing breast cancers and breast cancer cell lines. Southern hybridization of extracted DNA showed that none of the normal tissues expressing HER-2/*neu* had amplification of the gene. These results confirm that HER-2/*neu* is normally a membrane constituent of a variety of epithelial cell types.

## Introduction

The *neu* oncogene was first isolated from DNA extracted from ethylnitrosourea-induced adrenal neuroglioblastomas of neonatal rats (Shih *et al.*, 1981). The oncogene was identified by its ability to function as a dominant transforming gene in NIH3T3 transfection assays. Since this gene was identified in DNA from neuroglioblastomas it was referred to as *neu* (Schechter *et al.*, 1984). Subsequently, three different groups independently identified the human homolog of this gene (Coussens *et al.*, 1985; Semba *et al.*, 1985; King, Kraus & Aaronson, 1985) and, because of homology to the human epidermal growth factor receptor (HER) and *c-erb-B* proto-oncogene, it was referred to as HER-2 (Coussens *et al.*, 1985) or *c-erbB-2* (Semba *et al.*, 1985). Recently, amplification and overexpression of the HER-2/*neu* gene was found to be associated with shortened disease-free and overall survival in women with node-positive breast cancer (Slamon *et al.*, 1987; 1989a, b). In addition, an association between overexpression and clinical outcome has been seen in some women with

node-negative breast cancer (Wright *et al.*, 1989; Ro *et al.*, 1989; Paik *et al.*, 1990). HER-2/*neu* amplification and overexpression have also been found in human ovarian carcinomas where the alteration is again associated with a shorter overall survival (Slamon *et al.*, 1989a, b). Amplification of this gene is consistently associated with overexpression of both the 4.5 kb messenger RNA encoding the gene and the p185 protein product. Several lines of experimental evidence indicate that alterations in HER-2/*neu* can play an important role in the pathogenesis of some animal tumors. Transgenic mice containing a mutated *neu* transgene driven by the mouse mammary tumor virus promoter consistently develop breast carcinoma (Muller *et al.*, 1988). Transfection and subsequent amplification/overexpression or overexpression alone of a normal HER-2/*neu* gene (Hudziak *et al.*, 1987; diFiore *et al.*, 1987) renders NIH3T3 cells more tumorigenic in nude mice. The HER-2/*neu* gene encodes a membrane protein with an extracellular domain, which makes it a candidate target for immunotherapeutic approaches against those cells expressing high levels of gene product. Experimental data using *neu*-transformed cell lines grown *in vitro* as well as in nude mice suggest that this type of approach may be feasible (Drebin *et al.*, 1985). To exploit these potential therapies in patients it is important to understand the distribution and relative expression levels of HER-2/*neu* in normal tissues. Little information is currently available regarding this issue. This study describes the distribution of HER-2/*neu* expression in normal adult and fetal tissues and characterizes the expression levels.

## Results

HER-2/*neu* expression, in both fetal and adult tissues, was identified immunohistochemically on the membranes of epithelial cells (Table 1, Figures 1 and 2). This staining pattern was found throughout the gastro-intestinal, respiratory, urinary, and reproductive tracts, as well as the skin of fetal and adult specimens. Levels of expression were, in almost all instances, higher in fetal than in the corresponding adult tissues. Immunostaining of frozen, normal tissues ranged from barely detectable to, in a few specimens, moderate intensity (2+) (Table 1). Immunostaining in formalin-fixed, paraffin-embedded tissues was also seen on cell membranes; however, these sections consistently showed less immunostaining than the corresponding frozen sections and, frequently, immunostaining detectable in frozen sections was completely absent in paraffin-embedded sections of the same specimen. The same phenomenon has been previously described for this protein in human tumor tissue (Slamon *et al.*, 1989a, b). Because of this

Correspondence: M.F. Press

Received 12 October 1989; accepted in revised form 12 March 1990



**Table 1** Expression of HER-2/*neu* oncogene in fetal and adult tissues

Tissues	Immunostaining for HER-2/ <i>neu</i>	
	Fetal	Adult
Breast	NE	+
<i>Female reproductive</i>		
Ovary	—	—*
Fallopian tube	+	+
Uterus-endometrium	+	+
Uterus-cervix	+	wk/+
Vagina	+	+
<i>Male reproductive</i>		
Testis	—	—
Prostate	NE	wk/+
Epididymus	NE	—
<i>Digestive</i>		
Oropharynx	+	wk/+
Salivary gland	NE	wk
Esophagus	+	wk
Stomach	+	wk
Small intestine	+	wk
Large intestine	+	wk
Liver-hepatocytes	—	—
Bile ducts	+	wk
Pancreatic ducts	+	wk
Pancreatic acini	—	—
<i>Urinary</i>		
Kidney	+ / + +	wk/+
Ureter	+	wk
Bladder	+	—/wk
<i>Circulatory</i>		
Heart	—	—
Arteries	—	—
Veins	—	—
Capillaries	—	—
<i>Respiratory</i>		
Bronchi	+	+
Alveoli	0	—
<i>Hematologic</i>		
Liver	—	—
Spleen	—	—
Bone marrow	—	—
Lymph node	NE	—
<i>Musculoskeletal</i>		
Bone	—	—
Cartilage	—	—
Muscle	—	—
<i>Skin</i>		
Epidermis	+	+
Adnexae	0	wk
<i>Endocrine</i>		
Pituitary	—	—
Adrenal cortex	—	—
Adrenal medulla	—	—
Pancreatic islets	—	—
<i>Central Nervous System</i>		
Forebrain (cerebral cortex)	—	—
Midbrain	—	—
Hindbrain (cerebellum, medulla)	—	—
Spinal cord	—	—
Meninges	—	—
Eye	—	NE

\* Surface epithelium had weak membrane immunostaining, but the remainder of the ovary was not immunoreactive  
NE = not examined

difference, immunohistochemical analyses for the current study were performed using frozen specimens, circumventing the possibility that a weak or negative result would be due to fixation or tissue processing artifacts. The data on expression of HER-2/*neu* in normal fetal and adult tissues are summarized in Table 1 and are discussed in detail below.

### Gastrointestinal tract

HER-2/*neu* immunoreactive epithelium lined the fetal and neonatal gastrointestinal tract from the oropharynx to the large intestine. The epithelial cells of the common bile duct and pancreatic ducts also showed HER-2/*neu* membrane immunoreactivity. Membrane staining of epithelial cells ranged from weakly positive to distinctly positive (Figure 2P, Q). The lateral and basal cell membranes of most gastrointestinal epithelia were immunostained for HER-2/*neu*. Subsequent to the first trimester, the small and large intestine were easily distinguishable and it was apparent that the apical cell membranes of intestinal epithelial cells were negative or only weakly immunostained for HER-2/*neu*. Cells of the lamina propria, muscularis and serosa showed no immunoreactivity.

The epithelium of the adult gastrointestinal tract showed membrane immunoreactivity for HER-2/*neu*; however, the amount of immunostaining was generally reduced below the level observed in fetal tissue (Figure 2, Q vs. R) and in some cases, was barely detectable. Stratified squamous epithelium of the oropharynx and esophagus was weakly immunostained. Ductal epithelium of salivary glands was also immunoreactive. The columnar epithelium of the gastric pits was weakly immunostained while the epithelial cells of the gastric glands (parietal cells, chief cells) showed no HER-2/*neu* immunoreactivity. In the cardia and antrum the foveolae, which are lined almost entirely by mucus-secreting epithelial cells, showed weak immunostaining for HER-2/*neu* throughout their depth. Similarly, both the small intestinal epithelium (Figure 2) and the colonic epithelium were weakly immunoreactive for HER-2/*neu*. The immunostaining was again found along the lateral and basal cell membranes of these epithelial cells. In the small intestine, the epithelial cells lining the villi showed slightly more immunoreactivity than the epithelial cells of the crypts. Epithelial cells of Brunner's glands also had HER-2/*neu* membrane immunostaining. As in the fetal tissue, none of the cells of the lamina propria, muscularis mucosa, submucosa, muscularis propria or serosa showed HER-2/*neu* immunostaining. Membranes of ductal epithelial cells in the pancreas were weakly immunostained but acini and islet cells were not. Intrahepatic bile ducts were the only cell types in the adult liver which had detectable membrane staining (Figure 2L, M). This membrane staining was very weak even in larger bile ducts and often not identified in smaller bile ducts. Epithelial cells of the gall bladder also showed membrane immunostaining.

### Respiratory tract

The epithelium of the developing lungs (presumptive trachea, bronchi, and bronchioles) was immunoreactive for HER-2/*neu* in all stages of fetal development and in the neonate (Figure 2E, F), with the exception of the 0.3 cm fetus where the lung buds were not identified. Mesenchymal and vascular cells were negative for HER-2/*neu*.

Adult lungs showed HER-2/*neu* low level immunoreactivity on bronchial and bronchiolar epithelial cell membranes (Figure 2G, H), especially the lateral and basal portions of the cell membranes. The alveoli were

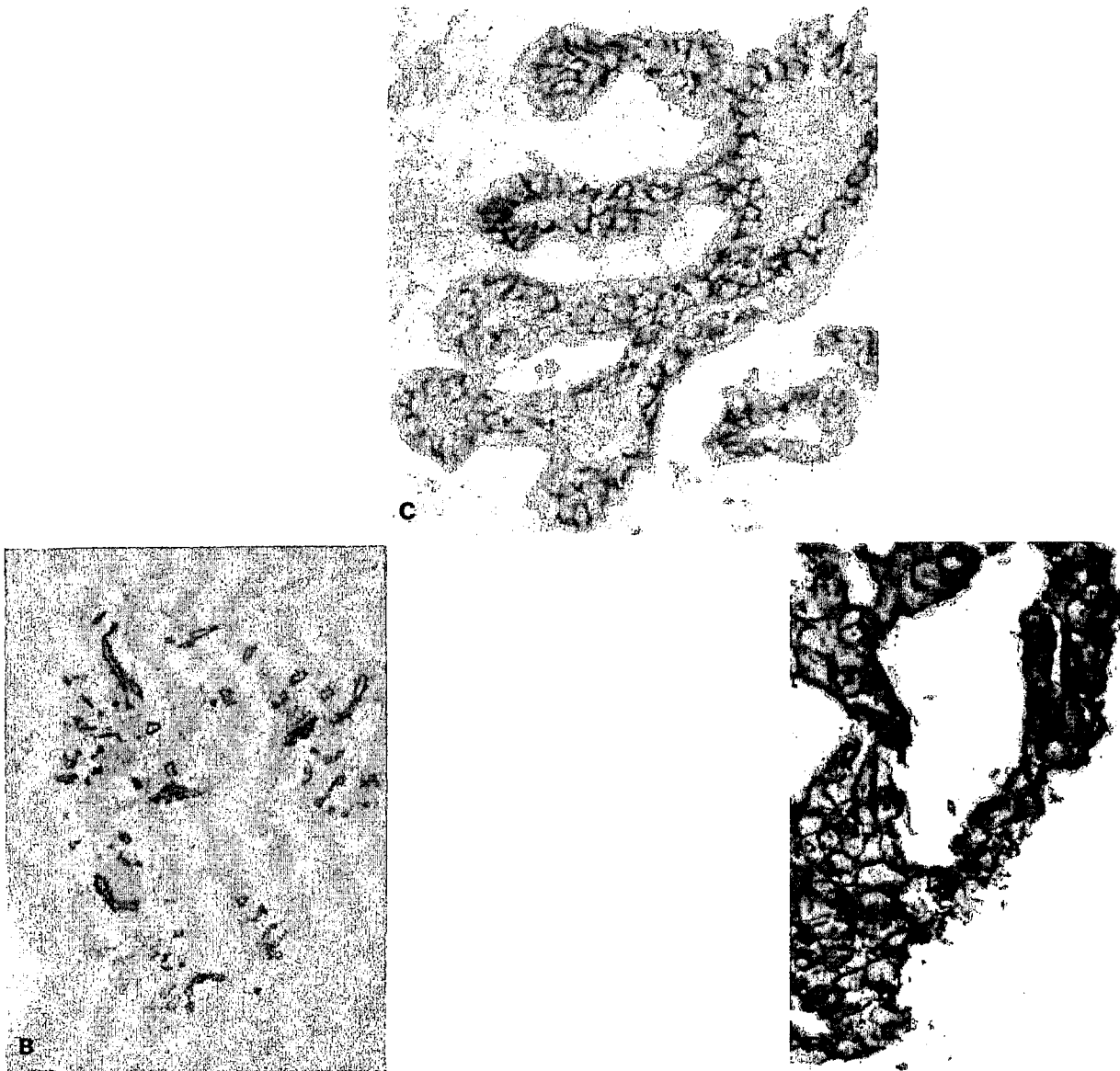


**Figure 1** Normal adult breast. All normal breast specimens had at least weak membrane immunostaining in frozen tissue sections. This illustrative case, obtained at reduction mammoplasty, had the strongest HER-2/neu membrane immunostaining (2+) in our series of 21 normal breast samples. (A) Hematoxylin and eosin stained section showing normal breast lobules and ducts. Magnification, 150 $\times$ . (B) Immunohistochemical localization of HER-2/neu demonstrates immunostaining throughout the ductal and lobular epithelial cells in a frozen tissue section. Magnification, 150 $\times$ . (C) Immunostaining of epithelial cell membranes in a terminal duct lobular unit. Frozen tissue section. Magnification, 1450 $\times$ . (D) Negative control section in which pre-immune serum was used instead of HER-2/neu-immune serum. Frozen tissue section. Magnification, 1450 $\times$ . (E) A portion of the same specimen, fixed in formalin and processed for paraffin-embedding, was sectioned and processed for HER-2/neu localization as in C. Note the relative lack of immunostaining. Magnification, 1450 $\times$ . (F) A breast carcinoma known to have 5 to 20-fold amplification and overexpression of the HER-2/neu gene demonstrates strong (3+) membrane staining for comparison with C and E. Frozen tissue section. Magnification, 1450 $\times$

not immunoreactive nor were pulmonary blood vessels, lymphatics or connective tissue.

#### Urinary tract

Mesonephric and metanephric epithelium was immunostained for HER-2/neu in all fetuses where the kidneys were examined (nine cases) as well as in the neonate. Renal epithelium of the developing kidney, i.e., epithelium lining the parietal surface of Bowman's capsule (Figure 2S), the proximal tubule, loops of Henle, distal tubule and collecting tubule (Figure 2T), expressed HER-2/neu (Figure 2). The intensity of the immunostaining ranged from weak in Bowman's capsule and the proximal tubules to moderate (2+) immunostaining in the collecting tubules of the kidney. Urothelium of

the renal pelvis and developing bladder also expressed the protein.

In the adult kidney the distribution of immunostaining is similar to that observed in the fetuses, but the intensity was much weaker in the glomeruli, proximal and distal tubules. The collecting tubules were more strongly immunostained (+/+/+) (Figure 2U, V) than the glomeruli and tubules of the adult kidney. The urothelium of the ureter and bladder were only weakly immunoreactive.

#### Female reproductive tract

Epithelial cells throughout the developing mullerian ducts of the embryos and fetuses were immunostained

Fetus

Adult

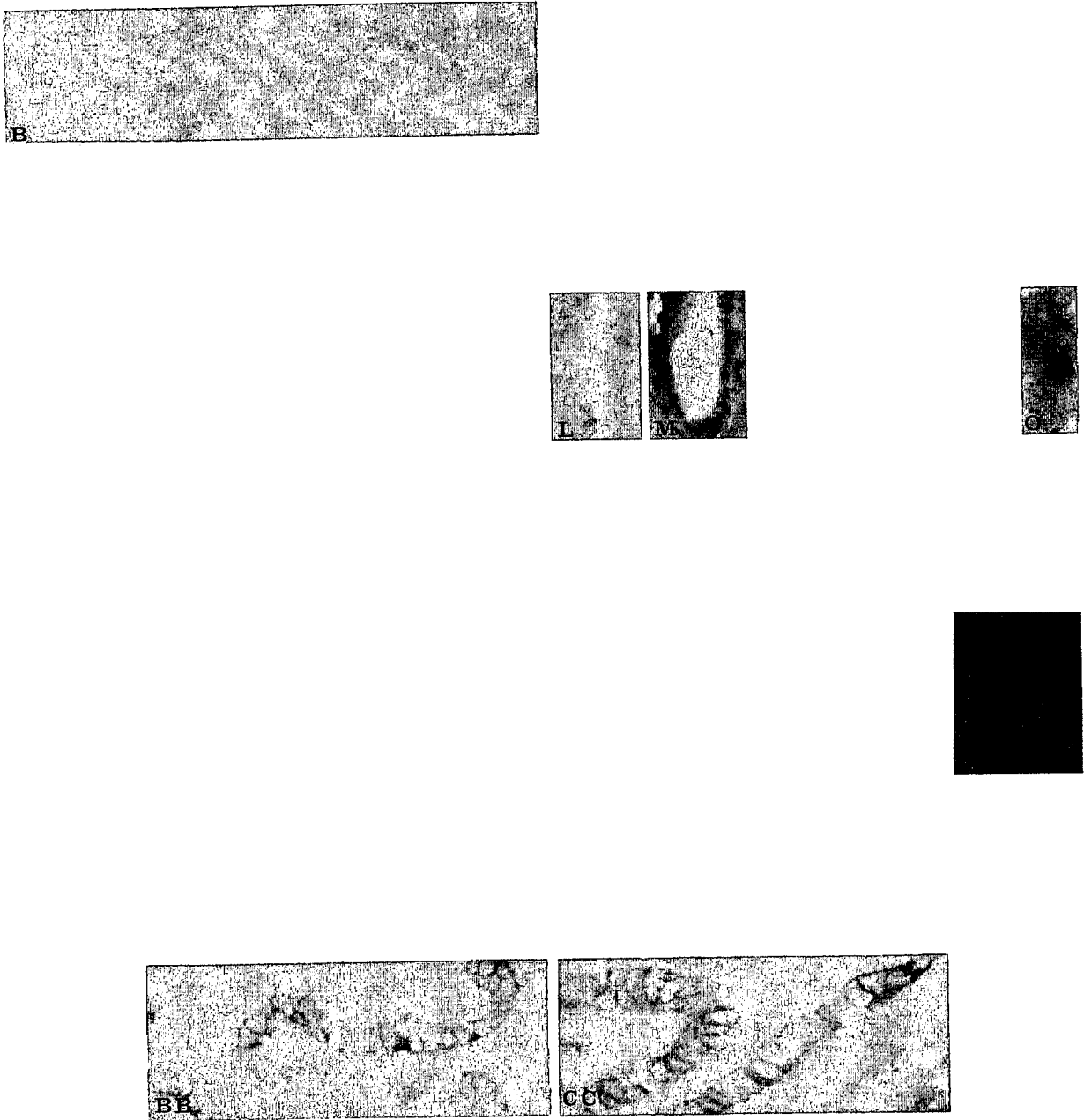


**Figure 2** Immunohistochemical identification of HER-2/*neu* in normal fetal and adult tissues. The left half of the figure is devoted to illustrating the results obtained in fetal tissues. The right half illustrates the results obtained in the corresponding adult tissues. All of the results illustrated were obtained with frozen tissue sections. (A) Histologic section of fetal brain (developing cerebral cortex) stained with hematoxylin and eosin corresponding to the immunostained area shown in B. 725 $\times$ . (B) Fetal brain (developing cerebral cortex) incubated with HER-2/*neu* immune serum (#60) as part of the peroxidase antiperoxidase technique shows no immunostaining. No counterstain. 725 $\times$ . (C) Histologic section of adult cerebral cortex stained with hematoxylin and eosin corresponding to D. (D) Adult cerebral cortex similarly shows no immunoreactivity with HER-2/*neu* immune serum. No counterstain. 725 $\times$ . (E) Histologic section of a bronchus in fetal lung stained with hematoxylin and eosin corresponding to the area shown in F. 1450 $\times$ . (F) Bronchial epithelium of fetal lung shows membrane staining for HER-2/*neu*. No counterstain. 1450 $\times$ . (G) Adult bronchial epithelium also shows HER-2/*neu* membrane staining. No counterstain. 1450 $\times$ . (H) Serial section of adult lung stained with hematoxylin and eosin showing the same bronchus at a lower magnification. 725 $\times$ . (I) Histologic section of fetal liver stained with hematoxylin corresponding to area shown in J. 1450 $\times$ . (J) Fetal liver shows no HER-2/*neu* immunostaining in hepatocytes or hematopoietic cells by immunohistochemistry. No counterstain. 1450 $\times$ . (K) HER-2/*neu* immunoreactivity is identified in cell membranes of the fetal biliary epithelium. No counterstain. 1450 $\times$ . (L) Weak HER-2/*neu* immunostaining is also identified on cell membranes of adult biliary epithelium. 1450 $\times$ . No counterstain. (M) Histologic section of biliary epithelium stained with hematoxylin and eosin corresponding to the area shown in L. 1450 $\times$ . (N) Immunoreactivity for HER-2/*neu* is not identified in hepatocytes of adult liver. No counterstain. 1450 $\times$ . (O) Histologic section of normal adult liver stained with hematoxylin and eosin corresponding to area shown in N. 1450 $\times$ . (P) Histologic section of fetal small intestine stained with hematoxylin and eosin corresponding to

for HER-2/*neu*. The various components of the female reproductive tract (vagina, cervix, uterus and fallopian tube) could be identified in fetuses larger than 10 cm and all were immunoreactive for HER-2/*neu* (Figure 2 W, X, AA, BB). As in the gastro-intestinal tract, the protein was localized to the lateral and basal cell membranes of these cells. The apical portion of the cuboidal and columnar epithelial cells (microvillus brush border) usually lacked HER-2/*neu* immunostaining (Figure 2X). Stromal cells, smooth muscle cells, blood vessels and mesothelial cells also lacked immunoreactivity for HER-2/*neu*. Finally, the developing ovaries from fetuses were not immunostained for HER-2/*neu*.

The adult vaginal epithelium was immunoreactive for the protein throughout its entire thickness including basal cells, parabasal cells, intermediate cells and superficial cells. The superficial cells showed variable immunostaining ranging from not present to weak. Immunostaining was strongest in the parabasal and intermediate cells. This immunostaining pattern was present in vaginal tissue sampled throughout the menstrual cycle. Vaginal samples obtained during menstruation or the early follicular phase were immunostained throughout the full thickness but displayed weaker staining. During the remainder of the menstrual cycle the immunostaining was slightly stronger. The submucosa and muscularis of the vagina were not immunoreactive for HER-2/*neu*.

Immunostaining of the adult cervix was identified in the ectocervical squamous and endocervical columnar epithelia. Stromal cells, smooth muscle cells of the muscularis and cells of blood vessels did not express HER-2/*neu*.

HER-2/*neu* immunoreactivity was present in the adult uterine epithelium (Figure 2Y, Z). Endometrial surface and glandular epithelia were stained throughout the menstrual cycle and again the immunoreactivity was identified predominantly along the lateral and basal aspects of cell membranes. Stromal cells of the endometrium were HER-2/*neu* negative during the normal menstrual cycle and after menopause. However, during the first and second trimesters of gestation some decidualized stromal cells did express the protein. Glandular epithelial cells, especially hypersecretory glands of the gravid uterus showed stronger HER-2/*neu* immunostaining than during the menstrual cycle. This increased membrane immunostaining was most apparent along the basal aspects of cell membranes. Decidualized stromal cells identified on the maternal surface of the placenta at delivery also showed membrane immunoreactivity.

The adult fallopian tube showed weak to moderate immunostaining of tubal epithelial cells throughout the

menstrual cycle (Figure 2 CC, DD). Immunostaining was less intense during menstruation and the early proliferative phase. Stromal cells, blood vessels, smooth muscle cells of the muscularis and mesothelial cells of the serosa were not immunoreactive.

With the exception of the surface epithelial cells, the ovary was not immunoreactive for HER-2/*neu*. Weak immunostaining of surface epithelium was identified in two of three ovaries where the epithelium had not become detached; one ovary was removed from a postmenopausal woman and the other from a woman of reproductive age during the luteal phase of the menstrual cycle.

#### Breast

Breast tissue was not identified in any of the embryos or fetuses. Adult breast consistently showed weak to low levels of HER-2/*neu* immunoreactivity in both ductal and lobular epithelia. The basal and lateral cell membranes were immunostained at levels comparable to those observed in most fetal epithelial cells. Immunostaining did not vary significantly during the menstrual cycle when 21 separate specimens distributed equally throughout the cycle were examined. In general, the amount of immunostaining in normal breast tissue was similar to that associated with non-HER-2/*neu*-amplified breast cancers, i.e. those which have a single copy of the gene and low levels of expression (Slamon *et al.*, 1989a, b). Of the 21 normal breast specimens evaluated, only one showed moderate levels (++) of staining (Figure 1b and c); however, this level was still lower than that observed in most amplified/overexpressing tumors (Figure 1f). The difference in HER-2/*neu* staining intensity seen in frozen (Figure 1b and c) and formalin-fixed, paraffin-embedded sections (Figure 1e) of the same specimen can be readily appreciated in this case. Other cells in the normal breast including myoepithelial cells, fibroblasts, fat cells, vascular smooth muscle and endothelial cells were not immunostained for HER-2/*neu*.

#### Male reproductive tract

Glandular epithelium of the adult prostate was weakly immunostained for HER-2/*neu*, while the stromal and vascular cells of the gland were negative. Fetal and adult testis as well as adult epididymus were not HER-2/*neu* immunoreactive.

#### Placenta

The squamous epithelium covering the fetal surface of the placenta and umbilical cord had immunoreactive

the area shown in Q. 1450 ×. (Q) HER-2/*neu* immunostaining of fetal small intestinal epithelial cells. No counterstain. 1450 ×. (R) Immunolocalization of HER-2/*neu* to the cell membranes of epithelial cells of the adult duodenum. No counterstain. 1450 ×. (S) Immunohistochemical localization of HER-2/*neu* in the metanephros showing immunostaining of cells lining Bowman's capsule of a glomerulus (g) and a cortical tubule. No counterstain. 1450 ×. (T) The developing collecting tubules in the medulla of the metanephros show membrane immunostaining of epithelial cells. No counterstain. 1450 ×. (U) Tubular epithelium of the adult medulla also shows membrane immunostaining for HER-2/*neu*. No counterstain. 1450 ×. (V) Histologic section of renal medulla corresponding to U. 1450 ×. (W) Histologic section of fetal endometrium stained with hematoxylin and eosin showing the same area as X. 1450 ×. (X) HER-2/*neu* is localized to the cell membranes, especially the lateral and basal cell membranes, of endometrial epithelial cells by immunohistochemistry in this fetal uterus. No counterstain. 2900 ×. (Y) The distribution of HER-2/*neu* in the adult endometrium is limited to the membranes of the epithelial cells. No counterstain. 1450 ×. (Z) Histologic section of Y stained with hematoxylin and eosin. 1450 ×. (AA) Histologic section of fetal fallopian tube stained with hematoxylin and eosin corresponding to area shown in BB. 1450 ×. (BB) Immunohistochemical localization of HER-2/*neu* in fetal fallopian tube. The immunostaining is present on cell membranes of epithelial cells. No counterstain. 1450 ×. (CC) HER-2/*neu* is also localized to the cell membranes of epithelial cells in the adult fallopian tube. No counterstain. 1450 ×. (DD) Histologic section of CC stained with hematoxylin and eosin. 1450 ×

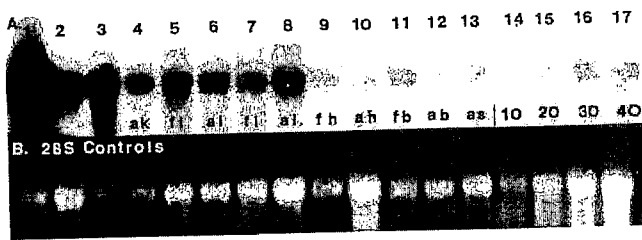


**Figure 3** (A) Northern blot analysis of HER-2/neu expression in normal fetal and adult tissues. The HER-2/neu message is identified as an autoradiographic signal in lanes 1 through 8 of this Northern blot. Only lane 1 (SKBR3, control breast cancer cell line with amplification and overexpression of the gene) has levels of expression significantly above the level found in a single-copy, low expression breast cancer shown in lane 2 (MCF-7 human breast cancer cell line). Expression of HER-2/neu message is identified in normal fetal and adult kidney (lane 3 and lane 4, fk and ak), fetal and adult lung (lanes 5 and 6, fl and al) and fetal and adult intestine (lanes 7 and 8, fi and ai) at levels similar to that in low expression breast cancers (e.g. lane 2). The 4.5 kb transcript is not identified in total RNA from fetal liver (fh, lane 9), adult liver (ah, lane 10), fetal cerebral cortex (fb, lane 11), adult cerebral cortex (ab, lane 12) and adult spleen (as, lane 13). In addition, to confirm the apparent lack of HER-2/neu expression in liver, 10, 20, 30 and 40 micrograms of total RNA from adult liver were loaded in lanes 14, 15, 16 and 17, respectively. Autoradiograms were produced by exposing the filter for 72 h at  $-70^{\circ}\text{C}$ . Exposure of the filter for an additional 48 h did not show an increase in HER-2/neu transcript. The Northern blots were prepared with total RNA from each sample as follows: 10 micrograms of total RNA were loaded in lanes 1-9 and 11-14; 20 micrograms in lanes 10 and 15; 30 micrograms in lane 16 and 40 micrograms in lane 17. (B) Controls-28S ribosomal RNA. To confirm that the loading and transfer of RNA had been performed properly the filters were stained with ethidium bromide to demonstrate the 28S and 18S subunits of ribosomal RNA. Staining of the 28S subunit is illustrated

cell membranes during gestation and at delivery. The epithelium of the allantoic remnant in the umbilical cord was also immunostained for HER-2/neu. Trophoblast of the chorionic villi expressed HER-2/neu during the first and second trimesters but only weakly or not at all at delivery. Interestingly, the immunostaining for HER-2/neu was along the apical cell membrane of the syncytial trophoblast. Some maternal decidualized stromal cells of gestational endometria were immunoreactive for HER-2/neu during the first and second trimester and at term and expressed the protein circumferentially along the cell membrane.

#### Skin

Skin of the embryos was composed of only a few layers of squamous epithelium and these cells expressed HER-2/neu. Adult skin showed immunoreactivity of keratinocytes but not melanocytes. Adnexal structures, especially hair follicles, sweat glands and sebaceous glands, were weakly immunostained.

#### Other tissues

The fetal and adult central nervous system was not immunoreactive for HER-2/neu (Table 1, Figure 2A-D). The developing eye, cerebral cortex, infundibulum, thalamus, pons, medulla oblongata showed no membrane immunostaining. Likewise, the mantle, marginal zones and dorsal root ganglia of the developing spinal cord showed no protein staining. Only epithelial cells of the choroid plexus showed weak immunoreactivity. Although cartilage did not express HER-2/neu, notochord of developing vertebral cartilage in embryos was

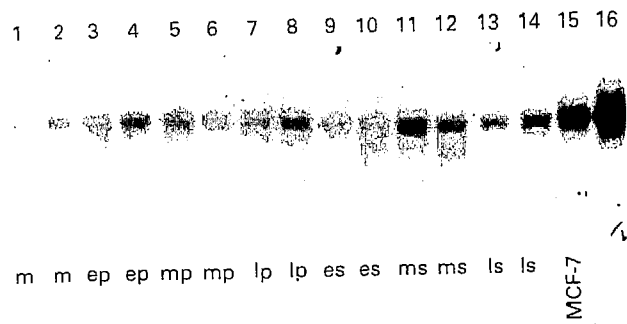


**Figure 4** Northern blot analysis of HER-2/neu expression in normal adult endometrium throughout the menstrual cycle. HER-2/neu message (4.5 kb) is identified in the RNA from two menstrual (m-lanes 1, 2), two early proliferative phase (ep-lanes 3, 4), two midproliferative phase (mp-lanes 5, 6), two late proliferative phase (lp-lanes 7, 8), two early secretory phase (es-lanes 9, 10), two midsecretory phase (ms-lanes 11, 12) and two late secretory phase (ls-lanes 13, 14) endometria. The low level of expression present in normal endometrium is clearly demonstrated by comparison of the autoradiographic signals obtained from endometrial samples (lanes 1-14) with the single copy, low HER-2/neu expressing breast cancer cell line, MCF-7 (lane 15). Lane 16 contains a breast cancer with 2 to 5-fold amplification of the HER-2/neu gene and moderate overexpression of the HER-2/neu message. The Northern blot was prepared as in Figure 3. Endometrial samples were dated from formalin-fixed, paraffin-embedded, hematoxylin and eosin stained tissue sections according to morphologic criteria described elsewhere (Press *et al.*, 1984; Press *et al.*, 1986; Press, Udove & Greene, 1988)

immunoreactive for the protein. Hematopoietic tissues including fetal liver (Figure 2I, J) spleen and adult bone marrow did not have HER-2/neu staining. In the adult liver only bile ducts showed membrane staining which was weak and inconsistently present (Figure 2L, M). Hepatocytes of adult liver were not immunostained (Figure 2N, O). The red and white pulp of adult spleen, adult lymph nodes and thymus, and lymphoid cells of adult tonsils were also not immunoreactive; however, the tonsillar squamous epithelium had membrane immunostaining. The fetal heart, adrenal gland (cortex and medulla), islet of Langerhans were not immunostained for HER-2/neu.

#### Expression of HER-2/neu characterized by Northern hybridization

Northern blot hybridization analyses were used for independent confirmation of HER-2/neu expression in fetal and adult tissues. Tissues which were immunostained by HER-2/neu antiserum had the 4.5 kb HER-2/neu message providing independent confirmation of expression (Figure 3, lanes 3-8). The MCF-7 human breast cancer cell line is an example of single DNA copy, low expression of HER-2/neu (Figure 3, lane 2; Figure 4, lane 15). The level of RNA expression in all normal fetal and adult tissues was similar to that found in single copy, low expressing breast cancers (Figure 3). RNA expression in the fetal kidney was higher than in other normal tissues. Fetal and adult liver, fetal and adult brain, fetal heart and adult spleen (Figure 3, lanes 9-14) did not express detectable levels of the HER-2/neu message, confirming the immunohistochemical data.

To determine if HER-2/neu expression levels varied with the menstrual cycle, we analyzed total RNA from 32 normal endometria including; 4 early proliferative phase, 4 midproliferative phase, 4 late proliferative phase, 4 early secretory phase, 4 midsecretory phase, 4 late secretory phase, 4 menstrual endometria and 4 gestational endometria. The amount of HER-2/neu

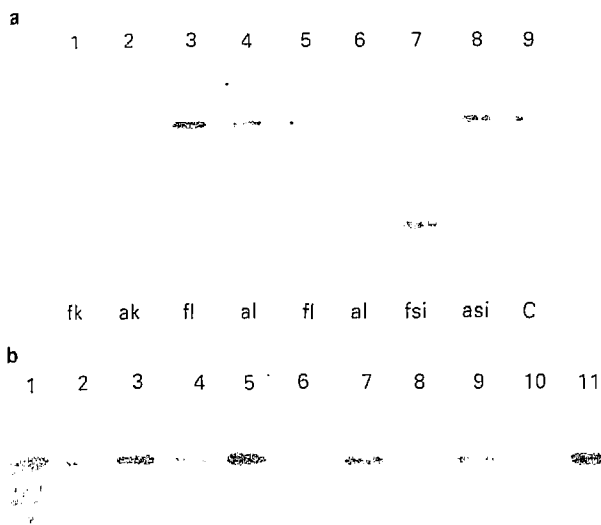


**Figure 5** Southern blot analysis of HER-2/*neu* gene copy number in normal adult and fetal tissues. (a) Comparison of selected fetal and adult normal tissues. A single copy of the HER-2/*neu* gene is present in each of fetal and adult kidney (lanes 1 and 2, fk and ak), fetal and adult lung (lanes 3, 5 and 4, 6; fl and al) and fetal and adult small intestine (lanes 7 and 8; fsi and asi). A single copy breast cancer cell line, MCF-7, (lane 9, C) is also included as a control. The DNA from the fetal small intestine illustrated in lane 7 shows a rearrangement of the HER-2/*neu* gene and was the only case which showed this change. The fetal kidney DNA of lane 1 is from the same case showing overexpression in Figure 3, lane 3. (b) Normal adult endometrium from menstrual (lanes 1 and 2), early proliferative (lanes 3 and 4), midproliferative (lane 5), late proliferative (lanes 6 and 7), early secretory (lane 8), midsecretory (lane 9) and late secretory (lane 10) have a single copy of the HER-2/*neu* gene. DNA from a human breast cancer cell line (lane 11) is used as the single copy control

message identified in endometria at any time point during the menstrual cycle did not exceed that of single copy, low expressor breast cancer cells as illustrated in Figure 4 (lanes 1–14) again using MCF-7 as the low expressor control (Figure 4, lane 15). While there was slight variation in a few cases, there was no systematic change in expression during the menstrual cycle. Gestational endometria showed similar levels of HER-2/*neu* RNA expression. This is comparable to the results obtained by immunohistochemistry.

#### Structure of the HER-2/*neu* gene in normal tissues

Southern hybridization was performed to determine if any of the tissues expressing HER-2/*neu* had alterations of the gene, i.e. amplification or rearrangements. Southern hybridization of DNA from tissue derived from fetal and adult kidney, lung, colon, liver, spleen and adult endometrium showed no evidence of gene amplification or rearrangement, (Figure 5), with the exception of a small intestine from one fetus which did show an apparent rearrangement (Figure 5a, lane 7).

#### Discussion

In this study HER-2/*neu* expression was analysed in a large variety of normal fetal and adult tissues. The cells expressing HER-2/*neu* were derived from all three germ layers. Ectodermal derivatives, i.e. skin and mammary

glands, mesodermal derivatives, i.e. kidney, ureter, vagina, cervix, uterus, fallopian tube and Wolffian duct, and endodermal derivatives, i.e. oropharynx, esophagus, stomach, intestines, pancreas, biliary tree, lungs, prostate, and bladder expressed the HER-2/*neu* gene. Extra-embryonic tissues expressing HER-2/*neu* were limited to the trophoblast of chorionic villi. Endothelial cells and mesothelial cells were the only polarized cells attached to basement membrane which did not express HER-2/*neu*. Interestingly, these two cell types are not considered 'true' epithelia (Eklom, 1989). The pattern of HER-2/*neu* expression emerging from this study is of weak levels of expression distributed in epithelial cells of most organs.

HER-2/*neu* expression in adult endometrium did not show cyclic variation with the menstrual cycle either by immunohistochemistry or by northern blot analysis. Likewise, immunohistochemical assay of normal adult breast also did not show cyclic variation. In another series of normal breasts, reported elsewhere, HER-2/*neu* expression was demonstrated with both northern hybridization and immunohistochemistry (Bartow *et al.*, 1989). The lack of cyclic variation indicates that HER-2/*neu* expression is not significantly altered by steroid hormones.

HER-2/*neu* was not preferentially expressed in dividing cells. Expression in secretory endometria was as great as, or slightly greater than, it was in proliferative endometria. Basal cells of squamous epithelia, columnar cells of crypts in the gastrointestinal tract, and cytotrophoblastic cells of placental chorionic villi, the proliferative compartment of their respective tissues, all showed similar or less immunostaining than adjacent epithelial cells.

The level of HER-2/*neu* expression in normal tissue, both by subjective evaluation of immunostaining results and by quantitation of northern hybridization, was consistently less than that observed in breast cancers with amplification and/or overexpression of the gene, and was similar to that observed in breast cancers lacking HER-2/*neu* amplification and overexpression. HER-2/*neu* protein product identified by immunohistochemistry was generally greater in fetal tissues than in their adult counterparts with the exception of the female reproductive tract and breast where it appeared to be comparable to fetal levels. Only the fetal metanephros (kidney) had levels of expression which overlapped with the low end of the spectrum of breast cancers showing overexpression of HER-2/*neu*. In contrast to mesothelium lining the peritoneal cavity, the surface epithelium of the ovaries was immunostained for HER-2/*neu*.

During the preparation of this manuscript four publications appeared reporting the distribution of HER-2/*neu* expression in normal human fetuses and/or adult tissues (Cohen *et al.*, 1989; DePotter *et al.*, 1989; Mori *et al.*, 1989; Quirke *et al.*, 1989). The distribution of HER-2/*neu* expression described here is in general agreement with only one of these reports (Mori *et al.*, 1989). Of these four publications only Mori *et al.* (1989) used frozen tissue for their study and only they described HER-2/*neu* as localized to cell membranes. Mori *et al.* (1989) reported their preliminary findings in three frozen human fetuses; 9, 14 and 24 weeks of age. They identified the protein on cell membranes of epithelial cells from a variety of organs (lung, esophagus,

stomach, intestines, kidney, and pancreas). Conversely, Quirke *et al.* reported broad expression of HER-2/*neu* including 'staining' of neural processes in both the central and peripheral nervous systems, chondrocytes of developing cartilage, osteocytes in bone, rhabdomyoblasts, cardiac muscle, respiratory epithelium and mesenchyme/smooth muscle, liver, mesonephric glomeruli, tubules and ducts, metanephric glomeruli and tubules, renal pelvis epithelium, gonadal blastema, adrenal gland, pancreatic acini, epidermis of skin and cyto- and syncytiotrophoblast from 11 formalin-fixed, paraffin-embedded fetuses. The cellular and subcellular distribution of this staining was unclear, but was not described as solely distributed on cell membranes. 'Membranous staining' is described only once, in the liver of a 6 week fetus. 'Strong punctate staining' was identified in the mesonephric tubules and in adult renal tubules. 'Cytoplasmic staining' was present in chondrocytes and in osteocytes. 'Oesophageal, gastric, small intestinal and colonic epithelium stained diffusely but with luminal accentuation'.

Localization of the putative receptor protein, HER-2/*neu*, to cell membranes which we (Slamon *et al.*, 1989a, b) and others (Van de Vijer *et al.*, 1988) consider to be characteristic was apparently not identified in these formalin-fixed, paraffin-embedded fetuses (Quirk *et al.*, 1989). The two antisera used by Quirk *et al.* (1989) to identify HER-2/*neu* in fetuses have been previously characterized as giving 'qualitatively and quantitatively different staining reactions. In all of the positive tumors, antiserum 20N predominantly stained the cytoplasm with only one tumor exhibiting membrane staining. . . . Antiserum 21N predominantly stained the cell membrane . . .' (Gusterson *et al.*, 1988). In the more recent publication reporting immunostaining in normal tissue 'the pattern of staining of both antibodies was identical, except for the strong staining of developing and mature red cells by 21N' (Quirk *et al.*, 1989). However, it is unclear whether the pattern was of membrane or cytoplasmic immunostaining or both. One possibility is that variations may be a result of differences in sample preparation, i.e. fixative, fixation time, embedding temperatures, etc.

Others, using Bouins-fixed, paraffin-embedded tissues, described HER-2/*neu* immunoreactivity in the gastrointestinal tract but likewise did not describe immunostaining on cell membranes (Cohen *et al.*, 1989).

DePotter *et al.* (1989), also using paraffin-embedded tissues, found 'a constant diffuse intracytoplasmic granular staining' in a variety of normal adult and fetal tissues. However, 'the cytoplasmic reacting protein was shown to be a different protein from the known *neu* oncogene product of 185 kd'; it had a molecular weight of 155 kd (DePotter *et al.*, 1989). They suggest that 'it could be a *neu*-like cross-reacting protein or a different *neu* oncogene product, derived by alternative splicing from the same gene and having a different destination in the cell'. No data was provided to show a change in the signal region of the peptide nor was any data provided showing alterations in the transmembrane domain which would prevent the protein product from accumulating in the cell membrane. Western immunoblots have been used in selected normal tissues to confirm that HER-2/*neu* has the characteristic 185 kd size (Mori *et al.*, 1989). Our experience with formalin-fixed, paraffin-embedded normal tissues as well as with breast cancers

(Slamon *et al.*, 1989a and b) is that HER-2/*neu*, when identified, is localized to cell membranes in this material. Samples with high levels of HER-2/*neu* amplification and marked overexpression can frequently have some cytoplasmic staining; however, we do not see this in the absence of accompanying membrane staining. Neither have we observed a redistribution of the HER-2/*neu* protein from the membrane to the cytoplasm with paraffin-embedding. The amount and intensity of the membrane immunostaining for HER-2/*neu* is consistently reduced when paraffin-embedded tissue is compared to frozen tissue sections derived from the same specimen (Slamon *et al.*, 1989a and b).

The assessment of the normal expression pattern of this gene is of some importance not only for general biologic consideration, but also because of potential utility of measurement of its expression in diagnostic and prognostic tests for human breast and ovarian cancer (Slamon *et al.*, 1989a). Moreover, therapeutic approaches directed at this protein will most likely be based on the differential high levels of expression seen in some tumors compared to normal tissues. As a result, knowledge of the amount and distribution of the HER-2/*neu* protein in normal tissues is of importance in interpreting diagnostic assays and could be of importance in anticipating toxicity of future therapeutic trials directed at the alteration in expression of this protein in some human tumors.

## Materials and methods

### Embryonic/fetal tissues

Both frozen and formalin-fixed, paraffin-embedded embryonic and fetal tissues were obtained from twelve human fetuses of between approximately 3 and 24 weeks gestation. The fetuses had crown rump lengths of 0.3, 1.7, 1.9, 2.5, 3.0, 4.0, 5.0, 8.0, 13.0, 15.0, 16.5, and 21.5 cm. Four of these fetuses were of undetermined sex, 3 were male and 5 were female. Tissue was obtained at autopsy from a female infant that expired after a 40 week gestation (6 lbs, 19 in.). The institutional clinical investigation committee reviewed and approved the study protocol in which these embryos and fetuses were obtained (UC protocol #4411).

### Adult tissues

Both frozen and formalin-fixed, paraffin-embedded tissues derived from surgical specimens were used for these studies. Normal adult tissues (followed by number of cases of each) analysed for HER-2/*neu* expression included lung ( $n = 12$ ), salivary gland ( $n = 4$ ), esophagus ( $n = 6$ ), stomach ( $n = 13$ ), small intestine ( $n = 8$ ), large intestine ( $n = 10$ ), liver ( $n = 10$ ), gall bladder ( $n = 2$ ), spleen ( $n = 2$ ), lymph node ( $n = 7$ ), thymus ( $n = 1$ ), pancreas ( $n = 4$ ), pituitary ( $n = 2$ ), thyroid ( $n = 7$ ), adrenal gland ( $n = 7$ ), kidney ( $n = 16$ ), bladder ( $n = 10$ ), testis ( $n = 8$ ), prostate ( $n = 12$ ), epididymus ( $n = 2$ ), ovary ( $n = 3$ ), skin ( $n = 10$ ), bone ( $n = 4$ ), muscle ( $n = 10$ ) and brain ( $n = 8$ ). In order to characterize HER-2/*neu* expression during the female reproductive cycle, tissue from normal vagina specimens of 21 cases, endometrium of 28 cases, fallopian tube of 21 cases, cervix of 21 cases, and breast of 21 cases, equally distributed throughout the menstrual cycle, were selected. Some of these cases have been reported previously in studies of either estrogen receptor (Press & Greene, 1984; Press *et al.*, 1984; Press *et al.*, 1986) or progesterone receptor expression in the female reproductive tract during the menstrual cycle (Press, Udove & Greene, 1988; Press & Greene, 1988). The normal breast samples were obtained from women

undergoing augmentation or reduction mammoplasties. Menstrual cycle dating was determined from historical information, from the date of the first menses following surgery and from serum steroid hormone levels in blood obtained immediately prior to surgery. Only one normal breast sample obtained from a woman who previously had a hysterectomy did not have the menstrual cycle date established.

#### Immunohistochemical assay

All normal tissues available for the study were analysed by immunohistochemistry. A rabbit polyclonal antiserum (#60), specific for HER-2/neu protein (Slamon *et al.*, 1989b), was used with the peroxidase antiperoxidase technique. The immunohistochemical technique involved the sequential application of the following antibodies: primary rabbit anti-HER-2/neu antiserum #60 (1:1000 dilution), a secondary or bridging goat antirabbit IgG (1:50 dilution, half hour) (Sternberger-Mayer, Inc.) and a tertiary rabbit peroxidase-antiperoxidase antibody (1:50, half hour) (Sternberger-Mayer, Inc.). Each antibody incubation was followed by rinsing the tissue sections in phosphate buffered saline three times (5 min each). The sites of immunoprecipitate formation were identified using light microscopy following treatment with a chromogen, 3-3'-diaminobenzidine. Tissues were grouped into one of the following expression categories depending on the amount of membrane immunostaining: negative (-), weak (wk), distinct (1+), moderate (2+), and strong/intense (3+). These categories are similar to those previously described for breast and ovarian cancers (Slamon *et al.*, 1989a, b). We do not report percentage of immunoreactive cells since relatively homogeneous immunostaining was observed in specific cell types throughout frozen sections of normal tissues (approximately 90% of the cells of a particular type showing similar immunostaining properties). Similar observations were made in frozen sections of breast and ovarian tumors (Slamon *et al.*, 1989a, b).

Negative control serial sections were prepared using pre-immune serum (1:1000 dilution) instead of the immune serum in the peroxidase anti-peroxidase technique. The specificity of the #60 antiserum was confirmed with competition studies using purified HER-2/neu protein (Slamon *et al.*, 1989b).

Immunostaining of frozen tissue sections, performed in a blinded fashion, was compared with immunostaining of formalin-fixed, paraffin-embedded tissue sections. Paraffin-embedded tissue sections were rehydrated by warming at 55–60°C for one hour and then transferring to xylene and a graded series of alcohols followed by phosphate buffered saline. The peroxidase antiperoxidase technique was performed as above except the incubation times with primary antibody differed. Frozen section localization of HER-2/neu

protein was not improved by incubation beyond one hour; however, in tests of optimum conditions for immunostaining, overnight incubation resulted in stronger membrane staining of cells in paraffin-embedded sections. Otherwise, the immunostaining protocols were identical.

#### Northern hybridization

Identification of the 4.5 kb messenger RNA encoding the HER-2/neu protein was done by Northern blot hybridization of total RNA extracted from selected normal adult and fetal tissues. RNA was isolated and the Northern hybridization performed as previously described (Thomas, 1980; Slamon *et al.*, 1989a, b). RNA was extracted from 28 cases of normal adult endometrium distributed throughout the menstrual cycle, 4 cases of gestational endometrium, 2 cases each of adult and fetal kidney, 2 cases each of adult and fetal lung, 2 cases each of adult and fetal liver, one case each of adult and fetal colon, three cases of fetal brain, one case of adult brain, one case of fetal heart, one case of fetal lower limb, and one case of adult spleen.

#### Southern hybridization

HER-2/neu gene copy level was determined by Southern hybridization of EcoRI digested DNA from selected normal adult and fetal tissues. The DNA was extracted from the same cases listed for Northern blot analyses. The Southern hybridization was performed as previously described (Southern, 1973; Slamon *et al.*, 1989a; Slamon & Clark, 1988). Autoradiograms were quantitated by soft laser densitometry. Autoradiograms obtained with probes for the myeloperoxidase and p53 genes, found on the long and short arms of chromosome 17, respectively, served as controls to demonstrate that similar amounts of DNA had been loaded into each lane.

#### Acknowledgements

We would like to thank Judith Udove, Tu Han, M. Jane Arbouleda, Marianne Friedman, and Jason Lukas for their technical assistance. We would also like to thank Tom Lampinen and Diane Alvarado for collecting some of the specimens used in this report. We appreciate the cooperation of the section of surgical pathology at the University of Chicago for permitting us to use paraffin-embedded blocks and obtain additional clinical information on cases collected as frozen specimens by one of us while on the faculty of the University of Chicago. This work was supported in part by grants from the National Cancer Institute (CA48780, CA47538, CA471779 and CA36827), Triton Biosciences, Inc. and the American Cancer Society (IN-21-29/003). D.J.S. is a recipient of an American Cancer Society Faculty Research Award.

#### References

- Bartow, S., Hildebrand, R., Boyd, M. & Press, M.F. (1989). *Lab. Invest.*, **62**, 8A, 1990. (abstract)
- Cohen, J.A., Weiner, D.B., More, K.F., Kokai, Y., Williams, W.V., Maguire, H.C., Jr, LiVolsi, V.A. & Greene, M.I. (1989). *Oncogene*, **4**, 81–88.
- Coussens, L., Yang-Feng, T.L., Liao, Y.-C., Chen, E., Gray, A., McGrath, J., Seeburg, P.H., Libermann, T.A., Schlessinger, J., Francke, U., Levinson, A. & Ullrich, A. (1985). *Science*, **230**, 1132–1139.
- De Potter, C.R., Daele, S.V., Van DeVijver, M.J., Pauwels, C., Maertens, G., De Boever, J., Vandekerckhove, D. & Roels, H. (1989). *Histopathology*, **15**, 351–362.
- DiFiore, P.P., Pierce, J.H., Kraus, M.H., Segatto, O., King, C.R. & Aaronson, S.A. (1987). *Science*, **237**, 178–182.
- Drebin, J.A., Link, V.C., Stern, D.F., Weinberg, R.A. & Greene, M.I. (1985). *Cell*, **41**, 695–706.
- Ekblom, P. (1989). *FASEB J.*, **3**, 2141–2150.
- Gusterson, B.A., Gullick, W.J., Venter, D.J., Powles, T.J., Elliott, C., Ashley, S., Tidy, A., Harrison, S. (1988). *Mol. Cell. Probes*, **2**, 383–391.
- Hudziak, R.M., Schlessinger, J. & Ullrich, A. (1987). *Proc. Natl. Acad. Sci. USA*, **84**, 7159–7163.
- King, C.R., Kraus, M.H. & Aaronson, S.A. (1985). *Science*, **229**, 974–976.
- Kokai, Y., Cohen, J.A., Drebin, J.A. & Greene, M.I. (1987). *Proc. Natl. Acad. Sci. USA*, **84**, 8498–8501.
- Kraus, M.H., Popescu, N.C., Amsbaugh, S.C. & King, C.R. (1987). *EMBO J.*, **6**, 605–610.
- Mori, S., Akiyama, T., Yamada, Y., Morishita, Y., Sugawara, I., Toyoshima, K. & Yamamoto, T. (1989). *Lab. Invest.*, **61**, 93–97.
- Muller, W.J., Sinn, E., Pattengale, P.K., Wallace, R. & Leder, P. (1988). *Cell*, **54**, 105–115.
- Paik, S., Hazan, R., Fisher, E.R., Sass, R.E., Fisher, B.,



- Redmond, C., Schlessinger, J., Lippman, M.E. & King, C.R. (1990). *J. Clin. Oncol.*, **8**, 103-112.
- Press, M.F. & Greene, G.L. (1984). *Lab. Invest.*, **50**, 480-486.
- Press, M.F., Nousek-Goebl, N.A., King, W.J., Herbst, A.L. & Greene, G.L. (1984). *Lab. Invest.*, **51**, 495-504.
- Press, M.F., Nousek-Goebl, N.A., Bur, M. & Greene, G.L. (1986). *Am. J. Pathol.*, **123**, 280-292.
- Press, M.F. & Greene, G.L. (1988). *Endocrinology*, **122**, 1165-1175.
- Press, M.F., Udove, J.A. & Greene, G.L. (1988). *Am. J. Pathol.*, **131**, 112-124.
- Quirke, P., Pickles, A., Tuzi, N.L., Mohamdee, O. & Gullick, W.L. (1989). *Brit. J. Cancer*, **60**, 64-69.
- Ro, J., El-Neggar, A., Ro, J.Y., Blick, M., Frye, D., Frascini, G., Fritsche, H. & Hortobagyi, G. (1989). *Cancer Res.*, **49**, 6941-6944.
- Schechter, A.L., Stern, D.F., Vaidyanathan, L., Decker, S.J., Drebin, J.A., Greene, M.J. & Weinberg, R.A. (1984). *Nature*, **312**, 513-516.
- Semba, K., Kamata, N., Toyoshima, K. & Yamamoto, T. (1985). *Proc. Natl. Acad. Sci. USA*, **82**, 6497-6501.
- Shih, C., Padhy, L.C., Murray, M. & Weinberg, R.A. (1981). *Nature*, **290**, 261-264.
- Slamon, D.J. & Clark, G.M. (1988). *Science*, **240**, 1796-1798.
- Slamon, D.J., Clark, G.M., Wong, S.G., Levin, W.J., Ullrich, A. & McGuire, W.L. (1987). *Science*, **235**, 177-182.
- Slamon, D.J., Godolphin, W., Jones, L.A., Holt, J.A., Wong, S.G., Keith, D.E., Levin, W.J., Stuart, S.G., Udove, J., Ullrich, A. & Press, M.F. (1989a). *Science*, **244**, 707-712.
- Slamon, D.J., Press, M.F., Godolphin, W., Ramos, L., Haran, P., Shek, L., Stuart, S.G. & Ullrich, A. (1989b). *Cancer Cells*, **7**, 371-380.
- Southern, E.M. (1975). *J. Mol. Biol.*, **98**, 503-517.
- Thomas, P.S. (1980). *Proc. Natl. Acad. Sci. USA*, **77**, 5201-5205.
- Van de Vijver, M.J., Peterse, J.L., Mooi, W.J., Wisman, P., Lomans, J., Dalesio, O. & Nusse, R. (1988). *N. Engl. J. Med.*, **319**, 1239-1245.
- Wright, C., Angus, B., Nicholson, S., Sainsbury, R.C., Cairns, J., Gullick, W.J., Kelly, P., Harris, A.L. & Horne, C.H.W. (1989). *Cancer Res.*, **49**, 2087-2090.

# EXHIBIT C

# Cell Cycle Phase-specific Cytotoxicity of the Antitumor Agent Maytansine<sup>1</sup>

Potú N. Rao,<sup>2</sup> Emil J. Freireich, Marion L. Smith, and Ti Li Loo

Department of Developmental Therapeutics, The University of Texas System Cancer Center, M. D. Anderson Hospital and Tumor Institute, Houston, Texas 77030

## ABSTRACT

The objective of this investigation was to study the effects of maytansine on the cell cycle kinetics of HeLa cells. The results of this study indicate that maytansine is a very potent mitotic inhibitor and that it has no effect on macromolecular synthesis. Maytansine-induced cytotoxicity was dependent upon the position of the cell in the cell cycle. Mitotic and G<sub>2</sub> cells are most sensitive to this agent, while G<sub>1</sub> phase cells are the most resistant, with S-phase cells being intermediate. Small ( $0.82 \times 10^{-8}$  M) fractionated doses given at an interval of 8 hr have been found to be more cytotoxic than was a large ( $1.64 \times 10^{-8}$  M) single dose. In evaluating the drug combinations, we observed that the schedule in which 1- $\beta$ -D-arabinofuranosylcytosine treatment was followed by maytansine treatment exhibited greater cell kill than the reverse sequence. No schedule-dependent effects were observed when maytansine was tried in combination with Adriamycin.

## INTRODUCTION

Maytansine, a naturally occurring ansa macrolide, isolated from the East African shrub *Maytenus serrata* (4, 5), has been reported to have significant antitumor activity against several experimental animal tumors, including P388 lymphocytic leukemia, B16 melanoma, and Walker 256 carcinoma (11). The antitumor activity of maytansine appears primarily to be due to its stathmokinetic effects, as in the case of *Vinca* alkaloids (12). Phase 1 clinical trials with maytansine in our department at M. D. Anderson Hospital and Tumor Institute appear to be promising because the antitumor activity of maytansine in patients with melanoma, breast carcinoma, and head and neck clear cell carcinoma is associated with little or no myelosuppression (2). Responses were also observed by other investigators in patients with acute lymphocytic leukemia, non-Hodgkin's lymphoma, ovarian cancer (3), and carcinoma of the breast (1). Maytansine is now in Phase 2 clinical trials.

Since maytansine is associated with some dose-dependent gastrointestinal toxicity (2, 3), we decided to study the effects of scheduling, dose, and dose fractionation of maytansine alone and in combination with ara-C<sup>3</sup> or Adriamycin on HeLa cells *in vitro*.

<sup>1</sup> This research is supported in part by Grants CA-11520, CA-14528, and CA-19856 and Contract CM-53773 from the National Cancer Institute, and Grant GM-23252 from the National Institute for General Medical Sciences, NIH, Department of Health, Education, and Welfare.

<sup>2</sup> To whom requests for reprints should be sent.

<sup>3</sup> The abbreviations used are: ara-C, 1- $\beta$ -D-arabinofuranosylcytosine; dThd, thymidine.

Received July 24, 1978; accepted May 15, 1979.

## MATERIALS AND METHODS

**Cells.** HeLa cells used in this study were grown in Lux plastic dishes as monolayer cultures in McCoy's Medium 5A supplemented with 16% heat-inactivated fetal calf serum and 1% penicillin (10,000 units/ml):streptomycin (10,000  $\mu$ g/ml). These cells have a cell cycle time of approximately 22 hr and a plating efficiency of about 90%.

**Cell Synchrony.** HeLa cells were synchronized in S phase by the excess dThd (2.5 mM) double-block method (8). Cells in S and G<sub>2</sub> phases were obtained by trypsinizing monolayer cultures at 1 and 7 hr, respectively, after reversal of the second dThd block. A pulse label of 30 min with [<sup>3</sup>H]dThd gave a labeling index of 95% for S-phase population and 15% for the G<sub>2</sub> population. The mitotic index in these populations was less than 1%. Mitotic HeLa cells of 98% purity or better were obtained by selective detachment after the exposure to nitrous oxide (at 80 psi and 37°) of a monolayer culture that was partially synchronized into S phase by a single dThd block (7). G<sub>1</sub> phase cells were obtained by incubating the N<sub>2</sub>O-arrested mitotic cells under regular culture conditions for 3 hr. During this 3-hr incubation, the mitotic index decreased from 98% to below 5%, indicating the successful completion of mitosis following reversal of the N<sub>2</sub>O block.

**Drugs.** Maytansine (NSC 153858), ara-C (NSC 63878), and Adriamycin (NSC 123127) were supplied by the Drug Development Branch, National Cancer Institute, NIH. Stock solutions of these drugs were freshly prepared just before use and then serially diluted in complete culture medium to obtain the desired concentrations.

**Cell Cycle Kinetics.** A culture in exponential growth was trypsinized and plated in a number of Lux 35-mm plastic dishes at  $2 \times 10^5$  cells/dish about 20 hr before the experiment. The experiment was begun by replacing the medium in the dishes with fresh medium containing maytansine. The drug concentrations studied were 0, 0.5, 1.0, 2.0, 4.1, 8.2, 16.4, and 32.8 nM. For each concentration, there were 2 dishes, one for an 18-hr continuous treatment and the other for a pulse treatment of 60 min (followed by a wash to remove the drug) and a posttreatment incubation of 17 hr in regular medium. At the end of this period, the cells were collected by trypsinization, deposited directly on clean slides by the use of a cytocentrifuge, fixed in absolute methanol:glacial acetic acid (3:1, v/v), stained with acetoorcein, and scored for the percentage of cells in mitosis. Five hundred cells were scored for each point. The mitotic accumulation was plotted as a function of dose. The data presented represent an average of 3 experiments.

**Dose-Survival Studies.** The procedures for drug treatment and the determination of plating efficiency have been described previously (9). HeLa cells in exponential growth, which were trypsinized and plated in a number of dishes the day before

the experiment, were exposed to various concentrations of the drug for 1 hr or more, depending upon the purpose of the experiment. At the end of the treatment, medium containing the drug was removed, and cells were washed with drug-free medium, trypsinized, plated for colonies, and incubated for 10 days. The number of colonies observed in the treatments was expressed as a percentage of the value for the untreated control. The plating efficiency of the controls was  $85 \pm 7\%$  (S.D.).

**Evaluation of Drug Combinations.** For the *in vitro* evaluation of combined drug effects, a random population of HeLa cells was exposed first to one drug that was then removed by washing before the second drug was added to the medium. Soon after the drug treatments, cells were washed with regular medium, trypsinized, and plated for colonies. In this study, 2-drug combinations, maytansine:ara-C and maytansine:Adriamycin, were examined. The various schedules included maytansine followed by either ara-C or Adriamycin and the reverse sequence. The duration of exposure of cells to maytansine and Adriamycin was 60 min. However, with ara-C, the treatment was 16 hr because it has been shown that a 16-hr incubation of a random population of HeLa cells with a sublethal dose (0.8  $\mu\text{g/ml}$ ) of ara-C reversibly blocked about 90% of the cells in S phase (9).

## RESULTS

**Effect on Cell Cycle Traverse and Macromolecular Synthesis.** The purpose of this set of experiments was to determine the optimum dose and duration of treatment of HeLa cells with maytansine to produce the maximum cytotoxic effects. The primary effect of maytansine on HeLa cells was the arrest of cells in metaphase. The degree of mitotic accumulation in a random population of HeLa cells after 18 hr of continuous exposure or after 17 hr of incubation following a 1-hr treatment with maytansine is presented in Chart 1. In general, the effects of maytansine on mitotic accumulation were similar to those of Colcemid. The effects of a pulse (60 min) exposure of cells to the drug were reversible at lower ( $0.05$  to  $0.2 \times 10^{-8}$  M) but

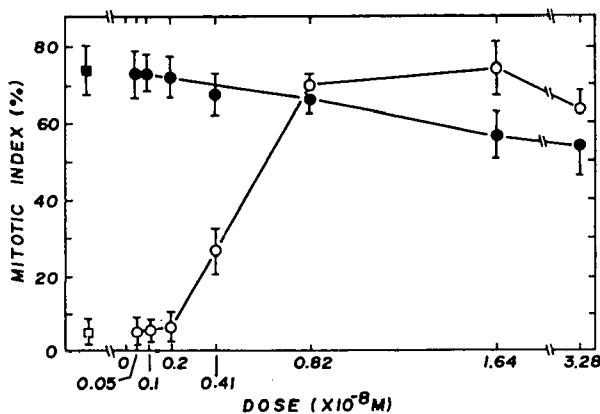


Chart 1. Effect of various concentrations of maytansine on the mitotic accumulation of HeLa cells in exponential growth. ○, a pulse treatment; cells were exposed to maytansine for 60 min; the drug was removed by washing and then incubated in regular medium for 17 hr. ●, cells were incubated with maytansine for 18 hr. Cells exposed to Colcemid ( $1.37 \times 10^{-7}$  M or  $0.05 \mu\text{g/ml}$ ) served as a control to monitor the antimetabolic effects of maytansine. ■, 18 hr continuous Colcemid treatment; □, 1 hr Colcemid treatment followed by 17 hr incubation in regular medium. Bars, S.D.

not at higher concentrations.

Maytansine has no inhibitory effect on the rate of incorporation of tritium-labeled precursors into DNA, RNA, and protein during a 3-hr period (Table 1). However, there was some increase in the incorporation of [ $^3\text{H}$ ]leucine in the presence of Colcemid or maytansine in the medium.

**Effect on Cell Survival.** The effect of a 1-hr treatment with various concentrations of maytansine on the plating (cloning) efficiency of HeLa cells was studied. Initially, the plating efficiency decreased with an increase in dose, but it soon reached a plateau (Chart 2). Further increase in dose had little or no effect on survival until the concentration reached  $6.56 \times 10^{-8}$  M. However, an increase in the duration of treatment resulted in a decrease in the plating efficiency (Chart 3).

**Effect of Dose Fractionation on Survival.** Based on the dose-survival curve in Chart 2, a maytansine concentration of  $1.64 \times 10^{-8}$  M was selected. This dose was fractionated into 2 doses ( $0.82 \times 10^{-8}$  M each), and each was applied for 1 hr, with or without an interval between them. These results indicate that the longer the interval between the split doses (up to a maximum of 8 hr studied) the greater was the decrease in cell survival (Chart 4).

**Cell Cycle Phase-Specific Effects of Maytansine on Plating Efficiency.** When HeLa cells synchronized in various phases of the cell cycle were exposed to maytansine ( $1.64 \times 10^{-8}$  M) for 1 hr, the percentage of survival varied depending upon the phase of the synchronized population (Chart 5). The greatest drug sensitivity was observed in mitotic populations followed by  $G_2$ , S, and  $G_1$ , in order of decreasing sensitivity.

**In Vitro Evaluation of Drug Combinations.** In view of the cell

Table 1  
Effect of maytansine on the incorporation of tritium-labeled precursors in DNA, RNA, and protein  
The data represent the average of 4 experiments.

Treatment	Relative cpm/ $10^6$ cells		
	[ $^3\text{H}$ ]dThd	[ $^3\text{H}$ ]Uridine	[ $^3\text{H}$ ]Leucine
Control	100	100	100
Colcemid (0.05 $\mu\text{g/ml}$ )	$106.4 \pm 4.39^a$	$94.5 \pm 7.20$	$121.2 \pm 11.10$
Maytansine ( $0.656 \times 10^{-8}$ M; $0.5 \text{ ng/ml}$ )	$102.7 \pm 8.10$	$111.3 \pm 10.60$	$152.0 \pm 13.8$

<sup>a</sup> Mean  $\pm$  S.D.

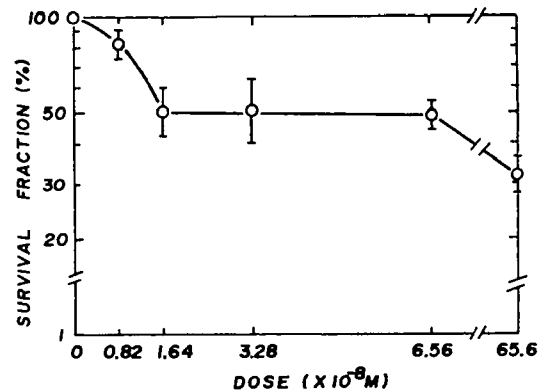


Chart 2. Effect of a 1-hr treatment with various concentrations of maytansine (○) on the plating efficiency of HeLa cells in exponential growth. Bars, S.D.

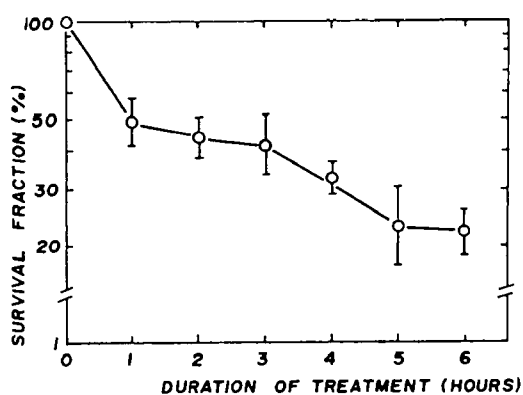


Chart 3. Effect of the duration of maytansine ( $1.64 \times 10^{-8}$  M) (O) treatment on the plating efficiency of HeLa cells in exponential growth. Bars, S.D.

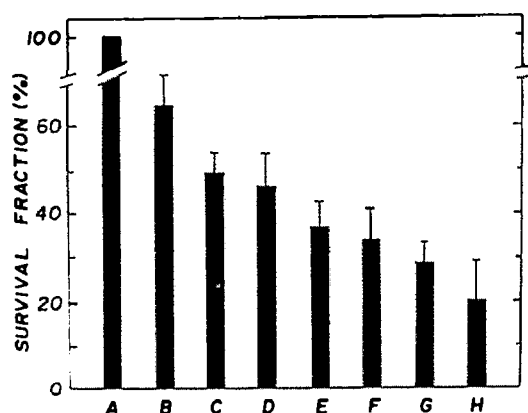


Chart 4. Effect of dose fractionation and the duration of interval between the treatments on the survival of HeLa cells in exponential growth. A, untreated control; B, maytansine treatment ( $0.82 \times 10^{-8}$  M) for 1 hr; C, maytansine treatment ( $1.64 \times 10^{-8}$  M) for 1 hr. For dose fractionation studies, 2 treatments of maytansine at  $0.82 \times 10^{-8}$  M for 60 min each were applied at zero (D), 2- (E), 4- (F), 6- (G), and 8- (H) hr intervals. Bars, S.D.

cycle phase-specific cytotoxicity of maytansine, we decided to study whether there would be any increase in cell kill by synchronizing with a low dose of ara-C and then exposing the cells to maytansine. Schedule-dependent cytotoxic effects were observed in the combination of maytansine with ara-C but not with Adriamycin (Chart 6). Exposure of cells to ara-C for 16 hr followed by a 1-hr treatment with maytansine reduced the plating efficiency to about 25%, as compared with 41% survival when the sequence was reversed. The data presented are the averages of 3 experiments.

### DISCUSSION

The results of this study indicate that maytansine is primarily a mitotic inhibitor. As a mitotic inhibitor, it is effective over a wide range of concentrations (Chart 1). The lowest effective concentration (0.5 nM) for maytansine in HeLa cells is about 200 times smaller than that for Colcemid ( $1.37 \times 10^{-7}$  M). Similarly, maytansine has been shown to be at least 100 times more potent as an antimetabolic agent than vincristine in sea urchin eggs (10).

Continuous treatment of HeLa cells with higher doses of maytansine may slow down the progression of cells through the cell cycle to some extent, as indicated by a slight reduction in the degree of mitotic accumulation (Chart 1). Such retarding

effects are not observed if the duration of treatment is limited to 1 hr. A 60-min treatment with concentrations of maytansine above  $0.82 \times 10^{-8}$  M produces a mitotic block in HeLa cells that remained irreversible up to 18 hr. At concentrations of  $0.2 \times 10^{-8}$  M or lower, the antimetabolic effects are quickly reversible by washing and resuspending the cells in drug-free medium. Similar results were obtained with murine leukemia cells by Wolpert-Defilippes *et al.* (12).

A 3-hr incubation of a random culture of HeLa cells with maytansine at concentrations of  $6.6 \times 10^{-8}$  M had no effect on the incorporation of [ $^3$ H]dThd and [ $^3$ H]uridine into DNA and RNA, respectively. A measurable increase in the uptake of [ $^3$ H]leucine into both Colcemid- and maytansine-treated cells is unexpected. Probably, these agents, due to their disorganizing effects on the cytoskeleton, may increase the permeability of

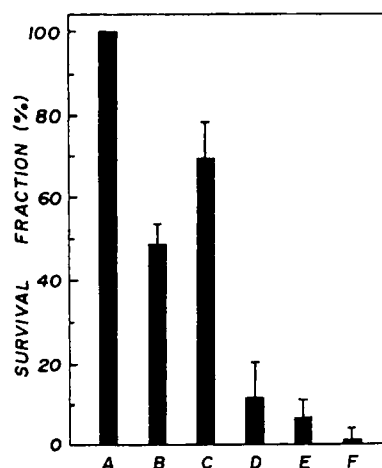


Chart 5. Effect of maytansine ( $1.64 \times 10^{-8}$  M for 60 min) on the plating efficiency of HeLa cells synchronized in various phases of the cell cycle. The number of colonies observed in the treatment is expressed as a percentage of the untreated control for each phase of the cell cycle. A, control, a random culture. Maytansine treatments: B, random culture; C, G<sub>1</sub> phase; D, S phase; E, G<sub>2</sub> phase; F, mitotic populations. Bars, S.D.

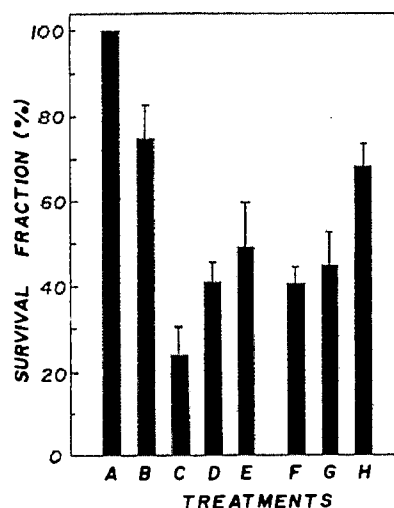


Chart 6. Effect of maytansine in combination with ara-C or Adriamycin on the survival of HeLa cells in exponential growth. The treatments included ara-C (0.8  $\mu$ M) for 16 hr, Adriamycin (0.2  $\mu$ g/ml) for 1 hr, and maytansine ( $1.64 \times 10^{-8}$  M) for 1 hr. A, untreated control; B, ara-C treatment; C, ara-C followed by maytansine; D, maytansine followed by ara-C; E, maytansine alone; F, maytansine followed by Adriamycin; G, Adriamycin followed by maytansine; H, Adriamycin alone. Bars, S.D.

the cell membranes to [<sup>3</sup>H]leucine, thus facilitating greater uptake and consequently greater incorporation of label into the protein than occurs in the control. These results are at variance with those of Wolpert-Defillippes *et al.* (12), who reported that, in murine leukemic cells, DNA synthesis was inhibited to the greatest extent. However, they measured the uptake of labeled precursors into DNA, RNA, and protein by pulse-labeling of cells that were incubated with maytansine over a period of 12 hr. A 12-hr exposure to maytansine at 10<sup>-7</sup> M would certainly block more than 50% of these cells in mitosis. The arrest of a significant fraction of the cell population in mitosis would result in a considerable reduction in the incorporation of label into DNA, RNA, and protein when compared with untreated control cultures.

The dose-survival curve for maytansine (Chart 2) quickly reaches a plateau with an increase in the concentration, indicating that there are 2 cell types in the population, one sensitive and the other relatively resistant. However, with a fixed dose, there is a direct correlation between the duration of treatment and the percentage increase in cell kill (Chart 3). Dose fractionation studies reveal that small fractionated doses are more cytotoxic than is a large single dose (Chart 4). The longer the interval between the fractionated doses, the lower is the plating efficiency up to 8 hr. These results suggest that most of the sensitive fraction in the cell population is killed by the first treatment, whereas the second treatment kills those that move from a resistant to a more sensitive phase of the cell cycle.

Studies with synchronized populations reveal that cells in mitosis are the most sensitive and those in G<sub>1</sub> are the most resistant to this agent (Chart 5). The closer the cell is to mitosis, the more sensitive it is to the cytotoxic effects of maytansine. Depolymerization and inhibition of polymerization of tubulin has been shown to account for the antimitotic effects of maytansine (10). Since oxidation of the sulfhydryl groups in tubulin inhibits its polymerization, the effect of maytansine may be due to its binding to these groups (10). It is also conceivable that tubulin, which is the most important constituent of the mitotic apparatus, accumulates gradually during the cell cycle reaching a peak at the beginning of mitosis (6). Thus, cells in G<sub>2</sub> and mitosis would have a full complement of these proteins, whereas those in G<sub>1</sub> would have the least proteins, with S-phase cells being intermediate. As soon as the cells were exposed to cytotoxic doses of maytansine, the spindle protein (tubulin) would be inactivated (depolymerized) by the irreversible binding of the drug. If the drug were removed after a brief exposure of 60 min, cells in G<sub>1</sub> and to some extent those in S could synthesize new tubulin and thus overcome the antimitotic effects of maytansine. Hence, G<sub>1</sub> cells would be more resistant to maytansine than those in other phases of the cell cycle, as we have observed. In the light of these observations, we can

explain the pattern of the dose-survival curve (Chart 1) as follows. The initial sharp decrease in the plating efficiency represents the killing of cells that were in the sensitive phases of the cell cycle by low concentrations of maytansine. On the other hand, the plateau is represented by the more resistant G<sub>1</sub> fraction, which constitutes about 50% of the population and remains unaffected over a relatively wide range of drug concentrations.

*In vitro* evaluation of the cytotoxic effects of maytansine in combination with ara-C revealed schedule-dependent effects (Chart 6). Administration of maytansine following a 16-hr ara-C treatment is more cytotoxic than the reverse sequence. This could be due to the synchronization of cells in S phase by the ara-C treatment. Our results (Chart 5) indicate that S-phase cells are more sensitive than those in G<sub>1</sub>. Since Adriamycin does not induce cell synchrony, the sequence of administration of Adriamycin and maytansine made no difference in cell survival.

## ACKNOWLEDGMENTS

We thank Dr. Howard Thames for his assistance in statistical analysis.

## REFERENCES

- Blum, R. H., and Kahert, T. Maytansine. A Phase I study of an ansa macrolide with antitumor activity. *Cancer Treat. Rep.*, 62: 435-438, 1978.
- Cabanillas, F., Rodriguez, V., Hall, S. W., Burgess, M. A., Bodey, G. P., and Freireich, E. J. Phase I study of maytansine using a 3-day schedule. *Cancer Treat. Rep.*, 62: 425-428, 1978.
- Chabner, B. A., Levine, A. S., Johnson, B. L., and Young, R. C. Initial clinical trials of maytansine, an antitumor plant alkaloid. *Cancer Treat. Rep.*, 62: 429-433, 1978.
- Kupchan, S. M., Komoda, Y., Brantman, A. R., Dailey, R. G., Jr., and Zimmerly, V. A. Novel maytansinoids. Structural interrelations and requirements for antileukemic activity. *J. Am. Chem. Soc.*, 96: 3706-3708, 1974.
- Kupchan, S. M., Komoda, Y., Court, W. A., Thomas, G. J., Smith, R. M., Karim, A., Gilmore, C. G., Haltiwanger, R. C., and Bryan, R. F. Maytansine, a novel antileukemic ansa macrolide from *Maytenus ovatus*. *J. Am. Chem. Soc.*, 94: 1354-1356, 1972.
- Lawrence, J. H., and Wheatley, D. N. Synthesis of microtubule protein in HeLa cells approaching division. *Cytobios*, 13: 167-179, 1975.
- Rao, R. N. Mitotic synchrony in mammalian cells treated with nitrous oxide at high pressure. *Science*, 160: 774-776, 1968.
- Rao, P. N., and Engelberg, J. Effects of temperature on the mitotic cycle of normal and synchronized mammalian cells. In: I. L. Cameron and G. M. Padilla (eds.), *Cell Synchrony—Biosynthetic Regulation*, pp. 332-352. New York: Academic Press, Inc., 1966.
- Rao, P. N., Freireich, E. J., Bodey, G. P., Gottlieb, J. A., and Smith, M. L. *In vitro* evaluation of 1-β-D-arabinofuranosylcytosine-β-2'-deoxyguanosine combination chemotherapy. *Cancer Res.*, 34: 2539-2543, 1974.
- Remillard, S., and Rebhun, L. I. Antimitotic activity of the potent tumor inhibitor maytansine. *Science*, 189: 1002-1005, 1975.
- Sieber, S. M., Wolpert, M. K., Adamson, R. H., Cysyk, R. L., Bono, V. H., and Johns, D. G. Experimental studies with maytansine—a new antitumor agent. *Bibl. Haematol.*, 43: 495-500, 1976.
- Wolpert-Defillippes, M. K., Adamson, R. H., Cysyk, R. L., and Johns, D. G. Initial studies on the cytotoxic action of maytansine, a novel ansa macrolide. *Biochem. Pharmacol.*, 24: 751-754, 1975.

# **EXHIBIT D**

target (Fig. 2B) or 180° out of phase with it (Fig. 2D). In both situations the unit continued to modulate in relation to the track-target's velocity, increasing its rate with the leftward movement. All 13 track-related Purkinje cells tested on all of these paradigms showed essentially the same pattern of firing. In the few units examined under conditions in which the movements of the target and chair were completely dissociated, track-target motion relative to earth-fixed surroundings was still the crucial factor. Irregularities in firing which are apparent as noise in the reciprocal interval plots tend to obscure the correlation with target velocity; they may reflect microvariations in the monkey's performance which are beyond the resolution of our oculogram recordings but are nonetheless significant.

That these neural correlates of visual tracking in the primate flocculus are probably not mere epiphenomena but may instead reflect some vital role in the programming of pursuit eye movements is suggested by the deficits which follow lesions in this area. Severe, and relatively specific, impairments of smooth pursuit eye movements are often associated with cerebellar atrophy in man (8), and total cerebellectomy in the mature monkey results in the permanent loss of such eye movements (9). Deficits in optokinetic responses after bilateral flocculectomy in monkeys have been reported, but, unfortunately, the animals were not examined specifically for pursuit eye movements of the kind under consideration here (10).

We hypothesize that Purkinje cell output from the primate flocculus provides oculomotor centers with target velocity information essential for visual tracking and represents an output of the smooth pursuit subsystem. In addition, we have some data which may help explain how the flocculus generates these velocity command signals. Most units in the flocculus showed no evidence of a CS, and we assume that they represent one or another of the various input elements known to influence Purkinje cells. The majority of such units fired vigorously in relation to saccadic eye movements often with both transient and tonic components but no apparent special concern with tracking; others seemed to be driven by vestibular inputs, modulating nicely in phase with chair (that is, head) velocity. We became aware of a class of visually driven units lacking CS's; these were especially sensitive to retinal image slip in the region of the fovea and often were more responsive to ipsilateral target movements. Firing of these units may be the putative error signal that ultimately sustains pursuit eye movements. These units

closely resemble those recently described for the monkey's nucleus of the transpeduncular tract (11), a part of the accessory optic system; at least in the rabbit, this tract projects to the flocculus (12). Signal processing in the pursuit system may require a precise velocity representation of the target (13); we propose that this is the function of the Purkinje cells in the primate flocculus. A true neuronal facsimile of the track target's absolute velocity would require the summing of three signals: velocity of the target's retinal image (target motion relative to eye motion), eye velocity (eye motion relative to head motion), and head velocity (head motion relative to earth motion); we know that information concerning the first and last of these reaches the flocculus, and the second might easily be derived from the numerous inputs related to eye movements. A possible complication arises if the system has predictive capabilities, since the tracking waveforms contrived in our study were usually highly periodic (sinusoids and linear ramps).

F. A. MILES  
J. H. FULLER

Laboratory of Neurophysiology,  
National Institutes of Health,  
Bethesda, Maryland 20014

## Antimitotic Activity of the Potent Tumor Inhibitor Maytansine

**Abstract.** *Maytansine, at  $6 \times 10^{-8}M$ , irreversibly inhibits cell division in eggs of sea urchins and clams. It causes the disappearance of a mitotic apparatus or prevents one from forming if added at early stages. Maytansine does not affect formation of the mitotic organizing center but does inhibit in vitro polymerization of tubulin. Maytansine and vincristine inhibit in vitro polymerization of tubulin at about the same concentrations, but vincristine is about 100 times less effective as an inhibitor of cleavage in marine eggs.*

Maytansine, a novel ansa macrolide (Fig. 1), isolated from various *Maytenus* species, is an antitumor agent (1) that significantly inhibits mouse P-388 lymphocytic leukemia in dosages of micrograms per kilogram of body weight, and is active over a 50- to 100-fold dosage range. Maytansine also shows significant inhibitory activity against the L-1210 mouse leukemia, the Lewis lung carcinoma, and the B-16 melanocarcinoma murine tumor systems. This agent is being tested toxicologically in preparation for clinical trials (2).

We report now on the antimitotic effects of maytansine. At a concentration of  $6 \times 10^{-8}M$ , it totally inhibited cleavage in sea urchin eggs when applied at fertilization (3). At  $4 \times 10^{-8}M$ , 10 to 20 percent of the eggs divided (although cleavage was

- ### References and Notes
1. C. Rashbass, *J. Physiol.* **159**, 326 (1961).
  2. N. Sugie and M. Wakakuwa, *IEEE (Inst. Elec. Electron. Eng.) Trans. Syst. Sci. Cyb.* **6**, 103 (1970). This study on man showed that eye-tracking performance is independent of head movement. No similar data are available for the monkey, although J. Dichgans *et al.* [*Brain Res.* **71**, 225 (1974)] attest to the efficacy of the vestibulo-ocular reflex in this species.
  3. R. H. Wurtz, *J. Neurophysiol.* **32**, 975 (1969).
  4. E. V. Everts, *Electroencephalogr. Clin. Neurophysiol.* **24**, 83 (1968).
  5. M. Ferin, R. A. Grigorian, P. Strata, *Exp. Brain Res.* **12**, 1 (1971).
  6. About one-quarter of the units identified as Purkinje cells showed no consistent modulation with any of the parameters considered in our study, except for rather weak, transient pauses during saccadic movements. Some of these neurons may have been involved in vertical tracking, a possibility we did not investigate.
  7. That Purkinje cell activity in primate flocculus modulates when the oscillating animal tracks a target moving with him but not when the target is stationary was first reported by S. G. Lisberger, and A. F. Fuchs [*Brain Res.* **69**, 347 (1974)].
  8. J. Corvera, G. Torres-Courtney, G. Lopez-Rios, *Ann. Otol. Rhinol. Laryngol.* **82**, 855 (1973); R. W. Baloh, H. R. Konrad, V. Honrubia, *Neurology* **25**, 160 (1975); D. S. Zee *et al.*, *Trans. Am. Neurol. Assoc.*, in press.
  9. G. Westheimer and S. M. Blair, *Invest. Ophthalmol.* **12**, 618 (1973).
  10. S. Takemori and B. Cohen, *Brain Res.* **72**, 213 (1974).
  11. G. Westheimer and S. M. Blair, *Invest. Ophthalmol.* **13**, 533 (1974).
  12. K. Maekawa and J. I. Simpson, *J. Neurophysiol.* **36**, 649 (1973). The visual responses in the rabbit flocculus are mediated by climbing fibers, in contrast to the presumed mossy fiber responses reported here.
  13. L. R. Young, in *The Control of Eye Movements*, P. Bach-y-Rita and C. C. Collins, Eds. (Academic Press, New York, 1971), p. 429.

17 March 1975; revised 27 May 1975

somewhat irregular). The remaining eggs formed irregular furrows that either did not separate equal-sized blastomeres or they subsequently retracted. When the eggs were treated with  $10^{-8}M$  (or less) maytansine, the cleavage time, cleavage pattern, and later development were normal.

The critical time in egg development for inhibition of cleavage by  $10^{-7}M$  maytansine was determined by adding the drug at 5-minute intervals, from the time of fertilization to first cleavage. Cleavage was totally inhibited when the drug was added at any time during the first half of the cleavage period; after that, an increasing number of cells went through some form of cleavage. However, even when the drug was added 10 minutes prior to cytokinesis, approximately 40 percent of the eggs did



not cleave, and those that did, looked irregular and did not cleave a second time. When drug was added to unfertilized eggs for at least 1 hour, it could be removed prior to fertilization, with normal cleavage and development following. Drug added immediately after fertilization could be removed by repeated washings in seawater up to 20 minutes after fertilization, with minimal effects on cleavage pattern or rate. If removed between 20 and 30 minutes, irregular cleavages occurred; and if removed 30 minutes or more after fertilization, cleavage (which occurs 60 to 90 minutes after this point in controls) was permanently inhibited. Both the minimum concentration and critical time for total inhibition of cleavage were the same for the eggs of the sea urchins *Strongylocentrotus purpuratus* and *Lytechinus pictus*.

We investigated the possibility that the critical process affected by maytansine is DNA synthesis by determining the incorporation of [<sup>3</sup>H]thymidine (4). The rate and amount of DNA synthesis was the same in eggs treated continuously with 10<sup>-7</sup>M maytansine from 10 minutes before fertilization as that in controls, even though cleavage was totally inhibited in treated eggs.

In sea urchin eggs treated with 10<sup>-7</sup>M maytansine before fertilization or starting 10 to 15 minutes after fertilization, fusion of the male and female pronuclei never occurred. A sperm aster (SA) (5) did not form in the egg. Since this body is necessary for the transport of the pronuclei to the egg center (5), pronuclear fusion does not occur in its absence. Further, since microtubules form an integral part of the SA (6), these observations suggested that maytansine may interfere with microtubule formation or tubulin mobilization into the aster.

To investigate the possibility that the drug might prevent the formation of mitotic apparatuses (MA's) as well as SA's, we used clam eggs (from *Spisula solidissima*) because of the ease with which the MA can be seen with a polarization microscope and the rapidity of MA formation [the MA starts to form about 10 minutes after fertilization or activation (7)]. Eggs treated with 10<sup>-7</sup>M maytansine in seawater were parthenogenetically activated with KCl-seawater solutions (7). Activation of the eggs was normal and rupture of the nuclear membrane occurred on schedule with drug treatment, but an MA did not form. When maytansine was applied as late as 10 minutes after activation, an MA was not obtained; but eggs treated with 10<sup>-8</sup>M maytansine had normal MA's (similar to those of the controls). Examination of eggs activated in the presence of maytansine at con-

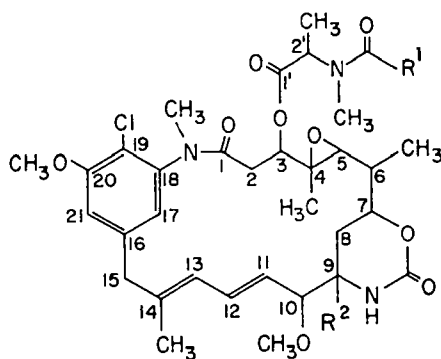


Fig. 1. Maytansine, R<sup>1</sup> = CH<sub>3</sub> and R<sup>2</sup> = OH; maytanbutine, R<sup>1</sup> = CH(CH<sub>3</sub>)<sub>2</sub> and R<sup>2</sup> = OH; maytanbutine 9-*n*-propyl thioether, R<sup>1</sup> = CH(CH<sub>3</sub>)<sub>2</sub> and R<sup>2</sup> = SCH<sub>2</sub>CH<sub>2</sub>CH<sub>3</sub>.

centrations between 10<sup>-8</sup>M and 10<sup>-7</sup>M revealed the following. At 3 × 10<sup>-8</sup>M, the MA was about one-half normal length and width (Fig. 2, a and b); at 6 × 10<sup>-8</sup>M (a dose that completely blocked polar body

formation) the MA was approximately one-third normal length and one-fourth normal width (Fig. 2c); at 10<sup>-7</sup>M a very small birefringent MA was present in the center of the egg and could not be seen without compressing the egg (Fig. 2d). Thus, maytansine regulates the size of the MA in a dose-dependent manner.

We studied the question of whether maytansine could affect SA's in sea urchin or MA's in clam eggs once the structure had already formed. We found that SA's in sea urchin eggs and already formed MA's in clam eggs could be made to shrink in a dose-dependent manner by application of maytansine. Although exact measurements have not yet been made, the final size of the MA appears to be the same whether the MA formed in the presence of certain concentrations of maytansine or whether that concentration is added subsequent to MA formation.

Maytansine inhibits the formation of

Fig. 2. (a) Normal eggs of the surf clam *Spisula solidissima* observed with a polarization microscope. Contrast in the MA depends on its orientation relative to the axes of the microscope and can be reversed by rotation of the MA axis by 90° or change in angle of a compensator (×300). (b) *Spisula* egg treated with 3 × 10<sup>-8</sup>M maytansine prior to activation. The MA is reduced in size; the egg will form a first polar body, but it is considerably delayed in time (×300). (c) *Spisula* egg treated with 6 × 10<sup>-8</sup>M maytansine prior to activation. The first polar body never forms (×300). (d) *Spisula* egg treated with 2 × 10<sup>-7</sup>M maytansine prior to activation and compressed to visualize very small MA still remaining in the cytoplasm (×300). (e) *Spisula* egg treated with 6 × 10<sup>-8</sup>M maytansine plus 3 percent HG; compare with (c). The degree of augmentation with glycols decreases with increasing concentration of maytansine (×300). (f) *Spisula* egg in 2 × 10<sup>-7</sup>M maytansine treated with 3 percent HG to "develop" the MA after 30 minutes. Double MA indicates replication of the MTOC (×300). (g) Eggs of sea urchin *S. purpuratus* treated with 2 × 10<sup>-7</sup>M maytansine to eliminate SA (×190). (h) Augmented SA in *S. purpuratus* eggs treated with 5 percent HG (×190). (i) *S. purpuratus* eggs treated with 5 percent HG to which 4 × 10<sup>-7</sup>M maytansine is then added. SA is reduced in size in a dose-dependent manner similar to the phenomenon in MA of clam eggs (×190).

the MA, either by inhibition of a mitotic organizing center (MTOC) (8), by interference with tubulin polymerization onto the center, or by some other mechanism. We tested the possibility that it might act on the MTOC by utilizing the long-chain glycol hexylene glycol (HG) since HG and other similar glycols cause augmentation of size and birefringence of SA's and MA's in a manner requiring the presence of an active MTOC (9). For these experiments both clam and sea urchin eggs were treated with maytansine before, at the same time as, or after treatment with 3 percent HG in seawater. At concentrations of  $10^{-7}M$  maytansine an SA or MA was formed which was intermediate in size between normal and augmented SA's (Fig. 2, g to i) and MA's; at  $3 \times 10^{-7}M$  maytansine, even the augmented structures could be caused to disappear. Further, clam eggs activated in maytansine and left for a half hour or so show multiple MA's or asters when augmented with glycols (Fig. 2f), suggesting that replication of the MTOC is not inactivated by the drug. Thus, maytansine does not appear to affect the ability of the MTOC to divide or to act as an organizing center for tubulin assembly. In this respect it acts in a manner similar to that of colchicine (8).

We then studied the effects of maytansine on brain tubulin polymerization (10), which can be used as a model for MA tubulin (11). Rabbit or pig brain tubulin was prepared by a slight modification of the method of Weisenberg (10) and purified through one or two cycles of polymerization. In each case polymerized microtubules were washed in buffer by centrifugation, a procedure that yields relatively pure tubulin after one cycle of polymerization, as judged by sodium dodecyl sulfate gel electrophoresis. Microtubules were depolymerized by cooling to  $0^{\circ}C$  in buffer in which guanosine triphosphate (GTP) was absent, and the resulting tubulin was used in subsequent experiments. Polymeri-

zation of tubulin was followed by turbidity increase at 310 nm (12) in a Gilford automatic recording spectrophotometer at  $37^{\circ}C$ . A sample of tubulin containing  $1 mM$   $Ca^{2+}$  and no added GTP was used as a blank, and turbidity was recorded as the difference between sample and blank. Polymerization was initiated by adding GTP to tubulin at  $37^{\circ}C$ . In initial experiments, maytansine was added to cold tubulin. Total inhibition of polymerization was found at  $10^{-5}M$  maytansine in tubulin solutions of 4 to 5 mg/ml. With  $5 \times 10^{-6}M$  maytansine the extent of polymerization of tubulin at 5 mg/ml was about 50 percent, as judged by turbidity at plateau levels. Maytansine added to polymerized tubulin caused a rapid decrease in turbidity to levels approximately the same as those attained when the same concentration was added before polymerization was started (Fig. 3). Inhibition of polymerization is about one-half at a mole ratio of 1 part of maytansine to 10 parts of tubulin, and total inhibition occurs at a mole ratio of 1 to 5.

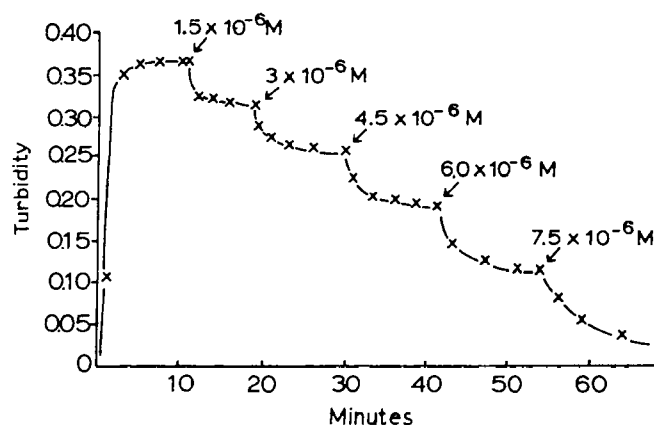
To ascertain whether the mole ratio of maytansine to tubulin required for inhibition of in vitro polymerization could account for its antimetabolic effects we assumed that maytansine would equilibrate between seawater and egg cytoplasm. The number of tubulin subunits in an MA the size of that of *S. purpuratus* is about  $2 \times 10^8$  (13). Since the egg diameter is 75  $\mu m$ , there should be about  $1.2 \times 10^7$  molecules of maytansine in each egg at  $10^{-7}M$  in the seawater if the drug equilibrates, and more if accumulation occurs. This is a ratio of 1 maytansine molecule to 16 tubulin molecules. Since brain tubulin has been shown to be a good model for MA tubulin (11), these results suggest that the inhibition of tubulin polymerization by maytansine can account for its in vivo antimetabolic effects, given the nature of the calculations. Initial uptake experiments with  $[^3H]$ maytansine suggest a rapid accumula-

tion of maytansine by eggs although the kinetics are not simple. They nevertheless suggest that enough maytansine enters the egg to support the above analysis.

Because the report of Wolper-Defilippes *et al.* (14) (which appeared as our experiments were nearing completion) suggested a relation of maytansine to vincristine in its antimetabolic effects, we compared the two drugs for inhibition of tubulin polymerization in vitro and for inhibition of cleavage in vivo. Sea urchin eggs did not cleave in  $10^{-5}M$  vincristine but formed irregular shallow furrows. At  $5 \times 10^{-6}M$  vincristine cleavage was approximately normal; thus, maytansine is at least 100 times more potent as an antimetabolic agent than vincristine. A difference in potency of about 15-fold was obtained with Chinese hamster ovary cells in culture. The molar concentration of vincristine necessary to inhibit polymerization of a given amount of brain tubulin, however, is actually somewhat lower for vincristine, and the kinetics of inhibition are very different. Colchicine inhibits tubulin polymerization in vitro at molar ratios even lower than that of maytansine (15) but requires a minimum dose of  $10^{-4}M$  or more for inhibition of cleavage in sea urchin eggs (16). Why such marked differences of potency for MA inhibition in vivo exist in the face of the ability of all agents to inhibit brain tubulin polymerization in vitro to approximately the same degree is not known, but may be due to differences in uptake. However, another possibility suggests itself since we have found that oxidation of the sulfhydryl groups in tubulin inhibits its polymerization (17); conceivably maytansine acts by binding certain key sulfhydryls of tubulin.

The latter suggestion is supported by the readiness with which maytanbutine, a homologous maytansine ester, alkylated *n*-propane thiol to form the 9-*n*-propyl thioether (18). Presumably, maytansine may alkylate protein thiols in an analogous manner (2). We have also found that geld-

Fig. 3. Change in turbidity at 310 nm (ordinate) as a function of time. Brain tubulin was prepared as described in the text and was resuspended at 4.7 mg/ml ( $4.27 \times 10^{-5}M$ , assuming a molecular weight of 110,000 for tubulin). Polymerization was followed at  $37^{\circ}C$  by recording turbidity increase at 310 nm after addition of GTP (12) with the use, as a blank, of a sample of the same tubulin that was made  $1 mM$  in  $CaCl_2$  and which had no added GTP (thus, polymerization was inhibited). Maytansine was added to sample and blank at the indicated points to give the final concentrations shown. The plateau levels reached were the same as those attained (within about 10 percent) if maytansine was added prior to initiation of polymerization by GTP. The turbidity in  $7.5 \times 10^{-6}M$  maytansine eventually reached the baseline. In each case a portion of the sample was checked for birefringence with a polarizing strain detector. Birefringence only disappeared in the  $7.5 \times 10^{-6}M$  sample when turbidity (compared to blank) vanished. We have found that birefringence of tubulin solutions always correlates with the presence of microtubules when viewed with the electron microscope. The ratio of tubulin to maytansine for decrease of turbidity by one-half was approximately 10:1 in four separate experiments performed at different tubulin concentrations. The ratio for complete depolymerization was approximately 5:1.



anamycin, an ansa macrolide closely related to maytansine (19) but lacking the carbinolamide functionality involved in -SH alkylation (and which does not show antileukemic activity), is 1000 times less effective in inhibition of sea urchin egg cleavage. However, at  $5 \times 10^{-3} M$  geldanamycin affects the MA in a manner analogous to that of maytansine and the effect is reversible.

Why some tumors should be sensitive to maytansine in vivo when it is an antimetabolic agent which can also inhibit normal cells is not clear. We know of no evidence that tubulin of tumor cells differs from that of normal cells. However, microtubules have been implicated in certain cell surface related processes in lymphocytes, polymorphonuclear leukocytes, and other cells (20); and, since tumor cell surfaces differ from those of normal cells (21), it is not unlikely that specificity resides in such cell surface properties.

STEPHEN REMILLARD  
LIONEL I. REBHUN

Department of Biology,  
University of Virginia,  
Charlottesville 22903

GARY A. HOWIE, S. MORRIS KUPCHAN  
Department of Chemistry,  
University of Virginia

#### References and Notes

- S. M. Kupchan, Y. Komoda, W. A. Court, G. J. Thomas, R. M. Smith, A. Karim, C. J. Gilmore, R. C. Haltiwanger, R. F. Bryan, *J. Am. Chem. Soc.* **95**, 1354 (1972).
- S. M. Kupchan, *Fed. Proc.* **33**, 2288 (1974).
- Maytansine is sparingly soluble in water. It was stored at 4°C at  $3 \times 10^{-3} M$  in dimethyl sulfoxide and diluted into seawater or tissue culture media as desired; final concentrations of dimethyl sulfoxide were never above 0.1 percent. These levels had no effects on egg development, cell morphology, or cell division in tissue culture.
- R. T. Hindgartner, B. Rad, D. E. Feldman, *Exp. Cell Res.* **36**, 53 (1964).
- E. B. Wilson, *The Cell* (Macmillan, New York, 1928), p. 400.
- L. I. Rebhun, M. Mellon, D. Jemiolo, J. Nath, N. Ivy, *J. Supramol. Struct.* **2**, 466 (1974); L. I. Rebhun, D. Jemiolo, N. Ivy, M. Mellon, J. Nath, *Ann. N.Y. Acad. Sci.*, in press.
- R. D. Allen, *Biol. Bull. (Woods Hole)* **105**, 213 (1953); L. I. Rebhun, *ibid.* **117**, 518 (1959).
- R. C. Weisenberg and A. C. Rosenfeld, *J. Cell Biol.* **64**, 146 (1975).
- L. I. Rebhun and N. Sawada, *Protoplasma* **68**, 1 (1969).
- R. C. Weisenberg, *Science* **177**, 1104 (1972).
- L. I. Rebhun, *Am. Zool.*, in press.
- F. Gaskin and C. R. Cantor, *J. Mol. Biol.* **89**, 737 (1974); Y. P. Lee, F. E. Samson, L. L. Houston, R. H. Himes, *J. Neurobiol.* **5**, 317 (1974).
- W. D. Cohen and L. I. Rebhun, *J. Cell Sci.* **6**, 159 (1969).
- M. K. Wolpert-Defilippes, R. H. Adamson, R. L. Cysyk, D. G. Jones, *Biochem. Pharmacol.* **24**, 751 (1975).
- L. Wilson, J. R. Bamberg, S. B. Mizel, L. M. Grishom, K. M. Creswell, *Fed. Proc.* **33**, 158 (1974).
- I. Cornman and M. E. Cornman, *Ann. N.Y. Acad. Sci.* **51**, 1443 (1951).
- M. Mellon, J. Nath, L. I. Rebhun, unpublished results.
- Maytanbutine 9-*n*-propyl thioether was obtained in 55 percent yield by treatment of maytanbutine in methylene chloride and trifluoroacetic acid with *n*-propyl thiol for 16 hours at room temperature. The physical constants for the thioether are: melting point (with decomposition) 202° to 204°C; specific rotation at 23°C for the sodium D line ( $[\alpha]_D^{23}$ ) -97° (c, 0.0421, chloroform); ultraviolet absorption maximum (ethanol) (log  $\epsilon$ ), 233 (4.41), 245 (4.38), 255 (4.41), 281 (3.71), 289 (3.69) nm; infrared ab-

sorption maximum (chloroform), 2.92, 3.34, 3.37, 3.41, 5.74, 5.86, 6.03, 6.12  $\mu m$ ; mass spectrum  $m/e$  777 (M<sup>+</sup>); elemental analysis, found: C, 59.96 percent; H, 7.34 percent; N, 5.55 percent; calculated for C<sub>39</sub>H<sub>56</sub>ClN<sub>3</sub>O<sub>9</sub>S, C, 60.17 percent; H, 7.26 percent; N, 5.40 percent.

- K. Sasaki, K. L. Rinehart, Jr., G. Slomp, M. F. Gnstic, E. C. Olsen, *J. Am. Chem. Soc.* **92**, 7591 (1970).
- R. D. Berlin and T. E. Ukena, *Nat. New Biol.* **238**, 120 (1972); G. M. Edelman, I. Yahara, J. L. Wang,

*Proc. Natl. Acad. Sci. U.S.A.* **70**, 1442 (1973); A. Hsieh and T. T. Puck, *ibid.* **68**, 358 (1971).

- R. Hynes, *Cell* **1**, 147 (1974).
- Supported by NSF grant BMS 73-00812 A01 (to L.J.R.), NIH grant CA-12059 (to S.M.K.), and an NIH postdoctoral fellowship (G.A.H.). We thank Dr. J. Nath and M. Mellon for help with the tubulin polymerization experiments and Dr. H. B. Wood, Jr., for a sample of geldanamycin.

11 April 1975; revised 13 May 1975

## Cancer by County: New Resource for Etiologic Clues

**Abstract.** Mapping of U.S. cancer mortality by county has revealed patterns of etiologic significance. The patterns for bladder cancer in males point to industrial determinants: some are known (chemical manufacturing) but others (automobile and machinery manufacturing) represent new leads for epidemiologic study. By contrast, the geographic clusters of high rates of stomach cancer in both sexes are consistent with ethnic susceptibility.

Geographic variation in cancer mortality in the United States has usually been evaluated on a state-by-state basis. The paucity of clues to cancer etiology arising from such surveys can be traced to the heterogeneity of statewide populations. Counties may provide a compromise, as units small enough to be homogeneous for demographic and environmental characteristics that might influence cancer risk, and yet large enough for stable estimates of site-specific cancer mortality. We have made some preliminary observations that illustrate the value of county mortality measurements in providing leads to the origins of cancers.

We obtained age-, race-, and sex-specific numbers of cancer deaths for the 3056 counties of the contiguous United States over a 20-year period, 1950-1969, from the National Center for Health Statistics, Rockville, Maryland. Corresponding county populations were provided by the 1950, 1960, and 1970 censuses (1), with in-

tercensal estimates derived by linear interpolation. For 35 cancer sites, we calculated age-standardized mortality rates by race and sex in each county, the standard being the age distribution of the entire U.S. population in 1960. Ninety-five percent confidence intervals were computed using the standard error of the age-standardized rate as determined by the method of Chiang (2). Differences between the county and national rates were statistically significant when the 95 percent confidence intervals for these rates did not overlap. Tabulations of cancer mortality rates by county were recently compiled (3).

Although population-based mortality data are a crude means of testing hypotheses concerning public health hazards, geographic correlations with environmental measurements can be done quickly and inexpensively, and may be a valuable first step in evaluating possible dangers. In this manner we have assessed cancer mortality patterns among people residing where drinking water is contaminated by asbestos (4), where homes are built on radioactive tailings from uranium mines (5), and where the chemical industry is highly concentrated (6).

The major contribution of the county resource, however, is in hypothesis formulation, namely the detection of geographic clustering that suggests etiologic clues, which can then be pursued by epidemiologic studies of an analytical type. Computer-generated maps were produced to visualize the spatial configuration of cancer mortality by county. We first plotted the distribution for bladder cancer, the tumor most strongly linked to occupational exposures (7). In white males there were clusters of elevated mortality in heavily industrialized areas (Fig. 1), a pattern that was not duplicated in females. The clusters in males suggest industrial hazards that should be evaluated.

To further characterize the possible hazards, we selected for correlation analysis a

Table 1. Industrial categories in which the percentage of men employed in counties where the bladder cancer risk is high differed significantly ( $P < .05$ ) from the percentage of men employed nationwide. See text for method of selecting high-risk counties. Abbreviations: Exp., expected; Obs., observed.

Industry	Percentage of employed men		
	In the U.S. (Exp.)	In high-risk counties (Obs.)	Obs./Exp.
Agriculture	15.8	4.2	0.3
Mining	2.2	0.3	0.1
Manufacturing	27.0	42.2	1.6
Furniture, lumber, wood	2.7	1.4	0.5
Nonelectrical machinery	2.8	6.3	2.3
Electrical machinery	1.3	2.8	2.2
Motor vehicles	1.9	4.8	2.5

# **EXHIBIT E**

# Growth Regulation of Human Breast and Ovarian Tumor Cells by Heregulin: Evidence for the Requirement of ErbB2 as a Critical Component in Mediating Heregulin Responsiveness

Gail D. Lewis, Julie A. Lofgren, Amy E. McMurtrey, Andrew Nuijens, Brian M. Fendly, Kenneth D. Bauer, and Mark X. Sliwkowski<sup>1</sup>

Genentech, Inc., South San Francisco, California 94080

## ABSTRACT

Alterations in the expression of the epidermal growth factor (EGF) receptor ErbB family are frequently encountered in a number of human cancers. Two of these receptors, ErbB3 and ErbB4, are known to bind a family of related proteins termed heregulins (HRGs) or *neu* differentiation factors. In biologically relevant systems, interaction of HRG with ErbB3 or ErbB4 results in the transactivation of ErbB2. In this report, we show that ErbB2 is a critical component in mediating HRG responsiveness in a panel of human breast and ovarian tumor cell lines. Because HRGs have been reported to elicit diverse biological effects on cultured cells, including growth stimulation, growth inhibition, and induction of differentiation, we systematically examined the effect of rHRG $\beta$ 1 on tumor cell proliferation. HRG binding studies were performed with a panel of breast and ovarian tumor cell lines expressing a range of levels of ErbB2. The biological responses to HRG were also compared to EGF and to the growth-inhibitory anti-ErbB2 antibody, 4D5. In most cases, HRG stimulation of DNA synthesis correlated with positive effects on cell cycle progression and cell number and with enhancement of colony formation in soft agar. On each cell line tested, the HRG effects were distinguishable from EGF and 4D5. Our findings indicate that HRG induces cell proliferation in a number of tumor cell lines. In addition, we show that methods for measuring cell proliferation, as well as experimental conditions, are critical for determining HRGs effect on tumor cell growth *in vitro*.

## INTRODUCTION

Clinical interest in the ErbB family of receptor tyrosine kinases stems from the observations that these receptors are frequently over-expressed in a number of human cancers (1-5). Five different gene products are known to activate the prototypical member of this family, EGFR.<sup>2</sup> In several different tumor types, the coexpression of EGFR with one of its cognate ligands, transforming growth factor  $\alpha$ , has been correlated with greater metastatic potential (6, 7). A second group of ligands, which collectively have been termed neuregulins, are known to arise from alternative splicing of a single gene mapped to human chromosome 8p22-p11 (8, 9). This family of proteins which includes HRG (10), NDF (11, 12), gp30 (13, 14), acetylcholine receptor-inducing activity (15), glial growth factor (16), and sensory and motor neuron-derived factor (17) are ligands for ErbB3 and ErbB4 (18). One hallmark of this class of receptors is their propensity for heterodimerization, which upon ligand stimulation can lead to transphosphorylation and ultimately transactivation (19). To date, no ligands have been characterized, to the extent that their cDNA clones have been obtained, that specifically interact with ErbB2. ErbB2 is, however, frequently transactivated by either EGFR ligands or neu-

regulins, and in several instances, the activation of ErbB2 has been shown to be essential for the generation of an active receptor signaling complex (20-22).

The importance of ErbB2 as a negative prognostic indicator in breast (23) and ovarian (24) cancer is now well established (25). Since HRG (10) and NDF (11) were originally identified based on their ability to activate ErbB2, it is of interest to determine the biological outcome of this activation on the growth of human breast and ovarian tumor cells. To address this question, we have undertaken a systematic study of HRG responsiveness using a panel of human breast and ovarian tumor cell lines with known ErbB2 levels. These cell lines were then characterized with regard to both their affinities and capacities to bind HRG. Antibodies directed against ErbB2 were used to determine if ErbB2 was essential in mediating HRG interactions with ErbB3 or ErbB4. To determine whether HRG treatment of these tumor cell lines resulted in cell proliferation (10) or growth inhibition (12, 26), we performed these assays under a series of well-defined experimental conditions and using a number of different assay formats. In addition, HRG responses were compared to EGF and a cytostatic monoclonal antibody directed against ErbB2, 4D5 (27, 28). Our conclusions from these studies are that ErbB2 plays a critical role in mediating HRG responsiveness over a wide range of ErbB2 expression levels. Cellular responses to exogenous HRG under carefully controlled experimental conditions are cell specific but, in general, result in the proliferation of human breast and ovarian tumor cells. These studies suggest that development of HRG antagonists or compounds that target HRG receptors may find clinical utility in the treatment of a number of important human cancers.

## MATERIALS AND METHODS

**Cells and Cell Culture.** The following cell lines were obtained from the American Type Culture Collection: MCF7, SK-BR-3, MDA-MB-175-VII, MDA-MB-231, MDA-MB-361, MDA-MB-453, MDA-MB-468, BT-474, HBL-100, T47D, BT-20, BT-483, Caov3, and SK-OV-3. For all experiments, cells were used between passages 5 and 15. All lines were maintained in Ham's F-12:DMEM (50:50) supplemented with 10% heat-inactivated FBS and 2 mM L-glutamine.

**HRG Binding Assays.** Tumor cells were plated in 24-well plates at  $10^5$  cells/well in F12/DMEM containing 10% FBS. After 48 h, the cultures were washed two times with F12/DMEM. Cells were placed on ice and briefly incubated with binding buffer (0.1% BSA in F12/DMEM). <sup>125</sup>I-labeled rHRG $\beta$ 1<sub>177-244</sub> (5 pM to 2 nM) was then added to each well. Binding reactions were performed for 4 h on ice. Kinetic studies showed that equilibrium was obtained at 4 h, and no significant changes in binding constants were observed if the reactions were conducted up to 16 h. Cells were then washed twice with 0.5 ml binding buffer, and bound radioactivity was determined after solubilization with 0.1% SDS in 0.1 N NaOH or with 8 M urea in 3 M acetic acid. Scatchard analysis was performed as described previously (10, 29). The values reported in Table 1 for these binding experiments are the average of three different binding experiments, each of which consisted of triplicate incubations for each concentration of <sup>125</sup>I-labeled rHRG $\beta$ 1<sub>177-244</sub> tested. Error values for both  $K_d$  and sites/cell were on the order of 10% or less for each binding experiment.

Received 10/16/95; accepted 1/17/96.

The costs of publication of this article were defrayed in part by the payment of page charges. This article must therefore be hereby marked *advertisement* in accordance with 18 U.S.C. Section 1734 solely to indicate this fact.

<sup>1</sup> To whom requests for reprints should be addressed, at Genentech, Inc., Mail Stop 63, South San Francisco, CA 94080. Phone: (415) 225-1247; Fax: (415) 225-5945; E-mail: marks@gene.com.

<sup>2</sup> The abbreviations used are: EGFR, epidermal growth factor receptor; HRG, heregulin; NDF, *neu* differentiation factor; FBS, fetal bovine serum; PI3-kinase, phosphatidylinositol 3'-kinase.

Inhibition of HRG binding to tumor cell lines by anti-ErbB2 antibodies were also performed on ice with monolayer cultures in a 24-well-plate format. Anti-ErbB2 monoclonal antibodies were added to each well and incubated for 30 min.  $^{125}\text{I}$ -labeled rHRG $\beta 1_{177-244}$  (25 pM) was added, and the incubation was continued for 4 to 16 h. For several cell lines, incubations were performed for 4 h, since longer incubations at reduced temperatures resulted in cells detaching from the plate.

**Tyrosine Phosphorylation Assays.** MCF7 cells were plated in 24-well plates as described above for HRG binding experiments. Monoclonal antibodies to ErbB2 were added to each well and incubated for 30 min at room temperature; then rHRG $\beta 1_{177-244}$  was added to each well for a final concentration of 0.2 nM, and the incubation was continued for 8 min. Media was carefully aspirated from each well, and reactions were stopped by the addition of 100  $\mu\text{l}$  of SDS sample buffer (5% SDS, 25 mM DTT, and 25 mM Tris-HCl, pH 6.8). Each sample (25  $\mu\text{l}$ ) was electrophoresed on a 4–12% gradient gel (Novex) and then electrophoretically transferred to polyvinylidene difluoride membrane. Antiphosphotyrosine (4G10, from UBI, used at 1  $\mu\text{g}/\text{ml}$ ) immunoblots were developed, and the intensity of the predominant reactive band at  $M_r \sim 180,000$  was quantified by reflectance densitometry, as described previously (10, 29).

**Cell Proliferation Determined by [ $^3\text{H}$ ]Thymidine Incorporation into DNA.** Cells were seeded into 96-well plates at a density of  $10^4/\text{well}$  for treatments up to 3 days and  $5 \times 10^3/\text{well}$  for the 6-day incubation. Following an overnight incubation to allow for cell adherence, the medium was removed and replaced with medium containing 0.1% FBS to growth arrest the cells. After a 48-h incubation, this medium was replaced with medium containing 0.1, 1.0, or 10% FBS and rHRG $\beta 1$  (5 pM–10 nM), 3 nM EGF (Sigma Chemical Co.), or 10  $\mu\text{g}/\text{ml}$  (65 nM) of the anti-ErbB2 monoclonal antibody 4D5 (27, 28, 30). The cells were then incubated for 0.5, 1, 3, or 6 days, pulsed with 1  $\mu\text{Ci}/\text{well}$  [ $^3\text{H}$ ]thymidine (Amersham) for 4 h, and harvested onto Unifilter GF/C plates (Packard Instrument Co.) using a Packard Filtermate 196 harvester. After allowing the filter plates to dry, MicroScint 20 liquid scintillation cocktail (Packard) was added to each well; then the plates were heat-sealed and counted in a Packard Topcount.

**Cell Cycle Analysis.** Cells were plated at a density of  $2 \times 10^6$  cells/dish in  $60 \times 15\text{-mm}$  culture dishes and allowed to adhere overnight. The monolayers were then washed with PBS and incubated with medium containing 0.1% FBS for 48 h to arrest cell growth. The medium was removed and replaced with medium supplemented with 0.1, 1.0, or 10% FBS alone or containing 0.3 nM rHRG $\beta 1$ , 3 nM EGF, or 65 nM 4D5. After a 1-day incubation, the cells were trypsinized, washed with PBS, fixed in ice-cold methanol, and stored at  $-20^\circ\text{C}$ . The fixed cells were then washed twice with PBS and incubated with 100  $\mu\text{g}/\text{ml}$  RNase (Worthington Biochemical) for 30 min at  $37^\circ\text{C}$ . The RNase was removed by centrifuging the cells, and the pellet was incubated with 50  $\mu\text{g}/\text{ml}$  propidium iodide (Molecular Probes, Inc.) in PBS for DNA staining. The samples were then incubated overnight at  $4^\circ\text{C}$  and analyzed on an Epics Elite flow cytometer (Coulter Corporation) using Modfit LT software (Verity Software House).

**Cell Proliferation Assay with Crystal Violet.** Tumor cells were plated at a density of  $2 \times 10^4/\text{well}$  in 96-well plates in media containing 0.1% FBS and allowed to adhere for 2 h. Monoclonal antibodies (10 nM) or media alone were added, and the cells were incubated for 2 h at  $37^\circ\text{C}$ . rHRG $\beta 1$  (0.3 nM) was then added, and the cells were incubated for 3 days. Monolayers were then washed with PBS and fixed/stained with 0.5% crystal violet. Plates were air dried, the dye was eluted with 0.1 M sodium citrate (pH 4.2) in ethanol (50:50), and the absorbance was read at 540 nm to determine cell viability (30).

**Determination of Cell Number.** Cells were plated as described for the [ $^3\text{H}$ ]thymidine assays. After each incubation, the monolayers were washed once with PBS, cells were detached with trypsin, and viable cells were counted by trypan blue dye exclusion.

**Quantification of Cell Proliferation by Anchorage-independent Growth in Soft Agar.** Cells were seeded in  $60 \times 15\text{-mm}$  dishes onto a bottom layer of 0.5% Bacto-agar (Difco) at the following densities:  $10^4/\text{dish}$  for SK-OV-3;  $2 \times 10^4/\text{dish}$  for MCF7, SK-BR-3, MDA-MB-231, BT-474, and HBL-100; and  $10^5/\text{dish}$  for MDA-MB-361, MDA-MB-453, and MDA-MB-468. A top layer of 0.25% agar in medium containing 0.3 nM rHRG $\beta 1$  or 3 nM EGF or medium alone (as a control) was added to each dish. After 2–4 weeks, colonies were stained with 250  $\mu\text{g}/\text{dish}$  3-[4,5-dimethylthiazol-2-yl]-2,5-diphenyltetrazolium bromide (Sigma Chemical Co.) and enumerated using an Omnicon

3600 Tumor Colony Image Analysis System (Imaging Products International, Inc.).

## RESULTS

**Determination of HRG Binding.** Using  $^{125}\text{I}$ -labeled rHRG $\beta 1_{177-244}$  to perform direct binding experiments, we determined both the affinity and the number of HRG receptors by Scatchard analysis on 13 different cell lines of breast and ovarian origin. A summary of these data is shown in Table 1. For each of these cell lines, the binding data could be fit to a single class of high affinity binding sites. Only the immortalized human mammary epithelial cell line, HBL-100, lacked detectable HRG binding. Very low ( $<10,000$  receptors/cell) HRG binding could be detected on the ovarian cell line SK-OV-3 and the breast tumor cell lines MDA-MB-175-VII, MDA-MB-468, and BT-20. The following breast cancer cell lines, MCF7, MDA-MB-361, T47D, and BT-483, and the ovarian cancer cell line Caov3 were found to have between 10,000–22,000 receptors/cell, and these cell lines were arbitrarily characterized as containing intermediate levels of HRG binding sites. Cell lines having high numbers of HRG binding sites (*i.e.*,  $>25,000$  receptors/cell) were SK-BR-3, MDA-MB-453, and BT-474. Previously, we have determined that in the absence of ErbB2, ErbB3 binds HRG with a binding affinity of 0.9–2 nM (31). When COS7 cells or NIH3T3 cells coexpress ErbB2 with ErbB3, a higher affinity binding site of  $\sim 20$  pM is observed (29, 32). Using a similar COS7 cell system, Tzahar *et al.* (33) have reported recently that NDF binds to ErbB4 and ErbB3 with  $K_d$ s of 1.5 and 8 nM, respectively. These authors speculated that the difference in the binding constants may be related to cell-specific determinants or are due to the preparation or radiolabeling of the recombinant ligands. Recently, we have determined that ErbB4 or ErbB3 binds HRG with similar affinity, if either is expressed singly in cells of hematopoietic origin in the absence of any other ErbB receptors.<sup>3</sup> The average  $K_d$  for the 12 cell lines shown in Table 1 that exhibit HRG binding is  $99 \pm 14$  pM. The binding constants shown in Table 1 are at least an order of magnitude higher in affinity than what has been reported for ErbB3 or ErbB4 alone. These data suggest that other components besides ErbB3 or ErbB4 are contributing to the formation of a high affinity HRG binding site on these cells.

**Monoclonal Antibodies to ErbB2 Block HRG Binding to Breast and Ovarian Tumor Cells.** Based on our previous observations with COS7 cells expressing ErbB3 and ErbB2, as well as our experience with human Schwann cells, we hypothesized that the high-affinity HRG receptors present on these tumor cells were the result of heterodimer formation of ErbB3 with ErbB2 or possibly ErbB4 with ErbB2 (21, 29). To evaluate whether ErbB2 contributes to the formation of this high-affinity HRG binding site on human tumor cells, we surveyed a panel of well-characterized anti-ErbB2 antibodies (28) for their ability to inhibit HRG-stimulated tyrosine phosphorylation of proteins in the  $M_r$  180,000 range from whole-cell lysates of MCF7 cells. MCF7 cells are reported to express all known ErbB receptors, but at relatively low levels (34). Since ErbB2, ErbB3, and ErbB4 have nearly identical molecular sizes (35, 36), it is not possible to discern which protein is becoming tyrosine phosphorylated when whole-cell lysates are evaluated by Western blot analysis. However, these cells are ideal for HRG tyrosine phosphorylation assays because under the assay conditions used, in the absence of exogenously added HRG, they exhibit low to undetectable levels of tyrosine phosphorylation proteins in the  $M_r$  180,000 range. As shown in Fig. 1A, several of these antibodies, including 2C4, 7F3, and 4D5, significantly inhibited

<sup>3</sup> R. W. Akita, N. Chiang, L. Bald, G. Schaefer, B. M. Fendly, and M. X. Sliwkowski. Allosteric modulation of heregulin binding to ErbB3, manuscript in preparation.

Table 1 HRG receptors on human tumor cell lines

Direct binding of  $^{125}\text{I}$ -labeled rHRG $\beta 1_{177-244}$  to tumor cells. Breast and ovarian cancer cell lines were plated in 24-well plates at an initial density of  $10^5$  cells/well and allowed to grow for 48 h. The cultures were washed twice with F12/DMEM and then placed on ice to thermally equilibrate.  $^{125}\text{I}$ -labeled rHRG $\beta 1_{177-244}$  (5 pM to 2 nM) was then added to each well. Binding reactions were performed for 4 h on ice. Scatchard analysis was performed as described previously (10, 29). The values reported are the average and SD for three different binding experiments, each of which consisted of triplicate incubations for each concentration of  $^{125}\text{I}$ -labeled rHRG $\beta 1_{177-244}$  tested. Error values for both  $K_d$  and sites per cell were  $<10\%$  for each binding experiment. The cell number was determined by trypan blue exclusion.

Cell line	$K_d$ (pM)	Sites/cell	ErbB-2 expression <sup>a</sup>
HBL-100	ND <sup>b</sup>	ND	Normal/low
SK-OV-3	84 $\pm$ 18	2500 $\pm$ 440	+++
MDA-MB-175	232 $\pm$ 103	2900 $\pm$ 1700	+
MDA-MB-468	68 $\pm$ 6	4000 $\pm$ 500	ND
BT-20	57 $\pm$ 3	7300 $\pm$ 400	Normal/low
MCF7	91 $\pm$ 16	12,700 $\pm$ 1300	Normal/low
MDA-MB-361	87 $\pm$ 3	14,500 $\pm$ 1000	++
T47D	81 $\pm$ 8	15,900 $\pm$ 800	+
BT-483	81 $\pm$ 6	20,100 $\pm$ 1000	Normal/low
Caov3	140 $\pm$ 3	21,700 $\pm$ 1200	Normal/low
SK-BR-3	54 $\pm$ 8	27,300 $\pm$ 1500	+++
MDA-MB-453	76 $\pm$ 3	29,000 $\pm$ 500	++
BT-474	137 $\pm$ 25	34,600 $\pm$ 2200	+++

<sup>a</sup> Values taken from Lewis *et al.* (30).

<sup>b</sup> ND, not detected.

the generation of a HRG-induced tyrosine phosphorylation signal at  $M_r$  180,000. In the absence of HRG, none of these antibodies were able to stimulate tyrosine phosphorylation of proteins in the  $M_r$  180,000 range (data not shown). Also, these antibodies do not cross-react with EGFR (28), ErbB3, or ErbB4.<sup>4</sup> Antibodies 2C4 and 7F3 significantly inhibited HRG stimulation of p180 tyrosine phosphorylation to  $<25\%$  of control. However, 4D5 was able to block HRG stimulation of tyrosine phosphorylation by  $\sim 50\%$ . Previously, 2C4 and 7F3 were assigned the same ErbB2 epitope as reported in the original characterization of this antibody panel, and this epitope is different than that recognized by 4D5 (28). Fig. 1B shows dose-response curves for 2C4 or 7F3 inhibition of HRG stimulation of p180 tyrosine phosphorylation as determined by reflectance densitometry. Evaluation of these inhibition curves using a 4-parameter fit yielded an  $\text{IC}_{50}$  of  $2.8 \pm 0.7$  nM and  $29.0 \pm 4.1$  nM for 2C4 and 7F3, respectively. Varying concentrations of 2C4 or 7F3 were incubated with MCF7 cells in the presence of  $^{125}\text{I}$ -labeled rHRG $\beta 1$ , and the inhibition curves are shown in Fig. 1C. Analysis of these data yielded an  $\text{IC}_{50}$  of  $2.4 \pm 0.3$  nM and  $19.0 \pm 7.3$  nM for 2C4 and 7F3, respectively. A maximum inhibition of  $\sim 74\%$  for 2C4 and 7F3 are in agreement with the tyrosine phosphorylation data. We concluded from these experiments that in MCF7 cells, ErbB2 was critical for HRG stimulation of tyrosine phosphorylation and was an important component for high-affinity HRG binding.

It was of interest to determine whether the effect of the anti-ErbB2 antibodies observed on MCF7 was a general phenomenon. To address this question, human tumor cell lines were incubated with 2C4 or 7F3 and the degree of specific  $^{125}\text{I}$ -labeled rHRG $\beta 1$  binding was determined. The results from this study are shown in Fig. 2. Binding of  $^{125}\text{I}$ -labeled rHRG $\beta 1$  could be significantly inhibited by either 2C4 or 7F3 in all cell lines, with the exception of the breast cancer cell line MDA-MB-468, which has been reported to express little (37) or no ErbB2 (30, 38). The remaining cell lines are reported to express ErbB2, with the level of ErbB2 expression varying widely among these cell lines (30, 38). In fact, the range of ErbB2 expression in the cell lines tested varies by more than 2 orders of magnitude. For

example, BT-20, MCF7, and Caov3 express  $\sim 10^4$  ErbB2 receptors/cell, whereas BT-474 and SK-BR-3 express  $\sim 10^6$  ErbB2 receptors/cell (30). Given the wide range of ErbB2 expression in these cells and the data in Fig. 2, it was concluded that the interaction between ErbB2 and ErbB3 or ErbB4, was itself a high-affinity interaction that takes place on the surface of the plasma membrane. At present, it is unclear whether these complexes involving ErbB2-ErbB3 or ErbB2-ErbB4 are preexisting in the absence of HRG or whether the association with

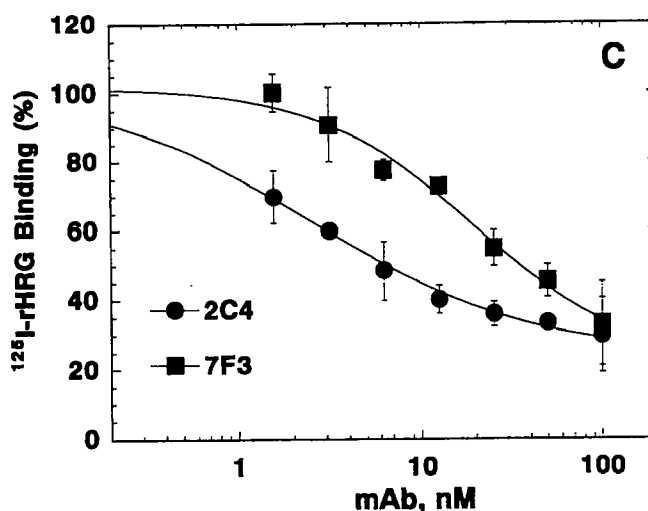
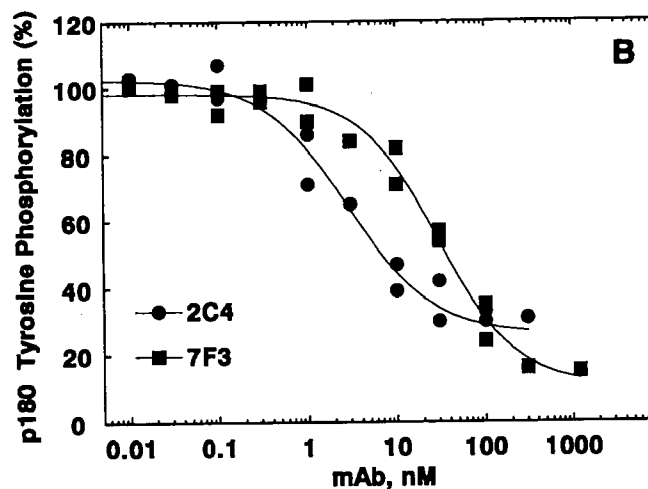
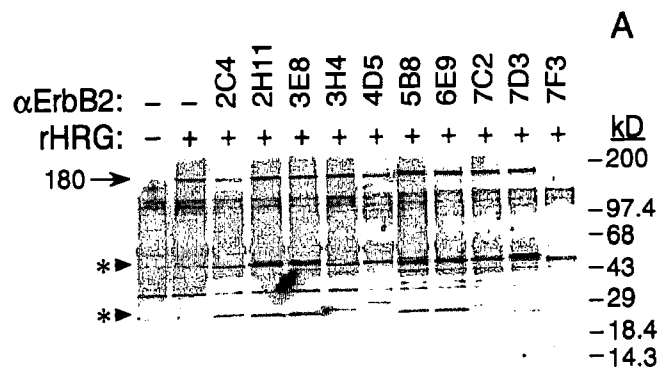


Fig. 1. Effect of anti-ErbB2 antibodies on rHRG $\beta 1$  activation of MCF7 cells. A, effect of the anti-ErbB2 antibodies on the generation of a phosphotyrosine signal at  $M_r$  180,000. Antiphosphotyrosine immunoblots were developed as described in "Materials and Methods." \*, immunoreactive bands that result from the interaction of the murine monoclonal antibody with the secondary antibody detection system. B, dose-response curves for 2C4 or 7F3 inhibition of HRG stimulation of tyrosine phosphorylation. C, dose-response curves for the inhibition of  $^{125}\text{I}$ -labeled rHRG $\beta 1_{177-244}$  binding to MCF-7 cells by 2C4 or 7F3; bars, SE.

<sup>4</sup> L. Bald, M. X. Sliwkowski, R. Akita, N. Chiang, C. Wirth, R. Taylor, N. Dybdal, and B. M. Fendly. Deciphering heregulin-mediated signaling through ErbB4: application of anti-ErbB4 monoclonal antibodies, manuscript in preparation.

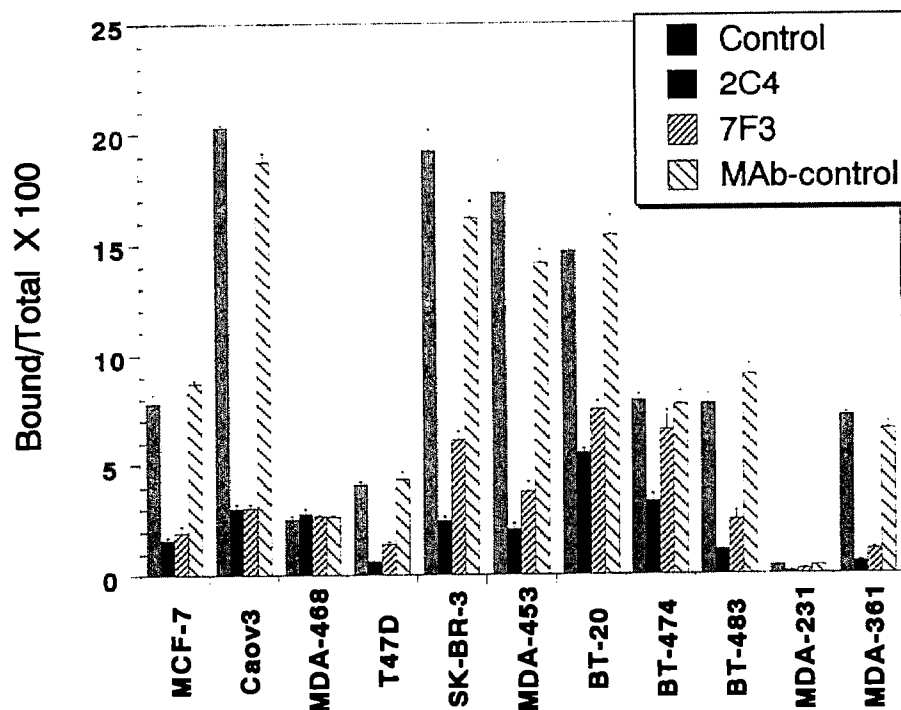


Fig. 2. Inhibition of specific  $^{125}\text{I}$ -labeled rHRG $\beta$ <sub>177-244</sub> binding to a panel of human tumor cell lines by the anti-ErbB2 monoclonal antibodies 2C4 or 7F3. Monoclonal antibody-controls are isotype-matched murine monoclonal antibodies that do not block rHRG binding. Nonspecific  $^{125}\text{I}$ -labeled rHRG $\beta$ <sub>177-244</sub> binding was determined from parallel incubations performed in the presence of 100 nM rHRG $\beta$ <sub>1</sub>. Values for nonspecific  $^{125}\text{I}$ -labeled rHRG $\beta$ <sub>177-244</sub> binding were less than 1% of the total for all of the cell lines tested; bars, SE.

ErbB2 is driven by the formation of HRG-ErbB3 or HRG-ErbB4 complexes.

#### Stimulation of Mitogenesis by HRG in Human Tumor Cells.

We initially reported that HRG stimulated the growth of SK-BR-3 breast tumor cells as measured by crystal violet staining (10). Having determined the levels of HRG receptors in a number of different human tumor cell lines, we examined the mitogenic response of these cells to rHRG $\beta$ <sub>1</sub>. Dose-response curves consisting of 5 pM-10 nM rHRG $\beta$ <sub>1</sub> in different serum concentrations were generated for all of the cell lines listed in Table 1. Prior to treatment with rHRG $\beta$ <sub>1</sub>, cells were growth arrested by incubation in medium containing 0.1% FBS for 48 h. Fig. 3 shows typical curves for three breast tumor cell lines after treatment for 3 days. MCF7 responsiveness to rHRG $\beta$ <sub>1</sub> was dependent on serum concentration in the assay medium. When assayed in 0.1% FBS, MCF7 cells showed a 4-5-fold stimulation of [ $^3\text{H}$ ]thymidine incorporation after treatment for 1 day (data not shown) and 3 days (Fig. 3a), with the maximal response occurring between 0.1 and 1 nM rHRG $\beta$ <sub>1</sub>, consistent with the affinity constant shown in Table 1. rHRG $\beta$ <sub>1</sub> also stimulated DNA synthesis 2-2.5-fold in 1% FBS but had no effect in 10% FBS (Fig. 3a). A likely explanation for this effect is that MCF7 cells contain high levels of estrogen receptors (39) and, in the absence of other exogenously added growth factors, requires estrogen for growth (40). Alternatively, the presence of peptide growth factors such as insulin-like growth factor-1 may reduce cellular responses to HRG (41). Sufficient quantities of these factors are present when cells are cultured in 10% serum; however, 0.1% serum is not sufficient. In low serum concentrations, HRG activation of ErbB receptor pathways is then sufficient for stimulating mitogenic activity. These data are consistent with those reported recently by Pietras *et al.* (42), which demonstrate a direct interaction between HRG-mediated activation of ErbB pathways and cross-talk with estrogen receptor pathways. In contrast, the ErbB2 overexpressing breast tumor cell lines, SK-BR-3 and MDA-MB-453, showed enhanced incorporation of [ $^3\text{H}$ ]thymidine in a serum-dependent manner after 1 day of treatment with rHRG $\beta$ <sub>1</sub> (data not shown) and after 3 days of treatment (Fig. 3, b and c). Although

there was no effect in 0.1% FBS, [ $^3\text{H}$ ]thymidine incorporation increased in cells exposed to rHRG $\beta$ <sub>1</sub> in 1 or 10% FBS.

**Comparison of the HRG Response to EGF and 4D5.** Since responsiveness of a number of tumor cell lines to either EGF or the anti-ErbB2 monoclonal antibody 4D5 has been extensively studied, we compared treatment of these cell lines with either EGF or 4D5 under identical conditions as a comparison to rHRG $\beta$ <sub>1</sub>. *In vitro*, EGF inhibits the growth of tumor cell lines such as MDA-MB-468 (43) and A431 (44, 45), both of which overexpress EGFR. Conversely, cells that express normal/low or moderate levels of EGFR are frequently growth-stimulated by exogenous EGF (39). Inhibition of cell growth by 4D5 is dependent on the expression level of ErbB2 (30), *i.e.*, 4D5 is cytostatic only for cells that overexpress ErbB2. Using a 3-day assay, the data in Fig. 4 show that the changes in [ $^3\text{H}$ ]thymidine incorporation in these cell lines were distinct, depending on the treatment conditions. rHRG $\beta$ <sub>1</sub> stimulated thymidine incorporation in MCF7, SK-BR-3, BT-474, MDA-MB-453, MDA-MB-361, T47D, and BT-20 cells at all serum concentrations tested. However the magnitude of the response varied, depending on the serum concentrations present in the assay. In contrast, EGF (3 nM) stimulated [ $^3\text{H}$ ]thymidine incorporation in HBL-100, T47D, BT-20, and SK-OV-3 cells under all conditions tested. Both rHRG $\beta$ <sub>1</sub> and EGF stimulated MCF7 cells in both 0.1% and 1% FBS, although the magnitude of the response was less with EGF than with rHRG $\beta$ <sub>1</sub>. 4D5 had no effect on this cell line, as reported previously (30). DNA synthesis was inhibited by EGF and, more potently, by 4D5 in SK-BR-3 cells at all serum concentrations tested. Similarly, [ $^3\text{H}$ ]thymidine incorporation in BT474, MDA-MB-453, and MDA-MB-361 breast tumor cells was also inhibited by 4D5 since these cell lines overexpress ErbB2. rHRG $\beta$ <sub>1</sub> and 4D5 did not affect [ $^3\text{H}$ ]thymidine incorporation in the MDA-MB-231 and MDA-MB-468 breast tumor lines. Consistent with previous reports (43), EGF was inhibitory for MDA-MB-468 cells. No significant changes in MDA-MB-231 cells were detected with either rHRG $\beta$ <sub>1</sub>, EGF, or 4D5 under the conditions tested.



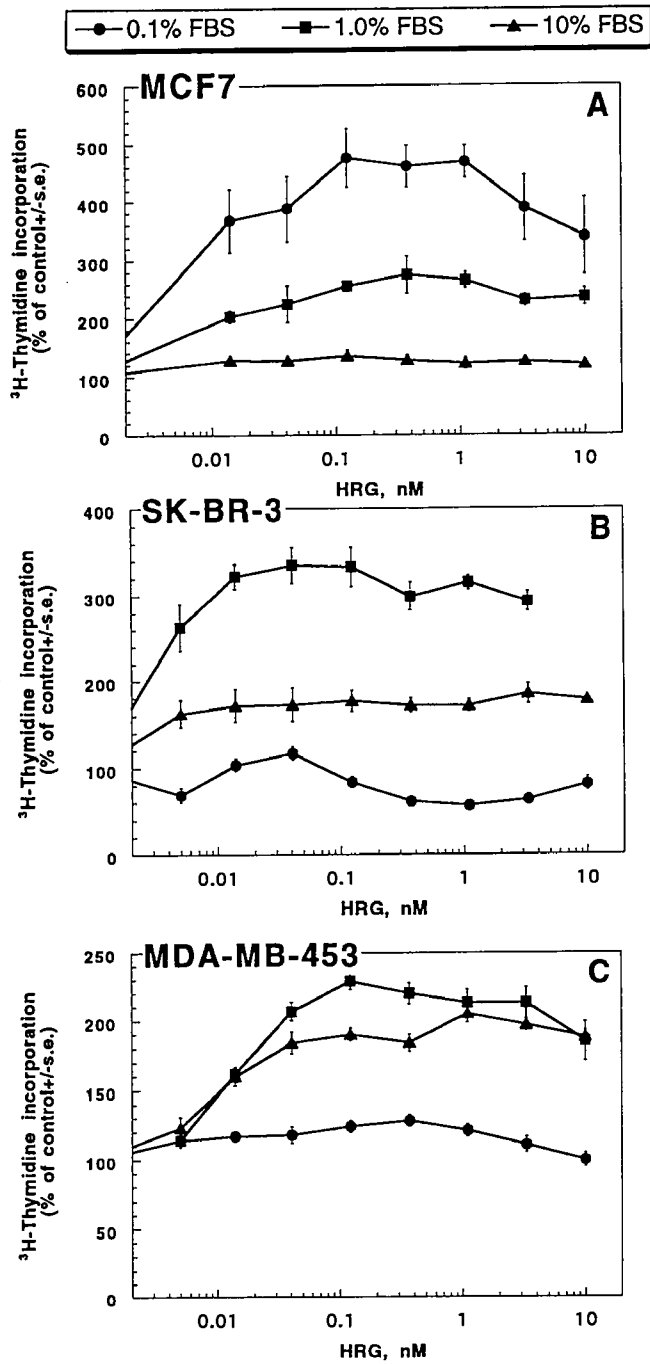


Fig. 3. Stimulation of DNA synthesis by rHRGβ1. MCF7 (A), SK-BR-3 (B), and MDA-MB-453 (C) breast tumor cells were plated at a density of 10<sup>4</sup> cells/well in 96-well microtiter plates and allowed to adhere overnight. The medium was then replaced with low serum medium (0.1% FBS) to growth arrest the cells. After 48 h, this medium was removed, and the cells were treated with different concentrations of rHRGβ1 in medium supplemented with 0.1 (●), 1 (■), or 10% FBS (▲) for 3 days. At the end of each incubation, the cells were radiolabeled with 1 μCi/well [<sup>3</sup>H]thymidine for 4 h, then harvested onto filter plates for scintillation counting. The data are expressed as the mean cpm of 4–8 replicates; bars, SE.

**Cell Cycle Changes Induced by rHRGβ1, EGF, and Murine Monoclonal Antibody 4D5.** To further characterize the effects of rHRGβ1, EGF, and 4D5 on tumor cell growth, analyses of cell cycle phase fraction distributions were performed. MCF7, SK-BR-3, and MDA-MB-453 breast tumor cells were serum starved and then treated for 1 day with 0.3 nM rHRGβ1, 3 nM EGF, or 66 nM 4D5 in 0.1, 1, or 10% FBS. Fig. 5 shows the results presented as the fraction of cells in

S phase as an indicator of proliferative status measured at ~30 h following treatment. For both MCF7 and SK-BR-3 cells, the changes in the percentage of S-phase cells after each treatment correlates well with the effects on [<sup>3</sup>H]thymidine incorporation (Fig. 3). rHRGβ1 caused a 3-fold increase in the percentage of MCF7 cells in S-phase in 0.1% FBS. EGF treatment induced a smaller proportion of cells to enter S phase in 0.1 and 1% FBS (1.6- and 1.3-fold, respectively),

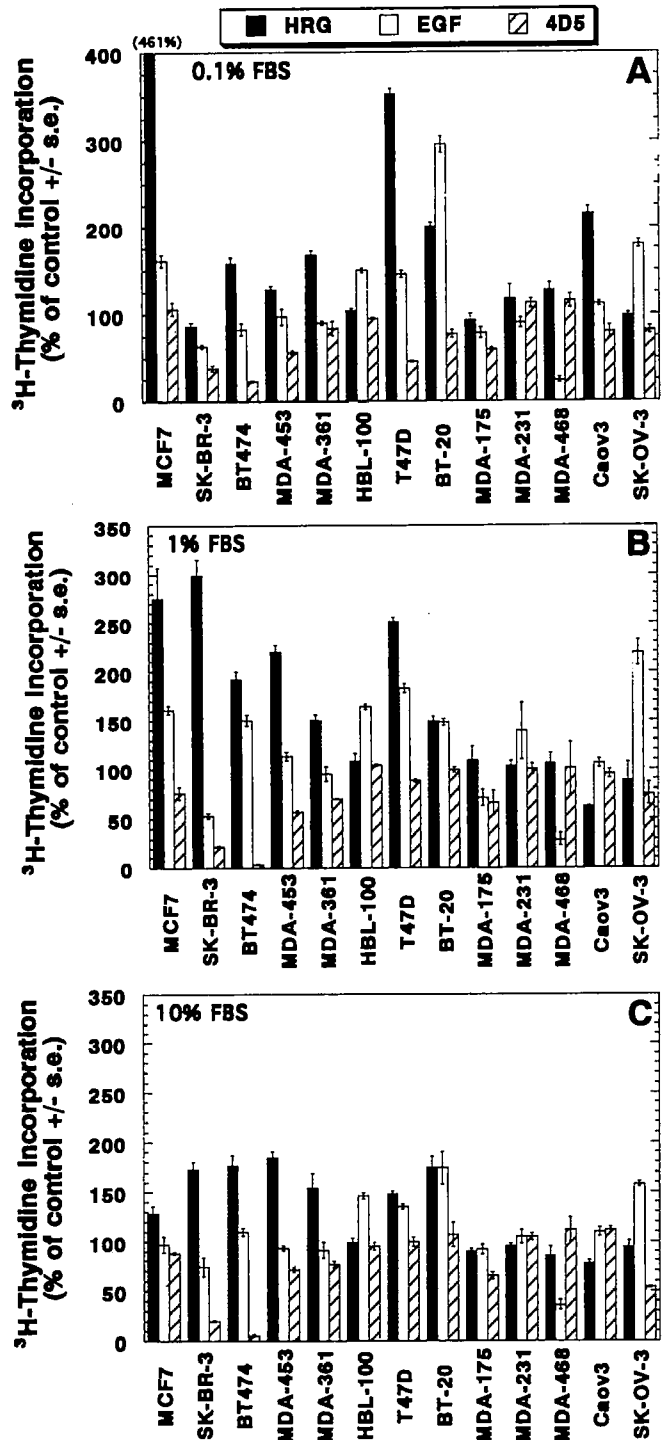


Fig. 4. Comparison of the response of different breast and ovarian tumor cell lines to rHRGβ1, EGF, and 4D5. Mitogenic assays were performed as described in Fig. 3. Cells were treated with 0.37 nM rHRGβ1, 3 nM EGF, or 66 nM 4D5 in medium containing 0.1% (A), 1% (B), or 10% (C) FBS for 3 days. The data are expressed as the percentage of [<sup>3</sup>H]thymidine incorporation (mean of 4–8 replicates; bars, SE) as compared to untreated control cells.

while 4D5 had no effect. With SK-BR-3 cells, rHRGβ1 stimulation of the percentage of cells in S phase was enhanced with increasing serum concentration (1.5–1.8-fold). EGF had an inhibitory effect in 0.1 and 1% FBS, and as expected, 4D5 decreased the percentage of S-phase cells at all concentrations of serum. MCF7 and SK-BR-3 cells were also treated for 3 days with rHRGβ1 with similar results. In contrast, the fraction of cells in S phase in the MDA-MB-453 cell line upon exposure to rHRGβ1 did not differ from controls in the three serum concentrations tested at 30 h. These results are different from the data shown in Fig. 4, where rHRGβ1 increased the incorporation of [<sup>3</sup>H]thymidine in the MDA-MB-453 cells in 1 and 10% FBS. On the other hand, EGF and 4D5 have similar effects on both [<sup>3</sup>H]thymidine incorporation and cell cycle progression. As expected, EGF-treated MDA-MB-453 cells were not different from control, since this cell line expresses little or no detectable EGFR (30, 38), whereas treatment with 4D5 reduced the number of S-phase cells. In contrast to previous reports (11, 26, 46), upon HRG treatment, there was no suggestion of a G<sub>2</sub>-M growth arrest nor was there evidence for induction of a ploidy abnormality. Explanations for these discrepancies can likely be attributed to differences in the purity of the NDF preparations or the particular cell lines being used in these earlier studies.

**Effect of rHRGβ1 on Cell Number.** Because of the discrepancy between the MDA-MB-453 [<sup>3</sup>H]thymidine incorporation and cell cycle experiments, it was necessary to determine actual cell number after rHRGβ1 treatment. Fig. 6 shows that the effects of rHRGβ1 on MCF7 and SK-BR-3 cell number are in agreement with the data in Figs. 3 and 5. The MCF7 breast tumor cells show the greatest increase in cell number to rHRGβ1 after 3 days of treatment in 0.1% FBS, while proliferation of SK-BR-3 cells is increased in higher serum concentrations. There was no change in MDA-MB-453 cell number after exposure to 0.3 nM rHRGβ1 in 0.1, 1, or 10% FBS. Therefore, it appears that the incorporation of [<sup>3</sup>H]thymidine in this cell line is not an indicator of DNA synthesis and cell proliferation. These results are in agreement with those reported earlier for the response of MDA-MB-453 cells to concentrated conditioned medium containing recombinant NDF (25). Our data for the responsiveness of MDA-MB-453 and SK-BR-3 cells differ from those reported earlier for NDFα (12) or purified natural gp30, which has been shown to be related to HRG/NDF (14, 26).

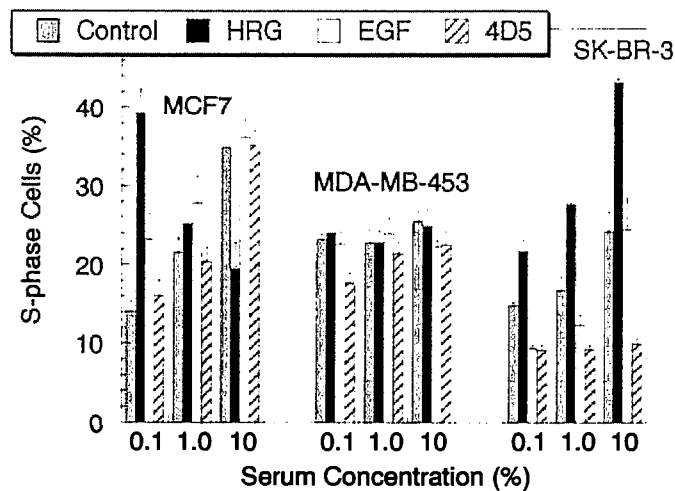


Fig. 5. Effects of rHRGβ1, EGF, and 4D5 on cell cycle progression in MCF7, SK-BR-3, and MDA-MB-453 breast tumor cells. Each treatment was done in triplicate, as described in "Materials and Methods." The data shown are pooled from three to four separate experiments; bars, SE.

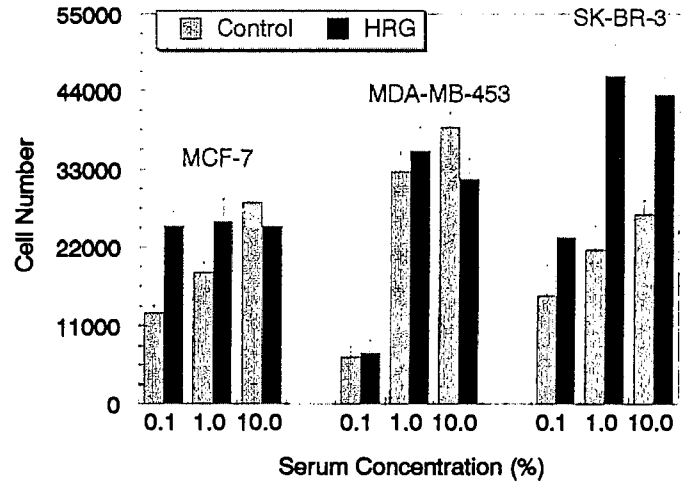


Fig. 6. Effect of rHRGβ1 on MCF7, SK-BR-3, and MDA-MB-453 cell number. Cells were treated as in Fig. 1, except at the end of the incubation, the monolayers were detached with trypsin, and viable cells were counted by trypan blue dye exclusion.

**HRG Stimulation of Tumor Cell Growth Is Inhibited by Anti-ErbB2 Monoclonal Antibodies 2C4 and 7F3.** Since 2C4 and 7F3 are cytostatic for cells that overexpress ErbB2 (30), we could not test the antagonist effect of 2C4 or 7F3 on HRG-induced growth of cells that overexpress ErbB2. The effect of 2C4 or 7F3 on three cell lines that express low/normal levels of ErbB2 is shown in Fig. 7. MCF7 and T47D are breast cancer cell lines that are known to express low to intermediate levels of all ErbB receptors (34, 36, 39). Although ErbB4 is not expressed in the ovarian cancer cell line Caov3 (35), other ErbB receptors are present (30) (data not shown). The effect of 2C4 or 7F3 on rHRGβ1 stimulation of cell growth using a 3-day crystal violet assay format is shown in Fig. 7. In each case, rHRGβ1-mediated growth was inhibited by 2C4 or 7F3 to levels close to those observed without HRG treatment. The results observed with 2C4 or 7F3 are similar to those reported recently by Graus-Porta *et al.* (22), using a version of T47D cells engineered to sequester ErbB2 in the endoplasmic reticulum with a single-chain anti-ErbB2 antibody. These data are also similar to those obtained when rHRGβ1 was tested in combination with 2C4 on human Schwann cells (21).

**Anchorage-independent Growth in Soft Agar.** For a final determination of the effects of rHRGβ1 on cell proliferation, we studied the anchorage-independent growth of different breast and ovarian tumor cell lines in soft agar and compared the response with EGF. To allow for enhanced proliferation of colonies in soft agar, cells were seeded at densities resulting in minimal colony formation in untreated cells, and all experiments had to be performed in 10% serum. As shown in Fig. 8, MCF7, T47D, SK-BR-3, BT474, and SK-OV-3 cells showed a greater than 2-fold increase in colony formation in response to treatment with 0.3 nM rHRGβ1. Growth in soft agar of the MDA-MB-468 cell line was also slightly enhanced. Since this cell line does not express ErbB2 (30, 38) and presumably low or undetectable levels of ErbB4 but does express ErbB3, this response might be mediated by ErbB3. Since ErbB3 is an impaired kinase (47, 48), these data suggest that ErbB3 may be heterodimerizing with another ErbB family member other than ErbB2. One plausible candidate for this active signaling complex may be EGFR-ErbB3 since MDA-MB-468 cells overexpress EGFR (49). Colony formation by MDA-MB-453 and MDA-MB-361 cells was inhibited by HRG treatment relative to control plates. In comparison, EGF had little effect on MCF7, MDA-MB-453, MDA-MB-361, or MDA-MB-231 cells. Growth in soft agar was stimulated by EGF in SK-OV-3 cells and was slightly enhanced in SK-BR-3 and BT474 cells. Treatment of MDA-MB-468 cells with EGF completely abolished colony formation.

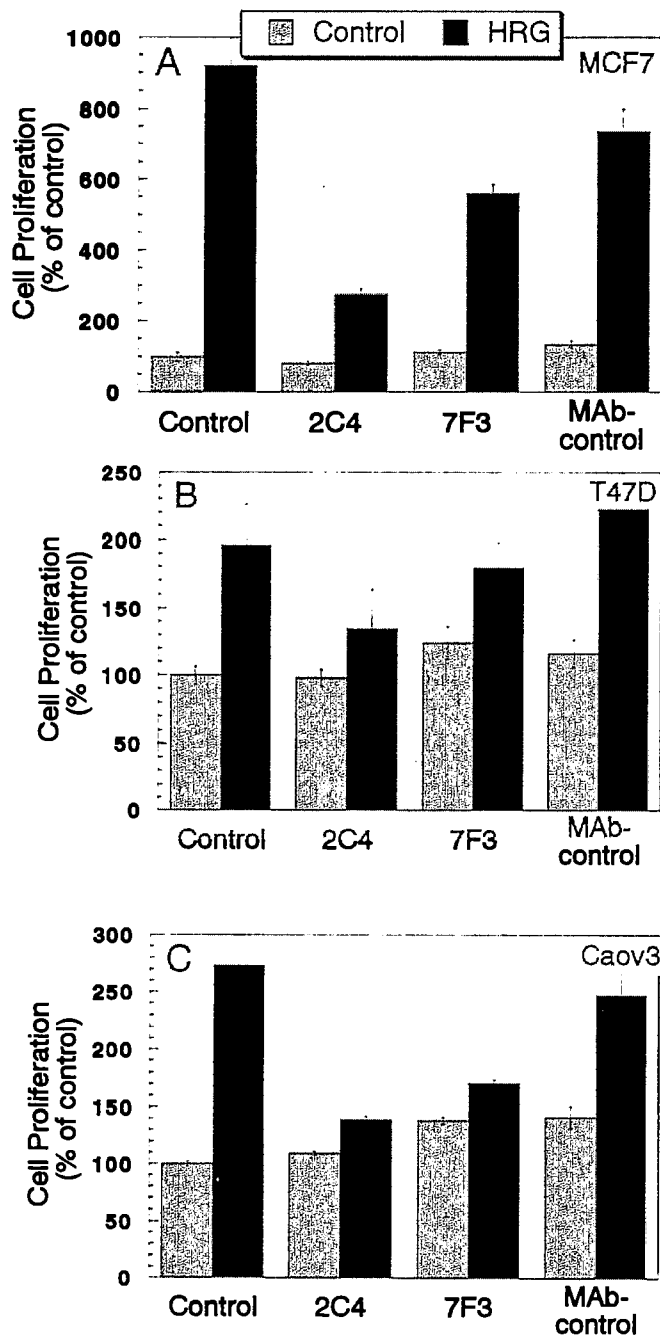


Fig. 7. Effect of 2C4 or 7F3 on rHRGβ1 induced proliferation of MCF7 (A), T47D (B), and Caov3 (C) tumor cell lines. Monoclonal antibodies (10 nM) or medium alone were added, and the cells were incubated for 2 h at 37°C. rHRGβ1 (0.3 nM) was then added, and the cells were incubated for 3 days. Monolayers were then washed with PBS and fixed/stained with 0.5% crystal violet; then the absorbance was read at 540 nm to determine cell proliferation (30).

**DISCUSSION**

In this study, we describe a systematic analysis of HRG responsiveness in a panel of human breast and ovarian cancer cell lines. High-affinity HRG receptors could be detected on most of these cell lines. However, the range of HRG receptor expression is significantly narrower than that observed for either EGFR or ErbB2. Since HRG binding requires the presence of ErbB3 or ErbB4, these data imply that ErbB3 and ErbB4 expression may be more tightly regulated in breast and ovarian tumors cells than either EGFR or ErbB2. Antibodies directed against ErbB2 inhibited HRG binding in these cell lines,

suggesting that the formation of this high-affinity binding site was likely the result of heterodimerization of ErbB2 with ErbB3 or with ErbB4. In addition, the binding affinity of HRG for ErbB4 appears to be considerably lower than the values determined here for this panel of human tumor cell lines (33). Although ErbB4 is expressed in some of these cell lines (34, 35), our analysis of ErbB4 expression in these cells using a panel of ErbB4-specific monoclonal antibodies indicates that the ErbB4 expression level is significantly lower than EGFR, ErbB2, or ErbB3.<sup>4</sup> ErbB4 is a fully functional HRG receptor (35, 50), and it has been demonstrated recently that ErbB4 is required for normal embryonic neural and cardiac development (51). Regardless of the relative expression levels or the activation of particular signal transduction pathways, the abrogation of HRG responsiveness by anti-ErbB2 monoclonal antibodies indicates that ErbB2 is critical in mediating HRG responsiveness. Our conclusion from these studies is that inhibition of HRG response by these blocking anti-ErbB2 antibodies is the result of inhibiting the recruitment of ErbB2 to a high-affinity complex with ErbB3 or ErbB4. Using different experimental approaches similar conclusions have also been drawn regarding the role of ErbB2 in mediating HRG responses in the breast cancer cell lines T47D (22) and MCF7 (52).

At present, more is known about the interaction of ErbB2 with ErbB3 than ErbB2 with ErbB4. Although ErbB3 can function as a HRG-binding protein, it is a unique receptor in that its intrinsic tyrosine kinase activity appears to be impaired (47, 48). When coexpressed with ErbB2, ErbB3 becomes phosphorylated on tyrosine residues in its cytoplasmic domain that generate a signal primarily through the PI3-kinase pathway (32, 53). Thus, a functional HRG receptor may be viewed as a heterodimer of ErbB3 with ErbB2, where ErbB2 modulates the affinity of ErbB3 for HRG binding and contributes an active tyrosine kinase domain. Conversely, ErbB3 is required for HRG binding and upon phosphorylation of its unique tyrosine residues in the cytoplasmic domain, ErbB3 is capable of coupling to PI3-kinase. This latter adapter function is analogous to the interaction of IRS-1 with insulin receptor. IRS-1 is the principal substrate of the activated insulin receptor tyrosine kinase. After becoming tyrosine phosphorylated, IRS-1 couples with PI3-kinase and other SH2-proteins for the propagation of downstream signaling (54). Coopera-

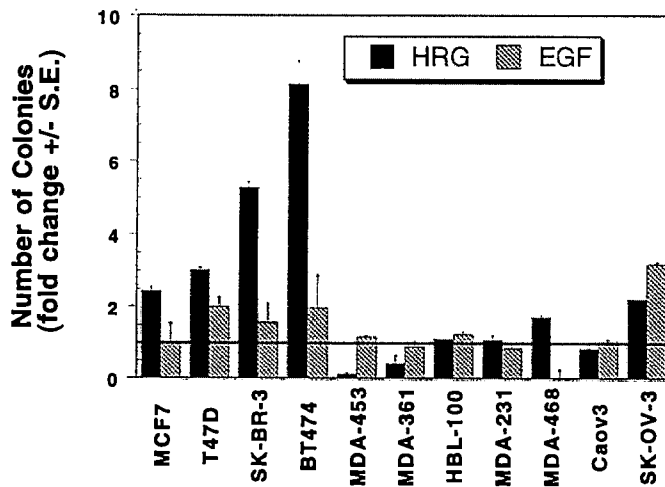


Fig. 8. Colony formation in soft agar by breast and ovarian tumor cell lines. Cells were seeded in 60 × 15-mm dishes onto a bottom layer of 0.5% agar and overlaid with 0.25% agar in Ham's F12:DMEM (50:50) medium supplemented with 10% heat-inactivated FBS and 2 mM L-glutamine. Treatment groups for each cell line were 0.3 nM rHRG, 3 nM EGF, or an untreated control (designated by horizontal bar). After 2–4 weeks, the colonies were stained with 3-[4,5-dimethylthiazol-2-yl]-2,5-diphenyltetrazolium bromide and counted using an Omnicon 3600 Image Analysis System. The data are represented as the fold change in the number of colonies per dish (bars, SE) that were greater than 80 μm relative to untreated control dishes. Each treatment group consisted of three replicate dishes.

tion between ErbB3 and ErbB2 in neoplastic transformation of NIH3T3 cells has also been demonstrated recently (53, 55).

We also studied the effects of rHRG on the growth of these cell lines using several different assay formats. In a number of these formats, it was found that the presence of serum profoundly influenced the magnitude of the HRG response on a number of these cell lines. In general, the results from these experiments agreed among the formats used. MCF7, Caov3, T47D, BT-20, BT-474, and SK-BR-3 cells were growth stimulated in a number of assays under defined serum concentrations. Our results with the stimulation of growth of these breast tumor cell lines are similar to those recently obtained with the mouse mammary epithelial cell line HC11 (56, 57) and the immortalized human epithelial cell line MCF-10A (41). Two notable exceptions in the present study were MDA-MB-453 and MDA-MB-361 cells. Although these cell lines were stimulated by rHRG treatment in the mitogenic assay, this incorporation of [<sup>3</sup>H]thymidine did not appear to lead to cell division. Indeed, anchorage-independent growth assays suggested that HRG treatment was growth inhibitory at high serum concentrations. There are several possible explanations for the apparent discrepancy between the stimulation of [<sup>3</sup>H]thymidine incorporation in the MDA-MB-453 and MDA-MB-361 cells and the negative results obtained with cell cycle, cell count, and soft agar experiments. Incorporation of [<sup>3</sup>H]thymidine into DNA occurs exclusively via the salvage pathway for DNA synthesis. Differences in rates of transport of labeled nucleotide into the cell, in activity of thymidine kinase or other synthetic or degradative enzymes, or in the size of intracellular nucleotide pools can lead to inconsistent results (58). Extranuclear labeling would also lead to enhanced incorporation independent of DNA synthesis. Studies showing increased [<sup>3</sup>H]thymidine incorporation without subsequent cell division have been reported (59, 60).

We compared the HRG response in these cell lines to 4D5, a cytostatic monoclonal antibody directed against ErbB2. Growth inhibitory response of cell lines to 4D5 is strictly dependent on ErbB2 expression levels (30) and appears to be independent of serum concentrations. The growth of cell lines such as BT-474 and SK-BR-3 is inhibited by 4D5, whereas under the same conditions, they are growth stimulated by HRG. Additionally, HRG-mediated growth responses in cell lines known to express low/normal levels of ErbB2 such as MCF7, T47D, and Caov3 were inhibited by two other anti-ErbB2 antibodies, 2C4 and 7F3. To explain these results with HRG and 4D5, we speculate that ErbB2 heterodimerization with other ErbB family members is itself a high-affinity interaction and is preferred to ErbB2 homodimerization. This hypothesis is supported by the observation that HRG activation of ErbB2 occurs at a wide range of ErbB2 expression levels. In the present study, ErbB2 activation occurs by at least two different mechanisms, heterodimerization or homodimerization. In addition to ErbB2, the heterodimerization pathway requires HRG and a receptor for HRG, *i.e.*, ErbB3 or ErbB4. Monoclonal antibodies directed against ErbB2, such as 2C4 or 7F3 and to a lesser extent 4D5, are capable of disrupting these ErbB2-ErbB3/4 interactions so that HRG activation of ErbB2 is ablated. Constitutive activation of ErbB2, which is likely the result of ErbB2 homodimerization or oligomerization, occurs at high ErbB2 receptor densities and is independent of HRG, ErbB3, and ErbB4 expression. In agreement with this hypothesis is the observation that a threshold of ErbB2 expression must be surpassed to transform rodent fibroblast (61). Moreover, reversion of this transformed phenotype can occur by treatment with anti-ErbB2 monoclonal antibodies (27). Additionally, the growth inhibitory properties of anti-ErbB2 monoclonal antibodies are observed only on human tumor cell lines that overexpress ErbB2 (30). Thus, activation of ErbB2 by HRG or ErbB2 overexpression can result in the proliferation of tumor cell growth. As observed, antibodies

that disrupt either of these activation pathways will have growth-inhibitory effects.

In comparison to HRG, treatment of these tumor cell lines with EGF under identical conditions produced only modest effects on growth proliferation. An exception was MDA-MB-468 cells, which were significantly growth inhibited by EGF (44, 45). Interestingly, the *in vitro* growth-inhibitory properties of EGF do not translate into a therapeutic benefit when the same cell lines are examined as xenografts *in vivo* (62, 63). *In vivo* experiments with MDA-MB-453 and MDA-MB-361 cells may be warranted given the growth-inhibitory effects observed with HRG treatment in the anchorage-independent growth assays. Recently, it has been demonstrated that HRG administration to athymic mice bearing MCF7 tumor xenografts is growth stimulatory to the tumors (42).

We conclude that expression of ErbB3 or ErbB4 with ErbB2 allow breast and ovarian tumor cells to be HRG responsive. The cell lines demonstrated to be HRG responsive do not express any known HRG isoform transcripts. HRG transcripts can be detected in fibroblasts as well as nontransformed breast cells and stromal elements in human breast tumors (53, 55, 64). These observations set the stage for potential paracrine stimulation of ErbB3/ErbB2- and ErbB4/ErbB2-expressing tumor cells and suggests that the interaction (53, 64) of HRG and its receptors may be important in transformation, tumor cell growth, or the maintenance of a transformed phenotype. Determination of the role that endogenous HRG plays in these processes may allow for therapies that target these receptors or this family of ligands.

## REFERENCES

1. Prigent, S. A., and Lemoine, N. R. The type 1 (EGFR-related) family of growth factor receptors and their ligands. *Progress Growth Factor Res.*, 4: 1-24, 1992.
2. Harris, J. R., Lippman, M. E., Veronesi, U., and Willett, W. Breast cancer. *N. Engl. J. Med.*, 327: 473-480, 1992.
3. Hynes, N. E. Amplification and overexpression of the *erbB-2* gene in human tumors: its involvement in tumor development, significance as a prognostic factor, and potential as a target for cancer therapy. *Semin. Cancer Biol.*, 4: 19-26, 1993.
4. Modjtahedi, H., and Dean, C. The receptor for EGF and its ligands: expression, prognostic value and target for therapy. *Int. J. Oncol.*, 4: 277-296, 1994.
5. Baselga, J., and Mendelsohn, J. Receptor blockade with monoclonal antibodies as anti-cancer therapy. *Pharmacol. & Ther.*, 64: 127-154, 1994.
6. Radinsky, R., Risin, S., Fan, D., Dong, Z., Bielenberg, D., Bucana, C. D., and Fidler, I. J. Level and function of epidermal growth factor receptor predict the metastatic potential of human colon carcinoma cells. *Clin. Cancer Res.*, 1: 19-31, 1995.
7. Scher, H. I., Sarkis, A., Reuter, V., Cohen, D., Netto, G., Petrylak, D., Lianes, P., Fuks, Z., Mendelsohn, J., and Cordon-Cardo, C. Changing pattern of expression of the epidermal growth factor receptor and transforming growth factor  $\alpha$  in the progression of prostatic neoplasms. *Clin. Cancer Res.*, 1: 545-550, 1995.
8. Lee, J., and Wood, W. I. Assignment of heregulin (HGL) to human chromosome 8p22-p11 by PCR analysis of somatic cell hybrid DNA. *Genomics*, 16: 790-791, 1993.
9. Orr-Urtreger, A., Trakhtenbrot, L., Ben-Levy, R., Wen, D., Rechavi, G., Lonai, P., and Yarden, Y. Neural expression and chromosomal mapping of Neu differentiation factor to 8p12-p21. *Proc. Natl. Acad. Sci. USA*, 90: 1867-1871, 1993.
10. Holmes, W. E., Sliwkowski, M. X., Akita, R. W., Henzel, W. J., Lee, J., Park, J. W., Yansura, D., Abadi, N., Raab, H., Lewis, G. D., Shepard, H. M., Kuang, W.-J., Wood, W. I., Goeddel, D. V., and Vandlen, R. L. Identification of heregulin, a specific activator of p185<sup>erbB2</sup>. *Science (Washington DC)*, 256: 1205-1210, 1992.
11. Peles, E., Bacus, S. S., Koski, R. A., Lu, H. S., Wen, D., Ogden, S. G., Levy, R. B., and Yarden, Y. Isolation of the neu/HER-2 stimulatory ligand: a 44 kd glycoprotein that induces differentiation of mammary tumor cells. *Cell*, 69: 205-216, 1992.
12. Wen, D., Peles, E., Cupples, R., Suggs, S. V., Bacus, S. S., Luo, Y., Trail, G., Hu, S., Silbiger, S. M., Levy, R. B., Ben Levy, R., Koski, R. A., Lu, H. S., and Yarden, Y. Neu differentiation factor: a transmembrane glycoprotein containing an EGF domain and an immunoglobulin homology unit. *Cell*, 69: 559-572, 1992.
13. Lupu, R., Colomer, R., Zugmaier, G., Sarup, J., Shepard, M., Slamon, D., and Lippman, M. E. Direct interaction of a ligand for the erbB2 oncogene product with the EGF receptor and p185<sup>erbB2</sup>. *Science (Washington DC)*, 249: 1552-1555, 1990.
14. Lupu, R., and Lippman, M. E. The role of erbB2 signal transduction pathways in human breast cancer. *Breast Cancer Res. Treat.*, 27: 83-93, 1993.
15. Falls, D. L., Rosen, K. M., Corfas, G., Lane, W. S., and Fischbach, G. D. ARIA, a protein that stimulates acetylcholine receptor synthesis, is a member of the neu ligand family. *Cell*, 72: 801-815, 1993.
16. Marchionni, M. A., Goodearl, A. D., Chen, M. S., Birmingham-McDonogh, O., Kirk, C., Hendricks, M., Danehy, F., Misumi, D., Sudhalter, J., Kobayashi, K., Wroblewski, D., Lynch, C., Baldassare, M., Hiles, I., Davis, J. B., Hsuan, J. J., Totty, N. F., Otsu, M., McBurney, R. N., Waterfield, M. D., Stobart, P., and Gwynne, D. Glial growth

- factors are alternatively spliced erbB2 ligands expressed in the nervous system. *Nature (Lond.)*, 362: 312-318, 1993.
17. Ho, W.-H., Armanini, M. P., Nuijens, A., Phillips, H. S., and Osheroff, P. L. SMDF, a novel heregulin isoform highly expressed in sensory and motor neurons. *J. Biol. Chem.*, 270: 14523-14532, 1995.
  18. Carraway, K. L., and Cantley, L. C. A new acquaintance for erbB3 and erbB4: a role for receptor heterodimerization in growth signaling. *Cell*, 78: 5-8, 1994.
  19. Earp, H. S., Dawson, T. L., Li, X., and Yu, H. Heterodimerization and functional interaction between EGF receptor family members: a new signaling paradigm with implications for breast cancer research. *Breast Cancer Res. Treat.*, 35: 115-132, 1995.
  20. Karunakaran, D., Tzahar, E., Liu, N., Wen, D., and Yarden, Y. Neu differentiation factor inhibits EGF binding: a model for *trans*-regulation within the ErbB family of receptor tyrosine kinases. *J. Biol. Chem.*, 270: 9982-9990, 1995.
  21. Levi, A. D., Bunge, R. P., Lofgren, J. A., Meima, L., Hefli, F., Nikolics, K., and Sliwkowski, M. X. The influence of heregulins on human Schwann cell proliferation. *J. Neurosci.*, 15: 1329-1340, 1995.
  22. Graus-Porta, D., Beerli, R. R., and Hynes, N. E. Single-chain antibody-mediated intracellular retention of ErbB-2 impairs Neu differentiation factor and epidermal growth factor signaling. *Mol. Cell. Biol.*, 15: 1182-1191, 1995.
  23. Slamon, D. J., Clark, G. M., Wong, S. G., Levin, W. J., Ullrich, A., and McGuire, W. L. Human breast cancer: correlation of relapse and survival with amplification of the *HER-2/neu* oncogene. *Science (Washington DC)*, 235: 177-182, 1987.
  24. Slamon, D. J., Godolphin, W., Jones, L. A., Holt, J. A., Wong, S. G., Keith, D. E., Levin, W. J., Stuart, S. G., Udove, J., Ullrich, A., and Press, M. F. Studies of the *HER-2/neu* proto-oncogene in human breast and ovarian cancer. *Science (Washington DC)*, 244: 707-712, 1989.
  25. Hynes, N. E., and Stern, D. F. The biology of erbB-2/*neu*/*HER-2* and its role in cancer. *Biochim. Biophys. Acta*, 1198: 165-184, 1994.
  26. Bacus, S. S., Huberman, E., Chin, D., Kiguchi, K., Simpson, S., Lippman, M., and Lupu, R. A ligand for the erbB-2 oncogene product (gp30) induces differentiation of human breast cancer cells. *Cell Growth & Differ.*, 3: 401-411, 1992.
  27. Hudziak, R. M., Lewis, G. D., Winget, M., Fendly, B. M., Shepard, H. M., and Ullrich, A. p185<sup>HER2</sup> monoclonal antibody has antiproliferative effects *in vitro* and sensitizes human breast tumor cells to tumor necrosis factor. *Mol. Cell. Biol.*, 9: 1165-1172, 1989.
  28. Fendly, B. M., Winget, M., Hudziak, R. M., Lipari, M. T., Napier, M. A., and Ullrich, A. Characterization of murine monoclonal antibodies reactive to either the human epidermal growth factor receptor or *HER2/neu* gene product. *Cancer Res.*, 50: 1550-1558, 1990.
  29. Sliwkowski, M. X., Schaefer, G., Akita, R. W., Lofgren, J. A., Fitzpatrick, V. D., Nuijens, A., Fendly, B. M., Cerione, R. A., Vandlen, R. L., and Carraway, K. L. Coexpression of erbB2 and erbB3 proteins reconstitutes a high affinity receptor for heregulin. *J. Biol. Chem.*, 269: 14661-14665, 1994.
  30. Lewis, G. D., Figari, I., Fendly, B., Wong, W. L., Carter, P., Gorman, C., and Shepard, H. M. Differential responses of human tumor cell lines to anti-p185<sup>HER2</sup> monoclonal antibodies. *Cancer Immunol. Immunother.*, 37: 255-263, 1993.
  31. Carraway, K. L., Sliwkowski, M. X., Akita, R., Platko, J. V., Guy, P. M., Nuijens, A., Diamonti, A. J., Vandlen, R. L., Cantley, L. C., and Cerione, R. A. The erbB3 gene product is a receptor for heregulin. *J. Biol. Chem.*, 269: 14303-14306, 1994.
  32. Carraway, K. L., Soltoff, S. P., Diamonti, A. J., and Cantley, L. C. Heregulin stimulates mitogenesis and phosphatidylinositol 3-kinase in mouse fibroblasts transfected with erbB2/*neu* and erbB3. *J. Biol. Chem.*, 270: 7111-7116, 1995.
  33. Tzahar, E., Levkowitz, G., Karunakaran, D., Yi, L., Peles, E., Lavi, S., Chang, D., Liu, N., Yayon, A., Wen, D., and Yarden, Y. ErbB-3 and ErbB-4 function as the respective low and high affinity receptors of all Neu differentiation factor/hergulin isoforms. *J. Biol. Chem.*, 269: 25226-25233, 1994.
  34. Jeschke, M., Wels, W., Dengler, W., Imber, R., Stocklin, E., and Groner, B. Targeted inhibition of tumor-cell growth by recombinant heregulin-toxin fusion proteins. *Int. J. Cancer*, 60: 730-739, 1995.
  35. Plowman, G. D., Culouscou, J. M., Whitney, G. S., Green, J. M., Carlton, G. W., Foy, L., Neubauer, M. G., and Shoyab, M. Ligand-specific activation of HER4/p180erbB4, a fourth member of the epidermal growth factor receptor family. *Proc. Natl. Acad. Sci. USA*, 90: 1746-1750, 1993.
  36. Kraus, M. H., Fedi, P., Starks, R., Muraro, R., and Aaronson, S. A. Demonstration of ligand-dependent signaling by the erbB-3 tyrosine kinase and its constitutive activation in human breast tumor cells. *Proc. Natl. Acad. Sci. USA*, 90: 2900-2904, 1993.
  37. Scott, G. K., Robles, R., Park, J. W., Montgomery, P. A., Daniel, J., Holmes, W. E., Lee, J., Keller, G. A., Li, W. L., Fendly, B. M., Wood, W. I., Shepard, H. M., and Benz, C. C. A truncated intracellular *HER2/neu* receptor produced by alternative RNA processing affects growth of human carcinoma cells. *Mol. Cell. Biol.*, 13: 2247-2257, 1993.
  38. Kraus, M. H., Popescu, N. C., Amsbaugh, S. C., and King, C. R. Overexpression of the EGF receptor-related proto-oncogene *erbB-2* in human mammary tumor cell lines by different molecular mechanisms. *EMBO J.*, 6: 605-610, 1987.
  39. Davidson, N. E., Gelmann, E. P., Lippman, M. E., and Dickson, R. E. Epidermal growth factor receptor gene expression in estrogen receptor-positive and negative human breast cancer cell lines. *Mol. Endocrinol.*, 1: 216-223, 1987.
  40. Read, L. D., Keith, D., Jr., Slamon, D. J., and Katzenellenbogen, B. S. Hormonal modulation of *HER-2/neu* protooncogene messenger ribonucleic acid and p185 protein expression in human breast cancer cell lines. *Cancer Res.*, 50: 3947-3951, 1990.
  41. Ram, T. G., Kokeny, K. E., Dilts, C. A., and Ethier, S. P. Mitogenic activity of neu differentiation factor/hergulin mimics that of epidermal growth factor and insulin-like growth factor-I in human mammary epithelial cells. *J. Cell. Physiol.*, 163: 589-596, 1995.
  42. Pietras, R. J., Arboleda, J., Reese, D. M., Wongvipat, N., Pegram, M. D., Ramos, L., Gorman, C. M., Parker, M. G., Sliwkowski, M. X., and Slamon, D. J. *HER-2* tyrosine kinase pathway targets estrogen receptor and promotes hormone-independent growth in human breast cancer cells. *Oncogene*, 10: 2435-2446, 1995.
  43. Filmus, J., Pollak, M. N., Cailleau, R., and Buick, R. N. MDA-468, a human breast cancer cell line with high number of epidermal growth factor (EGF) receptors, has an amplified EGF receptor gene and is growth inhibited by egf. *Biochem. Biophys. Res. Commun.*, 128: 898-905, 1985.
  44. Gill, G. N., and Lazar, C. S. Increased phosphotyrosine content and inhibition of proliferation in EGF-treated A431 cells. *Nature (Lond.)*, 293: 305-307, 1981.
  45. Barnes, D. W. Epidermal growth factor inhibits growth of A431 human epidermoid carcinoma in serum-free cell culture. *J. Cell Biol.*, 93: 1-4, 1982.
  46. Bacus, S. S., Gudkov, A. V., Zelnick, C. R., Chin, D., Stern, R., Stancovski, I., Peles, E., Ben-Baruch, N., Farbstein, H., Lupu, R., Wen, D., Sela, M., and Yarden, Y. Neu differentiation factor (heregulin) induces expression of intercellular adhesion molecule 1: implications for mammary tumors. *Cancer Res.*, 53: 5251-61, 1993.
  47. Guy, P. M., Platko, J. V., Cantley, L. C., Cerione, R. A., and Carraway, K. L. Insect cell-expressed p180<sup>erbB3</sup> possesses an impaired tyrosine kinase activity. *Proc. Natl. Acad. Sci. USA*, 91: 8132-8136, 1994.
  48. Kim, H. H., Sierke, S. L., and Koland, J. G. Epidermal growth factor-dependent association of phosphatidylinositol 3-kinase with the erbB3 gene product. *J. Biol. Chem.*, 269: 24747-24755, 1994.
  49. Soltoff, S. P., Carraway, K. L., Prigent, S. A., Gullick, W. G., and Cantley, L. C. ErbB3 is involved in activation of phosphatidylinositol 3-kinase by epidermal growth factor. *Mol. Cell. Biol.*, 14: 3550-3558, 1994.
  50. Plowman, G. D., Green, J. M., Culouscou, J. M., Carlton, G. W., Rothwell, V. M., and Buckley, S. Heregulin induces tyrosine phosphorylation of HER4/p180erbB4. *Nature (Lond.)*, 366: 473-475, 1993.
  51. Gassmann, M., Casagrande, F., Orioli, D., Simon, H., Lai, C., Klein, R., and Lemke, G. Aberrant neural and cardiac development in mice lacking the ErbB4 neuregulin receptor. *Nature (Lond.)*, 378: 390-394, 1995.
  52. Beerli, R., Graus-Porta, D., Woods-Cook, K., Chen, X., Yarden, Y., and Hynes, N. E. Neu differentiation factor activation of ErbB-3 and ErbB-4 is cell specific and displays a differential requirement for ErbB-2. *Mol. Cell. Biol.*, 15: 6496-6505, 1995.
  53. Alimandi, M., Romano, A., Curia, M. C., Muraro, R., Fedi, P., Aaronson, S. A., Di Fiore, P. P., and Kraus, M. H. Cooperative signaling of ErbB3 and ErbB2 in neoplastic transformation and human mammary carcinomas. *Oncogene*, 10: 1813-1821, 1995.
  54. White, M. F. The IRS-1 signaling system. *Curr. Opin. Genet. Dev.*, 4: 47-54, 1994.
  55. Wallasch, C., Weiss, F. U., Niederfellner, G., Jallal, B., Issing, W., and Ullrich, A. Heregulin-dependent regulation of *HER2/neu* oncogenic signaling by heterodimerization with *HER3*. *EMBO J.*, 14: 4267-4275, 1995.
  56. Marte, B. M., Jeschke, M., Graus-Porta, D., Taverna, D., Hofer, P., Groner, B., Yarden, Y., and Hynes, N. E. Neu differentiation factor/hergulin modulates growth and differentiation of HC11 mammary epithelial cells. *Mol. Endocrinol.*, 9: 14-23, 1995.
  57. Marte, B. M., Graus-Porta, D., Jeschke, M., Fabbro, D., Hynes, N. E., and Taverna, D. NDF/hergulin activates MAP kinase and p70/p85 S6 kinase during proliferation or differentiation of mammary epithelial cells. *Oncogene*, 10: 167-175, 1995.
  58. Maurer, H. R. Potential pitfalls of [<sup>3</sup>H]thymidine techniques to measure cell proliferation. *Cell Tissue Kinet.*, 14: 111-120, 1981.
  59. Davison, P., Liu, S., and Karasek, M. Limitations in the use of [<sup>3</sup>H]thymidine incorporation into DNA as an indicator of epidermal keratinocyte proliferation *in vitro*. *Cell Tissue Kinet.*, 12: 605-614, 1979.
  60. Jozan, S., Gay, G., Marques, B., Mirouze, A., and David, J. F. Oestradiol is effective in stimulating <sup>3</sup>H-thymidine incorporation but not on proliferation of breast cancer cultured cells. *Cell Tissue Kinet.*, 18: 457-464, 1985.
  61. Chazin, V. R., Kaleko, M., Miller, A. D., and Slamon, D. J. Transformation mediated by the human *HER-2* gene independent of the epidermal growth factor receptor. *Oncogene*, 7: 1859-1866, 1992.
  62. Ginsburg, E., and Vonderhaar, B. K. Epidermal growth factor stimulates the growth of A431 tumours in athymic mice. *Cancer Lett.*, 28: 143-150, 1985.
  63. Ozawa, S., Ueda, M., Ando, N., Abe, O., Hirai, M., and Shimizu, N. Stimulation by EGF of the growth of EGF receptor-hyperproducing tumour cells in athymic mice. *Int. J. Cancer*, 40: 706-710, 1987.
  64. Park, J. W., Slamon, D., and Shepard, H. M. Loss of heregulin expression is associated with malignancy. *Proc. Am. Assoc. Cancer Res.*, 84: 3107, 1993.

# **EXHIBIT F**

## p185<sup>HER2</sup> Monoclonal Antibody Has Antiproliferative Effects In Vitro and Sensitizes Human Breast Tumor Cells to Tumor Necrosis Factor

ROBERT M. HUDZIAK,<sup>1</sup> GAIL D. LEWIS,<sup>2</sup> MARCY WINGET,<sup>3</sup> BRIAN M. FENDLY,<sup>3</sup> H. MICHAEL SHEPARD,<sup>2</sup>  
AND AXEL ULLRICH<sup>1†\*</sup>

Departments of Developmental Biology,<sup>1</sup> Pharmacological Sciences,<sup>2</sup> and Medicinal and Analytical Chemistry,<sup>3</sup>  
Genentech, Inc., 460 Point San Bruno Boulevard, South San Francisco, California 94080

Received 3 October 1988/Accepted 8 December 1988

**The *HER2/c-erbB-2* gene encodes the epidermal growth factor receptorlike human homolog of the rat *neu* oncogene. Amplification of this gene in primary breast carcinomas has been shown to correlate with poor clinical prognosis for certain cancer patients. We show here that a monoclonal antibody directed against the extracellular domain of p185<sup>HER2</sup> specifically inhibits the growth of breast tumor-derived cell lines overexpressing the *HER2/c-erbB-2* gene product and prevents *HER2/c-erbB-2*-transformed NIH 3T3 cells from forming colonies in soft agar. Furthermore, resistance to the cytotoxic effect of tumor necrosis factor alpha, which has been shown to be a consequence of *HER2/c-erbB-2* overexpression, is significantly reduced in the presence of this antibody.**

*HER2/c-erbB-2*, the human homolog of the rat proto-oncogene *neu* (4, 34), encodes a 1,255-amino-acid glycoprotein with extensive homology to the human epidermal growth factor (EGF) receptor (4, 21, 33, 34, 42). The *HER2/c-erbB-2* gene product, p185<sup>HER2</sup>, has all of the structural features and many of the functional properties of subclass I growth factor receptors (reviewed in references 43 and 44), including cell surface location and an intrinsic tyrosine kinase activity. However, the ligand for this putative growth factor receptor has not yet been identified.

Amplification of the *HER2/c-erbB-2* gene has been found in human salivary gland and gastric tumor-derived cell lines (13, 34), as well as in mammary gland carcinomas (21, 22, 40, 42). Slamon et al. (35) surveyed 189 primary breast adenocarcinomas and determined that the *HER2/c-erbB-2* gene was amplified in about 30% of the cases. Most importantly, *HER2/c-erbB-2* amplification was correlated with a negative prognosis and high probability of relapse. Similar although less frequent amplification of the *HER2/c-erbB-2* gene has been reported for gastric and colon adenocarcinomas (45, 46). Experiments with NIH 3T3 cells also suggest a direct role for the overexpressed, structurally unaltered *HER2/c-erbB-2* gene product p185<sup>HER2</sup> in neoplastic transformation. High levels of *HER2/c-erbB-2* gene expression attained by coamplification of the introduced gene with dihydrofolate reductase by methotrexate selection (18) or by using a strong promoter (6) was shown to transform NIH 3T3 fibroblasts. Only cells with high levels of p185<sup>HER2</sup> are transformed, i.e., have an altered morphology, are anchorage independent, and will form tumors in athymic mice.

Overexpression of p185<sup>HER2</sup> may, furthermore, contribute to malignant tumor development by allowing tumor cells to evade one component of the antitumor defenses of the body, the activated macrophage (17). Macrophages play an important role in immune surveillance against neoplastic growth in vivo (1, 2, 38), and Urban et al. (39) have shown that tumor

cells made resistant to macrophages display enhanced tumorigenicity. Tumor necrosis factor alpha (TNF- $\alpha$ ) has been shown to play a role in activated macrophage-mediated tumor cell killing in vitro (3, 11, 23, 29, 39). NIH 3T3 cells transformed by a transfected and amplified *HER2/c-erbB-2* cDNA show increased resistance to the cytotoxic effects of activated macrophages or TNF- $\alpha$  in direct correlation with increased levels of p185<sup>HER2</sup> expression. Furthermore, breast tumor cell lines with high levels of p185<sup>HER2</sup> exhibit resistance to TNF- $\alpha$ . Resistance to host antitumor defenses could facilitate the escape of cells from a primary tumor to establish metastases at distant sites.

To further investigate the consequences of alteration in *HER2/c-erbB-2* gene expression in mammary gland neoplasia and to facilitate investigation of the normal biological role of the *HER2/c-erbB-2* gene product, we have prepared monoclonal antibodies against the extracellular domain of p185<sup>HER2</sup>. One monoclonal antibody (4D5) was characterized in more detail and was shown to inhibit in vitro proliferation of human breast tumor cells overexpressing p185<sup>HER2</sup> and, furthermore, to increase the sensitivity of these cells to the cytotoxic effects of TNF- $\alpha$ .

### MATERIALS AND METHODS

**Cells and cell culture.** Human tumor cell lines were obtained from the American Type Culture Collection. The mouse fibroblast line NIH 3T3/HER2-3<sub>400</sub>, expressing an amplified *HER2/c-erbB-2* cDNA under simian virus 40 early promoter control, and the vector-transfected control cell line NIH 3T3/CVN have been described previously (18).

Cells were cultured in a 1:1 mixture of Dulbecco modified Eagle medium and Ham nutrient mixture F-12 supplemented with 2 mM glutamine, 100 u of penicillin per ml, 100  $\mu$ g of streptomycin per ml, and 10% serum. Human tumor cell lines were cultured with fetal bovine serum (GIBCO Laboratories, Grand Island, N.Y.); NIH 3T3 derivatives were cultured with calf serum (Hyclone Laboratories, Inc., Logan, Utah.).

**Immunization.** Female BALB/c mice were immunized with NIH 3T3/HER2-3<sub>400</sub> cells expressing high levels of

\* Corresponding author.

† Present address: Max-Planck-Institut für Biochemie, 8033 Martinsried, Federal Republic of Germany.

p185<sup>HER2</sup>. The cells were washed once with phosphate-buffered saline (PBS) and detached from the plate with PBS containing 25 mM EDTA. After low-speed centrifugation, the cells were suspended in cold PBS ( $2 \times 10^7$  cells per ml). Each mouse was injected intraperitoneally with 0.5 ml of this cell suspension on weeks 0, 2, 5, and 7.

On weeks 9 and 13, 100  $\mu$ l of a Triton X-100 membrane preparation of p185<sup>HER2</sup>, partially purified by wheat germ agglutinin chromatography (700  $\mu$ g of protein per ml) (25), was administered intraperitoneally. Three days before fusion, 100  $\mu$ l of the enriched p185<sup>HER2</sup> protein was administered intravenously.

**Fusion and screening.** Mice with high antibody titers as determined by immunoprecipitation of p185<sup>HER2</sup> were sacrificed, and their splenocytes were fused as described previously (26). Spleen cells were mixed at a 4:1 ratio with the fusion partner, mouse myeloma cell line X63-Ag8.653 (20), in the presence of 50% polyethylene glycol 4000. Fused cells were plated at a density of  $2 \times 10^5$  cells per well in 96-well microdilution plates. The hypoxanthine-azaserine (12) selection for hybridomas was begun 24 h later. Beginning at day 10 postfusion, supernatants from hybridoma-containing wells were tested for the presence of antibodies specific for p185<sup>HER2</sup> by an enzyme-linked immunosorbent assay with the wheat germ agglutinin chromatography-purified p185<sup>HER2</sup> preparation (28). Enzyme-linked immunosorbent assay-positive supernatants were confirmed by immunoprecipitation and cloned twice by limiting dilution.

Large quantities of specific monoclonal antibodies were produced by preparation of ascites fluid; antibodies were then purified on protein A-Sepharose columns (Fermentech, Inc., Edinburgh, Scotland) and stored sterile in PBS at 4°C.

**Immunoprecipitations and antibodies.** Cells were harvested by trypsinization, counted in a Coulter counter (Coulter Electronics, Inc., Hialeah, Fla.), and plated 24 h before being harvested for analysis of p185<sup>HER2</sup> expression. Cells were lysed at 4°C with 0.8 ml of HNEG lysis buffer (18) per 100-mm plate. After 10 min, 1.6 ml of lysis dilution buffer (HNEG buffer with 1% bovine serum albumin and 0.1% Triton X-100) was added to each plate, and the extracts were clarified by centrifugation at  $12,000 \times g$  for 5 min.

Antibodies were added to the cell extracts and allowed to bind at 4°C for 2 to 4 h. Immune complexes were collected by adsorption to protein A-Sepharose beads for 20 min and washed three times with 1 ml of HNEG buffer-0.1% Triton X-100. Autophosphorylation reactions were carried out for 20 min at 4°C in 50  $\mu$ l of HNEG wash buffer containing 5 mM MnCl<sub>2</sub> and 3  $\mu$ Ci of [ $\gamma$ -<sup>32</sup>P]ATP (5,000 Ci/mmol, Amersham Corp., Arlington Heights, Ill.). The autophosphorylation reaction conditions have been described previously (18). Proteins were separated on sodium dodecyl sulfate (SDS)-7.5% polyacrylamide gels and analyzed by autoradiography.

The polyclonal antibody, G-H2CT17, recognizing the carboxy-terminal 17 amino acids of p185<sup>HER2</sup>, has been described previously (18). The anti-EGF receptor monoclonal antibody 108 (16) was provided by Joseph Schlessinger, Rorer Biotechnology, Inc.

**Fluorescence-activated cell sorting.** SK-BR-3 human breast tumor cells overexpressing the *HER2/c-erbB-2* gene (17, 22) or A431 human squamous carcinoma cells overexpressing the EGF receptor gene (14) were grown in T175 flasks. They were detached from the flasks by treatment with 25 mM EDTA-0.15 M NaCl, collected by low-speed centrifugation, and suspended at  $1 \times 10^6$  cells per ml in PBS-1% fetal bovine serum. One milliliter of each cell line was incubated with 10  $\mu$ g of either anti-*HER2/c-erbB-2* monoclonal antibody (4D5)

or a control antibody (40.1.H1) recognizing the hepatitis B surface antigen. The cells were washed twice and suspended on ice for 30 min in 1 ml of PBS-1% fetal bovine serum containing 10  $\mu$ g of goat anti-mouse immunoglobulin G F(ab')<sub>2</sub> fragments conjugated with fluorescein isothiocyanate dye (Boehringer Mannheim Biochemicals, Indianapolis, Ind.). Unbound fluorescein dye was removed by two further washes. The cells were suspended at  $2 \times 10^6$  per ml in PBS-1% fetal bovine serum and analyzed with an EPICS 753 (Coulter) fluorescence-activated cell sorter. Fluorescein was excited by 300 mW of 488-nm argon laser light, and the emitted light was collected with a 525-nm band-pass filter with a 10-nm band width.

**Down-regulation assay.** SK-BR-3 cells were plated at  $1.5 \times 10^5$  cells per 35-mm culture dish in normal medium. After a 6-h period to allow attachment, the medium was replaced by 1.5 ml of methionine-free labeling medium containing 150  $\mu$ Ci of [<sup>35</sup>S]methionine per ml and 2% dialyzed fetal bovine serum. The cells were metabolically labeled for 14 h and then chased with medium containing 2% dialyzed serum and unlabeled methionine. Either a control monoclonal antibody (40.1.H1) or anti-p185<sup>HER2</sup> (4D5) was added to a final concentration of 2.5  $\mu$ g/ml. At 0, 5, and 11 h, extracts were prepared with 0.3 ml of lysis solution and 0.6 ml of dilution buffer. The p185<sup>HER2</sup> was immunoprecipitated with 2.5  $\mu$ l of polyclonal antibody G-H2CT17. The washed immune complexes were dissolved in sample buffer, electrophoresed on a SDS-7.5% polyacrylamide gel, and analyzed by autoradiography. Each time point determination was performed in duplicate. Autoradiograph band intensities were quantitated by using a scanner (Ambis Systems).

**Cell proliferation assays.** The anti-p185<sup>HER2</sup> monoclonal antibodies were characterized by using the breast tumor cell line SK-BR-3. Cells were detached by using 0.25% (vol/vol) trypsin and suspended in complete medium at a density of 4

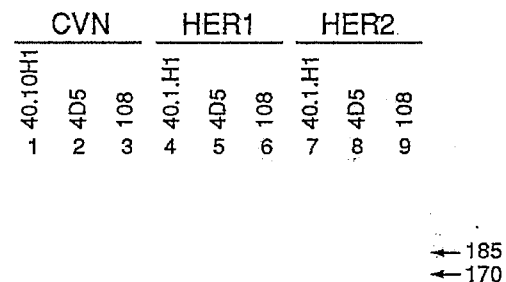


FIG. 1. Specificity of monoclonal antibody 4D5. Three cell lines, NIH 3T3/CVN, NIH 3T3/HER1-EGF receptor, and NIH 3T3/HER2-3<sub>400</sub>, were plated out at  $2.0 \times 10^6$  in 100-mm culture dishes. At 24 h, Triton X-100 lysates were prepared and divided into three portions. Either an irrelevant monoclonal antibody (6  $\mu$ g of anti-hepatitis B virus surface antigen, 40.1.H1; lanes 1, 4, and 7), anti-p185<sup>HER2</sup> monoclonal antibody 4D5 (6  $\mu$ g; lanes 2, 5, and 8), or anti-EGF receptor monoclonal antibody 108 (6  $\mu$ g; lanes 3, 6, and 9) was added and allowed to bind at 4°C for 4 h. The immune complexes were collected with 30  $\mu$ l of protein A-Sepharose. Rabbit anti-mouse immunoglobulin (7  $\mu$ g) was added to each 4D5 immunoprecipitation to improve the binding of this monoclonal antibody to the protein A-coated beads. Proteins were labeled by autophosphorylation and separated on an SDS-7.5% polyacrylamide gel. The gel was exposed to film at -70°C for 4 h with an intensifying screen. The arrows show the positions of proteins of *M*<sub>r</sub> 185,000 and 170,000.



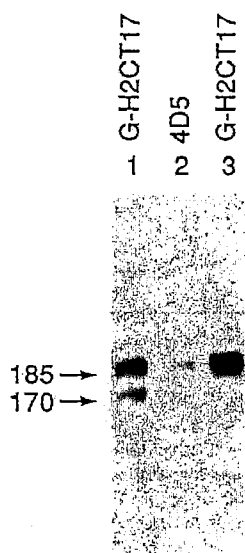


FIG. 2. Binding of monoclonal antibody 4D5 to unglycosylated receptor. NIH 3T3/HER2-3<sub>400</sub> cells were plated into two 100-mm plates at  $2 \times 10^6$  cells per plate. After 14 h, the antibiotic tunicamycin was added to one plate at  $3 \mu\text{g/ml}$ . After a further 5.5 h of incubation, Triton X-100 lysates were then prepared from each plate. Immunoprecipitations, the autophosphorylation reaction, and SDS-polyacrylamide gel electrophoresis were performed as described in the legend to Fig. 1. Lanes: 1, tunicamycin-treated cell lysate (one-third of a plate) immunoprecipitated with  $2.5 \mu\text{l}$  of a polyclonal antibody directed against the C terminus of p185<sup>HER2</sup>; 2, tunicamycin-treated cell lysate (one-third of a plate) immunoprecipitated with  $6 \mu\text{g}$  of 4D5; 3, untreated control lysate (one-third of a plate) immunoprecipitated with the polyclonal antibody. The arrows show the locations of proteins of  $M_r$  185,000 and 170,000.

$\times 10^5$  cells per ml. Aliquots of  $100 \mu\text{l}$  ( $4 \times 10^4$  cells) were plated into 96-well microdilution plates, the cells were allowed to adhere, and  $100 \mu\text{l}$  of media alone or media containing monoclonal antibody (final concentration,  $5 \mu\text{g/ml}$ ) was then added. After 72 h, plates were washed twice with PBS (pH 7.5), stained with crystal violet (0.5% in methanol), and analyzed for relative cell proliferation as described previously (36).

For assays in which monoclonal antibodies were combined with recombinant human TNF- $\alpha$  ( $5.0 \times 10^7$  U/mg; Genentech, Inc.), cells were plated and allowed to adhere as described above. Following cell adherence, control medium alone or medium containing monoclonal antibodies was added to a final concentration of  $5 \mu\text{g/ml}$ . Cultures were incubated for another 4 h, and then increasing concentrations of TNF- $\alpha$  were added to a final volume of  $200 \mu\text{l}$ . Following 72 h of incubation, the relative cell number was determined by crystal violet staining. Some samples were analyzed by crystal violet staining following cell adherence for determination of the initial cell number.

## RESULTS

**Specificity of monoclonal antibody 4D5.** Monoclonal antibodies directed against the extracellular domain of p185<sup>HER2</sup> were prepared by immunizing mice with NIH 3T3 cells transfected with a *HER2/c-erbB-2* cDNA (HER2-3<sub>400</sub>) (17, 18) and overexpressing the corresponding gene product, p185<sup>HER2</sup>. One antibody exhibited several interesting biological properties and was chosen for further characterization. Antibody 4D5 specifically immunoprecipitated a single <sup>32</sup>P-

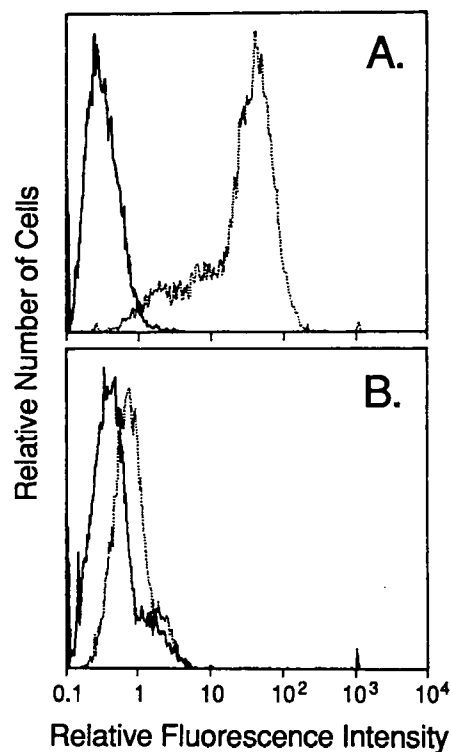


FIG. 3. Fluorescence-activated cell sorter histograms of human tumor cells binding anti-p185 monoclonal antibody 4D5. —, Binding by the control antibody, 40.1.H1, directed against the hepatitis B surface antigen; ·····, binding by the anti-*HER2/c-erbB-2* antibody, 4D5. The antibodies were first allowed to react with the cell surface. After a wash step, bound antibody was labeled by addition of fluorescein-conjugated F(ab')<sub>2</sub> fragment of goat anti-mouse immunoglobulin G. (A) Binding of the antibodies to the human breast tumor line SK-BR-3, which contains an amplification of the *HER2/c-erbB-2* gene and expresses high levels of the *HER2/c-erbB-2* gene product p185<sup>HER2</sup>. (B) Binding of the same antibodies to the human squamous epithelial cell line A431. This cell line expresses low levels of mRNA for *HER2/c-erbB-2* and high levels ( $2 \times 10^6$  receptors per cell) of the EGF receptor.

labeled protein of  $M_r$  185,000 from NIH 3T3 cells expressing p185<sup>HER2</sup> (Fig. 1, lane 8). This antibody did not cross-react with the human EGF receptor (HER1; Fig. 1, lane 5), even when overexpressed in a mouse NIH 3T3 background (Fig. 1, lane 6). Furthermore, it did not immunoprecipitate any proteins from NIH 3T3 cells transfected with a control plasmid (pCVN) which expresses the neomycin resistance and dihydrofolate reductase genes only (Fig. 1, lane 2).

To determine the nature of the epitope recognized by 4D5, NIH 3T3/HER2-3<sub>400</sub> cells were treated with tunicamycin, which prevents addition of N-linked oligosaccharides to proteins (15, 41). Cells treated with this antibiotic for 5.5 h contained two proteins which were immunoprecipitated by a polyclonal antibody against the carboxy-terminal peptide of p185<sup>HER2</sup> (Fig. 2, lane 1). The polypeptide of 170,000  $M_r$  represents unglycosylated p185<sup>HER2</sup>. The upper band of ca. 185,000  $M_r$  comigrated with glycosylated p185<sup>HER2</sup> from untreated cells (Fig. 2, lane 3). Monoclonal antibody 4D5 efficiently immunoprecipitated only the glycosylated form of p185<sup>HER2</sup> (Fig. 2, lane 2). This experiment suggests either that the epitope recognized by 4D5 consists partly of carbohydrate, or, alternatively, that the antibody recognizes a conformation of the protein achieved only when it is glycosylated.

TABLE 1. Inhibition of SK-BR-3 proliferation by anti-p185<sup>HER2</sup> monoclonal antibodies<sup>a</sup>

Monoclonal antibody	Relative cell proliferation <sup>b</sup>
7C2	79.3 ± 2.2
2C4	79.5 ± 4.4
7D3	83.8 ± 5.9
4D5	44.2 ± 4.4
3E8	66.2 ± 2.4
6E9	98.9 ± 3.6
7F3	62.1 ± 1.4
3H4	66.5 ± 3.9
2H11	92.9 ± 4.8
40.1.H1	105.8 ± 3.8
4F4	94.7 ± 2.8

<sup>a</sup> SK-BR-3 breast tumor cells were plated as described in Materials and Methods. Following adherence, medium containing 5 µg of either anti-p185<sup>HER2</sup> or control monoclonal antibodies (40.1.H1 and 4F4) per ml were added.

<sup>b</sup> Relative cell proliferation was determined by crystal violet staining of the monolayers after 72 h. Values are expressed as a percentage of results with untreated control cultures (100%).

The binding of monoclonal antibody 4D5 to human tumor cell lines was investigated by fluorescence-activated cell sorting (Fig. 3). This antibody was bound to the surface of cells expressing p185<sup>HER2</sup>. Figure 3A shows the 160-fold increase in cellular fluorescence observed when 4D5 was added to SK-BR-3 breast adenocarcinoma cells relative to a control monoclonal antibody. This cell line contains an amplified *HER2/c-erbB-2* gene and expresses high levels of p185<sup>HER2</sup> (17, 22). In contrast, the squamous carcinoma cell line A431, which expresses about  $2 \times 10^6$  EGF receptors per cell (14) but only low levels of p185<sup>HER2</sup> (4), exhibited only a twofold increase in fluorescence with 4D5 (Fig. 3B) when compared with a control monoclonal antibody.

The binding of 4D5 correlated with the levels of p185<sup>HER2</sup> expressed by these two cell lines. SK-BR-3 cells, expressing high levels of p185<sup>HER2</sup>, showed an 80-fold increase in relative fluorescence intensity compared with A431 cells. This experiment demonstrates that 4D5 specifically recognizes the extracellular domain of p185<sup>HER2</sup>.

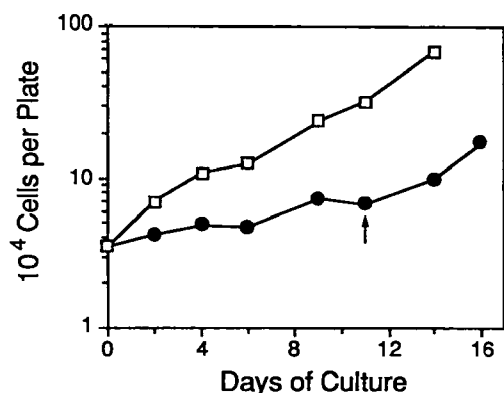


FIG. 4. Growth curve of SK-BR-3 cells treated with anti-*HER2/c-erbB-2* monoclonal antibody 4D5. Cells were plated into 35-mm culture dishes at 20,000 cells per plate in medium containing 2.5 µg of either control antibody (40.1.H1, anti-hepatitis B surface antigen) (□) or anti-p185<sup>HER2</sup> antibody 4D5 (●) per ml. On the indicated days, cells were trypsinized and counted in a Coulter counter. The determination for each time point and each antibody was done in duplicate, and the counts were averaged. The arrow indicates the day the cells were refed with medium without antibodies.

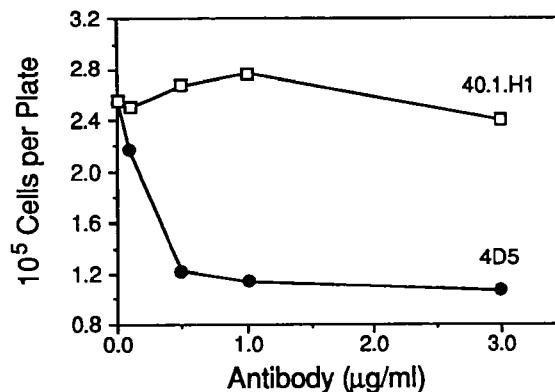


FIG. 5. Growth of SK-BR-3 cells in different concentrations of monoclonal antibody 4D5. The human breast tumor line SK-BR-3 was plated into 35-mm culture dishes at 20,000 cells per dish. Either 0.1, 0.5, 1.0, or 3.0 µg of a control monoclonal antibody (40.1.H1, anti-hepatitis B surface antigen) or monoclonal 4D5 antibody per ml was added at the time of plating. After 8 days of growth, the plates were trypsinized and the cells were counted in a Coulter counter. Each concentration of antibody was plated and counted in duplicate, and the cell numbers were averaged.

**Effects on cell proliferation.** We used the human mammary gland adenocarcinoma cell line, SK-BR-3, to determine whether monoclonal antibodies directed against the extracellular domain of p185<sup>HER2</sup> had any effect on the proliferation of cell lines overexpressing this receptorlike protein. SK-BR-3 cells were coincubated with several *HER2/c-erbB-2*-specific monoclonal antibodies or with either of two different control monoclonal antibodies (40.1.H1, directed against the hepatitis B surface antigen; 4F4, directed against recombinant human gamma interferon). Most anti-*HER2/c-erbB-2* monoclonal antibodies which recognize the extracellular domain inhibited the growth of SK-BR-3 cells (Table

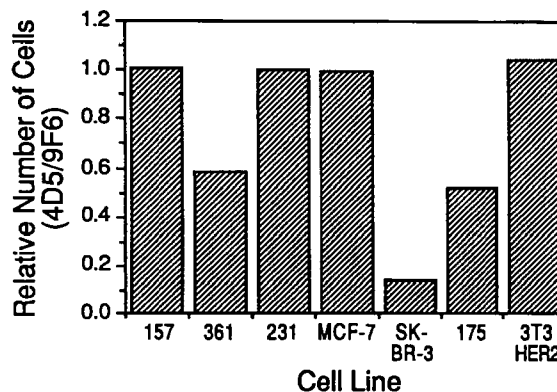


FIG. 6. Screening of breast tumor cell lines for growth inhibition by monoclonal antibody 4D5. Each cell line was plated in 35-mm culture dishes at 20,000 cells per dish. Either a control monoclonal antibody (9F6, anti-human immunodeficiency virus gp120) or the anti-p185<sup>HER2</sup> monoclonal antibody 4D5 was added on day 0 to 2.5 µg/ml. Because the different cell lines grow at different rates, the cell lines NIH 3T3/HER2-3<sub>400</sub> and SK-BR-3 were counted after 6 days, cell lines MDA-MB-157, MDA-MB-231, and MCF-7 were counted after 9 days, and cell lines MDA-MB-175VII and MDA-MB-361 were counted after 14 days. The difference in growth between cells treated with 4D5 and 40.1.H1 is expressed as the ratio of cell numbers with 4D5 versus a control monoclonal antibody, 9F6. Each cell line was assayed in duplicate for each antibody, and the counts were averaged.

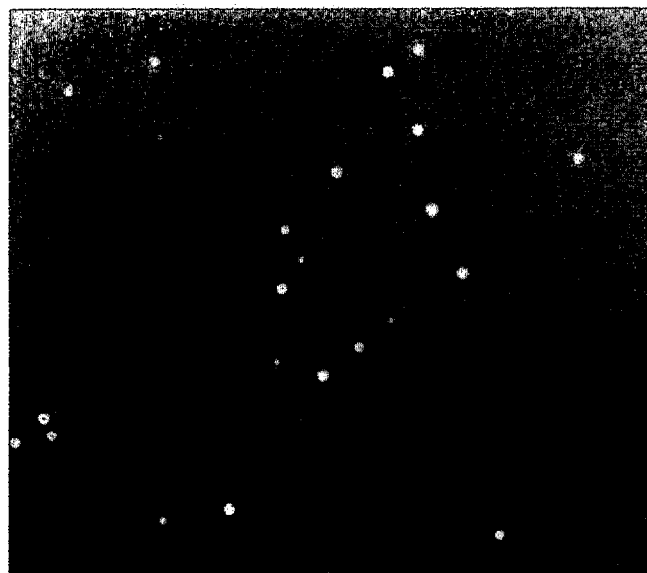


FIG. 7. Inhibition of anchorage-independent growth of NIH 3T3/HER2-3<sub>400</sub> cells by 4D5. Cells (20,000 per 60-mm plate) were plated in 0.2% soft agar over a 0.4% agar base. After 3 weeks, the plates were photographed at  $\times 100$  magnification by using a Nikon microscope with phase-contrast optics. (a) HER2-3<sub>400</sub> cells plated in agar containing 200 ng of a control antibody (TF-C8) per ml. (b) The same cells plated in agar containing 200 ng of 4D5 per ml.

1). Maximum inhibition was obtained with monoclonal antibody 4D5, which inhibited cellular proliferation by 56%. The control antibodies had no significant effect on cell growth.

Figure 4 compares the growth of SK-BR-3 cells in the presence of either a control antibody, 40.1.H1, or the anti-p185<sup>HER2</sup> antibody. Proliferation of the cells was inhibited when antibody 4D5 was present. The generation time increased from 3.2 to 12.2 days. To determine whether 4D5 treatment was cytostatic or cytotoxic, antibody was removed by medium change 11 days after treatment. The cells resumed growth at a nearly normal rate, suggesting that the antibody affected cell growth rather than cell viability. The dose-response curve (Fig. 5) showed that a concentration of 200 ng/ml inhibited growth by 50%, whereas maximum

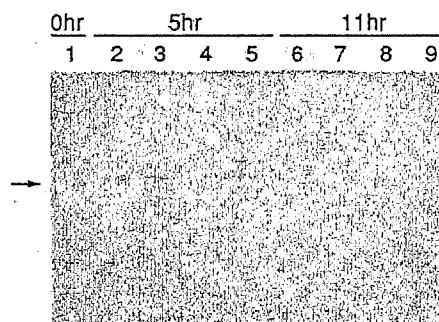


FIG. 8. Effect of antibody binding on p185<sup>HER2</sup> turnover. SK-BR-3 cells were labeled for 14 h with [<sup>35</sup>S]methionine. The label was then chased with cold methionine and either an irrelevant monoclonal antibody (40.1.H1, anti-hepatitis B surface antigen) or 4D5 was added to 2.5  $\mu$ g/ml. The cells on the plates were lysed at 0, 5, and 11 h, and <sup>35</sup>S-labeled p185<sup>HER2</sup> was quantitated by immunoprecipitation with the C-terminal specific polyclonal antibody. The 5- and 11-h time point determinations were performed in duplicate for each of the two antibodies. Proteins were separated by SDS-polyacrylamide gel electrophoresis. The fluor-treated gel was exposed to film for 4 h at room temperature. The arrow indicates the position of a protein of  $M_r$  185,000. Band intensities were quantitated by using an Ambis Systems scanner. Lanes; 1, 0 h; lanes 2 and 3, 40.1.H1 (5 h); lanes 4 and 5, 4D5 (5 h); lanes 6 and 7, 40.1.H1 (11 h); lanes 8 and 9, 4D5 (11 h).

effects were achieved by using a concentration of between 0.5 and 1  $\mu$ g/ml.

The effect of 4D5 on the proliferation of six additional breast tumor cell lines, as well as mouse NIH 3T3 fibroblasts transformed by p185<sup>HER2</sup> overexpression (NIH 3T3/HER2-3<sub>400</sub>), was tested in monolayer growth assays. Cells were plated at low density in medium containing 2.5  $\mu$ g of either a control antibody or 4D5 per ml. When the cultures approached confluency, cells were removed with trypsin and counted. 4D5 did not have any significant effect on the growth of the MCF-7, MDA-MB-157, MDA-MB-231, or NIH 3T3/HER2-3<sub>400</sub> cell lines (Fig. 6). It did, however, significantly affect the growth of the cell lines MDA-MB-361 (58% of control) and MDA-MB-175-VII (52% of control), which express high levels of p185<sup>HER2</sup> (17).

Interestingly, monoclonal antibody 4D5 had no effect on the monolayer growth of the NIH 3T3/HER2-3<sub>400</sub> cell line. However, it completely prevented colony formation by these cells in soft agar (Fig. 7), a property which had been induced by *HER2/c-erbB-2* amplification (18). In the presence of 200 ng of a control monoclonal antibody (antitissue factor, TC-C8) per ml, 116 (average of two plates) soft-agar colonies were counted, while the same cells plated simultaneously into soft agar containing 200 ng of 4D5 per ml did not yield any colonies.

**Monoclonal antibody 4D5 down-regulates p185<sup>HER2</sup>.** To determine whether the antiproliferative effect of 4D5 was due to enhanced degradation of p185<sup>HER2</sup>, we measured its rate of turnover in the presence or absence of antibody. p185<sup>HER2</sup> was metabolically labeled by culturing SK-BR-3 cells for 14 h in the presence of [<sup>35</sup>S]methionine. Cells were then chased for various times, and either a control antibody or 4D5 was added at the beginning of the chase period. At 0, 5, and 11 h, cells were lysed and p185<sup>HER2</sup> levels were assayed by immunoprecipitation and SDS-polyacrylamide gel electrophoresis. p185<sup>HER2</sup> is degraded more rapidly after exposure of SK-BR-3 cells to 4D5 (Fig. 8). Densitometric evaluation of the data showed that the p185<sup>HER2</sup> half-life of

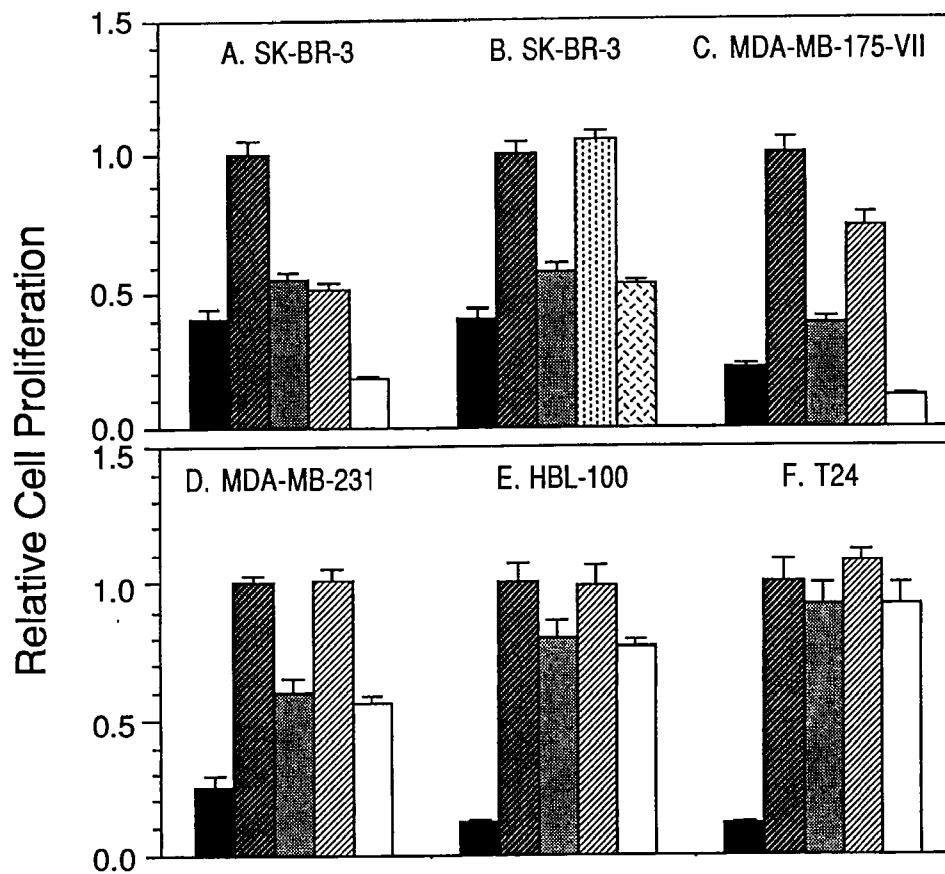


FIG. 9. Monoclonal antibody 4D5 sensitizes breast tumor cells to the cytotoxic effects of TNF- $\alpha$ . Cells were plated in 96-well microdilution plates ( $4 \times 10^4$  cells per well for SK-BR-3, MDA-MB-175-VII, and MDA-MB-231;  $10^4$  cells per well for HBL-100 and T24) and allowed to adhere for 2 h. Anti-*HER2/c-erbB-2* monoclonal antibody 4D5 (5  $\mu$ g/ml) or anti-hepatitis B surface antigen monoclonal antibody 40.1.H1 (5  $\mu$ g/ml) was then added for a 4-h incubation prior to the addition of TNF- $\alpha$  to a final concentration of  $10^4$  units/ml. After 72 h, the monolayers were washed twice with PBS and stained with crystal violet dye for determination of relative cell proliferation. In addition, some cell monolayers were stained with crystal violet following adherence in order to determine the initial cell density for comparison with cell densities measured after 72 h. The symbols denote initial cell density (■), untreated (control) cells (▨), cells treated with TNF- $\alpha$  (■), 4D5 (□), TNF- $\alpha$  plus 4D5 (□), 40.1.H1 (□); or TNF- $\alpha$  plus 40.1.H1 (□).

7 h decreased to 5 h in the presence of antibody (data not shown).

**Monoclonal antibody 4D5 enhances TNF- $\alpha$  cytotoxicity.** The addition of certain growth factors to tumor cells has been shown to increase their resistance to the cytotoxic effects of TNF- $\alpha$  (37). A prediction based on these findings would be that expression of oncogenes that mimic or replace growth factor receptor function may also increase the resistance of cells to this cytokine. Recently, it was shown that overexpression of the putative growth factor receptor p185<sup>HER2</sup> in NIH 3T3 cells caused an increase in the resistance of these cells to TNF- $\alpha$  (17). Furthermore, breast tumor cell lines with high levels of p185<sup>HER2</sup> also exhibited TNF- $\alpha$  resistance.

To further investigate the mechanism by which the 4D5 antibody inhibited cell growth, we investigated the response of three breast tumor cell lines to TNF- $\alpha$  in the presence or absence of this antibody. If the anti-p185<sup>HER2</sup> monoclonal antibody 4D5 inhibited proliferation of breast tumor cells by interfering with the signalling functions of p185<sup>HER2</sup>, addition of this antibody would be expected to enhance the sensitivity of tumor cells to TNF- $\alpha$ . Both SK-BR-3 (Fig. 9A) and MDA-MB-175-VII (Fig. 9C) were growth inhibited by both the monoclonal antibody 4D5 (5  $\mu$ g/ml; 50% and 25% inhibition, respectively) and high concentrations of TNF- $\alpha$

( $1 \times 10^4$  units/ml; 50% and 60% inhibition, respectively). However, the combination of TNF- $\alpha$  and monoclonal antibody 4D5 reduced the SK-BR-3 and MDA-MB-175-VII tumor cell number to a level below that initially plated, indicating the induction of a cytotoxic response. In a separate experiment, SK-BR-3 cell viability was determined directly by using trypan blue dye exclusion, yielding identical results to those described above that were obtained by using crystal violet staining (data not shown). A control monoclonal antibody, 40.1.H1, did not inhibit SK-BR-3 breast tumor cell proliferation, nor did it induce an enhanced sensitivity of this cell line to the cytotoxic effects of TNF- $\alpha$  (Fig. 9B). In addition, the growth of the breast tumor cell line MDA-MB-231, which does not express detectable levels of p185<sup>HER2</sup> (17), was unaffected by monoclonal antibody 4D5, and the growth inhibition seen with the combination of 4D5 and TNF- $\alpha$  was similar to that observed with TNF- $\alpha$  alone (Fig. 9D). Furthermore, neither HBL-100 (30), a nontransformed but immortalized human breast epithelial cell line (Fig. 9E), nor T24 (27), a human bladder carcinoma cell line (Fig. 9F), expressed high levels of p185<sup>HER2</sup> (data not shown), and neither demonstrated growth inhibition by 4D5 or an enhanced growth-inhibitory or cytotoxic response to the combination of TNF- $\alpha$  and monoclonal antibody 4D5. These results demonstrate that only tumor cells which

overexpress p185<sup>HER2</sup> will become sensitized to the cytotoxic effects of TNF- $\alpha$  by antibody 4D5.

#### DISCUSSION

We have prepared monoclonal antibodies against the extracellular domain of the *HER2/c-erbB-2* gene product, p185<sup>HER2</sup>, and have found that one of these, 4D5, strongly inhibits the growth of several breast tumor cell lines and furthermore sensitizes p185<sup>HER2</sup>-overexpressing breast carcinoma cell lines SK-BR-3 and MDA-MB-175-VII to the cytotoxic effects of TNF- $\alpha$ . Monoclonal antibody 4D5 is specific for p185<sup>HER2</sup> and shows no cross-reactivity with the closely related human EGF receptor expressed in mouse fibroblasts. Of six mammary carcinoma cell lines tested, only the three lines which express high levels of p185<sup>HER2</sup> (SK-BR3, MBA-MB-175, and MDA-MD-361 [17]) were growth inhibited, and 4D5 did not inhibit the proliferation of a nontransformed human breast epithelial cell line, HBL-100, or the bladder carcinoma cell line T24.

In the presence of the antibody, the inhibition of SK-BR-3 cell growth was nearly complete, but the effect was cytostatic rather than cytotoxic. This property of 4D5 is similar to that described for a subset of monoclonal antibodies to the EGF receptor (19, 31, 32) which inhibit the growth of A431 cells, a human squamous epithelial carcinoma line expressing high levels of the EGF receptor. In this case, these inhibitory antibodies compete with radiolabeled EGF for binding to the receptor, and antibodies which do not block EGF binding have no effect on A431 cell growth. It has been suggested (J. Mendelsohn and H. Masui, Clin. Res. 35:600A, 1987) that these antibodies inhibit cell growth by interfering with an autocrine system involving the EGF receptor and an essential growth factor, transforming growth factor alpha, that is produced by the cells (5). It is therefore intriguing to speculate that antibody 4D5 analogously interferes with ligand binding to the *HER2/c-erbB-2* gene product. Since an appropriate ligand for the putative *HER2/c-erbB-2* receptor has not yet been identified, this possibility cannot yet be tested directly.

The 4D5 antibody had no effect on the growth of NIH 3T3 cells transformed by *HER2/c-erbB-2* overexpression. However, it reversed one property conferred on these cells by amplification of the *HER2/c-erbB-2* cDNA: the formation of colonies in soft agar was prevented by 200 ng of 4D5 antibody per ml. This result is similar to those obtained by Drebin et al. (8) with a monoclonal antibody to the rat *neu* oncogene-encoded p185<sup>neu</sup>. They also observed that an anti-p185<sup>neu</sup> monoclonal antibody inhibited colony growth in soft agar and tumor formation by *neu*-transformed NIH 3T3 cells in athymic mice (7-10). This effect was attributed to a lowering p185<sup>neu</sup> levels by an increase in receptor turnover triggered by antibody binding. The apparent discrepancy between 4D5 effects on proliferation of breast tumor cells versus transfected mouse fibroblast cells is most probably a reflection of the fact that SK-BR-3 cells are authentic cancer cells, in contrast to the NIH 3T3 model system. Whereas SK-BR-3 cells may have evolved to be dependent on *HER2/c-erbB-2*-mediated signals for both growth and transformation characteristics, NIH 3T3 cells have acquired a transformed phenotype only as a result of *HER2/c-erbB-2* overexpression, but may proliferate normally in response to other serum growth factors, even in the presence of blocking anti-p185<sup>HER2</sup> antibody.

Previous work has shown that high-level expression of p185<sup>HER2</sup> will transform NIH 3T3 cells and has suggested a casual role for amplification of the *HER2/c-erbB-2* gene in

mammary gland neoplasia. We have shown here that *HER2/c-erbB-2* gene overexpression in NIH 3T3 cells is associated with increased resistance to the monokine TNF- $\alpha$  and that breast tumor cell lines which overexpress p185<sup>HER2</sup> are resistant to the cytotoxic effects of TNF- $\alpha$ . The mechanism by which 4D5 inhibits breast tumor cell proliferation and reverses phenotypes associated with high levels of p185<sup>HER2</sup> expression, such as resistance to TNF- $\alpha$ , is not clear. However, these results suggest that in addition to its ability to transform cells by virtue of overexpression (6, 18), *HER2/c-erbB-2* could play a role in tumor progression by allowing tumor cells overexpressing p185<sup>HER2</sup> to evade one component of the antitumor immunosurveillance of the host, the activated macrophage (17). These properties of the *HER2/c-erbB-2* gene product may in part explain the aggressive, single-step induction of mammary adenocarcinoma in transgenic mice bearing the *neu* oncogene (24), which encodes the mutated rat homolog of p185<sup>HER2</sup>.

The experiments presented here demonstrate that a monoclonal antibody which recognizes the extracellular domain of p185<sup>HER2</sup> inhibits the proliferation of breast tumor cells which overexpress this receptorlike protein. Moreover, treatment with this antibody also sensitizes these tumor cells to the cytotoxic effects of TNF- $\alpha$ . Monoclonal antibodies specific for p185<sup>HER2</sup> may therefore be useful therapeutic agents for the treatment of human neoplasias, including certain mammary carcinomas, which are characterized by the overexpressing of p185<sup>HER2</sup>.

#### ACKNOWLEDGMENTS

We thank Bill Lagrimas for help with the immunization procedure and Mary Napier and Michael Lipari for providing the wheat germ purified p185<sup>HER2</sup> preparation. We are grateful to Jeanne Arch for her patience and skill in typing this manuscript.

#### LITERATURE CITED

- Adams, D. O., and C. F. Nathan. 1983. Molecular mechanisms in tumor cell killing by activated macrophages. *Immunol. Today* 4:166-170.
- Adams, D. O., and R. Snyderman. 1978. Do macrophages destroy nascent tumors? *JNCI* 62:1341-1345.
- Beutler, B., and A. Cerami. 1986. Cachectin and tumour necrosis factor as two sides of the same biological coin. *Nature (London)* 320:584-588.
- Coussens, L., T. L. Yang-Feng, Y.-C. Liao, E. Chen, A. Gray, J. McGrath, P. H. Seeburg, T. W. Libermann, J. Schlessinger, U. Francke, A. Levinson, and A. Ullrich. 1985. Tyrosine kinase receptor with extensive homology to EGF receptor shares chromosomal location with *neu* oncogene. *Science* 230:1132-1139.
- Derynck, R., D. V. Goeddel, A. Ullrich, J. U. Gutterman, R. D. Williams, T. S. Bringman, and W. H. Berger. 1987. Synthesis of messenger RNAs for transforming growth factors  $\alpha$  and  $\beta$  and the epidermal growth factor receptor by human tumors. *Cancer Res.* 47:707-712.
- Di Force, P. P., J. H. Pierce, M. H. Kraus, O. Segatto, C. R. King, and S. A. Aaronson. 1987. *erbB-2* is a potent oncogene when overexpressed in NIH/3T3 cells. *Science* 237:178-182.
- Drebin, J. A., V. C. Link, and M. I. Greene. 1988. Monoclonal antibodies reactive with distinct domains of the *neu* oncogene-encoded p185 molecule exert synergistic anti-tumor effects *in vivo*. *Oncogene* 2:273-277.
- Drebin, J. A., V. C. Link, and M. I. Greene. 1988. Monoclonal antibodies specific for the *neu* oncogene product directly mediate anti-tumor effects *in vivo*. *Oncogene* 2:387-394.
- Drebin, J. A., V. C. Link, D. F. Stern, R. A. Weinberg, and M. I. Greene. 1985. Down-modulation of an oncogene protein product and reversion of the transformed phenotype by monoclonal antibodies. *Cell* 41:695-706.
- Drebin, J. A., V. C. Link, R. A. Weinberg, and M. I. Greene.

1986. Inhibition of tumor growth by a monoclonal antibody reactive with an oncogene-encoded tumor antigen. *Proc. Natl. Acad. Sci. USA* **83**:9129-9133.
11. Feinman, R., D. Henriksen-deStefano, M. Tsujimoto, and J. Vilcek. 1987. Tumor necrosis factor is an important mediator of tumor cell killing by human monocytes. *J. Immunol.* **138**: 635-640.
  12. Foug, S. K. H., D. T. Sasaki, F. C. Grumet, and E. G. Engleman. 1982. Production of functional human T-T hybridomas in selection of medium lacking aminopterin and thymidine. *Proc. Natl. Acad. Sci. USA* **79**:7484-7488.
  13. Fukushige, S.-I., K.-I. Matsubara, M. Yoshida, M. Sasaki, T. Suzuki, K. Semba, K. Toyoshima, and T. Yamamoto. 1986. Localization of a novel *v-erbB*-related gene, *c-erbB-2*, on human chromosome 17 and its amplification in a gastric cancer cell line. *Mol. Cell. Biol.* **6**:955-958.
  14. Haigler, H., J. F. Ash, S. J. Singer, and S. Cohen. 1978. Visualization by fluorescence of the binding and internalization of epidermal growth factor in human carcinoma cells. *Proc. Natl. Acad. Sci. USA* **75**:3317-3321.
  15. Heifetz, A., R. W. Keenan, and A. D. Elbein. 1979. Mechanism of action of tunicamycin on the UDP-GlcNAc:dolichyl-phosphate GlcNAc-1-phosphate transferase. *Biochemistry* **18**:2186-2191.
  16. Honegger, A. M., T. J. Dull, S. Felder, E. Van Obberghen, F. Bellot, D. Szapary, A. Schmidt, A. Ullrich, and J. Schlessinger. 1987. Point mutation at the ATP binding site of EGF receptor abolishes protein-tyrosine kinase activity and alters cellular routing. *Cell* **51**:199-209.
  17. Hudziak, R. M., G. D. Lewis, M. R. Shalaby, T. E. Eessalu, B. B. Aggarwal, A. Ullrich, and H. M. Shepard. 1988. Amplified expression of the HER2/ERBB2 oncogene induces resistance to tumor necrosis factor  $\alpha$  in NIH 3T3 cells. *Proc. Natl. Acad. Sci. USA* **85**:5102-5106.
  18. Hudziak, R. M., J. Schlessinger, and A. Ullrich. 1987. Increased expression of the putative growth factor receptor p185<sup>HER2</sup> causes transformation and tumorigenesis of NIH 3T3 cells. *Proc. Natl. Acad. Sci. USA* **84**:7159-7163.
  19. Kawamoto, T., J. D. Sato, A. Le, J. Polikoff, G. H. Sato, and J. Mendelsohn. 1983. Growth stimulation of A431 cells by epidermal growth factor: identification of high-affinity receptors for epidermal growth factor by an antireceptor monoclonal antibody. *Proc. Natl. Acad. Sci. USA* **80**:1337-1341.
  20. Kearney, J. F., A. Radbruch, B. Liesegang, and K. Rajewsky. 1979. A new mouse myeloma cell line that has lost immunoglobulin expression but permits the construction of antibody-secreting hybrid cell lines. *J. Immunol.* **123**:1548-1550.
  21. King, C. R., M. H. Kraus, and S. A. Aaronson. 1985. Amplification of a novel *v-erbB*-related gene in a human mammary carcinoma. *Science* **229**:974-976.
  22. Kraus, M. H., N. C. Popescu, S. C. Amsbaugh, C. R. King. 1987. Overexpression of the EGF receptor-related proto-oncogene *erbB-2* in human mammary tumor cell lines by different molecular mechanisms. *EMBO J.* **6**:605-610.
  23. Le, J., and J. Vilcek. 1987. Tumor necrosis factor and interleukin 1: cytokines with multiple overlapping biological activities. *Lab. Invest.* **56**:234-248.
  24. Muller, W. J., E. Sinn, P. K. Pattengale, R. Wallace, and P. Leder. 1988. Single step induction of mammary adenocarcinoma in transgenic mice bearing the activated *c-neu* oncogene. *Cell* **54**:105-115.
  25. Napier, M. A., M. T. Lipari, R. G. Courter, and C. H. K. Cheng. 1987. Epidermal growth factor receptor tyrosine kinase phosphorylation of glucose-6-phosphate dehydrogenase *in vitro*. *Arch. Biochem. Biophys.* **259**:296-304.
  26. Oi, V., and L. Herzenberg. 1980. Immunoglobulin-producing hybrid cell lines, p. 351. *In* B. Mishel and S. Schügi (ed.), *Selected methods in cellular immunology*. W. J. Freeman Co., San Francisco.
  27. O'Toole, C. M., S. Povey, P. Hepburn, and L. M. Franks. 1983. Identity of some human bladder cancer cell lines. *Nature (London)* **301**:429-430.
  28. Patzer, E. J., G. R. Nakamura, and A. Yaffe. 1984. Intracellular transport and secretion of hepatitis B surface antigen in mammalian cells. *J. Virol.* **51**:346-353.
  29. Philip, R., and L. B. Epstein. 1986. Tumor necrosis factor as immunomodulator and mediator of monocyte cytotoxicity induced by itself,  $\gamma$ -interferon and interleukin-1. *Nature (London)* **323**:86-89.
  30. Polanowski, G. P., E. V. Gaffney, and R. E. Burke. 1976. HBL-100, a cell line established from human breast milk. *In Vitro (Rockville)* **12**:328.
  31. Sato, J. D., T. Kawamoto, A. D. Le, J. Mendelsohn, J. Polikoff, and G. H. Sato. 1983. Biological effects *in vitro* of monoclonal antibodies of human epidermal growth factor receptors. *Mol. Biol. Med.* **1**:511-529.
  32. Sato, J. D., A. D. Le, and T. Kawamoto. 1987. Derivation and assay of biological effects of monoclonal antibodies to epidermal growth factor receptors. *Methods Enzymol.* **146**:63-81.
  33. Schechter, A. L., M.-C. Hung, L. Vaidyanathan, R. A. Weinberg, T. L. Yang-Feng, U. Francke, A. Ullrich, and L. Coussens. 1985. The *neu* gene: an *erbB*-homologous gene distinct from and unlinked to the gene encoding the EGF receptor. *Science* **229**:976-978.
  34. Semba, K., N. Kamata, K. Toyoshima, and T. Yamamoto. 1985. A *v-erbB*-related protooncogene, *c-erbB-2*, is distinct from the *c-erbB-1*/epidermal growth factor-receptor gene and is amplified in a human salivary gland adenocarcinoma. *Proc. Natl. Acad. Sci. USA* **82**:6497-6501.
  35. Slamon, D. J., G. M. Clark, S. G. Wong, W. J. Levin, A. Ullrich, and W. L. McGuire. 1987. Human breast cancer: correlation of relapse and survival with amplification of the HER-2/*neu* oncogene. *Science* **235**:177-182.
  36. Sugarman, B. J., B. B. Aggarwal, P. E. Hass, I. S. Figari, M. A. Palladino, and H. M. Shepard. 1985. Recombinant human tumor necrosis factor- $\alpha$ : effects on proliferation of normal and transformed cells *in vitro*. *Science* **230**:943-945.
  37. Sugarman, B. J., G. D. Lewis, T. E. Eessalu, B. B. Aggarwal, and H. M. Shepard. 1987. Effects of growth factors on the antiproliferative activity of tumor necrosis factors. *Cancer Res.* **47**:780-786.
  38. Urban, J. L., and H. Schreiber. 1983. Selection of macrophage-resistant progressor tumor variants by the normal host. *J. Exp. Med.* **157**:642-656.
  39. Urban, J. L., H. M. Shepard, J. L. Rothstein, B. J. Sugarman, and H. Schreiber. 1986. Tumor necrosis factor: a potent effector molecule for tumor cell killing by activated macrophages. *Proc. Natl. Acad. Sci. USA* **83**:5233-5237.
  40. van de Vijver, M., R. van de Berselaar, P. Devilee, C. Cornelisse, J. Peterse, and R. Nusse. 1987. Amplification of the *neu* (*c-erbB-2*) oncogene in human mammary tumors is relatively frequent and is often accompanied by amplification of the linked *c-erbA* oncogene. *Mol. Cell. Biol.* **7**:2019-2023.
  41. Waldman, B. C., C. Oliver, and S. S. Krag. 1987. A clonal derivative of tunicamycin-resistant Chinese hamster ovary cells with increased N-acetylglucosamine-phosphate transferase activity has altered asparagine-linked glycosylation. *J. Cell. Physiol.* **131**:302-317.
  42. Yamamoto, T., S. Ikawa, T. Akiyama, K. Semba, N. Nomura, N. Miyajima, T. Saito, and K. Toyoshima. 1986. Similarity of protein encoded by the human *c-erbB-2* gene to epidermal growth factor receptor. *Nature (London)* **319**:230-234.
  43. Yarden, Y., and A. Ullrich. 1988. Growth factor receptor tyrosine kinases. *Annu. Rev. Biochem.* **57**:443-478.
  44. Yarden, Y., and A. Ullrich. 1988. Molecular analysis of signal transduction by growth factors. *Biochemistry* **27**:3113-3119.
  45. Yokota, J., T. Yamamoto, N. Miyajima, K. Toyoshima, N. Nomura, H. Sakamoto, T. Yoshida, M. Terada, and T. Suigimura. 1988. Genetic alterations of the *c-erbB-2* oncogene occur frequently in tubular adenocarcinoma of the stomach and are often accompanied by amplification of the *v-erbA* homologue. *Oncogene* **2**:283-287.
  46. Zhou, D., H. Battifora, J. Yokota, T. Yamamoto, and M. J. Cline. 1987. Association of multiple copies of the *c-erbB-2* oncogene with spread of breast cancer. *Cancer Res.* **47**:6123-6125.

# **EXHIBIT G**

## ErbB2 Potentiates Breast Tumor Proliferation through Modulation of p27<sup>Kip1</sup>-Cdk2 Complex Formation: Receptor Overexpression Does Not Determine Growth Dependency

HEIDI A. LANE,\* IWAN BEUVINK, ANDREA B. MOTOYAMA, JOHN M. DALY,  
RICHARD M. NEVE, AND NANCY E. HYNES

*Friedrich Miescher Institute, CH-4002 Basel, Switzerland*

Received 9 August 1999/Returned for modification 1 November 1999/Accepted 3 February 2000

Overexpression of the ErbB2 receptor, a major component of the ErbB receptor signaling network, contributes to the development of a number of human cancers. ErbB2 presents itself, therefore, as a target for antibody-mediated therapies. In this respect, anti-ErbB2 monoclonal antibody 4D5 specifically inhibits the growth of tumor cells overexpressing ErbB2. We have analyzed the effect of 4D5-mediated ErbB2 inhibition on the cell cycle of the breast tumor cell line BT474. 4D5 treatment of BT474 cells resulted in a G<sub>1</sub> arrest, preceded by rapid dephosphorylation of ErbB2, inhibition of cytoplasmic signal transduction pathways, accumulation of the cyclin-dependent kinase inhibitor p27<sup>Kip1</sup>, and inactivation of cyclin-Cdk2 complexes. Time courses demonstrated that 4D5 treatment redirects p27<sup>Kip1</sup> onto Cdk2 complexes, an event preceding increased p27<sup>Kip1</sup> expression; this correlates with the downregulation of c-Myc and D-type cyclins (proteins involved in p27<sup>Kip1</sup> sequestration) and the loss of p27<sup>Kip1</sup> from Cdk4 complexes. Similar events were observed in ErbB2-overexpressing SKBR3 cells, which exhibited reduced proliferation in response to 4D5 treatment. Here, p27<sup>Kip1</sup> redistribution resulted in partial Cdk2 inactivation, consistent with a G<sub>1</sub> accumulation. Moreover, p27<sup>Kip1</sup> protein levels remained constant. Antisense-mediated inhibition of p27<sup>Kip1</sup> expression in 4D5-treated BT474 cells further demonstrated that in the absence of p27<sup>Kip1</sup> accumulation, p27<sup>Kip1</sup> redirection onto Cdk2 complexes is sufficient to inactivate Cdk2 and establish the G<sub>1</sub> block. These data suggest that ErbB2 overexpression leads to potentiation of cyclin E-Cdk2 activity through regulation of p27<sup>Kip1</sup> sequestration proteins, thus deregulating the G<sub>1</sub>/S transition. Moreover, through comparison with an ErbB2-overexpressing cell line insensitive to 4D5 treatment, we demonstrate the specificity of these cell cycle events and show that ErbB2 overexpression alone is insufficient to determine the cellular response to receptor inhibition.

The ErbB family of type I receptor tyrosine kinases has four members, ErbB1/epidermal growth factor receptor, ErbB2/Neu, ErbB3, and ErbB4. Although these receptors share common structural elements, including an extracellular ligand-binding domain and an intracellular tyrosine kinase domain, ligands have been identified only for ErbB1, ErbB3, and ErbB4 (for a review, see reference 16). ErbB2 remains an orphan receptor, with no diffusible ErbB2-specific ligand identified. However, ErbB2 can be transactivated through heterodimerization with other ErbB family members (11, 62) and appears to be their preferred heterodimerization partner (23, 30). ErbB2-containing heterodimers couple potently to major mitogenic signaling cascades, such as the mitogen-activated protein (MAP) kinase and phosphatidylinositol 3-kinase (PI3-kinase) pathways (16). Moreover, ErbB2 plays a role in the potentiation and prolongation of ErbB receptor signaling (4, 22, 30, 49).

The role of growth factors and their cognate receptors in cell growth and differentiation is now well established. Additionally, deregulation of growth factor receptors and/or elements of their signaling pathways occurs during the stepwise progression of a normal cell to a malignant phenotype. In this respect, two ErbB family members, ErbB1 and ErbB2, are involved in the development of many human cancers, including ovary and breast cancers. Indeed, amplification of the gene encoding ErbB2, leading to overexpression of the receptor, was one of

the first consistent genetic alterations found in primary human breast tumors (6, 70, 71). Furthermore, overexpression of ErbB2 correlates with a poor patient prognosis not only in breast cancer (24, 59, 70, 71) but also in other malignancies, such as ovarian (71) and gastric (84) cancers. These observations suggest that ErbB2 overexpression provides tumor cells with a growth advantage leading to a more aggressive phenotype. It seems likely, therefore, that an ErbB2-dependent sustained mitogenic stimulus may contribute to the uncontrolled cell growth associated with tumor progression. This phenomenon is presumably due to the formation of active receptor dimers which signal even in the absence of ligand. In agreement with this hypothesis, treatment with ErbB2-specific antibodies has been shown to selectively inhibit the growth of tumor cells which overexpress ErbB2 (26, 27, 29, 37, 38). However, despite the obvious involvement of ErbB2 in tumor progression, the underlying mechanisms by which overexpression of this receptor potentiates tumor cell growth remain poorly understood.

In addition to perturbations in signal transduction networks, aberrant expression of key cell cycle regulators also contributes to deregulated cell proliferation during tumor development (reviewed in references 18 and 28). In nonimmortalized, somatic cells genetic integrity during cell division is maintained through the proper execution of an intrinsic cell cycle machinery. The replication, repair, and segregation of DNA must be accurately performed in order to prevent the genetic changes associated with malignant transformation. The major regulators of cell cycle progression are the cyclin-dependent kinases (Cdk2s), the periodic activation and inactivation of which reg-

\* Corresponding author. Mailing address: Friedrich Miescher Institute, R-1066.210, Maulbeerstrasse 66, CH-4058 Basel, Switzerland. Phone: 41 61 697 8089; Fax: 41 61 697 3976. E-mail: hlane@fmi.ch.



ulate not only progression through each cell cycle stage but also transitions from one cell cycle stage into another (for a review, see reference 47). In G<sub>1</sub>, for example, passage of cells from growth factor dependency to growth factor independence (through the restriction point) is mediated by the sequential activation of cyclin D-dependent kinases Cdk4 and -6 and cyclin E-dependent kinase Cdk2 (for a review, see reference 68). These kinases phosphorylate and inactivate growth suppressor proteins of the retinoblastoma protein (pRb) family, allowing the expression of genes whose activities are required for S-phase entry (75). The importance of this pathway in growth control is highlighted by the fact that many of its components are commonly mutated, deleted, or aberrantly expressed in human cancer (for reviews, see references 18 and 28).

The activity of G<sub>1</sub> Cdks is stringently regulated, not only by association with specific regulatory cyclin subunits and phosphorylation/dephosphorylation events but also through association with specific Cdk inhibitors (CKIs) (47, 67, 68). There are two classes of CKIs, the INK4 proteins (INK4a to -d), which act specifically on cyclin D-dependent kinases, and the CIP/KIP family (p21<sup>Cip1/Waf1</sup>, p27<sup>Kip1</sup>, and p57<sup>Kip2</sup>), which bind all G<sub>1</sub> cyclin-Cdk complexes (67, 68). In fibroblasts, regulation of p27<sup>Kip1</sup> function is an essential step in the pathway linking mitogenic signals to passage through the restriction point (14). This is thought to be due to p27<sup>Kip1</sup>-mediated regulation of cyclin E-Cdk2 activity. Indeed, *in vitro*, p27<sup>Kip1</sup> is a more effective inhibitor of cyclin E-Cdk2 than of cyclin D-Cdk4 (56, 76). Additionally, *in vivo*, p27<sup>Kip1</sup> mediates inhibition of cyclin E-Cdk2 in cells that are exposed to growth-inhibitory agents (57, 72).

Although it was first assumed that CKIs act solely as inhibitors of Cdk complexes, members of the CIP/KIP family also promote the assembly of Cdk4-cyclin D complexes (34). Indeed, both p21<sup>Cip1/Waf1</sup> and p27<sup>Kip1</sup> are essential for Cdk4-cyclin D activity (13), being found in active kinase complexes in proliferating cells (8, 34, 73, 85). Furthermore, the sequestration of p27<sup>Kip1</sup> (and p21<sup>Cip1/Waf1</sup>) into higher-order complexes with cyclin D-dependent kinases appears to play a role in the activation of cyclin E-Cdk2 as cells progress through late G<sub>1</sub>. In this respect, the proto-oncogene *c-myc*, which is clearly involved in the regulation of cyclin E-Cdk2 activity (7, 36), has been shown to play a major role in p27<sup>Kip1</sup> sequestration through modulation of cyclin D protein levels (10, 54), as well as possibly other unknown p27<sup>Kip1</sup> sequestration proteins (2, 77). This suggests that a number of p27<sup>Kip1</sup>-sequestering proteins may exist. The relative contribution of each to cell cycle control may depend on cellular context.

In this study, we have addressed the question of why ErbB2 overexpression in tumors is associated with more aggressive growth characteristics. In this regard, an anti-ErbB2 monoclonal antibody (MAb 4D5), directed to the extracellular domain of the receptor, has been previously shown to specifically inhibit the growth of tumor cells overexpressing the ErbB2 receptor (27, 37, 38). These observations suggest that the growth of tumors overexpressing ErbB2 may be potentiated by increased ErbB2 receptor signaling. To gain insight into the consequence of ErbB2 overexpression for tumor development, we have examined how receptor overexpression impinges on cytoplasmic signaling pathways and elements of cell cycle control by analyzing the molecular mechanism of action of this growth-inhibitory antibody. We show that 4D5 treatment of BT474 cells, a human breast carcinoma cell line overexpressing ErbB2, results in a stable G<sub>1</sub> accumulation. This correlates with rapid downregulation of ErbB2 receptor signaling, increased p27<sup>Kip1</sup> levels, and inactivation of the cyclin E-Cdk2

complex. We further demonstrate that ErbB2 receptor inhibition leads to a redistribution of p27<sup>Kip1</sup> protein onto Cdk2 complexes. This event precedes increases in p27<sup>Kip1</sup> expression, paralleling the loss of proteins involved in p27<sup>Kip1</sup> sequestration, and is sufficient to totally inhibit Cdk2 activity and establish the G<sub>1</sub> block. These data suggest that in breast tumor cells ErbB2 overexpression provides an essential signaling element, leading to the potentiation of cyclin E-Cdk2 activity through sequestration of the CKI p27<sup>Kip1</sup>. Analysis of a second overexpressing cell line (SKBR3), which exhibits reduced proliferation in response to 4D5 treatment, supports this hypothesis. Furthermore, through comparison with an ErbB2-overexpressing, gastric carcinoma cell line (MKN7) insensitive to 4D5 treatment, we demonstrate that the growth response to 4D5-mediated inhibition of ErbB2 receptor function is tumor specific and may correlate with ErbB receptor expression profiles and/or the absence of compensatory mitogenic signaling pathways.

#### MATERIALS AND METHODS

**Cell culture, growth assays, lysate preparation, and flow cytometry.** Breast carcinoma (BT474, T47D, and SKBR3) cells were obtained from the American Type Culture Collection (Manassas, Va.) and grown in Dulbecco's modified Eagle's medium (GIBCO BRL, Gaithersburg, Md.), supplemented with 10% fetal calf serum, at 37°C and 5% CO<sub>2</sub>. Gastric carcinoma (MKN7) cells were kindly provided by C. Benz (University of California, San Francisco) and cultured as described above except that the Dulbecco's modified Eagle's medium was mixed 1:1 with Ham's F-12 (GIBCO BRL). BT474, SKBR3, and MKN7 cells were considered ErbB2 overexpressors by the criterion that they express approximately  $0.5 \times 10^6$  to  $1.0 \times 10^6$  receptors/cell (I. Harwerth and N. E. Hynes, unpublished results; see also reference 37). For growth assays, cells were plated at a density of 2,000 cells/cm<sup>2</sup> or as stated in the text. After 24 h of incubation, the medium was changed and either the purified mouse MAb 4D5 (kindly supplied by Genentech, Inc., South San Francisco, Calif.) or FRP5 (25) was added to a final concentration of 10 µg/ml. Both of these antibodies are of the isotype immunoglobulin G1. Cells were trypsinized at the times stated and counted in a hemocytometer. Cells grown for more than 4 days were refed with fresh medium, with or without antibody, on day 4.

For direct measurements of DNA synthesis, cells were seeded onto acid-washed glass coverslips and cultured in the presence of antibody as described above. After the times stated, bromodeoxyuridine (BrdU) was added for 4 h, the cells were fixed, and BrdU incorporation into nuclei was revealed by immunofluorescence as previously described (35). Cells were counted, and the percentage with BrdU-labeled nuclei was calculated.

For preparation of protein lysates, cells were plated at a density of  $3 \times 10^4$  cells/cm<sup>2</sup>. After 24 h of incubation, the medium was changed and 4D5 or FRP5 was added to a final concentration of 10 µg/ml. At the times indicated, cells were first washed with ice-cold phosphate-buffered saline (PBS) containing 1 mM phenylmethylsulfonyl fluoride and then with buffer containing 50 mM HEPES (pH 7.5), 150 mM NaCl, 25 mM β-glycerophosphate, 25 mM NaF, 5 mM EGTA, 1 mM EDTA, 15 mM pyrophosphate, 2 mM sodium orthovanadate, 10 mM sodium molybdate, leupeptin (10 µg/ml), aprotinin (10 µg/ml), and 1 mM phenylmethylsulfonyl fluoride (protease inhibitors from Sigma Chemical, St. Louis, Mo.). Cells were extracted in the same buffer containing 1% NP-40. After homogenization, lysates were clarified by centrifugation and frozen at -80°C. Protein concentrations were determined with the Bio-Rad (Munich, Germany) protein assay reagent.

To analyze the cell cycle profile of cells, cultures were seeded and treated with antibody as for the preparation of protein lysates. At the times indicated, cells were trypsinized, washed twice with ice-cold PBS, and resuspended in propidium iodide buffer (1 mM sodium citrate [pH 4.0], 1.5 mM NaCl, 5 mM EDTA, 5 mM EGTA, 0.1% NP-40, 4 µg of propidium iodide/ml, and 80 µg of RNase A/ml in PBS). After 30 min of incubation on ice, cell cycle distribution was monitored with a Becton Dickinson FACScan flow cytometer.

**Immunological techniques.** For immunoblot analysis of cell cycle regulators and signal transducers, clarified protein lysates (30 to 50 µg) were electrophoretically resolved on denaturing sodium dodecyl sulfate (SDS)-polyacrylamide gels (7.5 to 14%), transferred to polyvinylidene difluoride (Boehringer Mannheim GmbH, Mannheim, Germany), and probed with the following primary antibodies: anti-cyclin A and -p45<sup>SKIP2</sup> (kindly supplied by W. Krek, Friedrich Miescher Institute, Basel, Switzerland); anti-c-Myc (9E10), -cyclin E (C-19), -cyclin D2 (C-17), -cyclin D3 (C-16), -Cdk2 (M2), and -Cdk4 (C-22; from Santa Cruz Biotechnology, Santa Cruz, Calif.); anti-cyclin D1 (DCS-6; Novocastra Laboratories Ltd., Newcastle upon Tyne, United Kingdom); anti-pRb (G3-245; Pharmingen, San Diego, Calif.); anti-p27<sup>Kip1</sup> (Transduction Laboratories, Lexington, Ky.); and anti-protein kinase B (PKB), -phospho-PKB (serine 473), -Erk1/2, and -phospho-Erk1/2 (threonine 202/tyrosine 204; New England Biolabs, Inc., Bev-

erly, Mass.). Decorated proteins were revealed using horseradish peroxidase-conjugated anti-mouse or anti-rabbit immunoglobulins followed by enhanced chemiluminescence (ECL kit; Amersham Pharmacia Biotech, Buckinghamshire, United Kingdom).

For Cdk2-p27<sup>Kip1</sup> and Cdk4-p27<sup>Kip1</sup> coimmunoprecipitation experiments, clarified protein lysates (70 to 150  $\mu$ g for Cdk2 and 350  $\mu$ g for Cdk4) were precleared with 10  $\mu$ l of protein A Sepharose (Sigma) and then precipitated with 2  $\mu$ g of anti-Cdk2 (M2) or anti-Cdk4 (H-22; Santa Cruz Biotechnology) antibody previously coupled to protein A-Sepharose. Beads were washed thoroughly in extraction buffer, and Cdk-p27<sup>Kip1</sup> levels were analyzed by immunoblotting as described above.

For analysis of ErbB receptor protein and phosphotyrosine levels, protein extracts were either precipitated with an antibody specific for ErbB1 (500  $\mu$ g with antibodies 528 and R-1 mixed 1:1), ErbB3 (400  $\mu$ g with antibody C-17), ErbB4 (500  $\mu$ g with antibody C-18; from Santa Cruz Biotechnology), or ErbB2 (60 to 200  $\mu$ g with antibody 21N; specific for the intracellular domain of the receptor [49]). ErbB protein and tyrosine phosphorylation levels were analyzed by immunoblotting as described above, using anti-ErbB1 (1005; Santa Cruz Biotechnology), ErbB3 (C-17), ErbB4 (C-18), or ErbB2 (21N) antibody and a phosphotyrosine-specific MAb as previously described (49). Stripping of membranes for reprobing was performed as previously described (49).

**Histone H1 kinase assays.** Histone H1 kinase assays were performed using Cdk2 (M-2) immunoprecipitates (from 50  $\mu$ g of lysate protein) or cyclin E (C-19) immunoprecipitates (from 75  $\mu$ g of lysate protein) as previously described (81) except that the amount of histone H1 (Boehringer Mannheim) per assay was increased to 5  $\mu$ g and the final reaction volume was reduced to 20  $\mu$ l. Phosphorylated proteins were resolved by SDS-polyacrylamide gel (10%) electrophoresis (PAGE) and analyzed by autoradiography and scintillation counting.

**p27<sup>Kip1</sup> antisense assays.** Antisense and mismatch p27<sup>Kip1</sup> phosphorothioate oligonucleotides, modified by the addition of a propynyl group to the pyrimidine bases, were prepared and purified by reversed-phase chromatography by Microsynth (Balgach, Switzerland). Due to sequence conservation between the murine and human p27<sup>Kip1</sup> genes, the antisense and mismatch sequences utilized were the same as those previously used for the inhibition of p27<sup>Kip1</sup> expression in murine fibroblasts (14). BT474 cells were plated as stated above for the preparation of cell lysates. After 24 h of incubation, cells were treated with 50 nM oligonucleotides mixed with LipofectAMINE (or LipofectAMINE alone as a control) for 5.5 h as instructed by the manufacturer (GIBCO BRL). After this time, cells were washed and refed with normal culture medium. The cells were then allowed to recover for 3 to 5 h before the addition of antibody 4D5 (10  $\mu$ g/ml). At the times stated (i.e., subsequent to antibody addition), cells were either extracted for lysate production or trypsinized for flow cytometry as described above.

**In vivo [<sup>32</sup>P]orthophosphate-labeled tryptic phosphopeptide mapping of the ErbB2 receptor.** Cells were cultured as stated above for the preparation of cell lysates. After 24 h of incubation, cells were deprived of phosphate for 12 h (using phosphate-free medium supplemented with 10% normal phosphate-containing medium) and labeled with [<sup>32</sup>P]orthophosphate (Amersham) for 4 h. In the continued presence of [<sup>32</sup>P]orthophosphate, cells were subsequently treated with antibody 4D5 or FRP5 (10  $\mu$ g/ml) for 1 h; equal cell numbers were extracted for each treatment (twice as many MKN7 as BT474 cells were extracted due to the lower stoichiometry of ErbB2 phosphorylation in this cell line), and the ErbB2 receptor was immunoprecipitated as described above. Phosphorylated ErbB2 was excised from the gel, and tryptic phosphopeptide mapping was performed as previously described (49).

## RESULTS

**Treatment of BT474 cells, but not MKN7 cells, with MAb 4D5 induces a stable growth arrest.** Primary tumors overexpressing ErbB2 show a more aggressive phenotype which is associated with poor patient prognosis. The precise role of ErbB2 overexpression in tumor development, however, is not determined. To address this question, we have screened a number of ErbB2-overexpressing tumor cell lines for MAb 4D5 sensitivity. An isotype-matched MAb (FRP5), which recognizes the extracellular domain of ErbB2 but is not growth inhibitory (25, 26), was used as a negative control. From this analysis, and in agreement with previous work (37, 38), the growth of the breast carcinoma cell line BT474 was found to be drastically inhibited by 4D5 treatment over a 7-day period (Fig. 1A, bottom). This correlated with a 10-fold decrease in S-phase fraction, as determined by pulse-labeling of antibody-treated cells with BrdU followed by immunofluorescence (Fig. 1B). In contrast, the growth of MKN7 cells, an ErbB2-overexpressing, gastric carcinoma cell line, was unaffected by 4D5 (Fig. 1A, top; see also reference 37). In both cell lines, FRP5

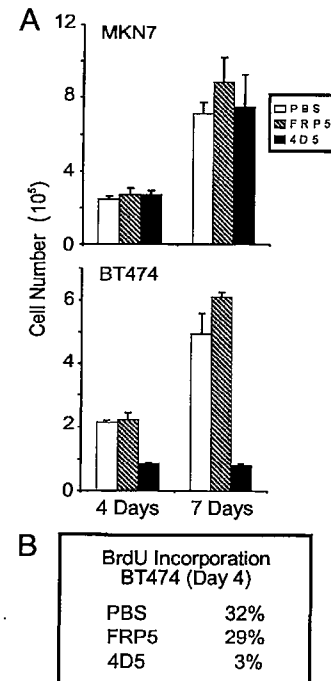


FIG. 1. Proliferation assays of BT474 and MKN7 cells treated with anti-ErbB2 antibodies. MKN7 and BT474 cells were seeded at a density of 2,000 cells/cm<sup>2</sup>; after 24 h of incubation, the medium was changed and either MAb FRP5 or MAb 4D5 was added to a final concentration of 10  $\mu$ g/ml, or an equal volume of PBS was added. After 4 and 7 days of incubation, cells were trypsinized and total cell number was calculated (A), or after 4 days, cells were pulse-labeled with BrdU for 4 h and BrdU incorporation into nuclei was revealed by immunofluorescence (B). Shown are the percentages of nuclei labeled with BrdU during the pulse period.

had little effect; after 7 days of incubation, FRP5-treated cells displayed slightly increased cell numbers compared to untreated controls (Fig. 1A), possibly due to the partially agonistic effects of this antibody on the ErbB2 receptor (25, 41). These data indicate, therefore, that although both of these cell lines overexpress ErbB2 (Fig. 2A; see Materials and Methods), they exhibit quite different responses to 4D5 treatment. This variability between cellular responses to 4D5 treatment has been previously reported (37, 38) and may reflect different dependencies on ErbB2 overexpression among tumor cell lines.

**MAb 4D5-mediated growth inhibition is independent of effects on receptor phosphorylation.** Both MAb FRP5 and 4D5 efficiently bind the extracellular domain of ErbB2 (25, 37). The growth defect seen, therefore, is presumably caused by a sustained antibody-specific effect on the ErbB2 receptor, which in BT474 cells is manifested by growth inhibition. Immunoblot analysis of ErbB receptor immunoprecipitates revealed that BT474 and MKN7 cells express quite different ErbB receptor complements (Fig. 2A). While both clearly overexpressed ErbB2, in contrast to a low-expressing breast tumor cell line (T47D), ErbB2 derived from BT474 cell extracts was highly phosphorylated in comparison with that derived from MKN7 (Fig. 2A, compare top and bottom panels). This elevated ErbB2 tyrosine phosphorylation correlated with coexpression of ErbB3 (Fig. 2A, top), the preferred and most potent heterodimerization partner of ErbB2 (55, 79), and suggests that ErbB2 is more active as a tyrosine kinase in BT474 cells than in MKN7 cells. Interestingly, although ErbB3 protein could

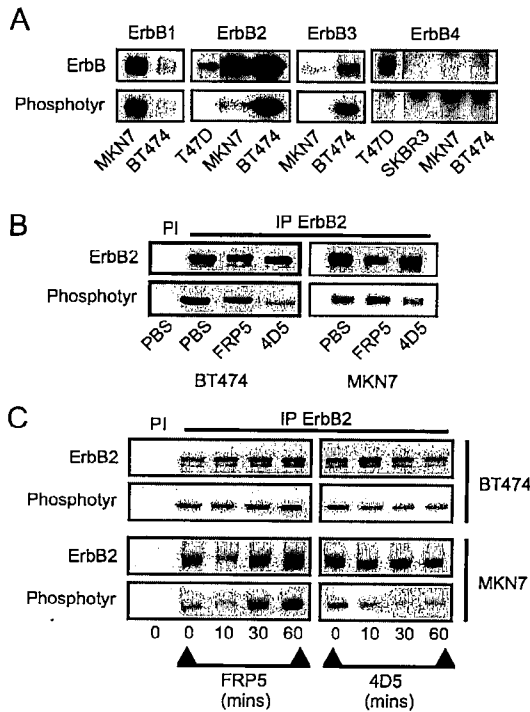


FIG. 2. Screen of ErbB receptor protein and tyrosine phosphorylation levels and effects of anti-ErbB2 antibody treatment on tyrosine phosphorylation of the ErbB2 receptor in BT474 and MKN7 cells. Cells were seeded at a density of  $3 \times 10^4$  cells/cm<sup>2</sup>. After 24 h of incubation, extracts were made and ErbB receptor protein (ErbB) and phosphotyrosine (Phosphoty) levels were analyzed following immunoprecipitation of the appropriate receptor (A). Cells were seeded as described above, and either MAb FRP5 or MAb 4D5 was added to a final concentration of 10  $\mu$ g/ml or an equal volume of PBS was added. Extracts were prepared, and ErbB2 protein and phosphotyrosine levels were assessed after 48 h of incubation (B) or at the times indicated (C) following immunoprecipitation (IP) with the ErbB2-specific polyclonal antibody 21N. Preimmune control precipitations are indicated (PI). In panels B and C, longer exposures were required for MKN7 cells due to the lower ErbB2 tyrosine phosphorylation levels in these cells than in BT474 cells. The exposures shown, therefore, do not represent a quantitative comparison of the two cell lines but were chosen to most clearly represent phosphorylation changes induced as a result of 4D5 treatment.

not be detected by immunoblotting in MKN7 cells, ErbB1 was highly expressed and highly phosphorylated in this cell line (Fig. 2A, top and bottom panels). In BT474 cells, however, ErbB1 expression was equivalent to that of a moderately expressing cell line (data not shown). ErbB4 protein, in contrast, was just detectable in BT474 cells compared to a known non-expressing (SKBR3) and moderately expressing (T47D) cell line. No ErbB4 was detected in MKN7 cells, and in all cell lines, tyrosine phosphorylation was undetectable (Fig. 2A, compare top and bottom panels), indicating that ErbB4 is not a major signaling element in these cells in the culture conditions used. These observations suggest that the relative activity of overexpressed ErbB2 may depend on the coexpression of other ErbB receptors, such as ErbB3. Furthermore, in MKN7 cells, overexpression of ErbB1 alone is insufficient to fully activate ErbB2.

To address the question of whether differences in cellular response to 4D5 treatment are reflected by differential effects on ErbB2 receptor signaling capacity, immunoblot analyses of ErbB2 receptor protein and phosphotyrosine levels after antibody treatment were performed. After 48 h of 4D5 treatment, a dramatic decrease in ErbB2 tyrosine phosphorylation was observed in BT474 cells (Fig. 2B, left). This was accompanied by a resultant increase in the electrophoretic mobility of the

receptor. However, no significant decrease in ErbB2 receptor levels was observed, even after these long treatment times. Furthermore, a similar analysis of 4D5-treated MKN7 cells also revealed receptor dephosphorylation with no effect on protein levels (Fig. 2B, right). To analyze the kinetics of receptor dephosphorylation, time courses of 4D5 treatment of BT474 and MKN7 cells, with FRP5 as a control, were performed. Strikingly, decreased ErbB2 tyrosine phosphorylation was observed within 10 min of 4D5 treatment in both cell lines, and this lower level was maintained for 1 h (Fig. 2C). Decreases in total receptor phosphorylation were also observed if cells were cultured in medium containing <sup>32</sup>P<sub>i</sub> and subsequently treated for 1 h with 4D5, followed by immunoprecipitation of the ErbB2 receptor (Fig. 3A). Additionally, in agreement with previous reports (25, 41), FRP5 treatment of both cell lines rapidly induced ErbB2 phosphorylation (Fig. 2C and 3A). Taken together, these data indicate that treatment of BT474 or MKN7 cells with MAb 4D5 or FRP5 results in comparable effects on ErbB2 phosphorylation.

To determine whether the 4D5-induced changes in ErbB2 receptor phosphorylation was due to dephosphorylation of specific sites or represented a general effect on receptor phosphorylation, tryptic phosphopeptide mapping of <sup>32</sup>P<sub>i</sub>-labeled ErbB2 immunoprecipitates from MAb-treated cell lines, as in Fig. 3A, was performed. In vivo-labeled ErbB2 from untreated, asynchronously growing BT474 cells exhibited phosphopeptide maps similar to those observed in MKN7 cells (Fig. 3B, compare top panels). As expected from the above results, FRP5 treatment of BT474 cells induced increases in the phosphorylation of a number of phosphopeptides (i.e., a through d) while not affecting the relative phosphorylation state of others (i.e., e and f; Fig. 3B, bottom left). In contrast, 4D5 treatment of BT474 cells led to the disappearance of b, c, and d and to a decrease in the intensity of a, e, and f, suggesting that it caused a general dephosphorylation of the ErbB2 receptor (Fig. 3B, bottom right). Quantitatively similar results were observed in MKN7 cells (data not shown). In conclusion, therefore, treatment with 4D5 induces general receptor dephosphorylation in both BT474 and MKN7 cells.

**MAb 4D5 treatment inhibits cytoplasmic signaling in BT474 cells but not in MKN7 cells.** ErbB2 plays a pivotal role in ErbB receptor-mediated activation of the major cytoplasmic, mitogenic signaling pathways, such as the MAP kinase and PI3-kinase pathways (4, 16, 22, 30, 49). We therefore investigated the effects of 4D5 treatment on these pathways in both BT474 and MKN7 cells (Fig. 4). As a readout for the MAP kinase and PI3-kinase pathways, the activation states of the Erk1/2 protein kinases and PKB, respectively, were measured by immunoblotting with antibodies specific for activating phosphorylation sites (see Materials and Methods). Consistent with effects on ErbB2 receptor phosphorylation (Fig. 2C), a dramatic decrease in PKB phosphorylation was observed within 10 min of 4D5 treatment in BT474 cells (Fig. 4, middle). This reduction was maintained for at least 4 h (Fig. 4 and data not shown). Equivalent effects on Erk1/2 phosphorylation were not observed, although a reduction in phosphorylation was seen at later times (Fig. 4, bottom, and data not shown). In this respect, however, in contrast to PKB phosphorylation, Erk1/2 phosphorylation appeared to be comparatively low in BT474 cells and was dramatically induced by FRP5 treatment (Fig. 4, middle and bottom; compare BT474 and MKN7). This indicates that the MAP kinase pathway may not be optimally activated under normal growth conditions in these cells. Surprisingly, a similar analysis of MKN7 cells gave no indication of 4D5-mediated downregulation of either of these pathways (Fig. 4, middle and bottom). A slight increase in Erk1/2 and

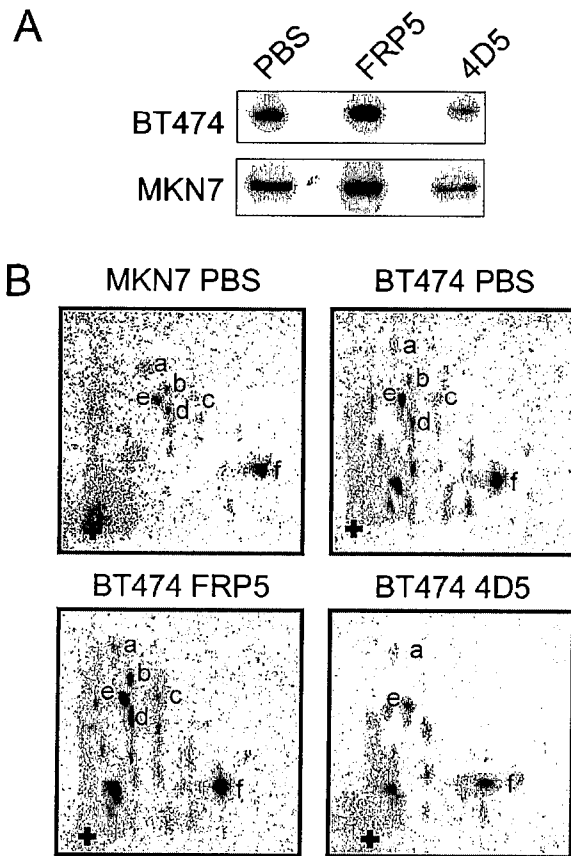


**FIG. 3.** In vivo [ $^{32}\text{P}$ ]orthophosphate labeling of the ErbB2 receptor in BT474 and MKN7 cells after anti-ErbB2 antibody treatment; tryptic phosphopeptide mapping. Cells were seeded as in Fig. 2. Twice as many MKN7 cells as BT474 cells were seeded (see Materials and Methods). After 24 h of incubation, cells were deprived of phosphate for 12 h and then prelabeled with [ $^{32}\text{P}$ ]orthophosphate followed by addition of MAb FRP5, MAb 4D5, or an equal volume of PBS for 1 h. Equal amounts of BT474 cell extracts (doubled in the case of MKN7 extracts) were immunoprecipitated with the anti-ErbB2 antibody 21N, and labeled proteins were identified by separation using SDS-PAGE (7.5% gel) (A). The labeled ErbB2 receptor protein was excised and analyzed by tryptic phosphopeptide mapping (B). Specific tryptic phosphopeptides are indicated by letters, and the origin is shown by a plus sign. Gels and tryptic phosphopeptide maps were analyzed with a phosphorimager. Although MKN7 samples were exposed for longer than BT474 samples, due to lower stoichiometry of phosphorylation, the same exposure is shown for each treatment protocol. The amount of label incorporated into the immunoprecipitated ErbB2 protein in panel A was quantified by scintillation counting. BT474 cells treated with MAb FRP5 and MAb 4D5 had 158 and 60%  $^{32}\text{P}$  incorporation, respectively, compared to the control (PBS)-treated cells. MKN7 cells treated with MAb FRP5 and MAb 4D5 had 139 and 75%  $^{32}\text{P}$  incorporation, respectively, compared to the control (PBS)-treated cells.

PKB phosphorylation was observed after 10 min of 4D5 treatment. However, this was not apparent at later times and was shown to be due to the medium change at the beginning of the experiment (Fig. 4 and data not shown). These data demonstrate that despite similar effects of 4D5 treatment on receptor phosphorylation levels in both BT474 and MKN7 cells, only BT474 cells exhibit downstream effects on cytoplasmic signaling molecules. This suggests that receptor dephosphorylation alone is insufficient to determine the cellular response of ErbB2-overexpressing tumor cells to 4D5-induced receptor inhibition.

**Mab 4D5 treatment induces a  $G_1$  arrest in BT474 cells which correlates with accumulation of p27<sup>Kip1</sup> and Cdk2 inactivation.** To more accurately define the 4D5-specific growth

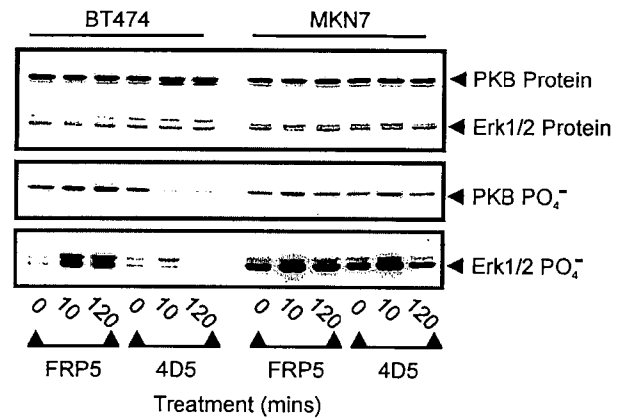


**FIG. 4.** Analysis of PKB and Erk1/2 phosphorylation after treatment of BT474 and MKN7 cells with anti-ErbB2 antibodies. Cells were seeded and treated with MAb FRP5 or MAb 4D5 as in Fig. 2. At the times indicated, cells were extracted and the protein levels (top) and phosphorylation ( $\text{PO}_4^-$ ) states of PKB (middle) and Erk1/2 (bottom) were evaluated by immunoblotting. Untreated cells ( $t = 0$ ) were included as controls.

suppression of BT474 cells, the cell cycle profiles of antibody-treated cells were analyzed after 48 h treatment using flow cytometry. As expected from previous proliferation assays (Fig. 1), FRP5 had no effect on cell cycle distribution compared to untreated controls (Fig. 5). However, 96% of 4D5-treated cells accumulated in  $G_1$  (Fig. 5). This  $G_1$  arrest was stable for up to a week (data not shown), indicating that these cells were blocked in the ability to progress into S phase of the cell cycle. No evidence of apoptosis was observed. Indeed, if 4D5 was removed from the culture medium, the cells were able to reenter the cell cycle (data not shown), confirming that this is a cytostatic rather than cytotoxic agent.

To identify the molecular basis of this  $G_1$  arrest, an initial screen of effects on the levels and activity of  $G_1$  regulators was performed. For this, BT474 cell extracts were prepared after 48 h treatment with MAb 4D5 or FRP5 and analyzed by immunoblotting (Fig. 6A and B). As expected, markers of S-phase progression (cyclin A and p45<sup>SKP2</sup>) as well as  $G_2/M$  (cyclin B1) were almost completely absent in 4D5-treated cells. Additionally, pRb was found exclusively in its hypophosphorylated, active, growth suppressor state. FRP5 treatment, in contrast, had no effect on the expression of these proteins or on pRb phosphorylation (Fig. 6A). Analysis of  $G_1$  Cdk and cyclin levels demonstrated no changes in Cdk4, Cdk6, cyclin E, or cyclin D1 expression, whereas cyclin D2 and D3 levels were reduced in 4D5-treated cells (Fig. 6A and B). Most strikingly, however, the CKI p27<sup>Kip1</sup> was dramatically increased in 4D5-treated cells, a phenomenon correlating with the disappearance of the faster-migrating, active form of Cdk2 (Fig. 6B). Immunoprecipitation of Cdk2, followed by either immunoblotting for associated p27<sup>Kip1</sup> or by histone H1 kinase assay, showed an increase in Cdk2-p27<sup>Kip1</sup> association and almost complete Cdk2 inactivation (Fig. 6C). No effects on the protein levels of other CKIs (including p21<sup>Cip1/Waf1</sup>, p57<sup>Kip2</sup>, p15<sup>INK4b</sup>, and p16<sup>INK4a</sup>) were observed (data not shown). Surprisingly, multiple independent kinase assays revealed that Cdk4 activity (the major cyclin D-dependent kinase expressed in BT474 cells) remained little affected in these experiments despite decreased cyclin D levels (data not shown). As cyclin D proteins are not completely lost, this maintenance of activity could be due to there being sufficient cyclin D to maintain Cdk4 activity. It should also be noted that FRP5-treated cells showed reproducible increases in cyclin D1 protein expression as well

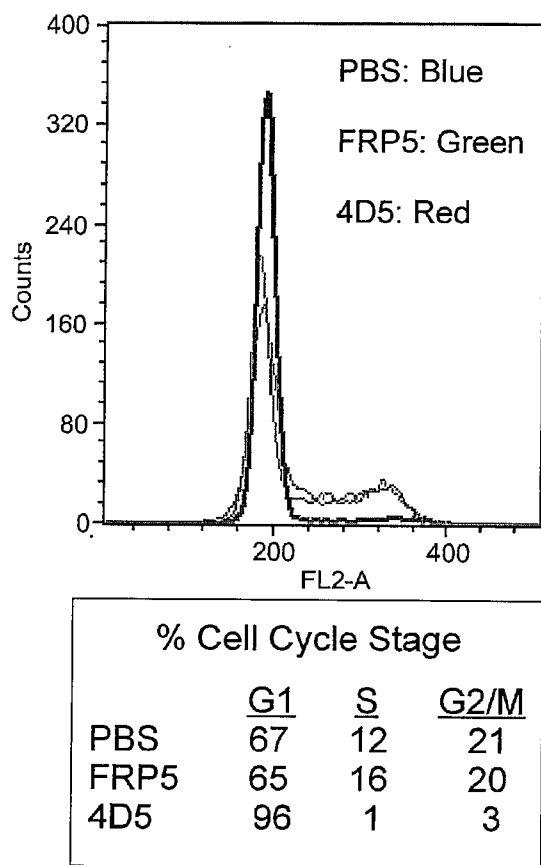


FIG. 5. Analysis of cell cycle distribution after treatment of BT474 cells with anti-ErbB2 antibodies. BT474 cells were seeded as in Fig. 2. After 24 h of incubation, the medium was changed, and MAb FRP5, MAb 4D5, or PBS was added as in Fig. 2. After 48 h, cells were harvested by trypsinization and nuclei were stained with propidium iodide. Shown is flow cytometry analysis of antibody-treated cells compared to PBS-treated controls (top). Percentages of cells in each cell cycle stage are indicated (bottom).

as increased Cdk2 activity (Fig. 6A and C). The partial agonistic effect of this antibody could explain this phenomenon (25, 41). Taken together, these data indicate that 4D5 treatment of BT474 cells induces increased p27<sup>Kip1</sup> protein levels, leading to the inhibition of Cdk2, events which do not occur with a noninhibitory control antibody.

To further determine a possible relationship between increased p27<sup>Kip1</sup> expression and the G<sub>1</sub> block, BT474 cells were treated for 4 to 48 h with 4D5 and, at the times shown (Fig. 7), either extracted and analyzed for markers of G<sub>1</sub> arrest by Western blotting (Fig. 7B) or trypsinized, and the cell cycle profile was determined by flow cytometry (Fig. 7A). Untreated cells (time [t] = 0 h) and cells treated for 48 h with FRP5 were used as controls. The results showed that 4D5-induced effects on pRb phosphorylation, as well as on cyclin A, cyclin B1, and p45<sup>SKP2</sup> levels, became apparent only between 24 and 36 h (Fig. 7B), coincident with a large proportion of cells having accumulated in G<sub>1</sub> (Fig. 7A; 87 and 96% in G<sub>1</sub> at 24 and 36 h, respectively). In contrast, p27<sup>Kip1</sup> levels increased after 8 h, well before the G<sub>1</sub> block was evident (77.5 and 74% in G<sub>1</sub> at 0 and 8 h, respectively). The timing of p27<sup>Kip1</sup> accumulation would, therefore, suggest that p27<sup>Kip1</sup>-mediated inhibition of Cdk2-cyclin E activity is the direct cause of the G<sub>1</sub> block.

**MAb 4D5-induced Cdk2 inactivation parallels increased p27<sup>Kip1</sup>-Cdk2 association, downregulation of D-type cyclins**

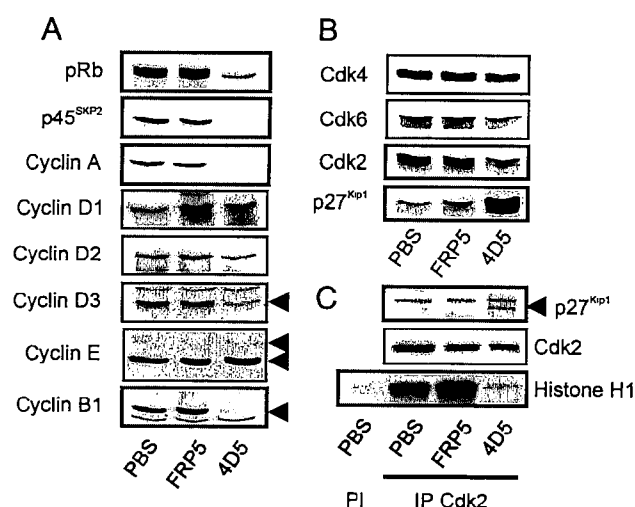


FIG. 6. Analysis of G<sub>1</sub> regulators in anti-ErbB2 antibody-treated BT474 cells. BT474 cells were seeded and treated with MAb FRP5, MAb 4D5, or PBS as in Fig. 2. After 48 h, cells were extracted and the protein levels of G<sub>1</sub> regulators were evaluated by immunoblotting (A and B). Additionally, p27<sup>Kip1</sup> association with Cdk2 complexes, and Cdk2 activity, was assessed through immunoprecipitation (IP) of Cdk2 followed by immunoblotting for associated p27<sup>Kip1</sup> protein or in vitro histone H1 kinase assay (C). Preimmune control precipitations are indicated (PI).

**and the c-Myc transcription factor, and loss of p27<sup>Kip1</sup> from Cdk4 complexes.** The above data support the hypothesis that in BT474 cells inhibition of ErbB2 receptor function through 4D5 treatment induces p27<sup>Kip1</sup> protein accumulation through an unknown mechanism. However, a closer analysis of the kinetics of Cdk2 inactivation demonstrated that after only 2 h of 4D5 treatment, Cdk2 activity had already decreased (Fig. 8A) despite no increase in p27<sup>Kip1</sup> levels at this time (Fig. 8B). Indeed, after 8 h, when p27<sup>Kip1</sup> levels were just starting to increase, total Cdk2 activity had decreased to approximately 50% of normal levels, reaching minimum levels after 24 h when p27<sup>Kip1</sup> protein levels were not yet maximal (Fig. 8). Furthermore, similar kinetics of inactivation were seen if Cdk2 activity was measured after immunoprecipitation of cyclin E (Fig. 8A). Subsequent analysis of Cdk2-p27<sup>Kip1</sup> association, in immunoprecipitates from the same samples, revealed that p27<sup>Kip1</sup> started to accumulate on Cdk2 within 2 h of 4D5 treatment, reaching a peak after 16 to 24 h (Fig. 8B). At later times (36 to 48 h), less p27<sup>Kip1</sup> appeared to be associated with Cdk2. However, this was coincident with decreased Cdk2 levels which, along with reduced pRb expression (Fig. 6A), was always observed after longer treatments with 4D5 and may represent a delayed program of adaptation to the G<sub>1</sub> block.

Increased association of p27<sup>Kip1</sup> with Cdk2 correlates with Cdk2 inactivation in 4D5-treated BT474 cells, and both events begin prior to the accumulation of p27<sup>Kip1</sup> protein. One must consider, therefore, that 4D5 treatment results in the rapid release of an intracellular pool of sequestered p27<sup>Kip1</sup> protein. Cyclin D-dependent kinase complexes, as well as the c-Myc transcription factor, play major roles in the regulation of p27<sup>Kip1</sup> sequestration (see the introduction). With this in mind, therefore, we performed a more detailed time course of 4D5 treatment and analyzed the extracts for correlations between changes in p27<sup>Kip1</sup>-Cdk2 association and c-Myc or cyclin D protein expression (Fig. 9A). Strikingly, c-Myc protein levels decreased within 1 h of 4D5 addition, reaching a minimum level within 2 h. This decrease correlated exactly with the initial accumulation of p27<sup>Kip1</sup> on Cdk2 in the same samples (Fig.

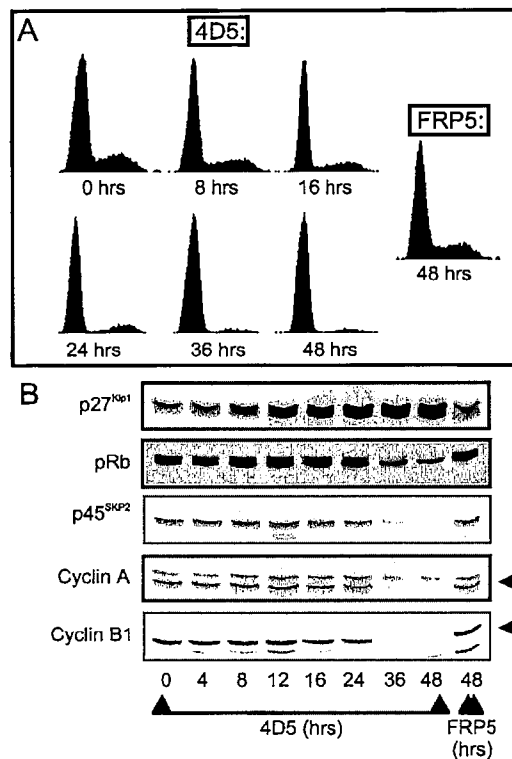


FIG. 7. Time course of the effect of MAb 4D5 treatment on the cell cycle distribution and the levels of cell cycle markers in BT474 cells. BT474 cells were seeded and treated with MAb FRP5 or MAb 4D5 as in Fig. 2. At the times shown, cells were trypsinized, and half of the sample was either stained with propidium iodide and analyzed for cell cycle distribution using flow cytometry (A) or extracted for immunoblot analysis of the proteins indicated (B). Untreated cells ( $t = 0$ ) and cells treated for 48 h with MAb FRP5 were included as controls.

9A) but was transient, as c-Myc protein levels began to recover after 16 h, reaching normal levels after 36 to 48 h (Fig. 9A and data not shown). Cyclin D levels also decreased with similar kinetics (Fig. 9A). The previous immunoblot analysis (Fig. 6A) demonstrated that after 48 h of 4D5 treatment, cyclin D1 was present at normal levels. Subsequent analysis of longer time courses indicated that, as with c-Myc, cyclin D1 levels did indeed recover at later times, reaching normal levels by 48 h (not shown). Taken together, the rapid downregulation of c-Myc and cyclin D proteins provides an explanation for the redistribution of p27<sup>Kip1</sup> onto Cdk2 complexes after 4D5 treatment. Indeed, in this context, loss of p27<sup>Kip1</sup> from cyclin D-Cdk4 complexes was observed after 4D5 treatment and correlated with increased p27<sup>Kip1</sup>-Cdk2 complex formation (Fig. 9B).

**Redirection of p27<sup>Kip1</sup> protein onto Cdk2 complexes occurs in the absence of increased p27<sup>Kip1</sup> expression in SKBR3 cells: correlation with partial Cdk2 inactivation and reduced proliferation levels.** To extend the observations made in BT474 cells, a similar cell cycle analysis was performed on a second ErbB2-overexpressing cell line (SKBR3) sensitive to 4D5 treatment. Intriguingly, growth assays demonstrated that the proliferation rate of these cells was reproducibly reduced by approximately 50% as a result of 4D5 treatment (Fig. 10A), indicating that these cells were less sensitive to antibody-mediated ErbB2 receptor inhibition than BT474 cells. This decrease in proliferation rate was not dependent on cell density (Fig. 10A, compare Expt. 1 with Expt. 2) and correlated with a 10 to 15%

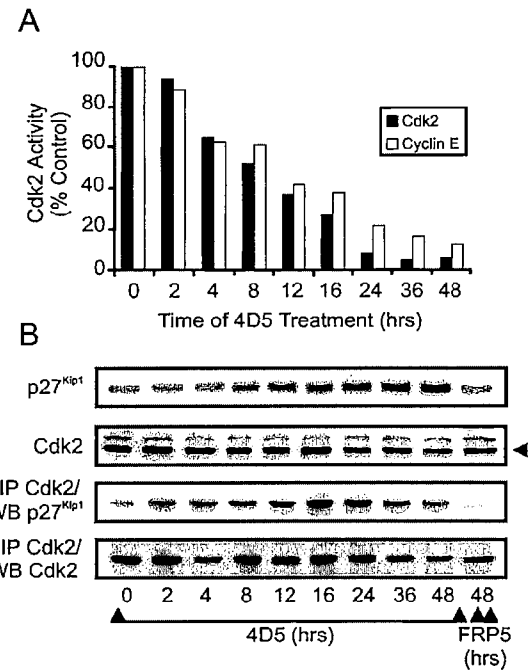


FIG. 8. Time course of Cdk2 inactivation and Cdk2-p27<sup>Kip1</sup> complex formation in MAb 4D5-treated BT474 cells. BT474 cells were seeded and treated with MAb FRP5 or MAb 4D5 as in Fig. 2. At the times indicated, cell extracts were prepared and immunoprecipitated with Cdk2-specific or cyclin E-specific antibodies followed by *in vitro* histone H1 kinase assay (A). Additionally, the levels of p27<sup>Kip1</sup> and Cdk2 protein in the same extracts were either analyzed directly by immunoblotting (WB) or after immunoprecipitation (IP) with Cdk2-specific antibodies (B). Untreated cells ( $t = 0$ ) and cells treated with MAb FRP5 for 48 h were included as controls. Cdk2 kinase activity is expressed as percentage of control ( $t = 0$ ) cells.

increase in the proportion of cells in G<sub>1</sub> as judged by flow cytometry (Fig. 10B and data not shown), suggesting a delay in G<sub>1</sub>-to-S progression. This possibility was supported by the observation that the phosphorylation state of pRb was reduced after 24 h of 4D5 treatment, with a higher proportion being found in the hypophosphorylated, growth suppressor state (Fig. 10C). Additionally, cyclin A protein expression was reduced, but not completely absent, consistent with the fact that these cells were still proliferating at a lower rate in the presence of 4D5 (Fig. 10C). As expected, treatment with the control antibody FRP5 had no growth-inhibitory effects and again appeared to be partially agonistic (Fig. 10).

Further analysis of 4D5-treated cells demonstrated that p27<sup>Kip1</sup> protein was indeed redirected onto Cdk2 complexes (Fig. 10C). This correlated with a reduction in c-Myc and cyclin D protein levels, a reduction in the intensity of the faster migrating, active form of Cdk2 and a reduction in Cdk2 activity to 43% of that seen in untreated cells (Fig. 10C). Interestingly, no increase in p27<sup>Kip1</sup> levels was observed after either 24 h (Fig. 10C) or 48 h (not shown) of 4D5 treatment. SKBR3 cells, therefore, exhibited 4D5-induced effects on p27<sup>Kip1</sup> sequestration protein levels and p27<sup>Kip1</sup>-Cdk2 complex formation similar to those observed in BT474 cells. In contrast, redirection of p27<sup>Kip1</sup> onto Cdk2 complexes in SKBR3 cells was insufficient to totally inactivate Cdk2, a situation reflected in the growth characteristics of these cells. These data suggest that the extent of growth inhibition elicited by 4D5 treatment is cell type specific and correlates with the degree of Cdk2 inactivation. Moreover, an increase in p27<sup>Kip1</sup> expression is not a universal response to ErbB2 inhibition in 4D5-sensitive cells.

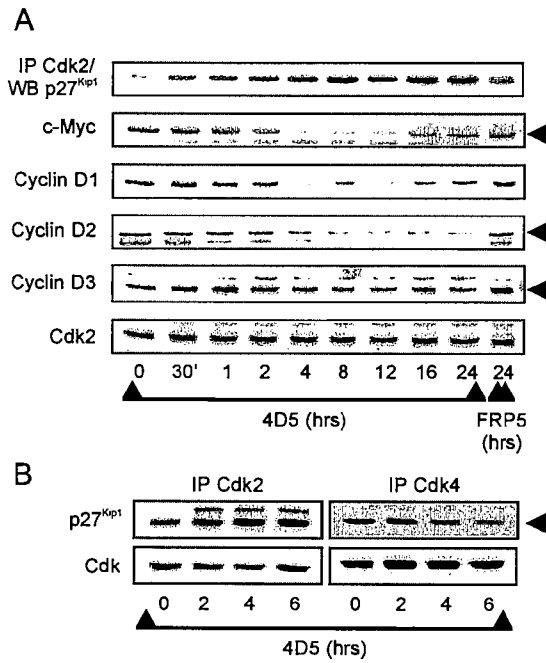


FIG. 9. Time course of MAb 4D5-induced effects on Cdk/p27<sup>Kip1</sup> association and levels of proteins involved in p27<sup>Kip1</sup> sequestration in BT474 cells. BT474 cells were seeded and treated with MAb FRP5 or MAb 4D5 as in Fig. 2. At the times indicated, cell extracts were prepared and analyzed by immunoblotting (WB) either directly or after immunoprecipitation (IP) with Cdk2-specific antibodies (A). Additionally, p27<sup>Kip1</sup> association with Cdk2 and Cdk4 was analyzed by immunoblotting after immunoprecipitation (IP) with Cdk2- or Cdk4-specific antibodies (B). Untreated cells (t = 0) and cells treated with MAb FRP5 for 24 h were included as controls.

**An equivalent response to MAb 4D5 treatment is not observed in MKN7 cells.** If the molecular events observed in BT474 and SKBR3 cells were indeed related to growth inhibition, it would be expected that they would not occur in

MKN7 cells, as these cells were not growth inhibited by treatment with 4D5 (Fig. 1A). To address this question, a time course of 4D5 treatment was performed with MKN7 cells. Here, no increase in p27<sup>Kip1</sup> protein levels or p27<sup>Kip1</sup>-Cdk2 association was observed, even after 24 h (Fig. 11) or 48 h (not shown) of 4D5 treatment. Furthermore, c-Myc and cyclin D protein levels were little affected (Fig. 11). These data suggest that the cell cycle effects observed in BT474 and SKBR3 cells are related to growth inhibition, rather than being nonspecific events.

**Increased p27<sup>Kip1</sup> levels are not required for MAb 4D5-induced p27<sup>Kip1</sup>-Cdk2 association, Cdk2 inactivation, and G<sub>1</sub> arrest in BT474 cells.** In BT474 cells, increased p27<sup>Kip1</sup>-Cdk2 complex formation correlated with Cdk2 inactivation and preceded increased p27<sup>Kip1</sup> expression. This observation prompted the question of whether increased p27<sup>Kip1</sup> expression is an essential component in mediating the G<sub>1</sub> block induced by ErbB2 receptor inhibition in BT474 cells, or whether it is simply a consequence of 4D5-induced Cdk2 inactivation. This question was particularly relevant considering the absence of p27<sup>Kip1</sup> induction in SKBR3 cells, which displayed only partial Cdk2 inhibition in response to 4D5 treatment (Fig. 10C). To address this issue, therefore, we used an antisense approach to assess the cell cycle effects of preventing 4D5-specific increases in p27<sup>Kip1</sup> protein levels in BT474 cells. For this, a specific 15-base p27<sup>Kip1</sup> antisense oligonucleotide and a mismatch control oligonucleotide were constructed as previously described (14) (see Materials and Methods) and introduced into BT474 cells by lipofection. Immunoblots of lipofection-treated BT474 cells, subsequently treated for 24 or 36 h with 4D5, revealed that although p27<sup>Kip1</sup> levels increased as a result of 4D5 treatment in both untreated and mismatch controls, p27<sup>Kip1</sup> protein levels were unaffected by 4D5 in cells treated with antisense oligonucleotide (Fig. 12A). These data demonstrate the efficacy of antisense-mediated inhibition of p27<sup>Kip1</sup> protein expression in this system. Strikingly, when the cell cycle profile of the same cells was analyzed by flow cytometry, antisense-treated cells were still found to be blocked in G<sub>1</sub>, as a result of 4D5 treatment, to an extent similar to that for untreated or

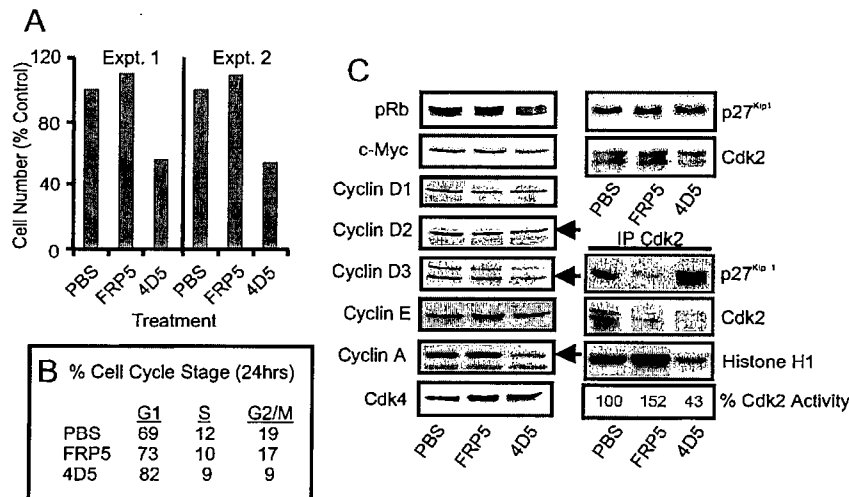


FIG. 10. Effects of anti-ErbB2 MAb treatment on SKBR3 cell proliferation and the expression and activity of G<sub>1</sub> regulators. SKBR3 cells were seeded as in Fig. 2. (A, Expt. 1; B and C) or at half the density (A, Expt. 2). After 24 h of incubation, PBS, MAb FRP5, or MAb 4D5 was added as in Fig. 2, and cells were treated as follows: (A) incubated for 4 days and trypsinized, after which total cell number was calculated; (B) incubated for 24 h, trypsinized, and treated with propidium iodide, after which cell cycle distribution was analyzed by flow cytometry; (C) incubated for 24 h, after which cell extracts were prepared and the protein levels of G<sub>1</sub> regulators were evaluated by immunoblotting, or p27<sup>Kip1</sup> association with Cdk2 complexes, and Cdk2 activity, was assessed through immunoprecipitation (IP Cdk2) of Cdk2 followed by immunoblotting for associated p27<sup>Kip1</sup> protein or in vitro histone H1 kinase assay. Cdk2 activity is indicated as a percentage of that in control (PBS)-treated cells.

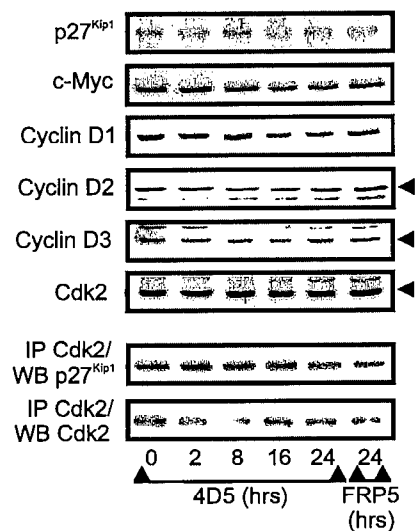


FIG. 11. Time course of the effects of MAb 4D5 treatment on  $G_1$  regulators in MKN7 cells. MKN7 cells were seeded at a density of  $3 \times 10^4$  cells/cm<sup>2</sup>. After 24 h of incubation, the medium was changed and MAb FRP5 or MAb 4D5 was added to a concentration of 10  $\mu$ g/ml for the times indicated. Cell extracts were prepared and analyzed by immunoblotting (WB) either directly or after immunoprecipitation (IP) with Cdk2-specific antibodies. Untreated cells ( $t = 0$ ) and cells treated with MAb FRP5 for 24 h were included as controls.

mismatch control-treated cells (Fig. 12B). Importantly, cells treated with oligonucleotide displayed a normal cell cycle profile when cultured for the same time in the absence of 4D5 (data not shown).

Consistent with the presence of a  $G_1$  block, Cdk2 activity was also decreased as a result of 4D5 treatment in all cases (Fig. 13A). Indeed, although Cdk2 inactivation appeared to be slightly delayed in antisense-treated cells (38%, compared to 18 and 12% in untreated and mismatch-treated cells, respectively, after 24 h incubation with 4D5), by 36 h almost total Cdk2 inactivation had occurred (4%, compared to 5 and 2.5% in untreated and mismatch-treated cells, respectively). Further analysis of Cdk2 immunoprecipitations for p27<sup>Kip1</sup> association indicated that after 24 h of treatment with 4D5 (a time when Cdk2 levels were unaffected), similar levels of p27<sup>Kip1</sup> protein became associated with Cdk2 in antisense-treated cells compared to controls (Fig. 13B). These data confirm that 4D5 treatment of BT474 cells induces the relocation of p27<sup>Kip1</sup> protein onto Cdk2 complexes. Furthermore, this movement is independent of increased p27<sup>Kip1</sup> protein levels and is sufficient to potentiate Cdk2 inactivation and, hence, establish a  $G_1$  block. Additionally, no induction of the expression of the CKI p21<sup>Cip1/Waf1</sup> was observed after lipofection of either the antisense or mismatch control oligonucleotide (data not shown). This attests to the specificity of this effect, ruling out nonspecific effects of single-stranded DNA on Cdk2 activity.

## DISCUSSION

**ErbB2 overexpression potentiates cyclin E-Cdk2 activity in breast tumor cells.** Examination of primary tumors overexpressing the ErbB2 receptor tyrosine kinase has revealed more aggressive tumor phenotypes, associated with poor patient prognosis (24, 59, 70, 71, 84). The extracellular accessibility and involvement in tumor malignancy suggest ErbB2, therefore, as an appropriate target for tumor-directed therapies. For this reason, elucidating the molecular mechanisms by which

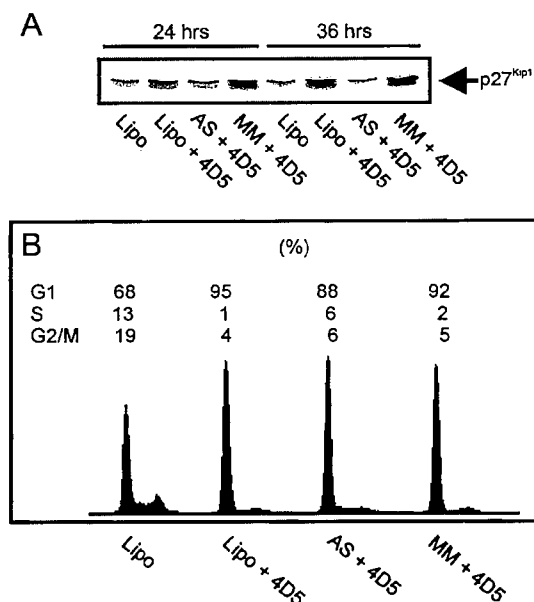


FIG. 12. Effect of antisense-mediated inhibition of MAb 4D5-induced p27<sup>Kip1</sup> accumulation on the cell cycle of BT474 cells. BT474 cells were seeded at a density of  $3 \times 10^4$  cells/cm<sup>2</sup>. After 24 h of incubation, cells were treated with LipofectAMINE alone (Lipo), p27<sup>Kip1</sup> antisense oligonucleotide (AS), or a mismatch control oligonucleotide (MM) as outlined in Materials and Methods. Cells were subsequently refed with normal growth medium; after 3 to 5 h, MAb 4D5 (+ 4D5) was added (10  $\mu$ g/ml) for 24 or 36 h. After these times, cell extracts were prepared and p27<sup>Kip1</sup> protein levels were examined by immunoblotting (A). After 36 h, cells were trypsinized and treated with propidium iodide, and cell cycle distribution was analyzed by flow cytometry (B). Cells treated with LipofectAMINE alone followed by no addition of MAb 4D5 were included as controls. The LipofectAMINE procedure itself had no effect on cell cycle distribution compared to untreated controls, as assessed after 36 h of incubation (not shown).

ErbB2 overexpression potentiates tumor cell growth is a priority. In this work, we have shown that MAb 4D5 treatment of the ErbB2-overexpressing breast tumor cell line BT474 results in a rapid reduction in ErbB2 receptor phosphorylation. Consistent with the relationship between tyrosine phosphorylation and receptor activity, a concomitant decrease in the activity of downstream cytoplasmic signaling pathways was also demonstrated. These observations imply antibody-mediated interference of receptor function in 4D5-treated cells. Consequently, BT474 cells respond to antibody treatment by growth arrest, suggesting that they are dependent on elevated ErbB2 receptor activity for proliferation. More specifically, 4D5 treatment results in a block of the  $G_1/S$  transition, characterized by a rapid increase in p27<sup>Kip1</sup> levels and inactivation of the cyclin E-Cdk2 complex.

Increased p27<sup>Kip1</sup> protein levels, with an associated  $G_1$  accumulation, have been previously observed in ErbB1-overexpressing human carcinoma cell lines after treatment with the ErbB1 growth-inhibitory MAb 225 (53, 81, 83), as well as in an ErbB2-overexpressing ovarian carcinoma cell line treated with 4D5 (83). This relationship could point to a general role for ErbB receptor overexpression in maintaining cyclin E-Cdk2 activity by directly controlling p27<sup>Kip1</sup> protein levels, thus deregulating control mechanisms regulating the  $G_1/S$  transition. The consequences of such a role for tumor development are obvious and would explain the more aggressive growth characteristics of tumors overexpressing ErbB2 receptors. However, through the work presented here, we provide evidence



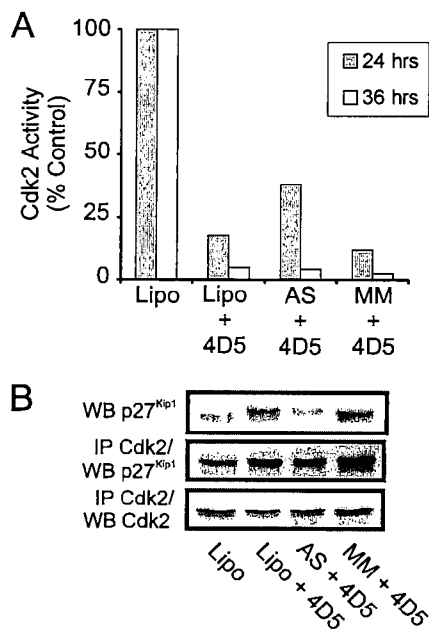


FIG. 13. Effect of antisense-mediated inhibition of MAB 4D5-induced p27<sup>Kip1</sup> accumulation on Cdk2 activity and p27<sup>Kip1</sup>-Cdk2 complex formation in BT474 cells. BT474 cells were seeded, treated with either LipofectAMINE alone (Lipo), antisense p27<sup>Kip1</sup> oligonucleotide (AS), or mismatch (MM) control oligonucleotide, and treated with MAB 4D5 (+ 4D5) as outlined in Fig. 12. After 24 and 36 h of incubation, cells were extracted and immunoprecipitated with Cdk2-specific antibodies followed by *in vitro* histone H1 kinase assay (A). After 24 h of incubation, the same extracts were analyzed for p27<sup>Kip1</sup> protein levels by immunoblotting (WB) directly or after immunoprecipitation (IP) of Cdk2 complexes. Cells treated with LipofectAMINE alone followed by no addition of MAB 4D5 were used as controls, and Cdk2 activity is expressed as a percentage of this control.

disputing this simple interpretation. First, a second ErbB2-overexpressing cell line (SKBR3), which is also growth inhibited as a result of 4D5 treatment, did not exhibit increased p27<sup>Kip1</sup> expression. Additionally, a more in-depth analysis of the effects of 4D5 treatment on p27<sup>Kip1</sup> function in BT474 cells demonstrated that the most immediate effect (within 2 h) of 4D5 treatment was to increase the availability of p27<sup>Kip1</sup>, allowing it to interact with cyclin-Cdk2 complexes. This occurred prior to increases in p27<sup>Kip1</sup> protein levels and paralleled Cdk2 inactivation kinetics. A similar shift of p27<sup>Kip1</sup> protein onto Cdk2 complexes was also observed in SKBR3 cells, correlating with reduced Cdk2 activity. We postulate, therefore, that elevated ErbB2 receptor signaling in overexpressing tumor cells potentiates G<sub>1</sub>/S progression by impeding p27<sup>Kip1</sup> association with cyclin E-Cdk2 complexes. This hypothesis is supported by further experiments, using an antisense p27<sup>Kip1</sup> oligonucleotide to prevent 4D5-induced increases in p27<sup>Kip1</sup> protein levels in BT474 cells. Here, increased p27<sup>Kip1</sup>-Cdk2 complex formation was still observed after 4D5 treatment, correlating with Cdk2 inactivation. Additionally, although increased p27<sup>Kip1</sup> levels may have contributed to the stability of the G<sub>1</sub> arrest at later times, this event was found not to be required to establish the G<sub>1</sub> block induced by 4D5 treatment in these cells.

It is known that p27<sup>Kip1</sup> levels are regulated principally by degradation (51). Furthermore, (i) phosphorylation of p27<sup>Kip1</sup> on threonine 187 by Cdk2 kinase and (ii) stable trimeric complex formation with cyclin-Cdk2 complexes act as signals for ubiquitination and hence target p27<sup>Kip1</sup> to the proteasome degradation machinery (43, 44, 66). From the results presented

here, p27<sup>Kip1</sup> accumulation in BT474 cells appears to be a secondary effect of 4D5-induced p27<sup>Kip1</sup>-Cdk2 complex formation, as the latter was sufficient to almost totally inhibit Cdk2 activity. In the absence of Cdk2 activity, p27<sup>Kip1</sup> protein would be inefficiently phosphorylated and stabilized. This supposition is supported by two observations. First, no p27<sup>Kip1</sup> induction was observed in 4D5-treated SKBR3 cells, which exhibited only partial Cdk2 inactivation as a result of p27<sup>Kip1</sup> redirection. Second, using [<sup>35</sup>S]methionine pulse-chase techniques after 16 h of 4D5 treatment, we have shown a doubling of p27<sup>Kip1</sup> protein half-life, with no specific effect on p27<sup>Kip1</sup> translation (unpublished data).

With these data in mind, therefore, we propose that the initial effect of inhibiting ErbB2 receptor function in 4D5-sensitive breast carcinoma cells is to redirect p27<sup>Kip1</sup> onto Cdk2 complexes resulting in inhibition of G<sub>1</sub>/S progression. The extent of Cdk2 inactivation following receptor inhibition appears to be cell type specific and in some cases is sufficient to instigate a complete G<sub>1</sub> block and induce increased p27<sup>Kip1</sup> protein expression. More specifically, we speculate that in some tumors ErbB2 overexpression promotes constitutive intracellular signaling leading to sequestration of p27<sup>Kip1</sup> away from Cdk2 complexes.

**ErbB2 overexpression regulates the expression of proteins involved in p27<sup>Kip1</sup> sequestration.** The D-type cyclins and the transcription factor c-Myc are involved in regulating p27<sup>Kip1</sup> sequestration in proliferating cells (8, 34, 73, 77, 85). In this respect, a reduction in the level of these proteins was observed in 4D5-treated BT474 and SKBR3 cells, correlating with p27<sup>Kip1</sup>-Cdk2 complex accumulation. Loss of p27<sup>Kip1</sup> sequestration proteins would provide an explanation for 4D5-induced p27<sup>Kip1</sup> relocation onto Cdk2 complexes. However, we acknowledge that alternative mechanisms of regulating p27<sup>Kip1</sup> availability in tumor cells may also be affected (50). Previous reports have shown that activation of the MAP (Erk1/2) kinase pathway leads to stabilization of the c-Myc protein (65) and increased cyclin D transcription (42). Furthermore, activation of the PI3-kinase/PKB pathway has been implicated in the translational induction of c-Myc (80) and stabilization of the D-type cyclins (13, 17). Here, we have shown that 4D5-treated BT474 cells exhibit a rapid and dramatic reduction in PKB phosphorylation, with less dramatic effects on Erk1/2, suggesting an effect on the activation state of these kinases. Additionally, effects on both PKB and Erk1/2 phosphorylation have also been demonstrated in SKBR3 cells (data not shown). Based on the literature, therefore, these observations could account for the decreased expression of c-Myc and D-type cyclins in cells sensitive to 4D5 treatment. Recently, the role of c-Myc in the regulation of cyclin D1 and D2 expression has been demonstrated (10, 54). Whether in our experiments downregulation of the D-type cyclins after 4D5 treatment was purely a consequence of reduced c-Myc protein levels is a matter for debate, particularly as in BT474 cells c-Myc protein levels recovered at later times (36 to 48 h) of 4D5 treatment, whereas cyclin D2 (and D3) levels did not. Intriguingly, changes in cyclin D1 protein levels did mirror fluctuations in c-Myc protein, suggesting that cyclin D1 expression is downstream of the c-Myc transcription factor in BT474 cells.

It should also be noted that no effect of 4D5-induced c-Myc downregulation was seen at the level of expression of cyclin E or the G<sub>1</sub> Cdk-regulatory phosphatase Cdc25A (Fig. 6A and data not shown). Both of these proteins have been postulated to be downstream transcriptional targets of c-Myc (2, 48). For Cdc25A, this now seems unlikely (48). Moreover, the exact relationship between c-Myc and cyclin E expression is not established. Indeed, the cyclin E promoter has no consensus

c-Myc binding sites, and in some systems c-Myc has been shown to increase cyclin E-Cdk2 activity in the absence of changes in cyclin E expression (61, 74). An additional point to consider is that cyclin E is constitutively overexpressed in breast tumor cells (31, 32). It is possible, therefore, that cyclin E levels were maintained after 4D5 treatment as a result of tumor-specific deregulation of cyclin E expression.

**Differential responses to MAb 4D5 treatment indicate differences in growth dependency in ErbB2-overexpressing tumor cells.** In vitro screening of ErbB2-overexpressing cell lines for 4D5-mediated growth inhibition has revealed variability in the response of tumor cells to antibody treatment (37, 38). Here, we have also shown that two overexpressing breast tumor cell lines, BT474 and SKBR3, respond to antibody-mediated inhibition of ErbB2 signaling to differing extents. Moreover, effects on cell proliferation appear to correlate with the extent of Cdk2 inhibition induced by antibody treatment. In this context, cyclin E-Cdk2 kinase activity is known to be heavily deregulated in breast tumor cells (31, 32). Indeed, increased cyclin E expression has been associated with a high proliferative capacity, highly aggressive tumors, and poor patient prognosis (45, 46, 58). Furthermore, cyclin E-Cdk2 activation levels in primary breast tumors correlate with the phosphorylation status of pRb and with proliferation rates (40), a finding which corroborates the observations presented here. The reason for the differences between the overall responses of BT474 and SKBR3 cells to 4D5 treatment is not known. However, we note that SKBR3 cells express approximately fourfold less p27<sup>Kip1</sup> protein than BT474 cells, as well as significantly higher levels of cyclin D2 (sevenfold), cyclin D3 (twofold), Cdk6 (fourfold), and c-Myc (twofold) proteins (unpublished data). It is possible, therefore, that cell-type-specific differences in the expression of p27<sup>Kip1</sup> and p27<sup>Kip1</sup> sequestration proteins may determine the potency of the growth response to ErbB2 receptor inhibition. This important question will be addressed in the future.

An additional consideration is that ErbB2-overexpressing tumor cells may exhibit graded responses to ErbB2 inhibition due to different dependencies on elevated ErbB2 receptor expression for the maintenance of mitogenic signaling pathways (discussed below). This possibility is exemplified in MKN7 cells, which also overexpress ErbB2 but are not growth inhibited by 4D5 treatment. Indeed, 4D5 treatment of MKN7 cells had no effect on p27<sup>Kip1</sup> sequestration or p27<sup>Kip1</sup> protein levels. Accordingly, major cytoplasmic signaling pathways, as well as c-Myc and cyclin D protein levels, remained essentially unchanged. These data indicate that the effects on the cell cycle machinery observed in 4D5-treated BT474 and SKBR3 cells are indeed related to growth inhibition. Furthermore, despite the fact that MKN7 cells dramatically overexpress ErbB2 to levels similar to those observed in BT474 cells (Fig. 2A; see also references 21 and 37) and also exhibit a general reduction in receptor phosphorylation as a result of 4D5 treatment, impaired ErbB2 receptor signaling does not seem to affect the maintenance of p27<sup>Kip1</sup> sequestration proteins or stimulate p27<sup>Kip1</sup>-Cdk2 complex formation in this case. The role of ErbB2 overexpression in the potentiation of Cdk2 activity in tumors, therefore, is not universal.

**ErbB2 receptor overexpression alone does not determine growth dependency.** Consistent with downstream effects on cytoplasmic signaling pathways, we have demonstrated that 4D5 treatment of BT474 cells results in a rapid and general reduction in ErbB2 phosphorylation. In contrast to a previous report examining the effect of 4D5 treatment on ovarian cancer cells (83), we observed no gross downregulation of ErbB2 protein levels. It is possible that slight decreases in ErbB2

expression were not detected by the immunoblotting approach that we used. With this in mind, therefore, we cannot rule out the possibility that partial receptor downregulation may have occurred after prolonged 4D5 treatment, as previously shown (27, 33). Until now, receptor analyses showing 4D5-induced reductions in ErbB2 phosphorylation were performed after long treatment periods, and tryptic phosphopeptide mapping was not carried out (27, 33). Moreover, it has also been suggested that 4D5 induces ErbB2 phosphorylation in BT474 cells (63). From detailed time courses of 4D5 treatment of BT474 cells, however, we have detected decreased receptor phosphorylation levels within 10 min of 4D5 addition. Furthermore, through phosphopeptide mapping, receptor dephosphorylation was shown to be general, including sites stimulated by treatment with MAb FRP5, a known ErbB2 partial agonist (25, 41). The lack of correlation between our observations and those of Scott and coworkers (63) could be due to differences in cell culture conditions before 4D5 addition. In our experiments, cells were treated with antibody at low densities (see Materials and Methods) when a normal cell cycle profile was evident (Fig. 7A). In contrast, 80 to 100% confluent cells were used by the above authors, which could have resulted in differences in response to antibody treatment.

Taken together, our data show that 4D5-induced inhibition of ErbB2 receptor signaling in BT474 cells affects downstream signaling events required for the maintenance of p27<sup>Kip1</sup> sequestration proteins and, hence, Cdk2 activity. It is tempting to propose, therefore, that the general dephosphorylation of ErbB2 induced by 4D5 treatment is sufficient to inhibit growth in ErbB2-overexpressing cell lines. However, as 4D5 treatment of the insensitive tumor cell line MKN7 also induced receptor dephosphorylation in a similar fashion, this event cannot be considered a marker for cellular response to 4D5 treatment. Consequently, one has to consider that other cell-type-specific factors may determine whether tumor cells become dependent on elevated ErbB2 signaling for proliferation.

It has been suggested that long-term resistance to 4D5 treatment may be due to intracellular expression of the extracellular domain of ErbB2, which interferes with internalized ErbB2-4D5 complexes (64). However, from the rapid kinetics of receptor dephosphorylation observed in both MKN7 and BT474 cells after addition of 4D5, this hypothesis would not explain the resultant differential effects on nuclear proteins. From the data presented in this paper, therefore, we speculate on a number of more plausible explanations for why there are differences between cellular responses to 4D5-induced ErbB2 receptor inhibition. First, although ErbB2 is overexpressed in MKN7 cells to levels similar to those in BT474 cells, the receptor is minimally phosphorylated in the former case (Fig. 2A). This implies that ErbB2 is not as active a signaling moiety in MKN7 cells as in BT474 cells. Of all ErbB receptor interactions, the ErbB2-ErbB3 heterodimer is considered the preferred and most potent signaling module (55, 79), coupling efficiently to the PI3-kinase pathway (20, 60). It is significant, therefore, that ErbB3 is overexpressed and active in BT474 cells but is undetectable in MKN7 cells. Moreover, the PI3-kinase pathway, as measured by PKB phosphorylation, is dramatically downregulated in BT474 as a result of 4D5 treatment but remains unaffected in MKN7 cells. Previously, ErbB3 expression has been shown to enhance ErbB2-mediated transformation and tumorigenic growth of NIH 3T3 cells (1, 78, 88). Furthermore, ErbB2-ErbB3 coexpression has been observed in human breast tumors (9, 69), where it has been postulated to play a critical role in tumor progression (69). ErbB3 may, therefore, collaborate with ErbB2, contributing to tumor development. The above data, together with the finding that

4D5-sensitive SKBR3 cells express similar levels of ErbB3 protein (as well as ErbB1 and ErbB2) as BT474 cells (data not shown) and reports that ErbB2-overexpressing cell lines with no or low ErbB3 expression are minimally growth inhibited by 4D5 treatment (37, 38), make it tempting to postulate that the strong proliferative signal resulting from an ErbB2-ErbB3 collaboration could lead to growth dependency during tumor development.

A second possible explanation for resistance to 4D5 treatment is the presence of alternative signaling pathways with the capacity to override ErbB2 receptor inhibition. In MKN7 cells a likely candidate is the ErbB1 receptor, which, in contrast to the situation in BT474 and SKBR3 cells, is overexpressed (see Fig. 2A and reference 37) and highly activated in these cells (Fig. 2A). The observations that ErbB-mediated signaling pathways overlap (5, 16), that epidermal growth factor rescues growth inhibition caused by 4D5 treatment (reference 83 and our unpublished data), and that the anti-ErbB1 MAb 225 augments 4D5-induced growth inhibition (83) provide compelling evidence for alternative routes by which tumor cells ensure maintenance of their proliferative capacity. With these two possibilities in mind, therefore, the involvement of all ErbB receptor family members in determining cellular responses to 4D5 treatment should be considered.

**Implications for tumor development.** Alterations targeting and, therefore, deregulating the G<sub>1</sub> Cdk/pRb phosphorylation pathway are commonly found in human cancers. In this respect, numerous correlations between abnormal p27<sup>Kip1</sup> expression and advanced tumor grade have been made (for examples, see references 12, 19, 39, 58, and 82). Enhanced proteasome-dependent p27<sup>Kip1</sup> degradation has been postulated to be a major influencing factor in these tumors (19, 39). Here, we show that ErbB2 overexpression can provide an additional level of p27<sup>Kip1</sup> deregulation during tumor development; maintaining p27<sup>Kip1</sup> sequestration proteins and, thus, potentiating cyclin E-Cdk2 activity. However, we further demonstrate that receptor overexpression levels alone cannot predict to what extent elevated ErbB2 receptor signaling will contribute to deregulation of the G<sub>1</sub>/S transition. Bearing this in mind, we note that even though all patients treated with a humanized version of 4D5 (Herceptin) presented with metastatic breast carcinomas overexpressing ErbB2, not all responded to treatment (3, 15, 52). It is tempting to speculate, therefore, that the ability of a given tumor cell to elicit p27<sup>Kip1</sup> relocation and, hence, Cdk2 inactivation in response to ErbB2 receptor inhibition may determine the potency of the clinical response to Herceptin. This ability may depend on the relative contribution of other growth factor receptors to ErbB2 activation and to the maintenance of specific intracellular, mitogenic signaling pathways. In some tumor cells, ErbB1 or ErbB3 expression is coamplified with ErbB2, leading to the suggestion that they may collaborate in the induction of human malignancies. The determination of whether such relationships do, indeed, exist has an impact not only on elucidating the mechanisms by which ErbB2 overexpression contributes to malignant transformation but also on therapeutic and screening strategies used in the clinic.

#### ACKNOWLEDGMENTS

This work was supported in part by a grant from the Swiss Cancer League to H.A.L. and J.M.D. R.M.N. was supported in part by a grant from The Basel Cancer League. A.B.M. acknowledges support from the Stipendium Kommission für Nachwuchskräfte aus Entwicklungsländern, Baselstadt, Switzerland.

We thank P. Dennis, G. Orend, and M. Gstaiger for critically reading the manuscript and all members of the laboratory for valuable

discussions. We also thank I. Hoffman (DKFZ, Germany) for continued support, W. Krek (FMI, Basel, Switzerland) for supplying anti-cyclin A and p45<sup>SKP2</sup> antibodies, C. Benz (UCSF, San Francisco, Calif.) for supplying MKN7 cells, and M. X. Sliwkowski and Genentech Inc. (South San Francisco, Calif.) for kindly supplying the 4D5 monoclonal, without which this work would not have been possible.

#### REFERENCES

1. Alimandi, M., A. Romano, M. C. Curia, R. Muraro, P. Fedi, S. A. Aaronson, P. P. Di Fiore, and M. H. Kraus. 1995. Cooperative signaling of ErbB3 and ErbB2 in neoplastic transformation and human mammary carcinomas. *Oncogene* 10:1813-1821.
2. Amati, B., K. Alevizopoulos, and J. Vlach. 1998. Myc and the cell cycle. *Frontiers Biosci.* 3:250-268.
3. Baselga, J., D. Tripathy, J. Mendelsohn, S. Baughman, C. C. Benz, L. Dantis, N. T. Sklarin, A. D. Seidman, C. A. Hudis, J. Moore, P. P. Rosen, T. Twaddell, I. C. Henderson, and L. Norton. 1996. Phase II study of weekly intravenous recombinant humanized anti-p185HER2 monoclonal antibody in patients with HER2/neu-overexpressing metastatic breast cancer. *J. Clin. Oncol.* 14:737-744.
4. Beerli, R. R., D. Graus-Porta, K. Woods-Cook, X. Chen, Y. Yarden, and N. E. Hynes. 1995. Neu differentiation factor activation of ErbB-3 and ErbB-4 is cell specific and displays a differential requirement for ErbB-2. *Mol. Cell. Biol.* 15:6496-6505.
5. Beerli, R. R., and N. E. Hynes. 1996. Epidermal growth factor-related peptides activate distinct subsets of ErbB receptors and differ in their biological activities. *J. Biol. Chem.* 271:6071-6076.
6. Berger, M. S., G. W. Locher, S. Saurer, W. J. Gullick, M. D. Waterfield, B. Groner, and N. E. Hynes. 1988. Correlation of *c-erbB-2* gene amplification and protein expression in human breast cancer with nodal status and nuclear grading. *Cancer Res.* 48:1238-1243.
7. Berns, K., E. M. Hijmans, and R. Bernards. 1997. Repression of c-Myc responsive genes in cycling cells causes G1 arrest through reduction of cyclin E/CDK2 kinase activity. *Oncogene* 15:1347-1356.
8. Blain, S. W., E. Montalvo, and J. Massague. 1997. Differential interaction of the cyclin-dependent kinase (Cdk) inhibitor p27<sup>Kip1</sup> with cyclin A-Cdk2 and cyclin D2-Cdk4. *J. Biol. Chem.* 272:25863-25872.
9. Bodey, B., B. Bodey, Jr., A. M. Groger, J. V. Luck, S. E. Siegel, C. R. Taylor, and H. E. Kaiser. 1997. Clinical and prognostic significance of the expression of the c-erbB-2 and c-erbB-3 oncoproteins in primary and metastatic malignant melanomas and breast carcinomas. *Anticancer Res.* 17:1319-1330.
10. Bouchard, C., K. Thieke, A. Maier, R. Saffrich, J. Hanley-Hyde, W. Ansoorge, S. Reed, P. Sicinski, J. Bartek, and M. Eilers. 1999. Direct induction of cyclin D2 by Myc contributes to cell cycle progression and sequestration of p27. *EMBO J.* 18:5321-5333.
11. Carraway, K. L., III, and L. C. Cantley. 1994. A new acquaintance for erbB3 and erbB4: a role for receptor heterodimerization in growth signaling. *Cell* 78:5-8.
12. Catzavelos, C., N. Bhattacharya, Y. C. Ung, J. A. Wilson, L. Roncari, C. Sandhu, P. Shaw, H. Yeger, I. Morava-Protzner, L. Kapusta, E. Franssen, K. I. Pritchard, and J. M. Slingerland. 1997. Decreased levels of the cell-cycle inhibitor p27<sup>Kip1</sup> protein: prognostic implications in primary breast cancer. *Nat. Med.* 3:227-230.
13. Cheng, M., P. Olivier, J. A. Diehl, M. Fero, M. F. Roussel, J. M. Roberts, and C. J. Sherr. 1999. The p21<sup>Cip1</sup> and p27<sup>Kip1</sup> CDK inhibitors are essential activators of cyclin D-dependent kinases in murine fibroblasts. *EMBO J.* 18:1571-1583.
14. Coats, S., W. M. Flanagan, J. Nourse, and J. M. Roberts. 1996. Requirement of p27<sup>Kip1</sup> for restriction point control of the fibroblast cell cycle. *Science* 272:877-880.
15. Cobleigh, M. A., C. L. Vogel, D. Tripathy, N. J. Robert, S. Scholl, L. Fehrenbacher, J. Wolter, V. Paton, S. Shak, G. Lieberman, and D. J. Slamon. 1999. Multinational study of the efficacy and safety of humanized anti-HER2 monoclonal antibody in women who have HER2-overexpressing metastatic breast cancer that has progressed after chemotherapy for metastatic disease. *J. Clin. Oncol.* 17:2639-2648.
16. Daly, R. J. 1999. Take your partners, please—signal diversification by the erbB family of receptor tyrosine kinases. *Growth Factors* 16:255-263.
17. Diehl, J. A., M. Cheng, M. F. Roussel, and C. J. Sherr. 1998. Glycogen synthase kinase-3 $\beta$  regulates cyclin D1 proteolysis and subcellular localization. *Genes Dev.* 12:3499-3511.
18. Elledge, S. J., J. Winston, and J. W. Harper. 1996. A question of balance: the role of cyclin-kinase inhibitors in development and tumorigenesis. *Trends Cell Biol.* 6:388-397.
19. Esposito, V., A. Baldi, A. De Luca, A. M. Groger, M. Loda, G. G. Giordano, M. Caputi, F. Baldi, M. Pagano, and A. Giordano. 1997. Prognostic role of the cyclin-dependent kinase inhibitor p27 in non-small cell lung cancer. *Cancer Res.* 57:3381-3385.
20. Fedi, P., J. H. Pierce, P. P. DiFiore, and M. H. Kraus. 1994. Efficient coupling with phosphatidylinositol 3-kinase, but not phospholipase C $\gamma$  or GTPase-activating protein, distinguishes ErbB-3 signaling from that of the

- Erb/EGFR family members. *Mol. Cell. Biol.* 14:492-500.
21. Fukushige, S.-I., K.-I. Matsubara, M. Yoshida, M. Sasaki, T. Suzuki, K. Semba, K. Toyoshima, and T. Yamamoto. 1986. Localization of a novel *v-erbB*-related gene, *c-erbB-2*, on human chromosome 17 and its amplification in a gastric cancer cell line. *Mol. Cell. Biol.* 6:955-958.
  22. Graus-Porta, D., R. R. Beerli, and N. E. Hynes. 1995. Single-chain antibody-mediated intracellular retention of ErbB-2 impairs neu differentiation factor and epidermal growth factor signaling. *Mol. Cell. Biol.* 15:1182-1191.
  23. Graus-Porta, D., R. R. Beerli, J. M. Daly, and N. E. Hynes. 1997. ErbB-2, the preferred heterodimerization partner of all ErbB receptors, is a mediator of lateral signaling. *EMBO J.* 16:1647-1655.
  24. Gullick, W. J., S. B. Love, C. Wright, D. M. Barnes, B. Gusterson, A. L. Harris, and D. G. Altman. 1991. *c-erbB-2* protein overexpression in breast cancer is a risk factor in patients with involved and uninvolved lymph nodes. *Br. J. Cancer* 63:434-438.
  25. Harwerth, L.-M., W. Wels, B. Marte, and N. E. Hynes. 1992. Monoclonal antibodies against the extracellular domain of the *erbB-2* receptor function as partial ligand agonists. *J. Biol. Chem.* 267:15160-15167.
  26. Harwerth, L.-M., W. Wels, J. Schlegel, M. Müller, and N. E. Hynes. 1993. Monoclonal antibodies directed to the *erbB-2* receptor inhibit *in vivo* tumour cell growth. *Br. J. Cancer* 68:1140-1145.
  27. Hudziak, R. M., G. D. Lewis, M. Winget, B. M. Fendly, H. M. Shepard, and A. Ullrich. 1989. p185<sup>HER2</sup> monoclonal antibody has antiproliferative effects *in vitro* and sensitizes human breast tumor cells to tumor necrosis factor. *Mol. Cell. Biol.* 9:1165-1172.
  28. Hunter, T., and J. Pines. 1994. Cyclins and cancer. II. Cyclin D and CDK inhibitors come of age. *Cell* 79:573-582.
  29. Jannot, Ch., R. R. Beerli, S. Mason, W. J. Gullick, and N. E. Hynes. 1996. Intracellular expression of a single-chain antibody directed to the epidermal growth factor receptor leads to growth inhibition of tumor cells. *Oncogene* 13:275-282.
  30. Karunagaran, D., E. Tzahar, R. R. Beerli, X. Chen, D. Graus-Porta, B. J. Ratzkin, R. Seger, N. E. Hynes, and Y. Yarden. 1996. ErbB-2 is a common auxiliary subunit of NDF and EGF receptors: implications for breast cancer. *EMBO J.* 15:254-264.
  31. Keyomarsi, K., and A. B. Pardee. 1993. Redundant cyclin overexpression and gene amplification in breast cancer cells. *Proc. Natl. Acad. Sci. USA* 90:1112-1116.
  32. Keyomarsi, K., D. Conte, Jr., W. Toyofuku, and M. P. Fox. 1995. Deregulation of cyclin E in breast cancer. *Oncogene* 11:941-950.
  33. Kumar, R., H. M. Shepard, and J. Mendelsohn. 1991. Regulation of phosphorylation of the *c-erbB-2/HER2* gene product by a monoclonal antibody and serum growth factor(s) in human mammary carcinoma cells. *Mol. Cell. Biol.* 11:979-986.
  34. LaBaer, J., M. D. Garrett, L. F. Stevenson, J. M. Slingerland, C. Sandhu, H. S. Chou, A. Fattaey, and E. Harlow. 1997. New functional activities for the p21 family of CDK inhibitors. *Genes Dev.* 11:847-862.
  35. Lane, H. A., and E. A. Nigg. 1996. Antibody microinjection reveals an essential role for human polo-like kinase 1 (Plk1) in the functional maturation of mitotic centrosomes. *J. Cell Biol.* 135:1701-1713.
  36. Leone, G., J. DeGregori, R. Sears, L. Jakoi, and J. R. Nevins. 1997. Myc and Ras collaborate in inducing accumulation of active cyclin E/Cdk2 and E2F. *Nature* 387:422-426.
  37. Lewis, G. D., I. Figari, B. Fendly, W. L. Wong, P. Carter, C. Gorman, and H. M. Shepard. 1993. Differential responses of human tumor cell lines to anti-p185<sup>HER2</sup> monoclonal antibodies. *Cancer Immunol. Immunother.* 37:255-263.
  38. Lewis, G. D., J. A. Lofgren, A. E. McMurtrey, A. Huijens, B. M. Fendly, K. D. Bauer, and M. X. Sliwkowski. 1996. Growth regulation of human breast and ovarian tumor cells by heregulin: evidence for the requirement of ErbB2 as a critical component in mediating heregulin responsiveness. *Cancer Res.* 56:1457-1465.
  39. Loda, M., B. Cukor, S. W. Tam, P. Lavin, M. Fiorentino, G. F. Draetta, J. Milburn Jessup, and M. Pagano. 1997. Increased proteasome-dependent degradation of the cyclin-dependent kinase inhibitor p27 in aggressive colorectal carcinomas. *Nat. Med.* 3:231-234.
  40. Lodén, M., N. H. Nielsen, G. Roos, S. O. Emdin, and G. Landberg. 1999. Cyclin E dependent kinase activity in human breast cancer in relation to cyclin E, p27 and p21 expression and retinoblastoma protein phosphorylation. *Oncogene* 18:2557-2566.
  41. Marte, B. M., D. Graus-Porta, M. Jeschke, D. Fabbro, N. E. Hynes, and D. Taverna. 1995. NDF/hergulin activates MAP kinase and p70/p85 S6 kinase during proliferation or differentiation of mammary epithelial cells. *Oncogene* 10:167-175.
  42. Meyerson, M., and E. Harlow. 1994. Identification of G<sub>1</sub> kinase activity for cdk6, a novel cyclin D partner. *Mol. Cell. Biol.* 14:2077-2086.
  43. Montagnoli, A., F. Fiore, E. Eytan, A. C. Carrano, G. F. Draetta, A. Hershko, and M. Pagano. 1999. Ubiquitination of p27 is regulated by Cdk-dependent phosphorylation and trimeric complex formation. *Genes Dev.* 13:1181-1189.
  44. Müller, D., C. Bouchard, B. Rudolph, P. Steiner, I. Stuckmann, R. Saffrich, R. Ansoorge, W. Huttner, and M. Eilers. 1997. Cdk2-dependent phosphorylation of p27 facilitates its Myc-induced release from cyclin E/Cdk2 complexes. *Oncogene* 15:2561-2576.
  45. Nielsen, N. H., C. Arnerlov, S. O. Emdin, and G. Landberg. 1996. Cyclin E overexpression, a negative prognostic factor in breast cancer with strong correlation to oestrogen receptor status. *Br. J. Cancer* 74:874-880.
  46. Nielsen, N. H., M. Lodén, J. Cajander, S. O. Emdin, and G. Landberg. 1999. G1-S transition defects occur in most breast cancers and predict outcome. *Breast Cancer Res. Treat.* 56:105-112.
  47. Nigg, E. A. 1995. Cyclin-dependent protein kinases: key regulators of the eukaryotic cell cycle. *Bioessays* 17:471-480.
  48. Obaya, A. J., M. K. Mateyak, and J. M. Sedivy. 1999. Mysterious liaisons: the relationship between c-Myc and the cell cycle. *Oncogene* 18:2934-2941.
  49. Olayoye, M. A., D. Graus-Porta, R. R. Beerli, J. Rohrer, B. Gay, and N. E. Hynes. 1998. ErbB-1 and ErbB-2 acquire distinct signaling properties depending upon their dimerization partner. *Mol. Cell. Biol.* 18:5042-5051.
  50. Orend, G., T. Hunter, and E. Ruoslahti. 1998. Cytoplasmic displacement of cyclin E-cdk2 inhibitors p21<sup>Cip1</sup> and p27<sup>Kip1</sup> in anchorage-independent cells. *Oncogene* 16:2575-2583.
  51. Pagano, M., S. W. Tam, A. M. Theodoras, P. Beer-Romero, G. Del Sal, V. Chau, P. R. Yew, G. F. Draetta, and M. Rolfe. 1995. Role of the ubiquitin-proteasome pathway in regulating abundance of the cyclin-dependent kinase inhibitor p27. *Science* 269:682-685.
  52. Pegram, M. D., A. Lipton, D. F. Hayes, B. L. Weber, J. M. Baselga, D. Tripathy, D. Baly, S. A. Baughman, T. Twaddell, J. A. Glaspy, and D. J. Slamon. 1998. Phase II study of receptor-enhanced chemosensitivity using recombinant humanized anti-p185HER2/neu monoclonal antibody plus cisplatin in patients with HER2/neu-overexpressing metastatic breast cancer refractory to chemotherapy treatment. *J. Clin. Oncol.* 16:2659-2671.
  53. Peng, D., Z. Fan, Y. Lu, T. Deblasio, H. Scher, and J. Mendelsohn. 1996. Anti-epidermal growth factor receptor monoclonal antibody 225 up-regulates p27<sup>Kip1</sup> and induces G1 arrest in prostatic cancer cell line DU145. *Cancer Res.* 56:3666-3669.
  54. Perez-Roger, I., S.-H. Kim, B. Griffiths, A. Sewing, and H. Land. 1999. Cyclins D1 and D2 mediate Myc-induced proliferation via sequestration of p27<sup>Kip1</sup> and p21<sup>Cip1</sup>. *EMBO J.* 18:5310-5320.
  55. Pinkas-Kramarski, R., L. Soussan, H. Waterman, G. Levkowitz, I. Alroy, L. Klapper, S. Lavi, R. Seger, B. J. Ratzkin, M. Sela, and Y. Yarden. 1996. Diversification of Neu differentiation factor and epidermal growth factor signaling by combinatorial receptor interactions. *EMBO J.* 15:2452-2467.
  56. Polyak, K., M.-H. Lee, H. Erdjument-Bromage, A. Koff, J. M. Roberts, P. Tempst, and J. Massagué. 1994. Cloning of p27<sup>Kip1</sup>, a cyclin-dependent kinase inhibitor and a potential mediator of extracellular antimitogenic signals. *Cell* 78:59-66.
  57. Poon, R. Y., H. Toyoshima, and T. Hunter. 1995. Redistribution of the CDK inhibitor p27 between different cyclin/CDK complexes in the mouse fibroblast cell cycle and in cells arrested with lovastatin or ultraviolet light. *Mol. Biol. Cell* 6:1197-1213.
  58. Porter, P. L., K. E. Malone, P. J. Heagerty, G. M. Alexander, L. A. Gatti, E. J. Firpo, J. R. Daling, and J. M. Roberts. 1997. Expression of cell-cycle regulators p27<sup>Kip1</sup> and cyclin E, alone and in combination, correlate with survival in young breast cancer patients. *Nat. Med.* 3:222-225.
  59. Press, M. F., M. C. Pike, V. R. Chazin, G. Hung, J. A. Udove, M. Markowicz, J. Danyluk, W. Godolphin, M. Sliwkowski, R. Akita, M. C. Paterson, and D. J. Slamon. 1993. Her-2/neu expression in node-negative breast cancer: direct tissue quantitation by computerized image analysis and association of overexpression with increased risk of recurrent disease. *Cancer Res.* 53:4960-4970.
  60. Prigent, S. A., and W. J. Gullick. 1994. Identification of c-erbB-3 binding sites for phosphatidyl 3' kinase and SHC using an EGF receptor/c-erbB-3 chimera. *EMBO J.* 13:2831-2841.
  61. Pusch, O., G. Barnaschek, M. Eilers, and M. Hengstschlager. 1997. Activation of c-Myc uncouples DNA replication from activation of G1-cyclin-dependent kinases. *Oncogene* 15:649-656.
  62. Riese, D. J., II, and D. F. Stern. 1998. Specificity within the EGF family/ErbB receptor family signaling network. *Bioessays* 20:41-48.
  63. Scott, G. K., J. M. Dodson, P. A. Montgomery, R. M. Johnson, J. C. Sarup, W. L. Wong, A. Ullrich, H. M. Shepard, and C. C. Benz. 1991. p185<sup>HER2</sup> signal transduction in breast tumour cells. *J. Biol. Chem.* 266:14300-14305.
  64. Scott, G. K., R. Robles, J. W. Park, P. A. Montgomery, J. Daniel, W. E. Holmes, J. Lee, G. A. Keller, W.-L. Li, B. M. Fendly, W. I. Wood, H. M. Shepard, and C. C. Benz. 1993. A truncated intracellular HER2/neu receptor produced by alternative RNA processing affects growth of human carcinoma cells. *Mol. Cell. Biol.* 13:2247-2257.
  65. Sears, R., G. Lone, J. DeGregori, and J. R. Nevins. 1999. Ras enhances Myc protein stability. *Mol. Cell* 3:169-179.
  66. Sheaff, R. J., M. Groudine, M. Gordon, J. M. Roberts, and B. E. Clurman. 1997. Cyclin E-CDK2 is a regulator of p27<sup>Kip1</sup>. *Genes Dev.* 11:1464-1478.
  67. Sherr, C. J., and J. M. Roberts. 1995. Inhibitors of mammalian G1 cyclin-dependent kinases. *Genes Dev.* 9:1149-1163.
  68. Sherr, C. J., and J. M. Roberts. 1999. CDK inhibitors: positive and negative regulators of G1-phase progression. *Genes Dev.* 13:1501-1512.
  69. Siegel, P. M., E. D. Ryan, R. D. Cardiff, and W. J. Muller. 1999. Elevated

- expression of activated forms of Neu/ErbB-2 and ErbB-3 are involved in the induction of mammary tumors in transgenic mice: implications for human breast cancer. *EMBO J.* 18:2149-2164.
70. Slamon, D. J., G. M. Clark, S. G. Wong, W. J. Levin, A. Ullrich, and W. L. McGuire. 1987. Human breast cancer: correlation of relapse and survival with the amplification of the HER-2/*neu* oncogene. *Science* 235:177-182.
  71. Slamon, D. J., W. Godolphin, L. A. Jones, J. A. Holt, S. G. Wong, D. E. Keith, W. J. Levin, S. G. Stuart, J. Udove, A. Ullrich, and M. F. Press. 1989. Studies of the HER-2/*neu* proto-oncogene in human breast and ovarian cancer. *Science* 244:707-712.
  72. Slingerland, J. M., L. Hengst, C. H. Pan, D. Alexander, M. R. Stampfer, and S. I. Reed. 1994. A novel inhibitor of cyclin-Cdk activity detected in transforming growth factor  $\beta$ -arrested epithelial cells. *Mol. Cell. Biol.* 14:3683-3694.
  73. Soos, T. J., H. Kiyokawa, J. S. Yan, M. S. Rubin, A. Giordano, A. DeBlasio, S. Bottega, B. Wong, J. Mendelsohn, and A. Koff. 1996. Formation of p27-CDK complexes during the human mitotic cell cycle. *Cell Growth Differ.* 7:135-146.
  74. Steiner, P., A. Philipp, J. Lukas, D. Godden-Kent, M. Pagano, S. Mittnacht, J. Bartek, and M. Eilers. 1995. Identification of a Myc-dependent step during the formation of active G<sub>1</sub> cyclin-cdk complexes. *EMBO J.* 14:4814-4826.
  75. Taya, Y. 1997. RB kinases and RB-binding proteins: new points of view. *Trends Biochem. Sci.* 22:14-17.
  76. Toyoshima, H., and T. Hunter. 1994. p27, a novel inhibitor of G<sub>1</sub> cyclin/cdk protein kinase activity, is related to p21. *Cell* 78:67-74.
  77. Vlach, J., S. Hennecke, K. Alevizopoulos, D. Conti, and B. Amati. 1996. Growth arrest by the cyclin-dependent kinase inhibitor p27<sup>Kip1</sup> is abrogated by c-Myc. *EMBO J.* 15:6595-6604.
  78. Wallasch, C., F. U. Weisse, G. Niederfellner, B. Jallat, W. Issing, and A. Ullrich. 1995. Heregulin-dependent regulation of HER2/*neu* oncogenic signaling by heterodimerization with HER3. *EMBO J.* 14:4267-4275.
  79. Weiss, F. U., C. Wallasch, M. Campiglio, W. Issing, and A. Ullrich. 1997. Distinct characteristics of heregulin signals mediated by HER3 or HER4. *J. Cell. Physiol.* 173:187-195.
  80. West, M. J., M. Stoneley, and A. E. Willis. 1998. Translational induction of the c-myc oncogene via activation of the FRAP/TOR signalling pathway. *Oncogene* 17:769-780.
  81. Wu, X., M. Rubin, Z. Fan, T. DeBlasio, T. Soos, A. Koff, and J. Mendelsohn. 1996. Involvement of p27<sup>Kip1</sup> in G<sub>1</sub> arrest mediated by an anti-epidermal growth factor receptor monoclonal antibody. *Oncogene* 12:1397-1403.
  82. Yasui, W., Y. Kudo, S. Semba, H. Yokozaki, and E. Tahara. 1997. Reduced expression of cyclin-dependent kinase inhibitor p27<sup>Kip1</sup> is associated with advanced stage and invasiveness of gastric carcinomas. *Jpn. J. Cancer Res.* 88:625-629.
  83. Ye, D., J. Mendelsohn, and Z. Fan. 1999. Augmentation of a humanized Anti-HER2 mAb 4D5 induced growth inhibition by a human-mouse chimeric anti-EGF receptor mAb C225. *Oncogene* 18:731-738.
  84. Yonemura, Y., I. Ninomiya, A. Yamaguchi, S. Fushida, H. Kimura, S. Ohoyama, I. Miyazaki, Y. Endou, M. Tanaka, and T. Sasaki. 1991. Evaluation of immunoreactivity for *erbB-2* protein as a marker of poor short-term prognosis in gastric cancer. *Cancer Res.* 51:1034-1038.
  85. Zhang, H., G. J. Hannon, and D. Beach. 1994. p21-containing cyclin-kinases exist in both active and inactive states. *Genes Dev.* 8:1750-1758.
  86. Zhang, K., J. Sun, N. Liu, D. Wen, D. Chang, A. Thomason, and S. K. Yasinaga. 1996. Transformation of NIH 3T3 cells by HER3 or HER4 receptors requires the presence of HER1 or HER2. *J. Biol. Chem.* 271:3884-3890.

# **EXHIBIT H**

# Monoclonal antibody drug conjugates in the treatment of cancer

Pamela A Trail\* and Albert B Bianchi†

Monoclonal antibodies directed to tumor-associated antigens have been chemically conjugated to drugs with different mechanisms of action and different levels of potency. Monoclonal-antibody-directed drug delivery has the potential to both improve efficacy and reduce systemic toxicity. Several immunoconjugates have demonstrated impressive antigen-specific antitumor activity in preclinical models. Phase I trials of a calicheamicin immunoconjugate for treatment of acute myeloid leukemia and a doxorubicin immunoconjugate for treatment of carcinoma have recently been completed.

## Addresses

Bristol-Myers Squibb Pharmaceutical Research Institute,  
P.O. Box 4000, Princeton, NJ 08543, USA

\*e-mail: Trailp@bms.com

† e-mail: Bianchia@bms.com

Correspondence: Pamela A Trail

**Current Opinion in Immunology** 1999, 11:584–588

0952-7915/99/\$ – see front matter © 1999 Elsevier Science Ltd.  
All rights reserved.

## Abbreviations

<b>AML</b>	acute myeloid leukemia
<b>DOX</b>	doxorubicin
<b>MAb</b>	monoclonal antibody
<b>MR</b>	molar ratio

## Introduction

The treatment of cancer is limited by a number of factors including the low therapeutic index of most chemotherapeutic agents, the emergence of drug- and radiation-resistant populations, tumor heterogeneity and the presence of metastatic disease. One of the means to improve the therapeutic index of drugs is by selective or 'targeted' delivery to tumor sites. Tumor-directed therapy has the potential to improve efficacy, by increasing the intratumoral concentration of the targeted agent, and to minimize toxicity by reducing systemic exposure. Monoclonal antibodies (MAbs), MAb fragments, hormones and growth factors have been used to deliver drugs, toxins, radionuclides, enzymes, photosensitizers and cytokines to tumors.

Unfortunately, the clinical efficacy of MAb-directed therapy is frequently limited by expression of the targeted antigen on normal as well as malignant cells. With the exception of MAbs to idiotypic domains of lymphocytes, truly tumor-specific MAbs have not been identified; rather, MAbs identify tumor-associated antigens expressed at higher density on malignant cells relative to normal cells. It is therefore necessary to balance the relative selectivity of the MAb with the potency of the agent delivered. Studies in preclinical models with human tumors in immunodeficient mice have demonstrated impressive activity for many of these conjugates. However, it is important to recognize that these models, while useful, frequently over-predict

activity and under-predict toxicity because the antigen targeted is tumor-specific in the mouse but tumor-associated in patients. Nevertheless, several immunoconjugates have shown impressive activity even though the targeted antigen is expressed on normal tissues of immunodeficient animals or normal tissues of immunocompetent animals bearing syngeneic tumors [1,2,3\*].

Significant progress has been made for MAb-directed therapies in the treatment of patients who have lymphoma [4,5\*\*]. In addition, the use of the MAb 17-1A following tumor resection has resulted in improved survival of patients with Dukes' C colorectal cancer [6\*] and improved response rates were seen in breast cancer patients receiving the anti-HER2 MAb, directed against the HER2 transmembrane tyrosine-kinase receptor coded by the *HER2* gene (also known as *neu* and as *c-erbB-2*), in combination with cisplatin [7]. However, only occasional responses have been reported for MAbs or immunoconjugates used as monotherapy in the treatment of patients with advanced solid tumors. The physical barriers of solid tumors — including elevated interstitial pressure, heterogeneous and reduced functional vasculature and the relatively large distances for MAbs to travel in the tumor interstitium [8\*] — contribute to the limited tumor penetration and minimal efficacy seen when MAb-directed therapies are used as single agents in patients with advanced disease.

Several modifications have been used to improve the efficacy of immunoconjugate therapy. Immunogenicity has been reduced by using chimeric [9\*\*] or humanized [5\*\*] MAbs. Attempts to decrease the amount of MAb needed for antitumor activity have included the use of more potent drugs [3\*,10] and alternative strategies such as branched linkers [11\*] and delivery of liposome-encapsulated drugs [12,13\*,14] to increase the quantity of drug delivered per antibody molecule. Improved MAb distribution in solid tumors has been addressed by using pharmacological approaches to improve penetration [15]. Recent studies have demonstrated that directing therapy to antigens expressed on the tumor vasculature (a readily accessible compartment), rather than to tumor-associated antigens of solid tumors, can produce impressive activity in preclinical models [16,17\*,18\*\*,19,20]. This review will concentrate on the results of recent clinical trials of MAb–drug immunoconjugates and highlight current strategies to improve the potency, specificity and efficacy of immunoconjugate therapy.

## MAb-directed delivery of enediyne

One means to improve immunoconjugate potency and efficacy is to increase the potency of the targeted drugs. Members of the enediyne family of antibiotics are among the

most toxic antitumor compounds described to date. This novel class of agents includes the calicheamicins, neocarzinostatin, esperamicins, dynemicins, kedarcidin and maduropeptin [21]. Although these agents are highly potent *in vitro*, their utility as antitumor drugs has — for the most part — been limited by their low therapeutic index. Antibody-directed delivery provides a potential means to exploit the impressive potency of these compounds while minimizing their systemic toxicity. The use of extremely toxic drugs requires careful MAb selection as even low levels of expression of the targeted antigen by normal cells may lead to significant toxicity. Neocarzinostatin [22–24] and several of the calicheamicins [3\*,5\*\*,10,25,26] have been used to produce extremely potent immunoconjugates.

The calicheamicins produce double-stranded breaks in DNA. Calicheamicin conjugates — in which a hydrazide of calicheamicin  $\gamma^1_1$  was linked to oxidized sugars on the internalizing anti-polyepithelial-mucin MAb CT-M-01 — produced potent antigen-specific activity against subcutaneous breast-tumor xenografts in athymic mice [10].

A Phase I study of CMA-676, an immunoconjugate of calicheamicin  $\gamma^1_1$  conjugated to a humanized (human IgG<sub>4</sub>) anti-CD33 MAb (hP67.6), has recently been completed [5\*\*]. The CD33 target antigen is expressed on acute myeloid leukemia (AML) and maturing hematopoietic cells but not on normal stem cells. Forty patients with refractory or relapsed AML were treated intravenously with 0.25–9.0 mg/m<sup>2</sup> of CMA-676. Toxicity was primarily hematologic; however neither the hematologic nor nonhematologic side effects was considered dose-limiting. Fever and chills occurred in 80% of patients and were the most common nonhematologic side effect. Leukemic cells were eliminated from the blood and marrow of 20% of treated patients. At the 9 mg/m<sup>2</sup> dose level, >75% saturation of CD33 sites was seen on peripheral-blood blast cells. Clinical responses were seen at dose levels of 1–9 mg/m<sup>2</sup>. Responses were seen only in patients whose peripheral blast cell demonstrated  $\geq 75\%$  saturation of CD33 and had low efflux of 3,3'-diethylloxycarbocyanine iodide, an assay that determines functional efflux mediated through MDR1- and non-MDR1-dependent mechanisms. The efflux data suggest that intracellular delivery of the calicheamicin by the hP67.6 MAb did not overcome multidrug resistance. Data from this Phase I trial in patients with advanced AML are encouraging and support evaluation of CMA-676 in a setting of newly diagnosed or minimal-residual disease.

Calicheamicin  $\theta^1_1$ , a more potent analog of calicheamicin  $\gamma^1_1$ , was conjugated to an anti-ganglioside-GD<sub>2</sub> MAb (14G2a) and showed impressive antitumor activity when used to treat experimental liver metastases in syngeneic immunocompetent mice [3\*]. Dose-dependent activity was observed against a neuroblastoma line heterogeneous for antigen expression. The conjugate of 14G2a with calicheamicin  $\theta^1_1$  was both more efficacious and less toxic

than unconjugated calicheamicin  $\theta^1_1$  or mixtures of 14G2a and calicheamicin  $\theta^1_1$ , indicating effective antibody-directed targeting. The use of a syngeneic tumor model heterogeneous for antigen expression more closely approximates the clinical situation and provides an important model system for evaluating immunoconjugate efficacy.

### MAb-directed delivery of anthracyclines

The anthracycline family of antitumor antibiotics, most notably doxorubicin (DOX) and daunorubicin, has been used extensively for drug targeting applications [27]. The immunoconjugate BR96–DOX [1,28] was evaluated in Phase I [9\*\*] and II [29\*] clinical trials. BR96–DOX (which is chimeric with human IgG<sub>1</sub>) binds a Le<sup>y</sup>-related, tumor-associated antigen expressed on most human carcinomas [30] and on normal cells of the gastrointestinal tract of humans, dogs and rats [1]. BR96–DOX induced cures of human lung, breast and colon carcinomas in athymic mice and rats [1,27,31] and syngeneic colon tumors in immunocompetent rats [2].

Although cures were seen in multiple preclinical models, only tumor stabilization and a small number of partial regressions were seen in a Phase I trial of patients with advanced disease. A therapeutically relevant anticonjugate response was not observed and there were no significant hematologic or cardiac toxicities. The dose-limiting toxicity was acute gastrointestinal toxicity with dose-related nausea, vomiting and gastritis [9\*\*].

A randomized Phase II trial was performed in patients with metastatic breast carcinoma [29\*]. Patients received 700 mg/m<sup>2</sup> of BR96–DOX (20 mg/m<sup>2</sup> DOX) or 60 mg/m<sup>2</sup> of DOX every three weeks. There was one partial response (in a patient with hepatic metastases) in the fourteen patients receiving BR96–DOX and one complete and three partial responses in the nine patients receiving DOX. Interestingly, two of the four patients who crossed over to the BR96–DOX arm of the trial after persistent stable disease during DOX treatment achieved partial regression of hepatic metastases following BR96–DOX therapy.

Localization of BR96 and DOX was seen in tumor biopsies of patients receiving BR96–DOX, indicating that BR96 successfully delivered DOX to tumors [9\*\*]. These data, taken together with the low clinical response rates, suggest that the dose that could be safely administered every three weeks was insufficient to maintain the intratumoral concentration of DOX required to achieve regression. Preclinical studies in antigen-expressing rats indicate that administering BR96–DOX in combination with cytotoxic drugs or at a low dose for an extended duration can substantially reduce both the dose per injection and the cumulative dose needed to cure established experimental tumors (PA Trail, unpublished data). It is likely that BR96–DOX, like most antibody therapies, will be most effective in minimal-disease settings.



Several novel conjugation strategies have been developed to improve the potency of anthracycline conjugates. An enzymatic coupling procedure that attaches DOX to galactose residues of an anti-carcinoembryonic-antigen MAb demonstrated antigen-specific activity *in vitro* and improved both the potency and efficacy (relative to unconjugated DOX) against tumors transplanted onto the chorioallantoic membrane of embryonated chicken eggs [32]. However, as conjugates were applied to tumor-containing discs on the chorioallantoic membrane, the relative utility of this method awaits demonstration of distal site activity in a more rigorous antitumor model that requires MAb-directed delivery.

The potency of immunoconjugates can be improved by increasing the quantity of drug delivered per MAb molecule. In the case of DOX immunoconjugates, significant losses in affinity and antigen-specific cytotoxicity were seen when  $\geq 10$  molecules of DOX were directly conjugated per MAb [33]. The use of branched linkers, in which each linker to the MAb carries two DOX molecules, resulted in an increase in the drug : MAb molar ratio (MR) from 8:1 to 16:1. This increase in the MR was accompanied by an increase in antigen-specific potency *in vitro* [11\*] and a two-fold decrease in the amount of MAb required to achieve partial regression of subcutaneous tumors in preclinical models. The use of water-soluble polymeric carriers [34] has also been attempted to increase conjugate MRs.

### Immunoliposomes

The encapsulation of drugs in MAb-targeted liposomes can be used to selectively increase the concentration of drug delivered to antigen-expressing cells [12,13\*,14,35]. The pharmacokinetics and clearance of liposomes were improved by incorporating lipid derivatives of polyethylene glycol (PEG) into liposome formulations [36,37]. These sterically stabilized liposomes enhance accumulation in tumours [38]. Importantly, immunoliposomes utilizing internalizing MAbs — such as anti-HER-2 [39] or anti-CD19 [13\*] — can be used to selectively deliver high concentrations of drug into the cytoplasm of antigen-expressing cells.

### Targeting the tumor vasculature

The progressive growth and metastasis of tumors requires the formation of new blood vessels (angiogenesis) from the pre-existing vasculature [40]. Immunoconjugates directed against antigens differentially expressed on tumor endothelium offer several potential advantages over targeting tumor-associated antigens expressed on cells of solid tumors. Directing therapy to the accessible vascular compartment reduces the impact of the physical barriers of solid tumors, such as heterogeneous blood flow and elevated interstitial pressure, which restrict the penetration and distribution of MAbs through the tumor parenchyma [8\*]. Endothelial cells are highly regulated, genetically stable cells that are less likely to develop the classical drug resistance observed in tumor cells [40]. In

addition, as angiogenesis is required for tumor progression, therapies directed against the tumor vasculature should have broad-spectrum activity. Several recent studies have demonstrated that targeting the tumor vasculature with MAbs [16,17\*,20], growth factor ligands [41,42] or peptides that bind  $\alpha_v$  integrins [18\*\*] can produce impressive antitumor activity. Identification of appropriate target antigens that are expressed on the tumor vasculature, but not on cells of normal vessels, is an area of ongoing interest. Potential antigens for vascular targeting include VEGFR-2 (vascular endothelial growth factor receptor 2), endoglin, endosialin, aminopeptidase A [16,19] and VEGF complexed with its receptor [43]. Screening of phage display libraries identified several peptides that selectively localized in the tumor vasculature. These peptides were conjugated to DOX and shown to have impressive antitumor activity that was associated with damage to the tumor vasculature [18\*\*]. The *in vivo* screening of phage peptide libraries is an interesting approach to identify novel molecules expressed on angiogenic blood vessels.

### Conclusions and future directions

Although immunoconjugates are not currently established chemotherapeutic agents, several of them have demonstrated evidence of biologic activity in patients with advanced disease [5\*\*,9\*\*,29\*]. The current objectives are aimed at improving the efficacy and therapeutic index of immunoconjugates by optimizing selectivity and potency. The development of MAb therapies directed against the tumor vasculature is an area of considerable interest and various research approaches to identify antigens and conjugation strategies with appropriate selectivity are being pursued.

The promise offered by MAb-based therapies has begun to be realized with the approval of an anti-CD20 MAb for treatment of non-Hodgkin's lymphoma and an anti-HER2 MAb for treatment of metastatic breast carcinoma. The calicheamicin conjugate CMA-676 [5\*\*] has shown encouraging data in a Phase I trial of patients with refractory AML. Although immunoconjugates may be active as single agents, it is likely that their major role — especially in treatment of solid tumors — will be in combination-chemotherapy regimens or minimal-disease settings. In addition to research efforts directed at improving immunoconjugate constructs, clinical studies to define optimal therapeutic strategies are underway and will further clarify the role of immunoconjugates as anticancer agents.

### References and recommended reading

Papers of particular interest, published within the annual period of review, have been highlighted as:

- of special interest
- \*\* of outstanding interest

1. Trail PA, Willner D, Lasch SJ, Henderson AJ, Hofstead SJ, Casazza AM, Firestone RA, Hellström I, Hellström KE: Cure of xenografted human carcinomas by BR96-doxorubicin immunoconjugates. *Science* 1993, 261:212-215.

2. Sjögren HO, Isaksson M, Willner D, Hellström I, Hellström KE, Trail PA: **Antitumor activity of carcinoma-reactive BR96-doxorubicin conjugate against human carcinomas in athymic mice and rats and syngeneic rat carcinomas in immunocompetent rats.** *Cancer Res* 1997, 57:4530-4536.
3. Lode HN, Reisfeld RA, Handgretinger R, Nicolaou KC, Gaedicke G, Wrasidlo W: **Targeted therapy with a novel enediyne antibiotic calicheamicin  $\theta^{11}$  effectively suppresses growth and dissemination of liver metastases in a syngenic model of murine neuroblastoma.** *Cancer Res* 1998, 58:2925-2928.  
 This paper describes an anti-GD<sub>2</sub> MAb (anti-ganglioside) conjugated to a potent calicheamicin analogue. This immunoconjugate showed impressive antitumor activity in a minimal-disease liver metastasis model. This model has relevance to the clinical situation because a syngeneic tumor with heterogeneous expression of the GD<sub>2</sub> antigen was used to evaluate immunoconjugate activity.
4. Press OW, Eary JF, Appelbaum FR, Martin PJ, Badger CC, Nelp WB, Glenn S, Butchko G, Fisher D, Porter B *et al.*: **Radiolabeled-antibody therapy of B cell lymphoma with autologous bone marrow support.** *N Engl J Med* 1993, 329:1219-1224.
5. Sievers EL, Appelbaum FR, Spielberger RT, Forman SJ, Flowers D, Smith FO, Shannon-Dorcy K, Berger MS, Bernstein ID: **Selective ablation of acute myeloid leukemia using antibody-targeted chemotherapy: a phase I study of an anti-CD33 calicheamicin immunoconjugate.** *Blood* 1999, 93:3678-3684.  
 This paper reports a phase I trial of an anti-CD33-calicheamicin conjugate, CMA-676, demonstrating a 20% response rate in patients with refractory AML. The study design included evaluation of the levels of saturation of CD33 sites and addressed the impact of a multi-drug-resistance phenotype on clinical response.
6. Riethmuller G, Holz E, Schlimok G, Schmiegel W, Raab R, Hoffken K, Gruber R, Funke I, Pichlmaier H, Hirche H *et al.*: **Monoclonal antibody therapy for resected Dukes' C colorectal cancer: seven-year outcome of a multicenter randomized trial.** *J Clin Oncol* 1998, 16:1788-1794.  
 This study of 189 patients shows that 17-1A antibody, when used to treat minimal residual disease (post resection of Dukes' C colon carcinoma), prevented the development of distant metastasis in approximately one third of patients. The therapeutic effect was maintained after seven years of follow-up evaluation.
7. Pegram MD, Lipton A, Hayes DF, Weber BL, Baselga MM, Tripathy D, Baly D, Baighman SA, Twaddell T, Glaspy JA, Slalom DJ: **Phase II study of receptor-enhanced chemosensitivity using recombinant humanized anti-p185HER2/neu monoclonal antibody plus cisplatin in patients with HER2/neu-overexpressing metastatic breast cancer refractory to chemotherapy treatment.** *J Clin Oncol* 1998, 16:2659-2663.
8. Jain RK: **Delivery of molecular and cellular medicine to solid tumors.** *J Control Release* 1998, 53:49-67.  
 This reviews the physical barriers of solid tumors that impair the penetration, distribution and efficacy of MAb-directed therapies.
9. Saleh MN, LoBuglio AF, Trail PA: **Immunoconjugate therapy of solid tumors: studies with BR96-doxorubicin.** In *Monoclonal Antibody-Based Therapy of Cancer*. Edited by Grossbard M. New York: Marcel Dekker, 1998:397-416.  
 This chapter discusses the preclinical biology and Phase I findings of BR96-DOX, an anticarcinoma immunoconjugate. Data from the Phase I trial demonstrate BR96-directed delivery of DOX in patient tumor biopsies and evidence of biologic activity. Low response rates indicate the need for further optimization for the conjugate to be clinically acceptable. It is suggested that BR96-DOX, like other MAB therapies, will be most effective when evaluated in minimal-disease settings.
10. Hinman LM, Hamann PR, Wallace R, Menendez AT, Durr FE, Upeslaciis J: **Preparation and characterization of monoclonal antibody conjugates of the calicheamicins: a novel and potent family of antitumor antibiotics.** *Cancer Res* 1993, 53:3336-3342.
11. King HD, Yurgaitis D, Willner D, Firestone RA, Yang MB, Lasch SJ, Hellstrom KE, Trail PA: **Monoclonal antibody conjugates of doxorubicin prepared with branched linkers: a novel method for increasing the potency of doxorubicin immunoconjugates.** *Bioconj Chem* 1999, 10:279-288.  
 The authors describe a novel conjugation strategy to increase immunoconjugate potency by increasing the amount of drug delivered per MAb. These linkers attach two DOX molecules per thiol to the MAb and the conjugates demonstrate potent antigen-specific cytotoxicity *in vitro*.
12. Park JW, Hong K, Kirpotin DB, Meyer O, Papahadjopoulos D, Benz CC: **Anti-HER2 immunoliposomes for targeted therapy of human tumors.** *Cancer Lett* 1997, 118:153-160.
13. Lopes de Menezes DE, Pilarski LM, Allen TM: ***In vitro* and *In vivo* targeting of immunoliposomal doxorubicin to human B-cell lymphoma.** *Cancer Res* 1998, 58:3320-3330.  
 A study demonstrating the potential to use internalizing MABs to deliver sterically stabilized DOX immunoliposomes in minimal-disease lymphoma models.
14. Tseng YL, Hong RL, Tao MH, Chang FH: **Sterically stabilized anti-idiotypic immunoliposomes improve the therapeutic efficacy of doxorubicin in a murine B-cell lymphoma model.** *Int J Cancer* 1999, 80:723-730.
15. Hornick JL, Khawli LA, Hu P, Sharifi J, Khanna C, Epstein AL: **Pre-treatment with a monoclonal antibody/interleukin-2 fusion protein directed against DNA enhances the delivery of therapeutic molecules to solid tumors.** *Clin Cancer Res* 1999, 5:51-60.
16. Huang X, Molema G, King S, Watkins L, Edgington TS, Thorpe PE: **Tumor infarction in mice by antibody-directed targeting of tissue factor to tumor vasculature.** *Science* 1997, 275:547-550.
17. Ran S, Gao B, Duffy S, Watkins L, Rote N, Thorpe PE: **Infarction of solid Hodgkin's tumors in mice by antibody-directed targeting of tissue factor to tumor vasculature.** *Cancer Res* 1998, 58:4646-4653.  
 This paper describes a strategy to inhibit tumor growth by selectively forming thrombi in the tumor vasculature. A MAB to a naturally occurring endothelial marker, vascular cell adhesion molecule 1 (VCAM-1), was used to target the extracellular domain of tissue factor.
18. Arap W, Pasqualini R, Ruoslahti E: **Cancer treatment by targeted drug delivery to tumor vasculature in a mouse model.** *Science* 1998, 279:377-380.  
 These studies use *in vivo* selection of phage display libraries to identify peptides that selectively localize in tumor blood vessels. This is an interesting approach to identify novel cell surface markers with selectivity for the tumor vasculature.
19. Arap W, Pasqualini R, Ruoslahti E: **Chemotherapy targeted to tumor vasculature.** *Curr Opin Oncol* 1998, 10:560-565.
20. Matsuno F, Haruta Y, Kondo M, Tsai H, Barcos M, Seon BK: **Induction of lasting complete regression of preformed distinct solid tumors by targeting the tumor vasculature using two new anti-endothelin monoclonal antibodies.** *Clin Cancer Res* 1999, 5:371-382.
21. Smith AL, Nicolaou KC: **The enediyne antibiotics.** *J Med Chem* 1996, 39:2103-2117.
22. Kondo S, Nakatsu S, Sakahara H, Kobayashi H, Konishi J, Namba Y: **Antitumor activity of an immunoconjugate composed of anti-human astrocytoma monoclonal antibody and neocarzinostatin.** *Eur J Cancer* 1993, 34:420-423.
23. Okamoto K, Yamaguchi T, Otsuji E, Yamaoka N, Yata Y, Tsuruta H, Kitamura K, Takahashi T: **Targeted chemotherapy in mice with peritoneally disseminated gastric cancer using monoclonal antibody-drug conjugate.** *Cancer Lett* 1998, 122:231-236.
24. Otsuji E, Yamaguchi T, Tsuruta H, Yata Y, Nishi H, Okamoto K, Taniguchi K, Kato M, Kotani T, Kitamura K *et al.*: **The effect of intravenous and intra-tumoural chemotherapy using a monoclonal antibody-drug conjugate in a xenograft model of pancreatic cancer.** *Eur J Surg Oncol* 1995, 21:61-65.
25. Schmidt CS, Wrasidlo W, Kaufmann O, Scherberich JE, Gaedicke G, Fischer P: **Monoclonal antibody 138H11 against gamma-glutamyltransferase provides a possible tool for targeting calicheamicin theta to renal cell carcinomas.** *Adv Exp Med Biol* 1998, 451:431-436.
26. Siegel MM, Tabei K, Kunz A, Hollander IJ, Hamann RR, Bell DH, Berkenkamp S, Hillenkamp F: **Calicheamicin derivatives conjugated to monoclonal antibodies: determination of loading values and distributions by infrared and UV matrix-assisted laser desorption/ionization mass spectrometry and electrospray ionization mass spectrometry.** *Anal Chem* 1997, 69:2716-2726.
27. Trail PA, Willner D, Hellstrom KE: **Site-directed delivery of anthracyclines for cancer therapy.** *Drug Dev Res* 1995, 34:196-209.
28. Willner D, Trail PA, Hofstead SJ, King HD, Lasch SJ, Braslawsky GR, Greenfield RS, Kaneko T, Firestone RA: **(6-maleimidocaproyl)-hydrazono of doxorubicin - a new derivative for the preparation of immunoconjugates of doxorubicin.** *Bioconj Chem* 1993, 4:521-527.

29. Tolcher AW, Sugarman S, Gelmon KA, Cohen R, Saleh M, Isaacs C, Young L, Healey D, Onetto N, Slichenmyer W: **Randomized phase II study of BR96-doxorubicin conjugate in patients with metastatic breast cancer.** *J Clin Oncol* 1999, **17**:478-484.
- This article describes a Phase II clinical study of BR96-DOX in patients with metastatic breast cancer.
30. Hellström I, Garrigues HJ, Garrigues U, Hellström KE: **Highly tumor-reactive, internalizing, mouse monoclonal antibodies to Ley-related cell surface antigen.** *Cancer Res* 1990, **50**:2183-2190.
31. Hellström I, Hellström KE, Siegall CB, Trail PA: **Immunoconjugates and immunotoxins for therapy of carcinomas.** In *Advances in Pharmacology*, vol 33, edn 1. Edited by August JT, Anders MW, Murad F, Coyle JT. San Diego: Academic Press; 1995:349-388.
32. Stan AC, Radu DL, Casares S, Bona CA, Brumeanu TD: **Antineoplastic efficacy of doxorubicin enzymatically assembled on galactose residues of a monoclonal antibody specific for the carcinoembryonic antigen.** *Cancer Res* 1999, **59**:115-121.
33. Shih LB, Goldenberg DM, Xuan H, Lu H, Sharkey RM, Hall TC: **Anthracycline immunoconjugates prepared by a site specific linkage via an amino-dextran intermediate carrier.** *Cancer Res* 1991, **51**:4192-4198.
34. Omelyanenko V, Gentry C, Kopeckova P, Kopecek J: **HPMA copolymer-anticancer drug-OV-TL16 antibody conjugates. II. Processing in epithelial ovarian carcinoma cells *in vitro*.** *Int J Cancer* 1998, **75**:600-608.
35. Crosasso P, Brusa P, Dosio F, Arpicco S, Pacchioni D, Schuber F, Cattel L: **Antitumoral activity of liposomes and immunoliposomes containing 5-fluorouridine prodrugs.** *J Pharm Sci* 1997, **86**:832-839.
36. Allen TM, Hansen C: **Pharmacokinetics of stealth versus conventional liposomes: effect of dose.** *Biochim Biophys Acta* 1991, **1068**:133-141.
37. Huwylar J, Yang J, Pardridge WM: **Receptor mediated delivery of daunomycin using immunoliposomes: pharmacokinetics and tissue distribution in the rat.** *J Pharmacol Exp Ther* 1997, **282**:1541-1546.
38. Hansen CB, Kao GY, Moase EH, Zalipsky S, Allen TM: **Attachment of antibodies to sterically stabilized liposomes: evaluation, comparison and optimization of coupling procedures.** *Biochim Biophys Acta* 1995, **1239**:133-144.
39. Kirpotin D, Park JW, Hong K, Zalipsky S, Li WL, Carter P, Benz CC, Papahadjopoulos D: **Sterically stabilized anti-HER2 immunoliposomes: design and targeting to human breast cancer cells *in vitro*.** *Biochemistry* 1997, **36**:66-75.
40. Folkman J: **New perspectives in clinical oncology from angiogenesis research.** *Eur J Cancer* 1996, **14**:2534-2539.
41. Olson TA, Mohanraj D, Roy S, Ramakrishnan S: **Targeting the tumor vasculature: inhibition of tumor growth by a vascular endothelial growth factor-toxin conjugate.** *Int J Cancer* 1997, **73**:865-870.
42. Arora N, Masood R, Zheng T, Cai J, Smith DL, Gill PS: **Vascular endothelial growth factor chimeric toxin is highly active against endothelial cells.** *Cancer Res* 1999, **59**:183-188.
43. Brekken RA, Huang X, King SW, Thorpe PE: **Vascular endothelial growth factor as a marker of tumor endothelium.** *Cancer Res* 1998, **58**:1952-1959.